PhD thesis

Ola M. Rygh

3D ultrasound based neuronavigation in neurosurgery

A Clinical Evaluation

NTNU
Norwegian University of
Science and Technology

Ola Morten Rygh

3D ultrasound-based neuronavigation in neurosurgery

A clinical evaluation

Thesis for the degree philosophiae doctor

Trondheim, June 2008

Norwegian University of Science and Technology
Faculty of medicine
Department of Neuroscience

Nevronavigasjon basert på tredimensjonal ultralyd - klinisk evaluering

Nevronavigasjon betyr å navigere ved hjelp av medisinske bildedata under nevrokirurgiske operasjoner, det vil si operasjoner på hjerne eller ryggmarg. Det har likhetstrekk med navigasjon med GPS, der posisjonen til en person eller en bil vises på et kart. I nevronavigasjon er det posisjonen til et kirurgisk instrument som vises på medisinske bildedata, for eksempel MR-bilder eller ultralydbilder. Dette gjør bildeinformasjonen lett tilgjengelig for kirurgen under operasjonen og hjelper kirurgen til å orientere seg før og under operasjonen.

I Trondheim er det et aktivt miljø som driver forskning og utvikling på nevronavigasjon og tredimensjonal (3D) ultralyd. Det er utviklet et system som bruker tredimensjonale ultralyd billeddata tatt underveis i operasjonen i tillegg til bildedata (for eksempel MR) tatt før operasjonen.

Formålet med denne avhandlingen var å undersøke nytten av det 3D ultralydbaserte navigasjonssystemet ved forskjellige operasjoner.

Hovedfunnene i avhandlingen:
1. Tredimensjonal ultralyd er svært nøyaktig til å avbilde grensen til hjernesvulster før en har påbegynt fjerning av svulsten, men under operasjonen er ultralydbildene noe mindre nøyaktige til å vise svulstens grenser, og det kan være overestimering av svulstvev på 3D ultralyd. Etter at svulsten er fjernet kan små områder som inneholder svulstvev eller infiltrer hjernevev oppfattes som normalt på 3D ultralyd.
2. Tredimensjonal ultralyd brukt til å vise blodkar (ultralyd angiografi basert på Dopplerteknikk) er nyttig til å vise blodkar ved fjerning av svulster som ligger nær viktige blodkar i hjernen, og kan gjøre operasjonene sikrere.
3. Tredimensjonal ultralyd kan brukes til å veilede kirurgen ved operasjoner på svulster i ryggmargen.
4. Tredimensjonal ultralyd kan brukes til å veilede kirurgen ved hjerneoperasjoner der en bruker kikkhulls-teknikk (endoskopi). Det er spesielt nyttig i tilfeller der en skal inn hjernens hulrom når disse er små og trange, eller når hjerneanatomien er avvikende.
5. Stereoskopisk visning (som gir kirurgen dybdesyn) av MR og ultralydbilder av blodkar er nyttig ved operasjoner på karnøster (arteriovenøse malformasjoner) i hjernen. Likevel er ultralydbilder av blodkar ved denne teknikken ofte ikke gode nok og teknikken må forbedres.

Dette forskningsarbeidet har vist at navigasjon basert på tredimensjonal ultralyd i hjerneoperasjoner og operasjoner på ryggmarg er et nyttig verktøy som kan bidra til å øke sikkerheten og bedre resultatene ved slike inngrep.

Cand.med. Ola Morten Rygh
Institutt for nevrovitenskap
Veiledere: Geirmund Unsgård og Toril A. Nagelhus Hernes

To my dear wife, son and daughter

CONTENTS:

ACKNOWLEDGEMENTS

This thesis is a result of the teamwork of researchers at SINTEF Health Research and the Norwegian University of Science and Technology (NTNU). This author had the fortune to take part in their journey, for which I am grateful. I am indebted to Professor Geirmund Unsgaard and Professor Toril A. Nagelhus Hernes for their inspiration and guidance. MSc. Tormod Selbekk and Dr.Ing Frank Lindseth at Sintef Health Research have been of invaluable help as well as good friends and research colleagues. I am also grateful to the other researchers at Sintef Health Research for taking me in as a member of the family during my residency there. The Norwegian Research Council provided funding for this work. Finally, I am grateful for the patience and support of my family, especially my wife.

Trondheim, June 2008

Ola M. Rygh

LIST OF PAPERS

Paper 1:

Rygh OM, Selbekk T, Torp SH, Lydersen S, Hernes TAN and Unsgaard G. Comparison of navigated 3D ultrasound findings with histopathology in subsequent phases of glioblastoma resection. Acta Neurochir (Wien) 2008; 150(10):1033-41.

Paper 2:

Rygh OM, Selbekk T, Lindseth F, Müller TB, Hernes TAN and Unsgaard G. Intraoperative navigated 3D ultrasound angiography in tumor surgery. Surg Neurol 2006; 66; 581-592.

Paper 3:

Kolstad F, Rygh OM, Selbekk T, Unsgaard G and Nygaard ØP. 3D-Ultrasound navigation in spinal cord tumor surgery. J Neurosurg Spine 2006; 5:264-70

Paper 4:

Rygh OM, Cappelen J, Selbekk T, Lindseth F, Hernes TA and Unsgaard G. Endoscopy guided by an intraoperative 3D ultrasound-based neuronavigation system. Minim Invasive Neurosurg 2006; 49: 1-9

Paper 5:

Unsgaard G, Ommedal S, Rygh OM and Lindseth F. Operation of Arteriovenous Malformations Assisted by Stereoscopic Navigation-controlled Display of Preoperative Magnetic Resonance Angiography and Intraoperative Ultrasound Angiography. Neurosurgery 2005; 56: 281-90

SUMMARY IN ENGLISH

Background and objectives:

Intraoperative ultrasound has been used for decades in neurosurgery for localization and characterization of pathology, particularly tumors. Furthermore, with Doppler imaging localization of vascular structures is also possible. Neuronavigation was developed as a tool for planning neurosurgical procedures and localization of lesions during surgery. Displacement of brain tissue during the course of surgery, called brain shift, is however recognized as a major source of inaccuracy in neuronavigation, and because of this intraoperative imaging is important for maintaining application accuracy in neuronavigation. A neuronavigation system with integrated 3D ultrasound, enabling intraoperative ultrasound imaging for use in navigation has been developed. The aims of this dissertation were to assess the clinical value of neuronavigation based on intraoperative 3D ultrasound and explore different applications of the technology.

Methods:

Five studies were performed, resulting in five papers (1-5):

1. A study comparing 3D ultrasound image findings with histopathology in the tumor border zone in three subsequent phases of tumor resection.
2. A study assessing the use and value of 3D ultrasound angiography in patients with supratentorial tumors.
3. A study exploring the feasibility and technical aspects of navigated 3D ultrasound for image guidance in spinal cord surgery.
4. A study evaluating navigated 3D ultrasound for image guidance of neuroendoscopic procedures.
5. A study exploring stereoscopic display in image guided AVM surgery, using preoperative MRI angiography and intraoperative 3D ultrasound angiography.

Results:

- 3D Ultrasound was found to accurately delineate tumor borders prior to resection, but it tended to overestimate tumor during resection and underestimate tumor after having completed the resection. On the other hand, residual tumor was rarely missed during resection.

- The application of navigated 3D ultrasound angiography was found useful in tumor cases with important vessels close to the tumor.
- Navigated 3D ultrasound was found feasible for the use in spinal cord tumor surgery.
- In neuroendoscopic procedures, image guidance based on intraoperative 3D ultrasound was found useful, particularly for inserting the endoscope in cases with small and narrow ventricles and orientation in cases with anomalous anatomy.
- Stereoscopic display of AVMs using 3D ultrasound angiography image data in some cases was of sufficient quality for interpretation. Updated imaging with 3D ultrasound angiography allowed for more accurate localization of feeder vessels and in one case residual AVM was identified.

Conclusions:

In this thesis, neuronavigation based on intraoperative 3D ultrasound and 3D ultrasound angiography has been evaluated in different clinical settings. Some limitations of the current ultrasound technology have been identified for delineation of tumor borders in subsequent stages of resection. Neuronavigation based on intraoperative 3D ultrasound angiography may have a place in some brain tumor cases, and in AVM surgery although further development is needed to increase image quality, particularly in the latter case. In spinal cord tumor surgery, neuronavigation with 3D ultrasound is feasible. Image guidance by intraoperative 3D ultrasound may increase safety in some neuroendoscopic procedures with small and narrow ventricles and anomalous anatomy.

Overall, 3D ultrasound in neuronavigation seemed to be useful in a range of clinical settings. Some limitations and issues for further development and research have been identified. With knowledge of the limitations, and in selected cases, neuronavigation based on 3D ultrasound may serve to increase the safety of the procedure and improve patient outcome.

SUMMARY IN NORWEGIAN

Bakgrunn og målsetninger:

Intraoperativ ultralyd har i flere tiår vært brukt i nevrokirurgi for å lokalisere og karakterisere patologi, særlig svulster. Ved hjelp av fargedoppler kan en også lokalisere blodkar. Nevronavigasjon har blitt utviklet som et verktøy for hjelp til planlegging av operasjoner og intraoperativ lokalisering av patologi under operasjoner. Forskyvning av hjernevev under operasjonen, kjent som "brain shift" er en kjent kilde til unøyaktig navigasjon i løpet av en operasjon, og derfor er intraoperativ avbilding viktig for å opprettholde nøyaktigheten til navigasjonssystemet under en operasjon. Et nevronavigasjonssystem som bruker 3D ultralyd for intraoperativ avbilding er utviklet. Målsetningen med denne avhandlingen var å vurdere den kliniske nytten ved nevronavigsasjon basert på intraoperativ 3D ultralyd og prøve ut forskjellige bruksområder av denne teknologien innen nevrokirurgi.

Metode

Fem studier ble utført:

1. En studie som sammenlignet bildefunn på ultralyd med histopatologi fra biopsier tatt i grensesonen mellom svulst og normalvev gjennom tre påfølgende faser av reseksjonen av hjernesvulster.
2. En studie som evaluerte nytten av intraoperativ 3D ultralyd angiografi ved reseksjon av supratentorielle svulster.
3. En studie av et system for 3D ultralyd basert navigasjon ved operasjoner på svulster i ryggmargen.
4. En studie av en løsning for bildeveiledete endoskopiske inngrep med navigert 3D ultralyd.
5. En studie av stereoskpisk visualisering av MR-angiografi og intraoperativ 3D ultralyd angiografi for navigert reseksjon av arteriovenøse malformasjoner.

Resultater:

- 3D ultralyd viste med stor grad av nøyaktighet grensen mellom svulstvev og normalvev før påbegynt reseksjon av en svulst. Imidlertid var det en tendens til overestimering av svulst i fasen under reseksjon og etter reseksjonen ble forekomsten av svulstvev og infiltrasjon i veggen til reseksjonshulen

underestimert. Resttumor ble i svært liten grad oversett på ultralyd under reseksjonen.

- Nevronavigasjon basert på 3D ultralyd angiografi ble funnet å være nyttig ved reseksjon av svulster som lå nært viktige blodkar.
- Det har latt seg gjøre å gjennomføre operasjoner på ryggmargen med billedveiledning fra navigert intraoperativ 3D ultralyd.
- Innen nevroendoskopiske inngrep er bildeveiledning med navigert 3D ultralyd nyttig der hjernens ventrikler er små og trange, og i tilfeller med avvikende anatomi.
- Stereoskopisk visualisering av arteriovenøse malformasjoner med 3D ultralyd angiografi gav i noen tilfeller tilfredsstillende bilder, men i andre tilfeller var billedkvaliteten for dårlig. Oppdaterte bildedata med 3D ultralyd angiografi bidro til mer nøyaktig lokalisering av feeder-blodkar, og i et tilfelle ble rest-AVM påvist.

Konklusjoner:

I denne avhandlingen har den kliniske nytteverdien av nevronavigasjon basert på intraoperativ 3D ultralyd og 3D ultralyd angiografi blitt undersøkt innen flere bruksområder i nevrokirurgien.

Noen begrensninger er påvist ved avbildning av svulst-grenser under og etter reseksjonen av en svulst. Nevronavigasjon basert på 3D ultralyd angiografi kan ha en plass i ved reseksjon av svulster i noen tilfeller der viktige blodkar ligger nær svulsten, og innen AVM-kirurgi men i sistnevnte tilfelle bør bildekvaliteten forbedres. I operasjoner på svulster i ryggmargen er det tenkelig at bildeveiledning med navigert 3D ultralyd kan ha en plass. Bildeveiledning med navigert 3D ultralyd innen nevroendoskopiske inngrep er nyttig i utvalgte tilfeller.

Bildeveiledning med navigert 3D ultralyd og 3D ultralyd angiografi kan være nyttig innen flere områder i nevrokirurgien. Teknologien har noen begrensninger som er viktige å være klar over, og på noen områder kan den videreutvikles. Med kunnskap om begrensningene og i utvalgte tilfeller kan nevronavigasjon basert på intraoperativ 3D ultralyd og 3D ultralyd angiografi øke sikkerheten ved nevrokirurgiske inngrep og bedre resultatet for pasienten.

ABBREVIATIONS

3D - Three-dimensional

2D - Two-dimensional

AVM - Arterio Venous Malformation

CAS - Computer Assisted Surgery

CCD - Charge Coupled Detector

CSF - Cerebro Spinal Fluid

CT - Computer Tomography

CUSA® - Cavitron Ultrasonic Surgical Aspirator®

DSA - Digital Subtraction Angiography

FDA - Food and Drug Administration

GPS - Global Positioning System.

LED - Light Emitting Diode

MRI - Magnetic Resonance Imaging

RMS - Root Mean Square

ROC - Receiver Operating Characteristic

1. INTRODUCTION

The thesis is a result of the ongoing research activity on image-guided surgery and ultrasound guided surgery at the St.Olav University Hospital, Trondheim, Norway, in close collaboration with SINTEF Health Research and the Norwegian University of Science and Technology (NTNU).
In 1995, the Ministry of Health and Social Affairs established a centre of competence for the advanced use of 3D ultrasound in surgery in Trondheim, which was a collaboration of the above-mentioned institutions. In 1998, the company MISON (Current name SONOWAND) was established as a result of this research activity. The research activity on ultrasound guided surgery and image-guided surgery has been concentrated on neurosurgery, vascular surgery and laparoscopic surgery. The research has resulted in several advances in these three fields. In the neurosurgical field, the commercially available 3D ultrasound-based neuronavigation system SonoWand was one of these.

1.1. INTRAOPERATIVE ULTRASOUND IN NEUROSURGERY

1.1.1 HISTORICAL PERSPECTIVE

The idea of using ultrasound in medical diagnosis arose around 1940. In their paper published this year, Gohr and Wedekind had suggested the possibility of ultrasonic medical diagnosis by echo-reflecting methods similar to those used for metal flaw detection [38]. In 1942 Dussik[26] proposed a technique for imaging the ventricles of the brain with ultrasound, using a through-transmission technique. During the early fifties the transmission technique was largely abandoned due to the superiority of the reflection technique. Several neurosurgeons were among the pioneers using ultrasound for medical diagnosis during the 50s. Among them was the neurosurgeon Lars Leksell from the University of Lund [84,85]. A-mode ultrasound (which was called echoencephalography in this context) was found to be a useful method for localizing intracerebral mass lesions and detecting midline shift [27,33,36,79,160,175]. The A-mode technique did not produce anatomical images, but detected highly reflective surfaces along the path of the ultrasound beam. In the 1960s, two-dimensional B-mode ultrasound became available, and the technology was further refined in the following years. With the advent of real-time B-mode sector scanning, the stage was set for

successful intraoperative imaging of the brain with ultrasound. The first preliminary reports on the use of B-mode ultrasound were published in 1980-81 [95,141,171]. In the early 80s several reports on the intraoperative use of B-mode ultrasound were published [17,40,71,80,95,133,137,139,141]. The technique was found to be helpful for localizing small subcortical neoplasms, as well as delineating solid and cystic portions of deep lesions. Additionally, ultrasound was found helpful for finding the shortest route of access to the tumor, reducing unnecessary dissection. First, abdominal probes were used, but soon more suitable probes for intraoperative ultrasound in neurosurgery became available. Further technical modifications allowed for smaller probes, enabling imaging trough small craniotomies and laminectomies, and even burr holes[96]. A variety of guidance systems for stereotactic real-time ultrasound-guided biopsies were also developed [8,28,69], allowing quick and precise placement of needles and catheters. Ultrasound guidance for inserting endoscopes has also been found useful [4,170].

To overcome the limitations of 2D, Koivukangas and co-workers explored 3D ultrasound techniques already in the 1980s, focusing first on ultrasound holographic imaging[74]. Concurrently, the arrival of navigation technology opened the prospect of integrating ultrasound in neuronavigation. Koivukangas and his group developed a neuronavigator arm where an ultrasound probe and various surgical instruments could be attached. The axis of the ultrasound probe or surgical instrument was displayed on images reconstructed from preoperative CT or MRI data [73]. This enabled simultaneous display of corresponding 2D ultrasound and reconstructed CT/MRI images.

A new method for integrating ultrasound with neuronavigation was presented in 1994 by Trobaugh and colleagues. Infrared light-emitting diodes were attached to the ultrasound probe, and this enabled tracking without the use of a mechanical arm. The technique was used for comparison of 2D ultrasound images with preoperative CT and MR to detect brain shift during surgery and for better interpretation of the ultrasound images. It was also possible to acquire 3D ultrasound data with the equipment, and it was suggested that 3D ultrasound could be used in frameless stereotactic neurosurgery [163,164]. Soon thereafter, other research groups also presented solutions where an ultrasound scanner was coupled with a conventional navigation system, displaying the real-time 2D ultrasound image together with the corresponding MRI slice [15,52,56]. In 1998, Jödicke reported the use of intraoperative 3D ultrasound

image data for identifying brain shift by comparing the ultrasound data with preoperative MRI [60]. For tracking of the ultrasound probe, magnetic localization was used. In 2000, Grønningsæter et al. presented a single-rack system with a neuronavigation system integrated with an ultrasound scanner that enabled neuronavigation using intraoperative 3D ultrasound in addition to preoperative MRI or CT [41]. It was developed in collaboration with clinical researchers at SINTEF Health Research and the Neurosurgical department in Trondheim. The system was launched commercially with the name SonoWand. In initial clinical evaluation studies, the system was found to be useful for maintaining accuracy of navigation in cases with brain shift, detecting residual tumor, improved anatomical orientation compared to conventional 2D ultrasound, and practical as less space-occupying than two-rack solutions [11,166].

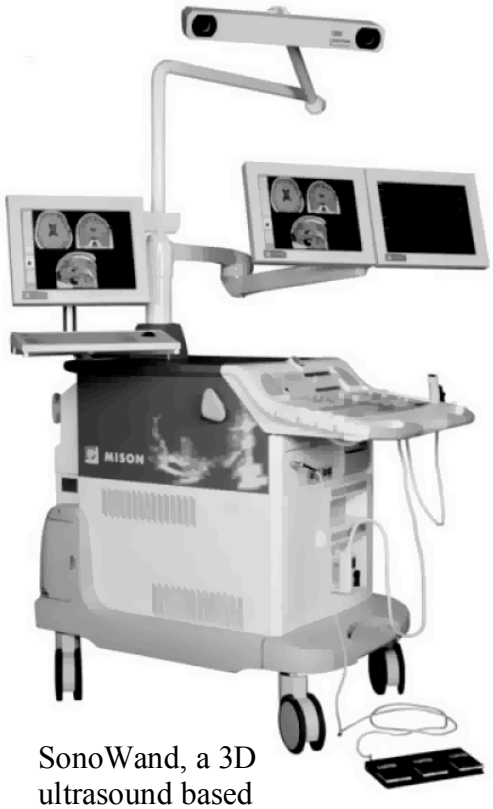

SonoWand, a 3D ultrasound based neuronavigation system

1.1.2 INTRAOPERATIVE ULTRASOUND DOPPLER IMAGING

In the late 1980s, also Doppler imaging techniques were evaluated for intraoperative use. In 1988, Black et al. [9] reported the use of intraoperative color-flow Doppler imaging of AVM's and aneurysms. They found the technique to be a useful adjunct in localizing vascular lesions, identifying feeding or draining vessels, and confirming intraoperative surgical excision of AVM's or ligation of giant aneurysms. Other authors followed, reporting the use of intraoperative Doppler imaging for the visualization of vessels in neurosurgical procedures [9,42,140,178,181].

1.1.3 VERSATILITY OF INTRAOPERATIVE ULTRASOUND

The main use of intraoperative ultrasound in neurosurgery has been in tumor surgery, for localization and detection of residual tumor.

Several other applications for intraoperative ultrasound has been reported: Shunt catheter placement, drainage of abscesses and hematomas, introduction of endoscopes, and ultrasound-guided biopsies [19,157,170]. Cavernous hemangiomas are readily depicted on ultrasound and have been reported to be resected more completely with a less traumatic approach with the aid of ultrasound guidance [78,180]. In pituitary surgery, intraoperative ultrasound has been applied and been found helpful [119].

Several research groups have explored the use of intraoperative ultrasound in spinal surgery [20,21,29,70,72,105,116,118,123,138,174]. Ultrasound was found useful in a variety if intraspinal lesions, such as intraspinal tumors, extramedullary masses, syringohydromyelia, and visualizing the degree of surgical decompression.

Noteworthy is also the endo-neuro-sonography technique developed by Resch and coworkers [126,127], where a small sono catheter (originally developed for intravascular use) is inserted into the working canal of an endoscope, giving a 360-degree axial (to the endoscope) real-time view of the anatomy, like a “mini-CT”. This is an example of how miniaturized probes may be used in special applications, which may be a part of the future in intraoperative ultrasound.

1.2 ULTRASOUND THEORY

1.2.1 BASIC PRINCIPLES OF ULTRASOUND

Ultrasound is sound waves (compression waves) that have frequencies above the audible range, which means any sound wave with a frequency more than 15-20 kHz. Ultrasound in medicine usually is in the range 2-10 MHz, but higher frequencies may be used for special purposes. The correlation between the wavelength (λ) and the frequency (f) is $\boldsymbol{\lambda = c / f}$, where c is the speed of the wave. In water, the speed of sound at 25°C is 1497 m/s. The speed of sound waves varies between soft tissues due to differences in mass density and volume compressibility. Still, in body tissues other than fat and bone, the speed of sound only varies 0.2-0.3%[3]. Ultrasound waves are reflected from boundaries between tissues and structure within the tissues (called

scatterers). The position of structures detected along the direction of the ultrasound beam is calculated from the speed of sound **c** and the time from emission of the ultrasonic pulse until the return of the echo. By mechanically or electronically steering the direction of emitted ultrasound pulses in a sector, reflected ultrasonic echoes in different directions and depths may be mapped. In a typical B-mode ultrasound image, the vertical position of each pixel is thus decided by the time from emitting the ultrasound pulse to the return of the ultrasound echo. The horizontal position is decided by the direction of the emitted ultrasound pulse. The amplitude of the returned ultrasound echo decides the brightness of each pixel. In a homogenous tissue, ultrasound reflected from structure within the tissue produces an interference pattern, called *speckle*, which appears as tissue structure.

Modern ultrasound transducers used in neurosurgery send out repetitive ultrasound wave pulses instead of a continuous wave. An ultrasound beam is generated by an array of ultrasound emitters in the probe. For optimal resolution the ultrasound beam is focused in a certain distance from the probe head. There are different ways to focus a beam. In a phased array probe, focusing is accomplished by a small time-delay (phasing) between the elements (eg ultrasound emitters) of the probe. This generates an interference pattern making the ultrasound beam converge at a focus point, similar to a magnifying glass converging light beams. Steering the beam is also accomplished with phasing, by creating an interference pattern resulting in a beam at a certain angle. Usually 100-200 ultrasound beams are sent out in different directions in a fan-like form to make a B-mode image. Typical ultrasound transducers can make an image in just a few milliseconds; therefore, real-time imaging is possible with ultrasound.

The *resolution* in an ultrasound image is proportional to the wavelength, i.e. inversely proportional to the frequency. This means that higher frequencies give better resolution. Unfortunately the *attenuation* of the ultrasound also increases with increasing frequency, so the choice of frequency for imaging has to be a compromise between penetration in the tissue and resolution. For imaging in neurosurgery, frequencies in the range 3-30 MHz have been evaluated [43]. A frequently used probe which gives a reasonable trade-off between penetration and resolution is for example a 4-8 MHz probe (commonly just called 5 MHz probe), which typically has a radial

(e.g. along the beam) resolution of 0.5 mm and a lateral resolution of 1.0 mm. Probes with higher frequencies (for example 10 MHz) may be used for better resolution.
A thorough description of ultrasound theory is beyond the scope of this text and can be found elsewhere [3].

1.2.2 ULTRASOUND ANGIOGRAPHY – COLOR FLOW AND POWER DOPPLER

When the object that reflects the ultrasound is moving, the frequency of the reflected ultrasonic echo will be altered from the frequency of the emitted ultrasound. This change in frequency is commonly called the Doppler effect. The Doppler Shift, f_d, is given by the Doppler equation: $f_d = 2\frac{v \cdot \cos\theta}{c} \cdot f_0$, where f_0 is the frequency of emitted ultrasound, c is the ultrasound wave velocity, v is the velocity of the object which reflects the ultrasound, and θ is the angle between the velocity direction and the ultrasound beam[3]. It follows from this that if the motion of the object is perpendicular to the ultrasound beam, no Doppler shift will be detected (cos 90 = 0). The actual Doppler shift detected represent the velocity component parallel to the ultrasound beam. Doppler imaging in ultrasound is usually used to display blood flow in vessels. In colorflow imaging, flow direction and velocity is displayed by estimating the mean Doppler frequency shift at a particular position in color. Velocities toward the transducer are displayed in tones of red and velocities away from the transducer are displayed in tones of blue. One of the drawbacks with colorflow imaging is aliasing, which may make the vessel look discontinuous. In "power Doppler" imaging, the amplitude (e.g. the and not the frequency shift) in the Doppler signal is encoded in color. Thus the directional information is discarded, but power Doppler has several advantages: It does not alias, there is less noise in the image and the technique is less angle dependent [135]. The biggest limitation is that it is extremely motion sensitive, and minimal soft tissue motion can seriously degrade the image. In spectral Doppler, the estimated velocities in a sample volume are displayed as a curve along an axis.

1.2.3 FROM 2D TO 3D ULTRASOUND

To produce a 3D volume from 2D images, one must know the relative position and angulation of each 2D image. The main types of 3D ultrasound data acquisition are: 1) Tracked freehand systems, 2) untracked freehand systems, 3) mechanical assemblies and 4) 2D arrays.

With a tracked freehand system, the ultrasound probe is equipped with a tracking device, and is tilted or translated over the area of interest. Two-dimensional images are digitized as the transducer is moved. A 3D volume is obtained by an algorithm using the image data from the digitized 2D ultrasound images[152]. Tracking techniques commonly used include articulated arm-tracking, magnetic field tracking and optical tracking. For intraoperative use, optical tracking is usually preferred, as magnetic field tracking may be vulnerable to metal objects in the vicinity, which may affect the accuracy of tracking. Optical tracking is on the other hand dependent on direct line of sight, e.g. no obstructing objects must come in the way between the object tracked and the cameras of the tracking system.

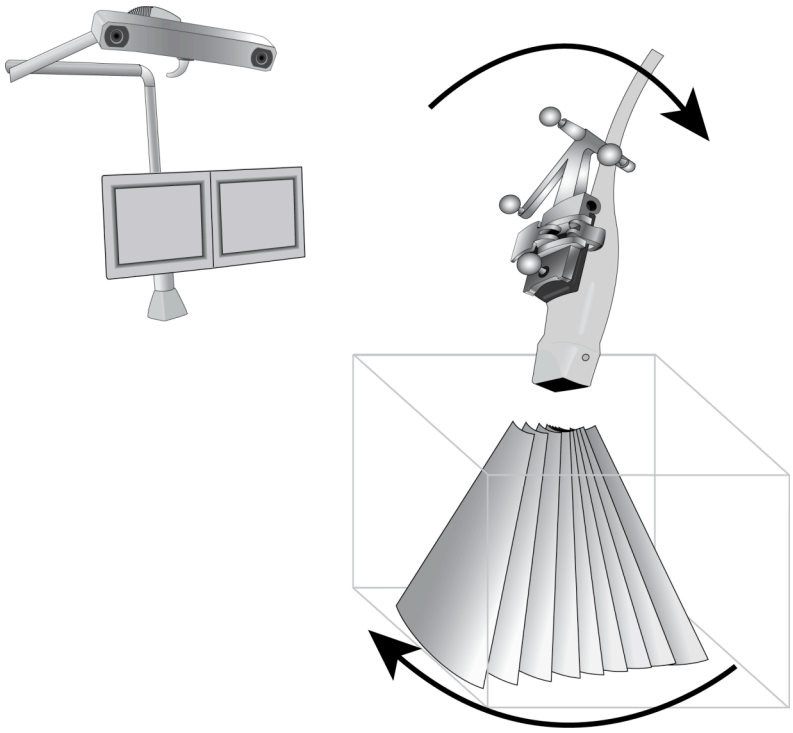

Figure 1: 3D ultrasound acquisition with freehand movement and optical tracking. The ultrasound probe is equipped with a tracking frame with reflecting spheres. The cameras of the tracking system thus traces the position and angulation of the ultrasound probe. A series of 2D images are collected and reconstructed into a 3D volume.

With mechanical assemblies, the transducer is moved mechanically. Using two-dimensional arrays, electronic scanning with a 2D transducer array may be used to obtain 3D images. Such 3D ultrasound probes generates pyramidal or conical US pulses and processes the echoes to generate 3D information in real time.

1.2.4 ULTRASOUND IMAGING OF BRAIN TUMORS

On real-time B-mode ultrasound, the echogenic tissue appears bright, while the least echogenic structure appear dark. For orientation during neurosurgical procedures (when used without navigation), anatomical landmarks such as the ventricles, choroid plexus, tentorium cerebelli and falx cerebri are used. All brain tumors appear hyperechoic (e.g. brighter) in comparison with brain tissue. Edema, which may have variable echogenicity, is with few exceptions distinguishable from tumor tissue [30,87,151]. The delineation of cystic and solid parts of a tumor as well as the differentiation between cyst and necrosis has been found to be more distinct than on CT images [170]. In tumor cases with previous treatment (eg. previous surgery or radiation therapy), ultrasound tends to overestimate tumor, probably because areas of gliosis appear hyperechoic and difficult to distinguish from tumor [49,82,86]. Used intraoperatively, residual tumor can be evaluated with ultrasound. Ultrasound imaging can be applied repetitively at different stages of the operation to determine the location and quantity of residual tumor [49,136]. Still, some authors have found ultrasound for residual tumor assessment at the end of resection unreliable [170].

In meningioma surgery, ultrasound has also been reported to be helpful for assessing whether the dural sinus is invaded or just compressed by the tumor [170].

1.3 NEURONAVIGATION

1.3.1 HISTORICAL PERSPECTIVE OF NEURONAVIGATION

The positioning of the craniotomy and the direction of dissection has traditionally been determined by anatomical knowledge, x-ray image findings and clinical findings. Surgical exposures were often much larger than otherwise necessary in order to access the lesion. The anatomic localization method has been the norm also after the introduction of CT and MRI. Without other means to match image space with physical space, the use of CT images and MRI was through their reconstruction within the mind of the neurosurgeon. Stereotactic devices were developed for more accurate targeting of lesions than the anatomic localization method offered. In 1933, Kirschner [68] used a stereotactic device to treat trigeminal neuralgia with electrocoagulation of the ganglion gasseri by targeting the foramen ovale at the skull base. In 1947, Spiegel and Wycis [154] did the first stereotactic thalamotomy using the corpus pineale as a reference point. With the development of CT in the early seventies [2,59], the usage of stereotactic technique broadened, and stereotaxy was used for biopsies, neuroendoscopy and localization of tumors. At present, stereotaxy still has its place in neurosurgery due to its high accuracy. It is now mostly used for implantation of deep brain stimulation electrodes. An important limitation of conventional stereotactic technique is its single path, lacking interactivity during surgery (in contrast to neuronavigation systems). The stereotactic head-frame may also be painful for the patient.

By the mid 1980s, the necessary prerequisites existed for computer assisted navigation in surgery: Computers and software with sufficient power to process image data in real time and positioning hardware with sufficient accuracy.

In 1986, Roberts [131] presented a microscope fitted for navigated neurosurgery. Reformatted CT image data according to the position of the microscope was projected into the optics of the microscope. This allowed the surgeon to see the relevant CT image data superimposed on the surgical site. In1987, the Japanese neurosurgeon Watanabe presented a “neuronavigator” arm, introducing the idea of frameless stereotaxy [75,172,173]. It consisted of a jointed positioning arm, where the angle of the

joints were measured with high accuracy and transferred to a computer. The positioning arm was attached to the head holding frame. Preoperative CT image data was used for navigation, with lead spheres as fiducial markers. In order to match physical to image space (e.g. registration), the pointer tip of the arm was directed at the lead spheres attached to the patients head, then the position of the lead spheres on the CT images were marked on the navigation computer. After the registration the position of the pointer tip of the arm was displayed and constantly updated on the corresponding CT images, enabling navigation. The neuronavigator was found useful for planning of the operation. The system was developed further for navigation with additional imaging modalities, such as MR images and the lateral view of an angiography. Thus, the system was developed into a multimodal navigation system. Furthermore, attaching ultrasound probes to the end of the arm was also tested. The neuronavigator arm was also combined with somatosensory evoked potentials for identification of the central sulcus in cases with distorted anatomy. Interestingly, Watanabe introduced the concept of a "virtual tip", a virtual elongation of the pointer, showing a spot at a known distance beyond the actual pointer tip, useful for planning of the approach. A similar feature has also been found most useful by our group. Soon after Watanabes publication of the neuronavigator arm, Schlöndorff and Mösges developed another arm-based navigation system (which was called CAS; Computer Assisted Surgery) [145]. Image data from CT, MR and DSA was used for navigation. They also used a mechanical arm with six degrees of freedom like Watanabe. To avoid the need for registration anew each time the head was repositioned, a fixed relation between the head holder and the navigating arm was later established [153]. A rigid endoscope could also be attached to the navigating arm, enabling image guidance of endoscopy. Other tools could also be used with the system, but this required exact information on the size and shape of each instrument. The ISG Viewing Wand System [25,83] was also a mechanical arm with six joints, and has been studied by several authors. Preoperative CT and MR images were imported and displayed in three orthogonal planes. In addition to a pointer, a neuroendoscope could be attached. The Viewing Wand was reported to enhance minimally invasive techniques and aiding in location of important structures in cases with distorted anatomy [143]. It was also reported useful in epilepsy surgery [113] and skull base tumor surgery [100,132], as well as pediatric neurosurgery of different sorts [24,117]. One of the

drawbacks were reported to be the added time for registration, but intraoperative location was performed faster [112]. Furthermore, the size and weight of the navigation arm was a practical shortcoming. Last but not least, the accuracy was reduced during surgery because of progressive displacement of the brain because of CSF drainage and pull of gravity (this phenomenon was later given the name of "brain shift"). Overall, the Viewing Wand was found accurate and reliable in clinical evaluations, achieving a useful registration in 310 of 325 cases as reported by Golfinos [39].

In Oulu, Finland, Koivukangas and colleagues, having a background in neurosurgical intraoperative ultrasound, designed a navigation system based on a six-jointed arm with six degrees of freedom. A common central axis of the navigator arm allowed for attachment of an ultrasound probe, and thus corresponding 2D ultrasound and reconstructed CT or MR image data could be viewed [73,144]. Several instruments could be used with the Oulu neuronavigator system in addition to the pointer and an ultrasound probe, among them a biopsy forceps or needle, a neuroendoscope, and furthermore a surgical microscope could be aligned with the central axis. The image data could be displayed as standard orthogonal slices or as oblique planes. The system remarkably also included voice control. Other arm-based neuronavigation systems have also been reported [34,35,158].

Arm-based neuronavigation systems, although accurate, had the disadvantage of being rather bulky and impractical. Because of this, armless navigation systems were developed, with the positioning based on other principles than the joints of a mechanical arm. For positioning, ultrasound (sonic digitizers), magnetic sources and light-emitting diodes were employed.

Roberts et al [131] were the first to employ ultrasonic sparks gaps and microphones to track the surgical microscope and displaying CT image data in the microscope. The system was reported to be useful for guiding tumor resection, but the distance between the sonic emitters and microphones had to be unobstructed and less than 2,5 meters and the overall accuracy was reported to be 3,5-6,5 mm [130]. Another system based on sonic digitizers was reported by Zweifel and coworkers in 1990 [183]. The ultrasonic transmitter was attached to the pointer. The microphones were positioned close to the patient's head, and the working space was limited. Therefore, this group later traded the sonic digitizers for a LED based positioning system [144].

In 1991, Kato and coworkers published a study where they used a frameless, armless navigational system with magnetic localization technology. They found the system valuable, but reported that accuracy was vulnerable to metal objects and electromagnetic noise surrounding the magnetic field source and sensor [65]. Tan et al. also reported on a neuronavigation system with a magnetic localization unit, also commenting that large metal objects such as metal cabinets or tables had to be kept several meters away to avoid affected navigation accuracy. They therefore stated that although an magnetic localizing device is well suited for presurgical planning, other frameless stereotactic methods should be considered for intraoperative use [159].

In 1991, Krybus and coworkers reported the use of optical tracking in neuronavigation [77]. In 1994, Zamorano et al reported on an infrared-based tracking system [182]. A cylindrical probe with 24 LEDs placed along an around it was designed for attachment of different surgical instruments, such as a biopsy needle or an endoscope. An ultrasound probe could also be attached. Also in 1994, Smith et al. published a paper [150] about the Neurostation™. It was based on infrared tracking with a bipolar forceps equipped with LEDs serving as the pointer. A reference frame with five LEDs was attached to the head holder and served as reference coordinates in physical space. Ryan and coworkers designed a smaller *dynamic reference frame* with LEDs which was attached to the patients skull by a screw, allowing continuous tracking of the patient[142]. The digitized coordinates of the pointer (which also was equipped with LEDs) were transformed into the coordinate system of the reference frame, thus making them independent of patient motion. In earlier systems without a reference frame arrangement, repositioning of the patients head (whether intentional or unintentional) required repeated registration of the patient, which could be cumbersome as fiducials may have been covered by drapes etc.

In later generations of optical tracking neuronavigation systems like the VectorVision [48] and SonoWand [46], reflective spheres served as points for tracing by the cameras, and the light sources were placed around the cameras on the camera array. This arrangement did not require power cables connected to the pointer and other tracked instruments, and in addition simplified sterilization procedures.

The displacement of intracranial structures during a craniotomy, called *brain shift*, was discovered as an important source of inaccuracy during evaluation studies of neuronavigation systems. In 1994, Nauta [108] reported a case where simultaneously

using the Viewing Wand and a stereotactic frame in a small tumor resection. The accuracy was good at the beginning of the procedure, but dropped to 5mm during the resection, both for the stereotactic frame and the neuronavigation system. It was proposed that the loss in accuracy was due to tissue position changes occurring during the procedure. In 1996, Sipos and coworkers published an application accuracy evaluation study of the Viewing Wand. They commented on shift of the intracranial contents being a source of application inaccuracy in navigation based on preoperative images, and suggested that intraoperative ultrasound may be a useful adjunct[149]. Several studies have followed, evaluating the extent, direction and occurrence of brain shift [7,22,50,51,55,88,107,109,111,125,129,162]. Brain shift increases during the course of the procedure [55]. The brain shift is also non-uniform, being largest at the cortical surface close to the resection area, and smaller in deeper structures of the brain [22]. To amend for inaccuracy in navigation due to brain shift, intraoperative imaging may be performed and the intraoperative images can replace or be matched with the previous (or preoperative) dataset. Solutions for intraoperative MRI and ultrasound to acquire intraoperative image data for neuronavigation have therefore been developed. In 1997, the Heidelberg group [165] were the first to report on intraoperative MRI for update of image data for neuronavigation. Today, most intraoperative MRI suites also have integrated neuronavigation systems [1].

At present, it seems that assistance of neuronavigation has been evaluated in most neurosurgical procedures. The main argument is that anything that helps the surgeon, also in the end is beneficial for the patient. Critics have argued that a neuronavigation system in some cases only is a plaything and in reality does not add extra value for the patient [67]. Whatever the true value of neuronavigation systems is, most neurosurgical centers seem to have one and they are probably used whenever the surgeon finds it helpful.

1.3.2 BASIC PRINCIPLES OF NEURONAVIGATION

To keep track of distance and direction within the skull is one of the main efforts during neurosurgical operations. Basically, in neuronavigation, technology is used to assist in orientation by displaying the position of a pointer on medical images. The technique has many similarities to the now widespread GPS devices, which show ones position on a map. Neuronavigation has also been called image guided surgery,

computer-assisted surgery, and frameless stereotaxy. This chapter gives a brief summary of neuronavigation technology.

In essence, a neuronavigation system consists of a computer connected to a positioning system. The computer is doing image data processing and computes positioning data. The positioning unit tracks the pointer position in space. Preoperative CT/MRI data is transferred to the computer by network or removable media.

A number of different navigation systems have been designed. They may be split up into categories based on whether they are: 1) Navigational microscopes or pointer-based systems, 2) Active robots or passive devices, and 3) Arm-based or armless pointers [44]. Armless systems may further be distinguished by whether the tracking is based on ultrasound, infrared light (IR), visible light or magnetism. Each of these has its benefits and disadvantages. It seems that the armless neuronavigation systems with optic tracking have won the competition and that these systems now dominate the market.

1.3.3 POSITIONING SYSTEMS

Ideally, a positioning or tracking system should be convenient, accurate, fast working and able to track several objects at the same time. Furthermore, it should be robust, not being influenced by the environment or objects nearby. It should not require direct line of sight. Lastly, it should be inexpensive[115].

1.3.3.1 ARM-BASED SYSTEMS

Arm-based positioning systems are made up of arms with joints. The joints have sensors that measure the joint angle, and the position of the pointer is calculated by the information from the joint sensors. The joints usually have six degrees of freedom, three of translation and three of rotation.

Arm-based systems have high technical accuracy and are not influenced by surrounding objects, air temperature and other external factors. They do not require unobstructed line-of sight. On the negative side, they require more space in the operating field than armless systems, and only one object can be tracked at a time.

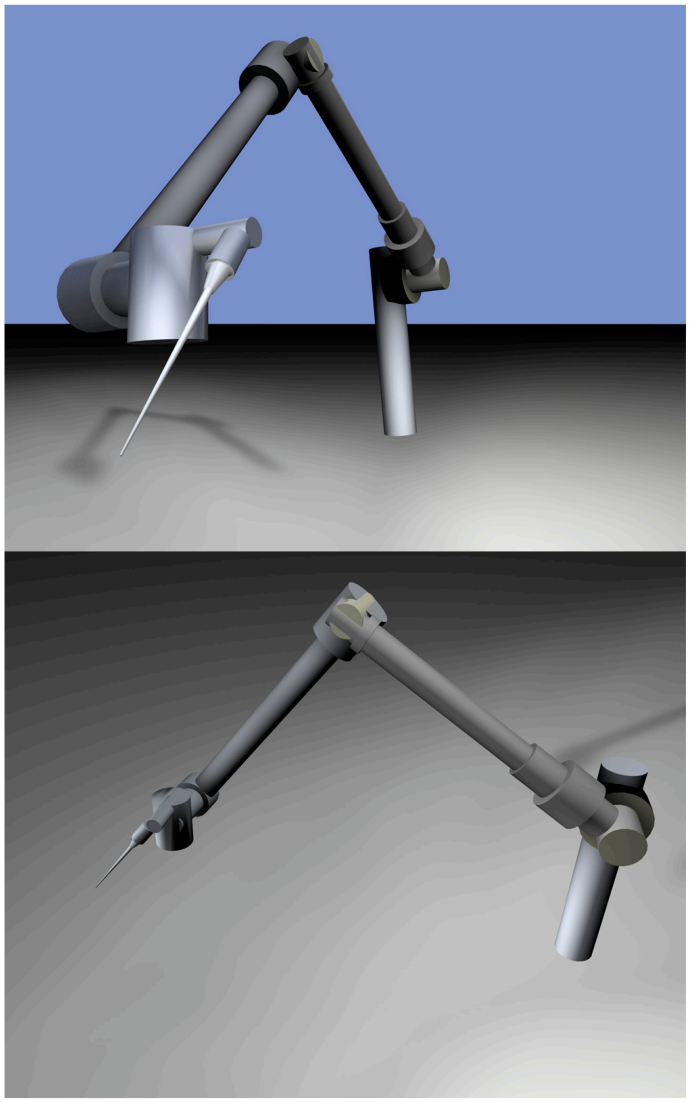

Figure 2: Example of a neuonavigator arm.

1.3.3.2 ARMLESS SYSTEMS:

Armless systems may be based on light, sound waves or magnetic fields. Two or more sensors determine the position of the pointer in space. The sensors may be infrared cameras, magnetic sensors or microphones depending on the physical principle used.

1.3.3.2.1 SONIC POSITIONING

Sonic positioning systems determine position by measuring time from the emission of sound (often called spark gaps in the literature) from an emitter to the detection by

three or more microphones. The position of the emitter is calculated by comparing the difference in time for the emitted sound pulse to reach each microphone. A disadvantage is that the speed of sound is dependent on air temperature and humidity, and this may affect positioning accuracy. In addition, echoes from walls may cause problems. Although using sound, these systems do require an unobstructed line-of sight between emitter and receivers.

1.3.3.2.2 MAGNETIC LOCALIZATION

These localization devices apply a magnetic field. The transmitter generates a magnetic field, and the receiver is localized and oriented by detection of gradients in the magnetic field. Usually the receiver is inside the pointer probe. They do not require an unobstructed line of sight (or sound) like the optical and sonic positioning systems, but accuracy may be affected by distortion of the magnetic field by metal objects

1.3.3.2.3 OPTICAL TRACKING

These systems use optical imaging for localization. They consist of light sources and optical sensors. The light sources may be active light emitters, usually light emitting diodes (LEDs) that emit infrared light, or passive reflectors of infrared light. Markers that have high contrast in the visible spectrum may also be applied. Optical sensors usually are a rack of charge-coupled devices that use a 2D array of pixel sensors (CCD cameras). To determine the position of an object, at least three emitters/reflectors are required. A triangulation technique is used to determine the position of the emitters. Positioning accuracy is in the submillimer range, and multiple objects can be tracked in real time. The environment does not influence the accuracy. The main drawback of optical tracking systems is that they require an unobstructed line of sight, which may be occluded by objects or personnel during the procedure. Furthermore, only rigid instruments may be tracked.

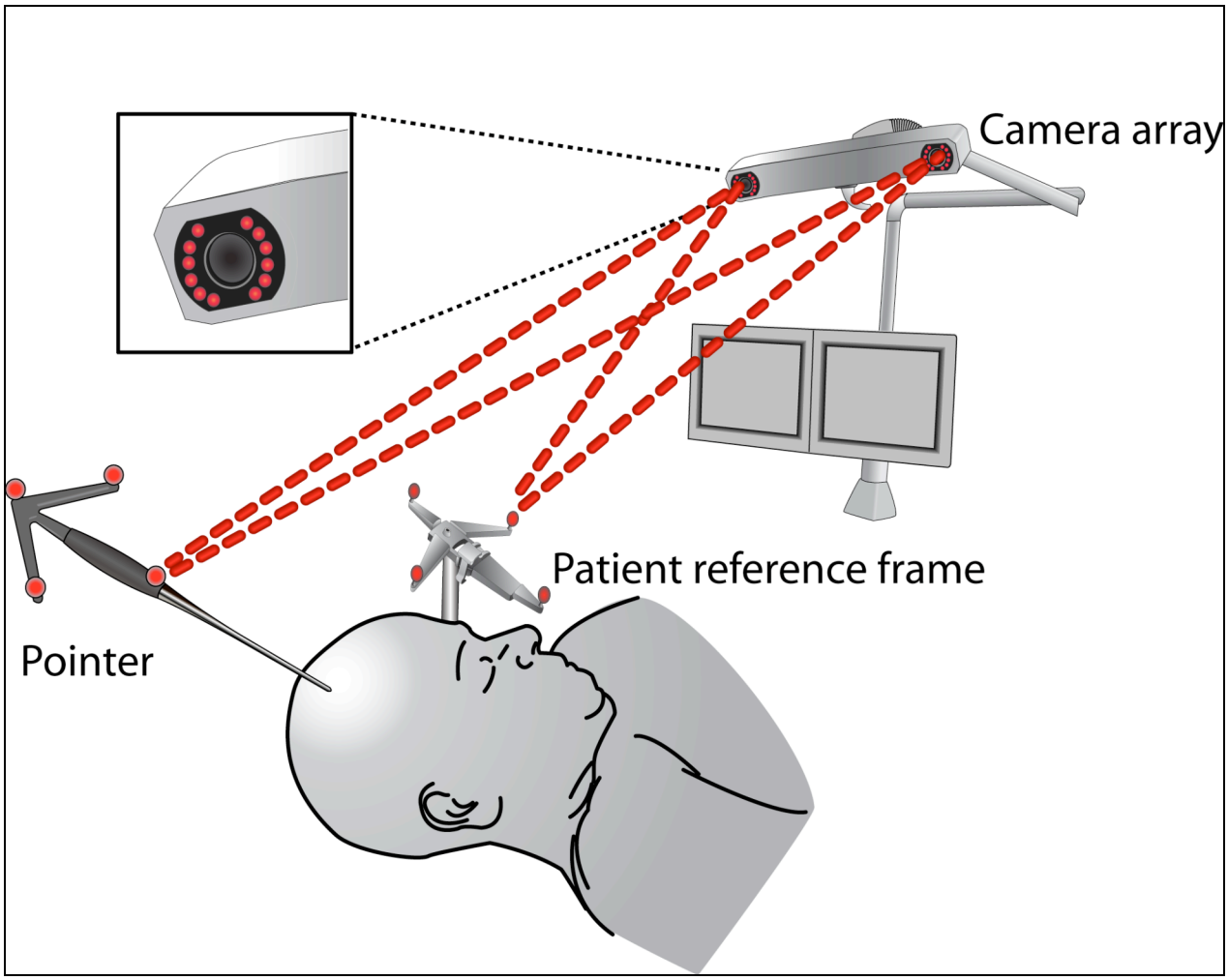

Figure 3: Neuronavigation with optical tracking. Infrared light sources are arranged around the CCD cameras, reflecting spheres attached to pointer and reference frame.

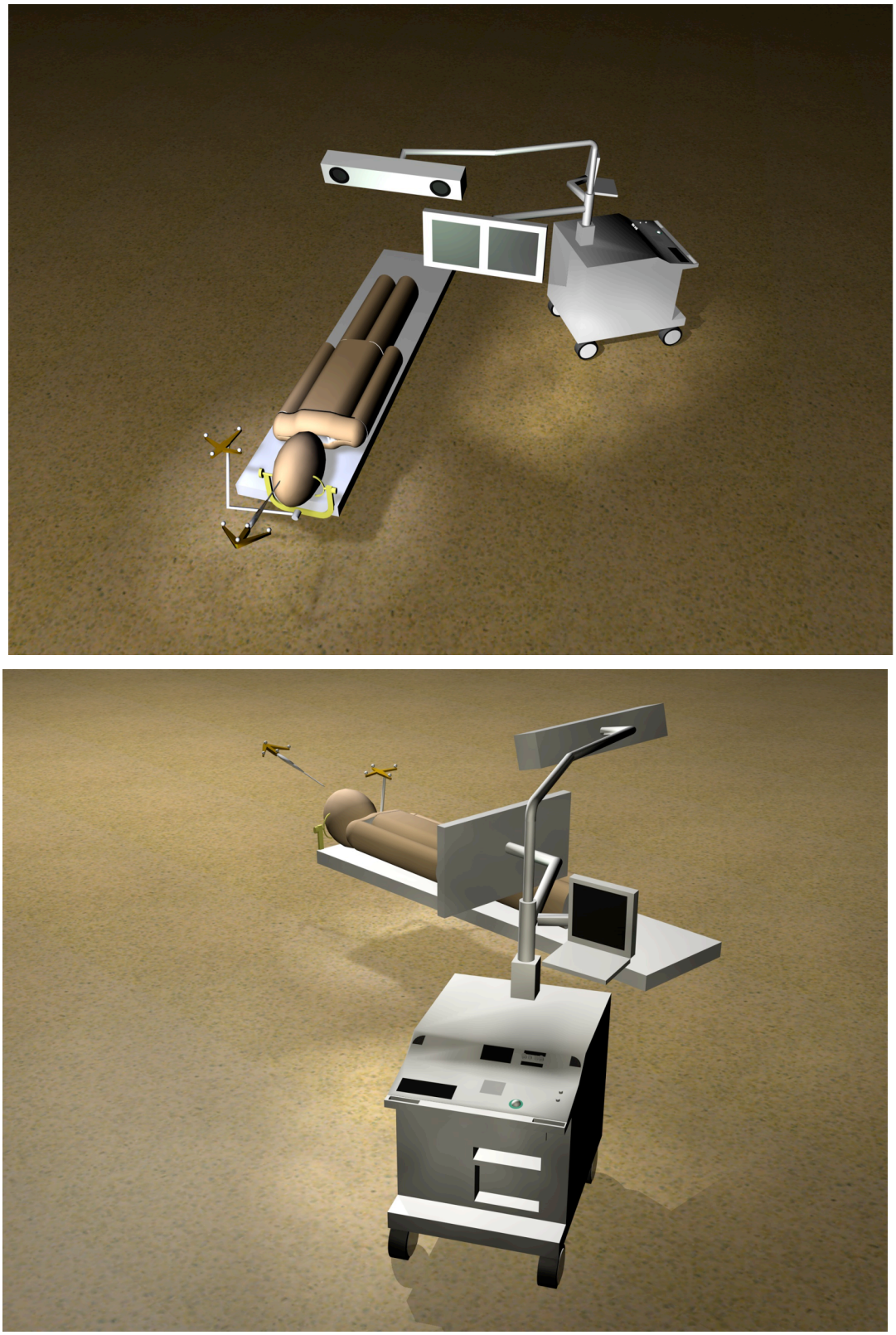

Figure 4: Armless, pointerbased navigation system, based on infrared light for tracking.

1.3.4 INSTRUMENT CALIBRATION

Basically any instrument can be tracked in neuronavigation, given it is equipped with emitters detected by the systems cameras or sensors. In the context of armless navigation systems based on infrared light with passive emitters such as reflecting spheres, a frame with reflecting spheres is attached to the instrument which is to be used in navigation. Then, the instrument has to be calibrated so that the navigation system will display the tip and trajectory of the instrument correctly. As an alternative, the manufacturer also can calibrate the instrument in advance. When properly calibrated, the instrument thus can be used in neuronavigation. Examples of instruments used in navigation are a biopsy forceps or needle, bipolar forceps, neuroendoscope, and a CUSA[168]. In case an ultrasound probe is to be used in neuronavigation, the *ultrasound probe* has to be calibrated in order to be used in navigation[81,102]. This may be performed each time the ultrasound probe is to be used, or in advance by the maker of the navigation system.

1.3.5 REGISTRATION

In order to use preoperative image data for navigation, a relationship between a real world coordinate system (the patient space) and the image space has to be established. This procedure is called registration or patient registration. First, corresponding points or surfaces are identified in the image dataset and on the patient. Next, a transformation matrix is established which correlates the coordinates of any point in the image space and the patient space. Fiducial-based paired-point transformation and surface contour matching are the two techniques frequently used for this purpose[44,115]. With **paired-point matching**, the coordinates of a matching set of points must be established in the image space and the patient. Usually markers glued to the skin are applied for this purpose, called **fiducial markers** of just fiducials. The main point is that these fiducial markers also are visible on the preoperative images. As the skin markers may move due to for example traction of the skin and thereby add registration error, markers attached to the skull with screws have been suggested to increase accuracy[13,99]. Anatomical structures may also be used instead of fiducials, for example the nasion and the exit of the auditory canal, however this approach usually gives a less accurate registration. If the patient changes position after registration, recalibration of the system is necessary. This is usually done automatically using a

patient reference frame fixed to the head holder. Without a patient reference frame, manual patient registration has to be performed over again, if not, the navigation map no longer corresponds to physical space.

An important exception from the rule that patient registration has to be performed in advance of navigation is navigation based on intraoperative imaging such as 3D ultrasound. When this is the case, the intraoperative images are acquired in the patient/physical space, and no further registration is necessary[168]. If navigation with preoperative images in addition to the intraoperative images also is desired, the registration procedure still has to be executed.

The accuracy of registration with the paired points method will be better when the number of corresponding points is increased. In addition, the registration points must not be clustered in a small area, as a small registration error may be magnified outside the area of registration points.

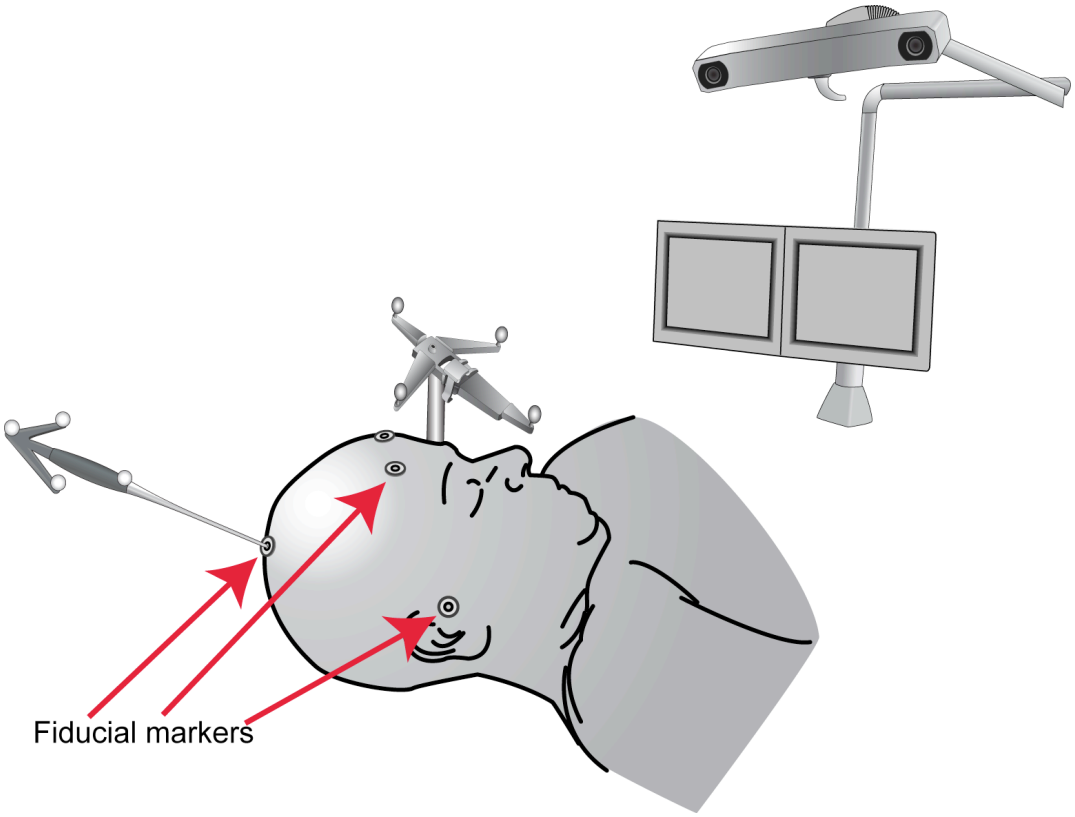

Figure 5: Registration with fiducial markers

Surface based transformations are methods for matching two rigid objects by minimizing the distance and rotation or a specific attribute between them[114]. In a neuronavigation context, the surface of the patient has to be matched with a 3D surface reconstruction from his/her images. This is may be done by using the pointer

to sample points on the surface of the patient, and then the best match of the sampled points with the 3D surface reconstruction is determined.

Strongly related to surface matching for registration is *image-to-image registration* of different imaging modalities to the basic preoperative CT/MRI data. Functional MRI and tractograms, intraoperative CT, MRI or ultrasound are all feasible for image-to-image registration with regular preoperative image data.

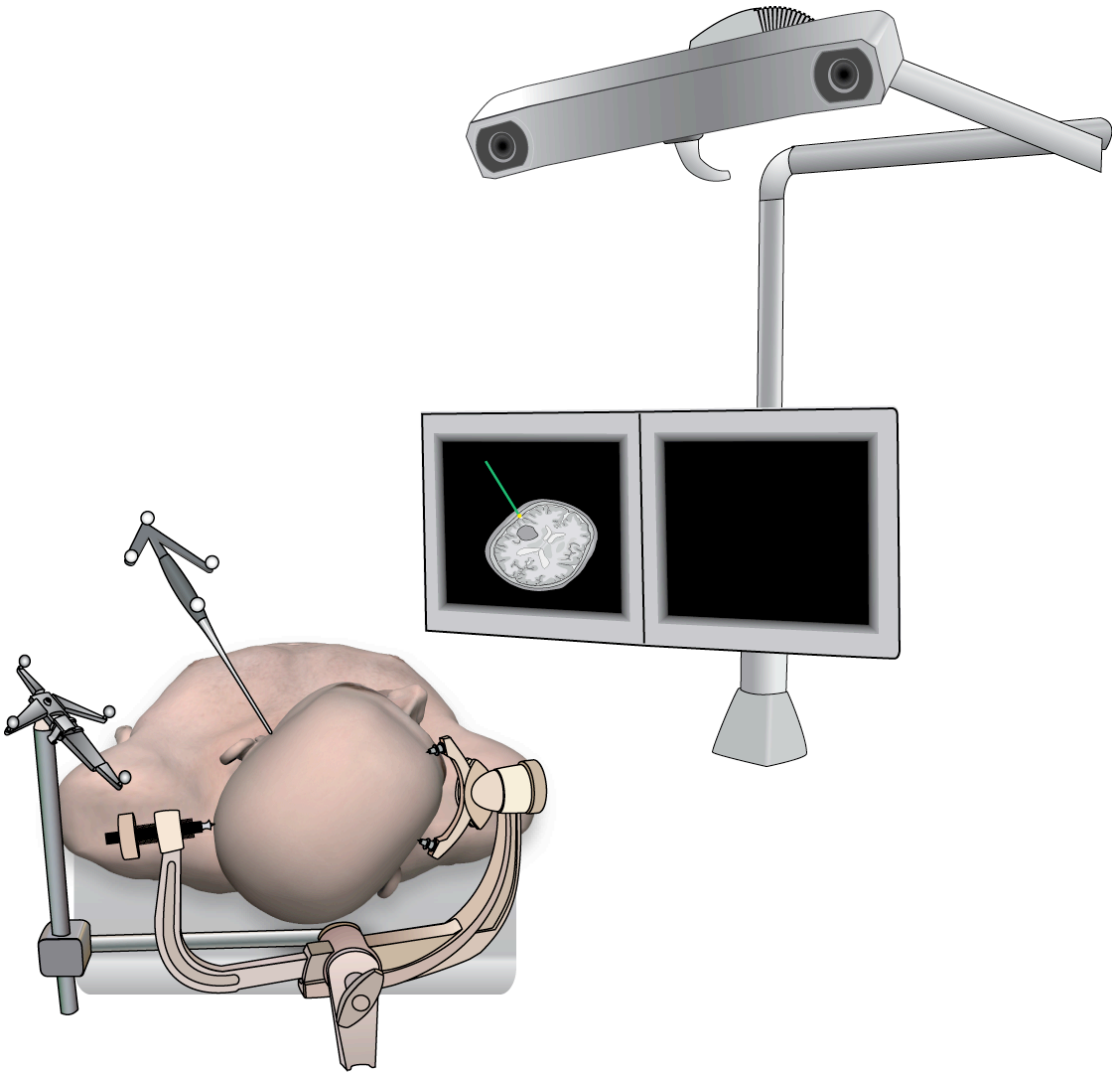

Figure 6: After patient registration, the navigation system is ready for use. The image displayed by the navigation system is determined by the position and trajectory of the pointer. On the screen, the pointer is marked. The patient reference frame is attached to the head-holder.

1.3.6 ACCURACY

The expression “precise”, in a technical context, is used for a group of measurements with a small standard deviation (e.g. the value of the measurements differ little), although the mean of these measurements can be far from the true value. On the other

hand, a group of measurements are *unbiased* if the mean is close to the true value. Only if both precise and unbiased, a set of measurements is accurate. In neuronavigation systems based on preoperative images the error sources may be numerous[91], and usually one distinguishes between three different types of accuracy [45]:

1. The technical accuracy, meaning how reliably the positioning system can define its own position. The technical error is usually in the sub millimetre range with present positioning systems.

2. Registration accuracy. Registration accuracy is a measure of how well the coordinates of physical space is corresponding to the coordinates in image space after registration. Registration accuracy depends on the method of registration: In paired-point matching, using anatomic landmarks for registration has the worst accuracy, while using adhesive skin fiducials is better. Attaching fiducials with screws in the skull has the best registration accuracy. Registration accuracy for adhesive skin fiducials is somewhere in between. Navigation systems based on paired-point transformation have a check for estimating the registration error, the root mean square (RMS). The RMS is the root mean square of the distance differences of the fiducials between the image and the physical space. The RMS using CT images with 2-3mm slice thickness is usually in the millimetre range, but typically below 4mm [44].

3. The application accuracy/Navigation accuracy is reflecting the targeting error during the operation. It depends on both technical accuracy and registration accuracy as well as additional factors [91]. In addition, displacement of the head in the clamp, displacement of the dynamic reference frame and displacement of brain tissue (called *brain shift*, discussed below) altogether influence the overall application accuracy. The application accuracy also varies in time and space as brain shift is non-uniform and may increase during a procedure [107,109].

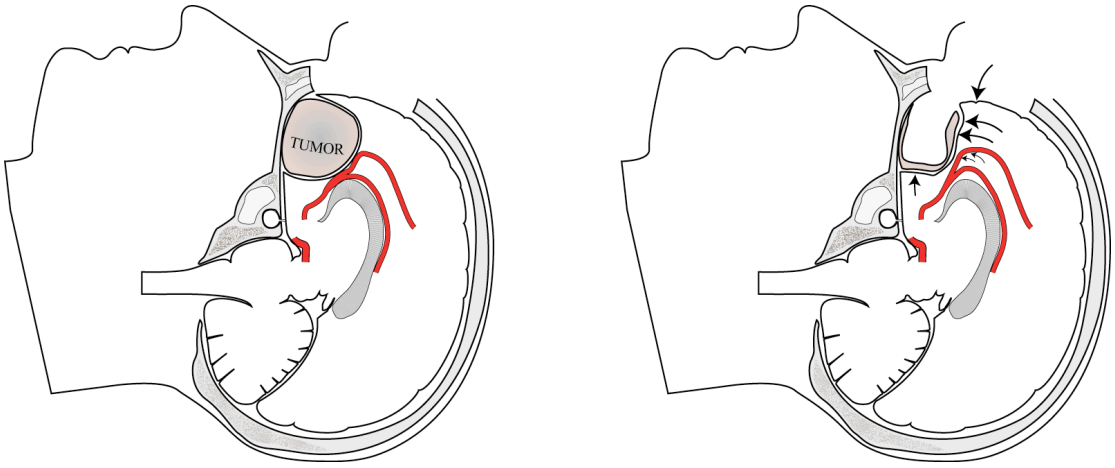

Figure 7: Brain shift. After some resection has been performed, brain shift may occur (arrows). Brain shift is non-uniform, and difficult to predict. The cortical surface, walls of the resection cavity, and important structures such as vessels may move.

1.3.7 VISUALIZATION AND DISPLAY

Image data may be displayed in different ways. It is a challenge to display the increasing amount of available data from different imaging modalities in a user-friendly way, and this has been an issue of interest for our research group [53,54,90,120,167]. As the image data is a 3D data volume, the 2D images displayed on screen are *image slices* trough the 3D dataset. The images may be displayed as conventional *orthogonal* slices, e.g. the way one usually view medical images, sliced in the sagittal, coronal and transversal planes. As an alternative to this, an image slice determined by the trajectory and rotation of the surgical tool or pointer may be displayed (this visualization mode is called “anyplane” in the SonoWand system), like the real-time image from an ultrasound probe. Some users of navigational systems find this more intuitive, as only the structures in the direction of the pointer is displayed. Another image slice perpendicular to the first plane may be displayed in order to view the anatomy in two planes, which ensures that structures above or below the first plane are not missed. A third image slice, perpendicular to the two other may also be introduced, thus being perpendicular to the axis of the pointer. In addition, 3D display modes may be applied, using stereoscopic display or surface and volume rendering techniques. When microscope integration is used, items of interest (for example the outline of a tumor) may be displayed and superimposed in the ocular of the operating microscope.

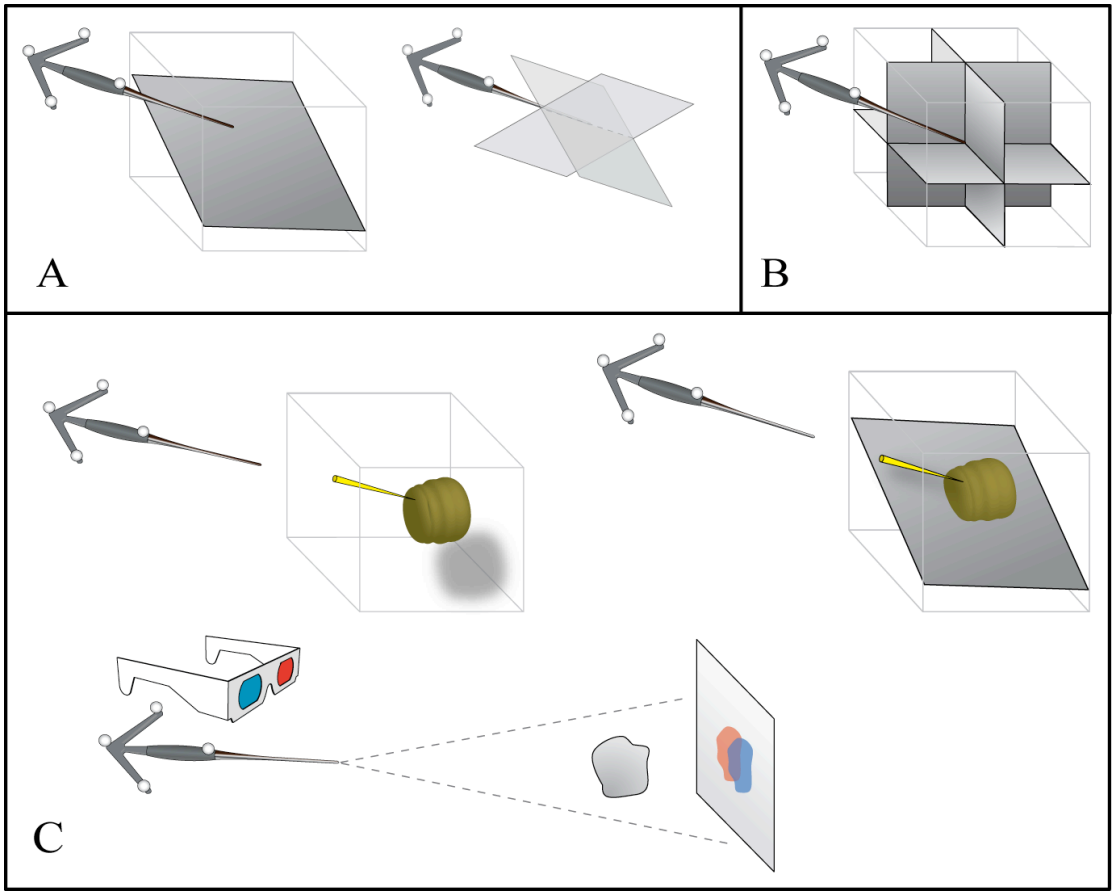

Figure 8: Different methods of visualization for image guidance. A: To the left: A single 2D slice from the 3D volume determined by the position and orientation of the instrument (called ”anyplane” in the SonoWand system). Right: Two perpendicular image slices determined by the position and orientation of the instrument. B: Three orthogonal slices determined by the position of the tool and the patient. C: Other visualization techniques. Top left: 3D visualization technique using volume or surface rendering of selected objects. Top right: Image slice and 3D display technique used simultaneously in one window/scene. Bottom: Stereoscopic visualization using red-blue glasses.

1.3.8 APPLICATIONS OF NEURONAVIGATION:

Neuronavigation systems are used for planning of the craniotomy and for intraoperative orientation and localization. Instead of standard approaches, using neuronavigation an approach may be tailored and allow smaller craniotomies. Essentially any target which is difficult to find and is below the cortical surface of the brain may be located easier with the help of neuronavigation, such as tumors, aneurysms, cavernous haemangiomas, AVMs and AVM feeder vessels. Image

guidance may allow an endoscope to be inserted into narrow ventricles in neuroendoscopic operations. Improved orientation provided by the neuronavigation system may be helpful, demonstrating anatomical relationships, and detecting residual tumor. In spinal surgery, neuronavigation may be used to assist proper screw positioning.

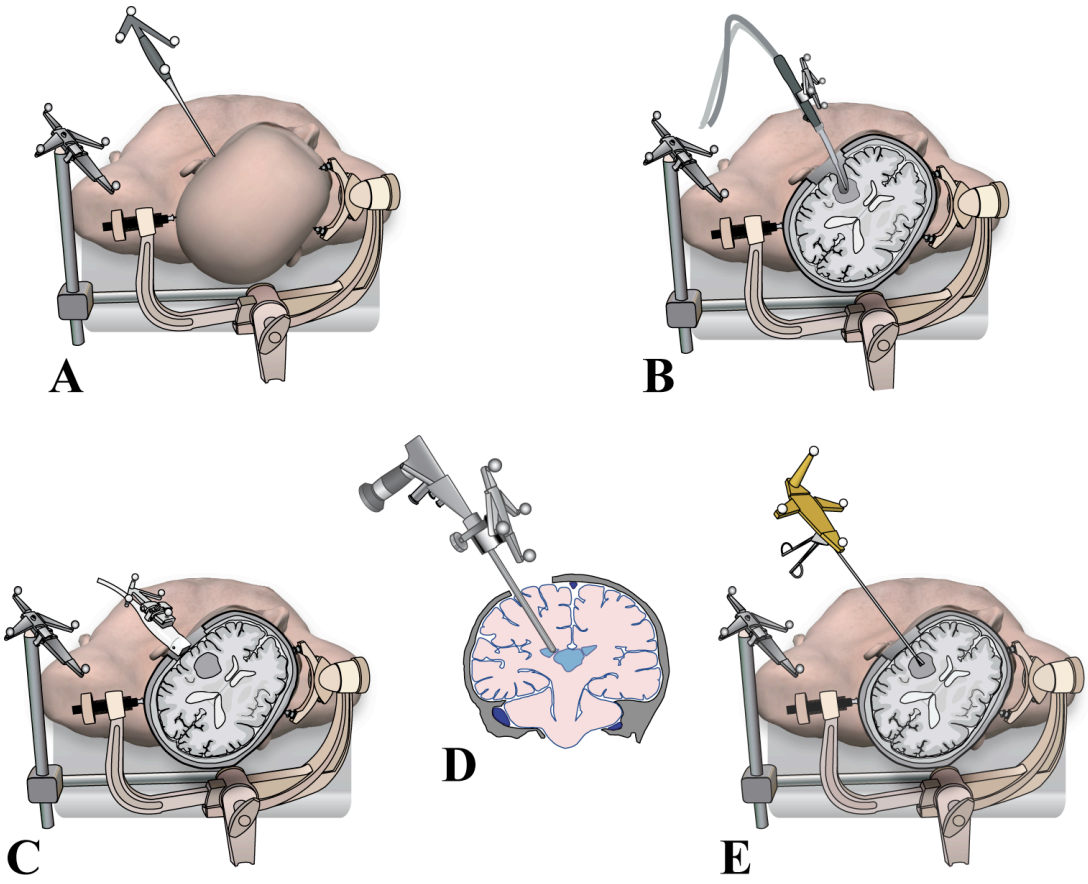

Figure 9; Examples of instruments that can be used in neuronavigation. A: Pointer. B: Cavitron Ultrasonic Surgical Aspirator (CUSA) C: Ultrasound probe. D: Endoscope. E: Biopsy forceps.

1.4. INTEGRATED 3D ULTRASOUND AND NEURONAVIGATION

1.4.1 INTRAOPERATIVE IMAGING AND ULTRASOUND IN NEURONAVIGATION

The use of intraoperative 3D ultrasound for updated image data to be used in neuronavigation was reported by Grønningsæter and colleagues in 2000 [46]. The virtue of the SonoWand system is that the ultrasound image data are transformed into a 3D dataset that may be used for navigation like any other image data. The usefulness of

the SonoWand system has been reported by other groups [11,134]. A couple of another 3D ultrasound based neuronavigation solutions has been reported as well [89,148]. Other neuronavigation solutions with intraoperative 2D ultrasound have also been introduced, for concurrent display of intraoperative (2D) ultrasound and preoperative MRI [61,66,156,161]. Intraoperative CT imaging has been explored as well [94], but never gained momentum.

Intraoperative MRI is the major alternative to ultrasound in intraoperative imaging[1]. Enthusiasts of both intraoperative MRI and ultrasound seem to have their arguments why their modality is superior. Intraoperative ultrasound is a low-cost alternative, not requiring extra staff and an expensive dedicated operating suite. Furthermore, intraoperative ultrasound allows for updating the intraoperative image data as often as desired, while intraoperative MR updates are more limited due to the extra time required for imaging. While devotees of intraoperative ultrasound argue that image quality is comparable to intraoperative MRI with state of the art ultrasound equipment, the general neurosurgical community does not seem convinced. Ultrasound will only show parts of the anatomy, while MRI shows the entire scene. Deeper structures tend to be less easily delineated by ultrasound, due to the attenuation of ultrasound waves the further they travel in tissues. Finally, intraoperative MRI with high field strengths may perform new MRI imaging techniques such as diffusion weighted MRI, functional MRI (although it requires awake craniotomies), MR-Angiography among others [1]. In this context it is important to remember that ultrasound and MRI are based on fundamentally different physical principles, and in some regards comparing the two modalities would be like comparing apples and oranges. Interestingly, Katisko and Koivukangas recently have explored using both intraoperative MRI and intraoperative ultrasound in neuronavigation [64], and this seem like a good idea as the two modalities in reality are complimentary.

1.4.2 3D ULTRASOUND IN NEURONAVIGATION.

In present solutions for 3D ultrasound, an ultrasound probe is calibrated either prior to the operation or comes pre-calibrated by the manufacturer. At the neurosurgical department in Trondheim, precalibrated 5 MHz and a 10 MHz probes are available for use with the SonoWand system. When the probe is calibrated, the 2D ultrasound image is positioned correctly in physical space by the positioning system. The 3D ultrasound image data is then acquired by moving the probe over the area of interest. (See chapter 1.2.3 for discussion on 3D ultrasound). In addition to standard B-mode images, also duplex images showing vessels with Doppler may be used.

The 3D ultrasound image volume is then ready for use in navigation, alone or in combination with preoperative image data such as MRI. Using preoperative images in addition to intraoperative 3D ultrasound is obviously useful for planning of the craniotomy, but also for orientation and interpretation of the ultrasound images. During the operation, new 3D ultrasound image data may be acquired whenever wanted. The ultrasound probe is in the surgical field only during 3D ultrasound image acquisition.

1.4.3 CLINICAL APPLICATION OF 3D ULTRASOUND.

3D ultrasound may be used in a number of different neurosurgical procedures. In most cases, preoperative MRI is also used in addition to 3DUS and is useful particularly for planning of the approach.

In *tumor resection*, 3D ultrasound is used for delineating the tumor borders, monitoring the resection and detection of residual tumor. In addition, complications such as hemorrhage may be detected. Navigation with 3D ultrasound may be done with a pointer or with a calibrated CUSA in which case the resection may be guided continuously[168]. Microscope integration is not yet available with 3D ultrasound. To make the resection as safe and complete as possible, it is essential to acquire new 3D ultrasound image data during the operation, especially at the end of the resection. The surgical approach should be made as vertical as possible to allow saline to fill the entire cavity when 3DUS image acquisition is done, to allow air bubbles to escape. In addition, there should not be any blood, debris, spatulas or cottonoids in the resection cavity when acquiring 3D ultrasound. Nearly all tumor types can be identified and outlined with 3D ultrasound[168]. As Paper 2 in this thesis points out, in some cases it

may be useful to use 3D ultrasound angiography to monitor important vessels close to the tumor border. During the course of the resection the ability of 3D ultrasound to delineate glioblastomas may decline, as Paper 1 in this study shows, and it is important to keep this and other limitations of 3D ultrasound in mind when performing a resection with 3D ultrasound image guidance.

Biopsies may be image guided with 3D ultrasound. Using 3D ultrasound for biopsies may be advantageous as accuracy loss due to brain shift and registration error will be minimal. A biopsy forceps equipped with a tracking frame is used, and must be calibrated in each case before use. To be able to perform image guided biopsies with 3D ultrasound, a burr hole large enough for the ultrasound probe must be made.

Navigated 3D ultrasound is well suited for resection and removal of *cavernous haemangiomas* as they are readily depicted on ultrasound. Also cavernous haemangiomas in the posterior fossa are suited for surgery with 3D ultrasound, and again, with minimal error due to brain shift and registration error.

Image guidance of *endoscopes* may be performed with 3D ultrasound, as Paper 4 in this thesis shows. In many cases image guidance of the endoscope with 3D ultrasound alone is sufficient. Image guidance is useful for choosing the best entry point and trajectory for the endoscope, as well as deciding the best site for doing a fenestration.

In *evacuation of intracerebral hematomas*, image guidance with 3D ultrasound is possible using a CUSA with tracking.

In *vascular neurosurgery*, image guidance with 3D ultrasound using power Doppler may be of value. In *aneurysm surgery*, navigation with 3D ultrasound angiography may be useful for locating aneurysms at atypical locations. In *AVM* surgery, navigated 3D ultrasound angiography and stereoscopic display of the 3D ultrasound angiogram may be useful for identifying feeders for clipping, and to check whether residual AVM is left after clipping, as Paper 5 shows. In addition, one other group has reported this [98].

3D ultrasound image guidance may be useful in surgery for *intraspinal pathology*. It may be helpful for both locating tumors in the spinal canal and medulla spinalis and for resection control. In Paper 3 this is discussed. Also in syrinx surgery using 3D ultrasound may be helpful [10].

1.4.4 MULTIMODAL NEURONAVIGATION.

Multimodality may be defined as the integration of multiple imaging modalities in neuronavigation, so that all relevant image data is displayed simultaneously on the same screen. Important progress in neuronavigation has in recent years been made in multimodality and visualization techniques.

To display the multimodal image data in an intuitive fashion is a challenge, and only the image data which is relevant should be displayed. Functional image such as BOLD-fMRI and tractograms which map important neural pathways in the white matter of the brain may be particularly useful. Several groups have reported the use of fMRI and tractograms for functional neuronavigation [12,18,57,62,76,104,110,120] Also other information which may be useful can be imported and used in neuronavigation, such as MR spectroscopy [155].

Ultrasound, with its practical advantages, may be the main intraoperative imaging modality in multimodal neuronavigation. Thus updated and accurate structural images are used for navigation, while important functional image data is simultaneously shown. An important area of research is methods for automatic multimodal co-registration between pre-operative MRI and fMRI/tractograms and intraoperative 3D ultrasound, which means to adjust preoperative image data using intraoperative imaging. This may be a feature of future neuronavigation systems[18,120].

2 AIMS OF THE RESEARCH

Since its introduction, the application of Neuronavigation based on 3D ultrasound has continuously been explored and evaluated by our research group. The purpose of the present PhD thesis was twofold: 1) Undertake a clinical evaluation of the present 3D ultrasound-based neuronavigation system. 2) To further explore the possibilities of neuronavigation based on 3D ultrasound.

2.1 AIMS OF STUDIES

The main use of intraoperative navigated 3D ultrasound at our department has been image guidance of brain tumor resection. Ultrasound is reported to readily show and delineate nearly all brain tumors [5,17,49,82,122,137,170,180]. The delineation of gliomas by 3D ultrasound has been studied in unresected tumors by our group [169]. 3D ultrasound was found to have good specificity and sensitivity in delineating tumor borders prior to resection. Furthermore, the use of ultrasound for evaluation of the completeness of resection has been reported, comparing image findings with histopathology [16,87,179]. These studies show that using ultrasound tumor remnants may be detected after resection with a reasonable degree of certainty. However, it is not clear to what extent intraoperative factors disturb the delineation of gliomas in subsequent phases of the resection. A study was initiated to assess this, and is reported on in **Paper 1**.

Using 3D ultrasound in image guidance of tumor resection includes the possibility of also employing ultrasound Doppler imaging. In our case, power Doppler was used. The aim of the study presented in **Paper 2** was to do a clinical evaluation of the benefits and shortcomings of 3D ultrasound angiography for image guidance in surgery of brain tumors. One aim of the study presented in **Paper 5** was to evaluate the application of navigated 3D ultrasound angiography and a stereoscopic display technique enabling navigation with the ultrasound angiographic image data in true 3D.

In spinal cord tumor surgery, ultrasound has earlier been applied and reported to be useful [70,116,121,123,138]. The experience with neuronavigation and intraoperative imaging with 3D ultrasound in this setting is however modest. The aim of a study undertaken by our research group was to assess the feasibility and technical aspects of navigated intraoperative 3D ultrasound in spinal cord surgery. This study is presented in **Paper**

3. In neuroendoscopy, the use of neuronavigation for image guidance is a recognized enhancement [6,14,23,31,32,47,58,92,106,128,146]. Orientation in cases with anomalous anatomy, introducing the endoscope into small and slender ventricles, visualization in obscure fluids and finding small subependymal tumor masses may all be obstacles in endoscopic neurosurgery. Still, due to brain shift navigation with preoperative images may be inaccurate. The use of the SonoWand system for 3D ultrasound guidance of neuroendoscopic procedures therefore was one of the logical applications of this system. An adapter for attaching it to one of the endoscopes at the department was designed. The design was put to use, and utilized successfully. An evaluation of this concept in a series of cases was the goal of the study presented in **Paper 4**.

3. MATERIALS AND METHODS

The navigation system used was an intraoperative ultrasound based neuronavigation system, SonoWand (SONOWAND AS, Trondheim, Norway) with a 4-8 MHz flat phased array probe (also called 5MHz due to the mostly used scan frequency) with optimal focusing properties at 3-6 cm and with the capability of acquiring power Doppler (ultrasound angiography) images[166,168]. On the ultrasound angiography images, vessels were displayed as an overlay in shades of red according to the power of the Doppler signal, over the tissue image. On B-mode images, the 4-8MHz probe has a radial and lateral resolution of approximately 0.5 and 1.0mm, respectively. In addition, the image plane itself has a certain width that varies with depth. This elevation resolution (perpendicular to the scan-plane) is less than 2 mm in the optimal depth range. In addition, a 10 MHz probe was used, which had better resolution and accordingly lower penetration.

For tracking of the ultrasound probe, a tracking frame was attached. Neuronavigation was performed with a tracked pointer device, or the CUSA with an attached tracking frame. Tracking of the CUSA enabled continuous monitoring of the position of the tip and the trajectory of this instrument (a concept called “on-line resection”). A biopsy forceps with tracking was also available for image guidance of biopsies. For acquisition of 3D ultrasound image data for navigation, the ultrasound probe was placed on the dura and tilted or translated over the area of interest by a free hand movement. The 2D ultrasound images acquired were reconstructed to a 3D ultrasound dataset ready for navigation. The ultrasound probe was not in the operating field after

the acquisition of a 3D ultrasound volume, unless when additional 3D ultrasound datasets were acquired or real-time 2D imaging was needed.

Image slices from the 3D ultrasound dataset was displayed on the screen of the navigation system, usually in addition to the preoperative MRI, which was displayed simultaneously on the same screen. With a simple pointer device surgical planning and navigation could be performed after fiducial-based patient registration. The patient reference frame was attached to the head-holder. Additional ultrasound and ultrasound angiography image data was acquired whenever required due to suspected brain shift, or for resection control.

The application accuracy of the SonoWand system has previously been reported to be as low as 2 mm when using intraoperative ultrasound to compensate for brain shift [91].

The operations in this research were carried out in the years 2003-2006, by senior neurosurgeons at the Neurosurgical Department in Trondheim. This author attended nearly all operations in which data for this research was collected. Research colleagues from SINTEF Health Research always attended the operations.

Data was collected by gathering images and recording information during the operations. Discussions with the operating surgeons in retrospect also was an important method of collecting information.

Ethical approval: In the "Endoscopy" study, ethical approval was not applied for. The patients were however informed about the equipment by the operating surgeon in advance. All other studies in this thesis were approved by the Regional Committee for Medical Research at the University of Science and Technology in Trondheim, and the patients gave written informed consent, and had the opportunity to ask questions about the project afterwards, as well as withdrawing from the study at any time.

Inclusion and exclusion of patients: Patients were considered eligible as they were assigned for surgery. Then, the patients were asked to participate and if they volunteered, they were included/excluded by the inclusion and exclusion criteria in each study.

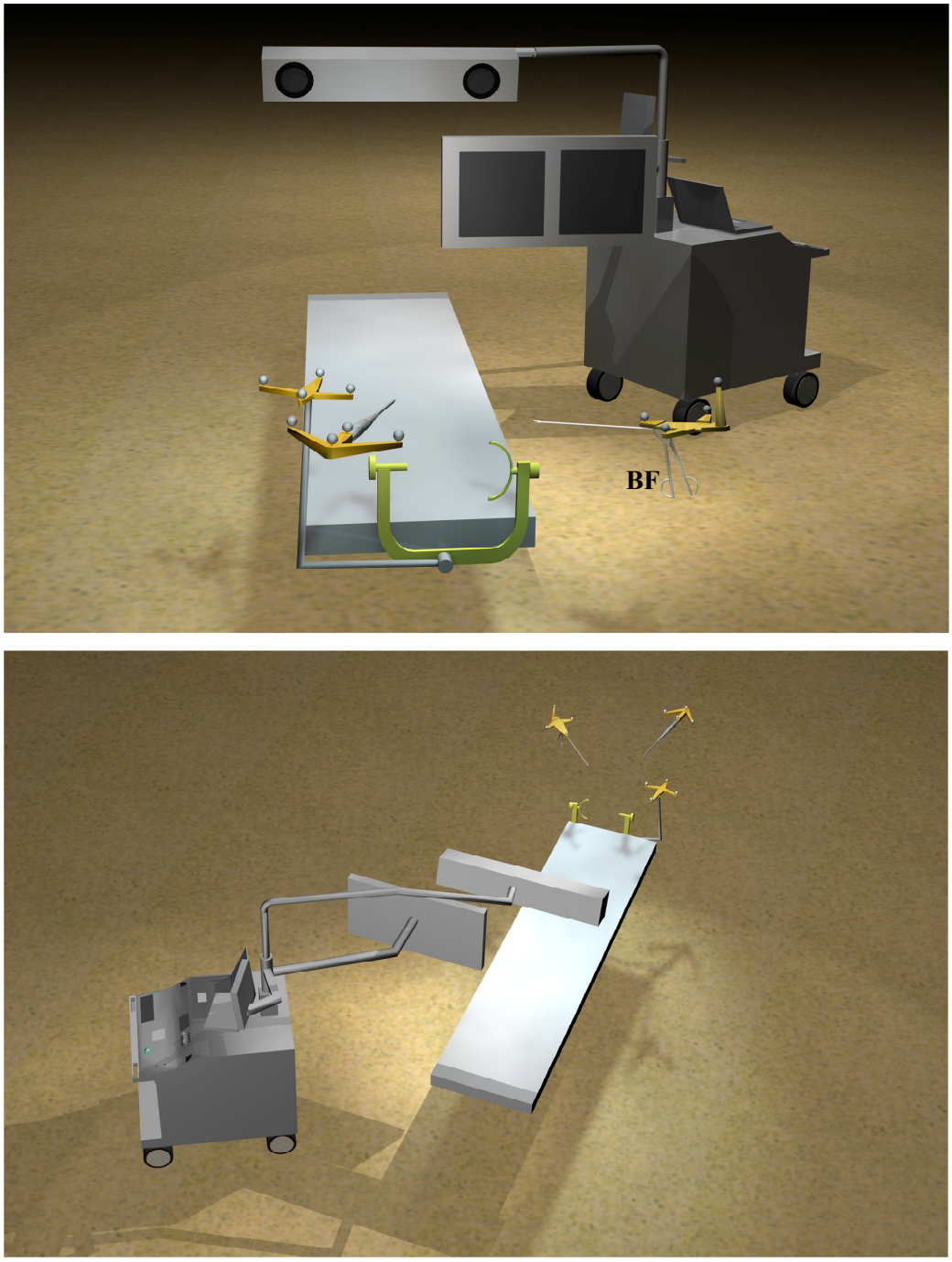

Figure 10: Setup of equipment in the operating room. The biopsy forceps (BF) is on the right hand side in the top image

4. SUMMARY OF STUDIES AND MAIN FINDINGS

PAPER 1

This paper presents a study where the ability of intraoperative navigated 3D ultrasound to distinguish normal from tumor tissue during subsequent phases of surgery is assessed. This was done by comparing image interpretation (e.g. whether the biopsy was sampled in tumor or normal tissue) of biopsy location and the corresponding histopathologic findings. In the study, ultrasound readily distinguished tumor from normal tissue before the resection. However, during resection (when a certain amount of tumor was removed), there were false positives on several occasions, in other words areas falsely interpreted as tumor. This reduced the specificity of ultrasound during resection. After completed resection, there were a considerable number of false negatives, in other words biopsy sites interpreted as normal but which showed tumor tissue or infiltration on histopathological examination. Thus the sensitivity after resection was low. The conclusion of the study was that the ultrasound tended to overestimate tumor in the situation where some resection had been carried out (during resection), while it underestimated the occurrence of tumor and infiltrated tissue in the resection cavity wall. On the other hand, sensitivity was acceptable during resection, and thus it seems that residual tumor masses are detected during resection. The specificity was acceptable after resection, reflecting that normal tissue was correctly diagnosed in most cases.

PAPER 2

This paper presents a collection of cases with intracranial supratentorial tumors in which navigation with intraoperative 3D ultrasound angiography (power Doppler) was used for image guidance. The main finding in this study was that navigated intraoperative 3D ultrasound angiography was easy to use and interpret, and that it was found useful by the surgeon in cases with important vessels situated close to the tumor.

PAPER 3

In spinal cord tumor surgery, neuronavigation may be useful, and this paper presents the use of intraoperative 3D ultrasound for image guidance in spinal cord tumor surgery. The main finding was that using intraoperative 3D ultrasound for neuronavigation was feasible. The paper also discusses the technical and practical issues of this application.

PAPER 4

This paper evaluates the use of intraoperative 3D ultrasound with neuronavigation for guidance of neuroendoscopy. The main finding was that this technique was practicable, and that the ultrasound images were of sufficient quality for image guidance of neuroendoscopic procedures. In cases with narrow ventricles and cases with anomalous anatomy image guidance was found useful for deciding entry point and trajectory for the endoscope and where to perform a fenestration. Still, issues of improvement of the equipment like an improved tracking frame developed exclusively for the endoscope were identified.

PAPER 5

This paper presents a study in which a navigated stereoscopic display module in the SonoWand system was assessed in AVM cases. The stereoscopic display was found easy to interpret. Intraoperative 3D ultrasound angiography image data were acquired and put on view with the stereoscopic display, but the image quality of 3D ultrasound angiography displayed in this manner was uneven. In some cases, the ultrasound angiography data was of sufficient quality and stereoscopic display of the AVM allowed feeder vessels to be identified and accurately targeted because accuracy of ultrasound image data was not affected by brain shift. Still, the vessels seemed bulkier when visualized by 3D ultrasound angiography than on MR-angiography. 3D ultrasound angiography was also useful to map the size of the nidus as it showed both arteries and veins, and in one case to detect residual AVM.

5. DISCUSSION

Interpretation of ultrasound images is highly dependent on the experience of the ultrasound user. In Paper 1, 2 and 5, the operating surgeons interpreting the ultrasound images had significant experience with ultrasound, while in paper 3 and 4, the operating surgeons had average experience with intraoperative ultrasound.

5.1 THE ABILITY OF INTRAOPERATIVE 3D ULTRASOUND TO DISTINGUISH BETWEEN TUMOR AND NORMAL TISSUE.

In **Paper 1**, it is shown that the ability of navigated intraoperative 3D ultrasound to distinguish tumor from normal tissue is reduced during resection and after resection, as compared to the situation prior to resection. Tumor tended to be overestimated during resection, as several biopsies deemed "normal" contained either tumor tissue or normal tissue.

The factors influencing the ultrasound image are multiple. Some of these factors can be assumed to be constant during all phases of the operation, such as for example the resolution of the ultrasound scanner. Other features may change. Intraoperative factors may theoretically cause the physical characteristics of the brain tissue to be altered in different ways that may affect how the tissue is imaged by ultrasound. For example, the effect of gravity in the absence of CSF may alter the echogenicity of the brain tissue. It is not known whether the surgeon performed the 3D ultrasound image acquisition differently in the different phases of the operation and if this was the case how it would affect the images. Finally, imaging artefacts due to blood, microscopic bubbles among other things may obviously be introduced by the surgery. To identify the causes of the reduced diagnostic accuracy of ultrasound during and after resection were however beyond the scope of this study.

The highly infiltrating nature of gliomas is an everlasting concern in the surgical treatment of these neoplasms. This issue also has a natural place in this discussion. It is to be expected to find infiltrated tissue and tumor remnants in the walls of the resection cavity after surgery. The resolution of ultrasound is of course limited, and small tumor remnants may not be detected.

Does ultrasound show infiltration? In the study presented in paper 1, the surgeon did not have the option of classifying an image finding as “infiltration”, while the pathologist did. Still, it is difficult enough to decide whether it is tumor or normal tissue on the ultrasound images and it was considered too complicated in addition to decide whether it was infiltration. On the other hand, the surgeon could choose between being certain or uncertain on whether the biopsy was sampled in normal or tumor tissue. This was chosen because it most closely reflected what is the real situation using 3D ultrasound (and in retrospect it allowed us to create ROC curves). **Table 2** in paper 1 shows the image findings in biopsies that contained infiltrated tissue. Before the resection 6 of 10 of biopsies that contained infiltration were deemed “tumor”, 2 biopsies “tumor, uncertain” and 2 biopsies “normal”. In the next phase, during resection also 6 of 10 biopsies that contained infiltration were judged “tumor”, while 1 biopsy “tumor, uncertain”, 1 “normal, uncertain”, and 2 “normal”. After completed resection the picture was different, with 1 of 16 biopsies which contained infiltrated tissue considered “tumor, uncertain” (none were considered “tumor”), 10 of 16 biopsies were considered “normal, uncertain”, while the remaining 5 were deemed “normal”. Thus it seems that the majority of the biopsies containing infiltration before and during surgery were deemed “tumor” or “tumor, uncertain”, while after resection the majority of biopsies were deemed “normal, uncertain” or “normal”. We were reluctant to draw further conclusions on this in part due to the fact that the study was not designed to assess whether infiltration shows on ultrasound.

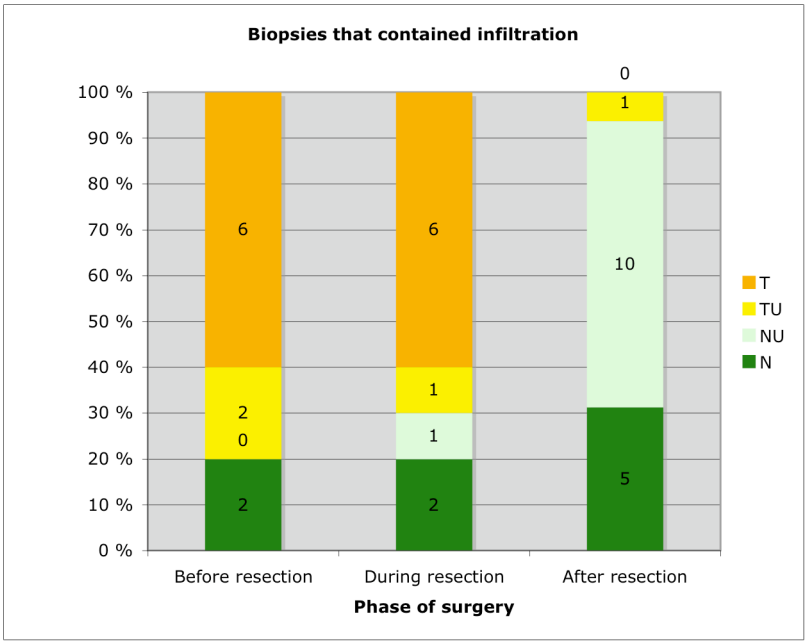

Figure 10: Bar chart of biopsies that were categorized "infiltration" by the pathologist.

Another observation is the *proportion of biopsies in which the surgeon was uncertain in the different phases* (regardless of whether it was "tumor, uncertain" or "normal, uncertain"). Before resection the surgeon was uncertain in 7% of biopsies, during resection 12% and after resection 56%. Thus it seems that the situation after resection was different. A possible explanation for this is that it simply is more difficult to appraise the images after resection, when there is no certain tumor left on the image for comparison with normal tissue.

Is the reduced diagnostic accuracy of ultrasound during and after surgery harmful for the patient? Overestimation of tumor may lead to a too aggressive resection, unnecessarily removing normal tissue. Still, the postoperative status of the patients who participated in this study was overall certainly acceptable, so it seems that at least in this study there was no such harmful effect. Underestimation of small tumor remnants and infiltrated tumor tissue after resection may be unfavourable for the patient, and if this is the case, the resection should be carried out more aggressively than the ultrasound image suggests. To find answers to this dilemma, further studies are needed.

Statistical considerations: Further statistical analyses than simple calculations of sensitivity, specificity, NPV and PPV are not included in **Paper 1**, and confidence intervals for the calculated values of sensitivity, specificity NPV and PPV are not presented. This was however given consideration, and an experienced medical statistician (SL) consulted on the issue. If confidence intervals were to be calculated, a random effects model would have to be considered as several biopsies were sampled from the same patient. McKnight et al used a bootstrap method when comparing histopathology with MR-spectroscopy to account for the multiple biopsy specimens excised from each patient [101]. We did not however find a suitable statistical method for our data for calculating valid confidence intervals taking random effects into consideration. A method for creating approximate confidence intervals (although probably too narrow) could have been using Agresti and Coulls method.

Limitations of the study. There are several methodological shortcomings in **Paper 1**, which are discussed in the paper. In addition, there are still other possible sources of error. It cannot be ruled out that the staff marking the biopsies and bringing them to the pathology lab might have been more tired at the end of the day, thus the risk of misplacing biopsies might have been greater for biopsies during and after surgery

introducing another possible source of error that is different for the subsequent phases of resection.

Obviously there also might have been a bias in the attitude of the surgeon in this phase, as he already had decided that the resection was complete. Still, the surgeon was certainly aware of this possible bias and tried to avoid it.

5.2 THE DETECTION AND DEPICTION OF VESSELS BY 3D POWER DOPPLER ULTRASOUND IMAGES

The findings that neuronavigation based on 3D ultrasound angiography is feasible in brain tumor surgery and useful in selected cases, mean that the addition of navigated ultrasound angiographic imaging should be considered in tumor surgery. In cases with important vessels situated close to the tumor, it may increase safety. Still, it is important when using this technique to be aware of its limitations. It is not possible to distinguish arteries from veins using power Doppler alone, and the vessels may appear to be bulkier than they are in reality due to blooming and the effect of the 2D ultrasound slice thickness.

The stereoscopic display of vessels is an alternative method of displaying the image information as 2D image slices. This might be a better way of displaying the angiographic information, as the whole vessels are displayed in a true 3D image. The experience with this display technique in AVM surgery reveals that it is vulnerable to shortcomings in the 3D ultrasound angiography technique. Successful imaging using stereoscopic display was variable, giving comprehensible images in some cases while not in other cases, in which the images were too blurry and bulky to be of value. Also in aneurysm surgery we had this experience (unpublished data). Another research group have also used stereoscopic visualization of AVMs with intraoperative 3D ultrasound angiography, and it seem that their experience was more positive [97], but the low resolution of power Doppler imaging was commented on as being a major limitation. The stereoscopic display of preoperative MR-angiography was in our experience consistently of good quality, ruling out that the stereoscopic technique was the cause of low image quality in some cases. Shortcomings in power Doppler imaging like blooming and flash artefacts are discussed in **Paper 2.**

During our research some important questions about the modality arose. The blooming effect make vessels appear larger than they really are, but how much larger? To what extent is the blooming effect related to the distance from the ultrasound probe? What is the smallest size of a vessel that may be detected by this method? And how does the distance from the ultrasound probe affect the size of the smallest detectable vessels? These questions may be the subject of further studies. Still, in the fast-moving world of medical technology, new technologies may arise before the existing ones are thoroughly tested. For example, wide-band Doppler technique coupled with improved signal and image processing seem promising, because it boasts better resolution and less blooming (T.Sato, http://www.toshiba-europe.com/medical/Materials/Whitepapers/Sato.pdf).

Contrast agents for use with ultrasound have for some years been available on the market. They are highly echogenic gas-filled microbubbles that are administered intravenously, and may be used for depiction of vessels. We considered the use of contrast agents for visualization of vessels, but discarded the idea partly due to the fact that the knowledge of hazardous effects of ultrasound contrast applications used intraoperatively in neurosurgery is limited. We also feared that the intravenous administration of the contrast agents would be an obstacle in the intraoperative setting. Still, the use of ultrasound contrast agents has been applied in neurosurgical intraoperative ultrasound, and the authors reported that it was feasible and they did not observe any harmful effects [63]. The use of ultrasound contrast agents for intraoperative angiographic imaging therefore cannot be ruled out.

5.3 THE USE OF 3D ULTRASOUND NAVIGATION IN SPINAL CORD SURGERY

In **Paper 3**, it was demonstrated that the use of a navigation system based on intraoperative 3D ultrasound was feasible in spinal cord tumor surgery. In our view, this has considerable advantages in comparison with 2D ultrasound, and these are discussed in the paper. Still, while conventional 2D ultrasound is real-time, the 3D ultrasound technique presented here is not. The unexposed spinal cord has been shown to move craniocaudally in a pulsatile fashion with each cardiac cycle[103]. To what extent and in what direction the spinal cord exposed after a laminectomy move

when the surgical opening is filled with saline is not known. If it does, it will probably vary with the size and location of the surgical opening, and whether the dura is opened or not. We did in one case in 14 patients with spinal lesions experience that the reconstructed images of the spinal cord appeared wavy when viewed in the sagittal plane, and suspected that this might have been due to pulsatile motion of the spinal cord while performing 3D image data acquisition.

In spinal surgery, the vertebras move due to breathing, and to a greater extent due to surgeon-induced motion [37]. As the vertebras move, the spinal cord will also shift. The attachment of the patient reference frame to the spinal process of a vertebra is therefore a better solution than attaching it to the operating table. To what extent the spinal cord and the vertebras move in a similar fashion due to breathing is not known, but we have assumed that the spinal cord and the vertebras move in a parallel fashion. This is almost certainly only an approximation. While we did not do a systematic evaluation of the application accuracy, our experience was that the agreement between the navigated images and the surface of the dura was very good, although agreement in the craniocaudal direction was impossible to assess with this approach. It thus seems that neuronavigation of the spinal cord has some intriguing challenges, and this preliminary study raises several important questions about accuracy that have to be further investigated.

We did not have the opportunity to test probes with higher frequencies than 10 MHz. It may be possible that probes with even higher frequencies give even better imaging results. Navigation with power Doppler imaging was performed a couple of times, and vessels successfully imaged. A systematic evaluation of the value of neuronavigation with intraoperative ultrasound angiography in spinal cord surgery was not done by us, but this technique may also be useful in selected cases as for example spinal AVMs.

5.4 THE USE OF 3D ULTRASOUND NAVIGATION IN ENDOSCOPY

In paper 4, it was shown that navigation based on 3D ultrasound was feasible for image guidance of neuroendoscopic procedures, furthermore it was found useful for deciding entry point and trajectory for the endoscope and where to perform a fenestration.

The field of neuroendoscopy is expanding, and the applications are many. It was beyond the scope of this study to evaluate the usefulness of this concept in each of the many applications. Besides, only one endoscope was used. The concept was based on the calibration of a rigid endoscope with a tracking frame attached. The tracking frame was originally designed for the CUSA, and an adapter was made so that the tracking frame could be attached. Still, assembling the endoscope, adapter and tracking frame correctly proved to be cumbersome, and was not a fail-safe procedure (e.g. the tracking frame could be mounted incorrectly resulting in erroneous navigation). Furthermore, the tracking frame in one case shifted (probably because it had been pushed during a manoeuvre), resulting in incorrect navigation. Therefore we believe that tracking frame solution exclusively for use with the endoscope should be developed. Furthermore, for calibration the endoscope was directed at a small hole in the centre of the reference frame. This hole was a bit to small for the endoscope to enter, so it did not reach the bottom of the hole. This was probably a source of a systematic inaccuracy yet probably small and no problems in navigation were discovered as a cause of this. In any case, the endoscope is designed for visual control of what is ahead of the endoscope so a small navigation error in the length of the endoscope may be acceptable. The solution presented here would not work with a flexible endoscope, because the calibration procedure is based on that the instrument does not change its geometry in the course of surgery. For tracking of a flexible endoscope tip, magnetic tracking could work. The clinical accuracy was not systematically tested, which should be done in the future.

In the solution presented in paper 4, the endoscope had to be removed for imaging, which was not regarded a problem. If it is essential not to remove the endoscope while performing 3D ultrasound image acquisition, a larger craniotomy may be made but of course in that case this has to be planned for ahead. We did not try image acquisition with the endoscope in place. An obvious drawback with image acquisition with the endoscope in position would of course be ultrasound image artefacts from the endoscope itself.

5.5 LIMITATIONS

The work presented here is essentially technical evaluation and development research. Complications related to the surgery and possibly the technical equipment was

recorded, but no attempts to measure benefits for the patients in terms of for example functional outcome and survival were made. Studies that assess the benefits of neuronavigation and intraoperative imaging are scarce, but exist[176,177]. To directly assess the advantages for the patients studies with fundamentally different designs would have to be carried out, for example randomisation and careful follow-up. Such studies were considered but abandoned due to several reasons. One main reason was the ethical questions of randomizing patients to a control group without image-guided operations, because of the strong belief in the benefits of this technique. (E.g. it would mean that patients in the control group would not be given what one believe to be the best treatment). Another type of study that was considered was to indirectly assess the benefits for the patients in terms of for example residual tumor volume measurements. This was also abandoned mainly because we did not have resources for this. Lack of resources was also an important reason why we chose not to have the ultrasound snapshots taken during biopsy sampling examined by another person in retrospect for assessment of inter observer variability. (Inter observer variability was however assessed in a previous biopsy study undertaken by our research group [169].)
In neuroendoscopy and spinal cord surgery, the studies presented were too small to identify indications for the use of navigated 3D ultrasound. Studies with considerably more patients would be needed for assessment of this issue.

6. FUTURE PERSPECTIVES

The future developments in navigated intraoperative 3D ultrasound will probably be along different paths. First, new probe technology and signal and image processing techniques may bring further improvements. Although image updates with 3D ultrasound may be performed as often as wanted, the technique is not real-time. However, new 3D ultrasound probes will enable real-time 3D ultrasound imaging. Still, using such probes for 3D imaging means that the probe will have to stay in the surgical field, which is a practical disadvantage for the surgeon and in addition may require larger craniotomies or an extra craniotomy for the probe. 1,5 D probes with thinner scan-planes will have improved resolution. Custom made probes for special applications for example in spinal surgery and pituitary surgery may have an impact. Regarding new signal and image processing techniques, using wide-band Doppler techniques is already mentioned above. Other novel signal and image processing techniques may also have an impact, such as strain imaging [147] and blood flow imaging [93], tissue harmonic imaging, and others.

A second path of development is the use of 3D ultrasound for updating preoperative images using image-to-image registration algorithms [54,120,124], which is a complicated task yet holds great promise if robust methods for this purpose are developed.

A third path of development that applies to the entire field of neuronavigation is new multimodal visualization techniques. Multimodal visualization means to display in an understandable fashion data from several new imaging techniques such as for example fMRI and tractograms together with pre- and intraoperative anatomical images in a single multimodal scene.

Whether the use of ultrasound contrast agents will find its place in intraoperative ultrasound imaging remains to be seen. If contrast agents that enhance the delineation of tumor borders and tumor remnants became available, it would be most helpful for inexperienced users of 3D ultrasound, and maybe for the experienced ones as well.

7. CONCLUSION

The work presented in this thesis has been a clinical evaluation of the use of intraoperative navigated 3D ultrasound in neurosurgery, and new knowledge has been obtained.

- New understanding about the significance of ultrasound diagnosis in the successive stages of resection is gained: The surgeon must be aware that the tumor border may be overestimated during the resection, while a tumor resection cavity that seem clean may contain small tumor remnants and infiltrated tissue.
- The application of 3D ultrasound angiography using power Doppler has been found to be useful in cases with important vessels passing close to the tumor.
- In image guided AVM surgery, 3D ultrasound image data may be used for stereoscopic visualization of the AVM, but the technique need further development to become robust enough for ordinary clinical use.
- In spinal cord tumor surgery, navigated 3D ultrasound has been found feasible for tumor localization and anatomical orientation.
- Image guidance in neuorendoscopy may be performed with 3D ultrasound, and has been found useful in cases with narrow ventricles and distorted anatomy for image guided endoscope insertion and fenestration.

Issues for further improvement and studies have been indicated.

REFERENCES

1. Albayrak B, Samdani AF, Black PM: Intra-operative magnetic resonance imaging in neurosurgery. **Acta Neurochir (Wien) 146:**543-556; discussion 557, 2004
2. Ambrose J, Hounsfield G: Computerized transverse axial tomography. **Br J Radiol 46:**148-149, 1973
3. Angelsen BAJ: **Ultrasound imaging - Waves, signals and signal processing**: NTNU, dept of physiology and biomedical engineering, 2000
4. Auer LM: Intraoperative ultrasound as guide for neurosurgical endoscopic procedures. **Acta Radiol Suppl 369:**164-166, 1986
5. Auer LM, van Velthoven V: Intraoperative ultrasound (US) imaging. Comparison of pathomorphological findings in US and CT. **Acta Neurochir (Wien) 104:**84-95, 1990
6. Badie B, Brooks N, Souweidane MM: Endoscopic and minimally invasive microsurgical approaches for treating brain tumor patients. **J Neurooncol 69:**209-219, 2004
7. Benveniste RJ, Germano IM: Correlation of factors predicting intraoperative brain shift with successful resection of malignant brain tumors using image-guided techniques. **Surg Neurol 63:**542-548; discussion 548-549, 2005
8. Berger MS: Ultrasound-guided stereotaxic biopsy using a new apparatus. **J Neurosurg 65:**550-554, 1986
9. Black KL, Rubin JM, Chandler WF, McGillicuddy JE: Intraoperative color-flow Doppler imaging of AVM's and aneurysms. **J Neurosurg 68:**635-639, 1988
10. Bonsanto MM, Metzner R, Aschoff A, Tronnier V, Kunze S, Wirtz CR: 3D ultrasound navigation in syrinx surgery–a feasibility study. **Acta Neurochirurgica 147:**533-541, 2005
11. Bonsanto MM, Staubert A, Wirtz CR, Tronnier V, Kunze S: Initial Experience with an Ultrasound-Integrated Single-Rack Neuronavigation System. **Acta Neurochir (Wien) 143:**1127-1132, 2001
12. Braun V, Albrecht A, Kretschmer T, Richter HP, Wunderlich A: Brain tumour surgery in the vicinity of short-term memory representation--results of neuronavigation using fMRI images. **Acta Neurochir (Wien) 148:**733-739, 2006
13. Brinker T, Arango G, Kaminsky J, Samii A, Thorns U, Vorkapic P, et al: An experimental approach to image guided skull base surgery employing a microscope-based neuronavigation system. **Acta Neurochir (Wien) 140:**883-889, 1998
14. Broggi G, Dones I, Ferroli P, Franzini A, Servello D, Duca S: Image guided neuroendoscopy for third ventriculostomy. **Acta Neurochir (Wien) 142:**893-898; discussion 898-899, 2000
15. Bucholz RD: The Correction of Stereotactic Inaccuracy Caused by Brain Shift Using an Intraoperative Ultrasound Device, First Joint Conference, Computer Vision. **Virtual Reality and Robotics in Medicine and Medical Robotics and Computer-Assisted Surgery, Grenoble, France:**459-466, 1997

16. Chacko AG, Kumar NKS, Chacko G, Athyal R, Rajshekhar V: Intraoperative ultrasound in determining the extent of resection of parenchymal brain tumours - a comparative study with computed tomography and histopathology. **Acta Neurochirurgica 145:**743-748, 2003
17. Chandler WF, Knake JE, McGillicuddy JE, Lillehei KO, Silver TM: Intraoperative use of real-time ultrasonography in neurosurgery. **J Neurosurg 57:**157-163, 1982
18. Coenen VA, Krings T, Weidemann J, Hans FJ, Reinacher P, Gilsbach JM, et al: Sequential visualization of brain and fiber tract deformation during intracranial surgery with three-dimensional ultrasound: an approach to evaluate the effect of brain shift. **Neurosurgery 56:**133-141; discussion 133-141, 2005
19. Di Lorenzo N, Esposito V, Lunardi P, Delfini R, Fortuna A, Cantore G: A comparison of computerized tomography-guided stereotactic and ultrasound-guided techniques for brain biopsy. **J Neurosurg 75:**763-765, 1991
20. Dohrmann GJ, Rubin JM: Cervical spondylosis and syringomyelia: suboptimal results, incomplete treatment, and the role of intraoperative ultrasound. **Clin Neurosurg 34:**378-388, 1988
21. Dohrmann GJ, Rubin JM: Intraoperative ultrasound imaging of the spinal cord: syringomyelia, cysts, and tumors--a preliminary report. **Surg Neurol 18:**395-399, 1982
22. Dorward NL, Alberti O, Velani B, Gerritsen FA, Harkness WF, Kitchen ND, et al: Postimaging brain distortion: magnitude, correlates, and impact on neuronavigation. **J Neurosurg 88:**656-662, 1998
23. Dorward NL, Alberti O, Zhao J, Dijkstra A, Buurman J, Palmer JD, et al: Interactive image-guided neuroendoscopy: development and early clinical experience. **Minim Invasive Neurosurg 41:**31-34, 1998
24. Drake JM, Prudencio J, Holowaka S, Rutka JT, Hoffman HJ, Humphreys RP: Frameless stereotaxy in children. **Pediatr Neurosurg 20:**152-159, 1994
25. Drake JM, Rutka JT, Hoffman HJ: ISG Viewing Wand System. **Neurosurgery 34:**1094-1097, 1994
26. Dussik K: Possibility of using mechanical high frequency vibrations as a diagnostic aid, Z. f. **Neurol. Psychiatr 174:**153-168, 1942
27. Dyck P, Kurze T, Barrows HS: Intra-operative ultrasonic encephalography of cerebral mass lesions. **Bull Los Angeles Neurol Soc 31:**114-124, 1966
28. Enzmann DR, Irwin KM, Marshall WH, Silverberg GD, Britt RH, Hanbery JW: Intraoperative sonography through a burr hole: guide for brain biopsy. **AJNR Am J Neuroradiol 5:**243-246, 1984
29. Enzmann DR, Murphy-Irwin K, Silverberg GD, Djang WT, Golden JB: Spinal cord tumor imaging with CT and sonography. **AJNR Am J Neuroradiol 6:**95-97, 1985
30. Enzmann DR, Wheat R, Marshall WH, Bird R, Murphy-Irwin K, Karbon K, et al: Tumors of the central nervous system studied by computed tomography and ultrasound. **Radiology 154:**393-399, 1985
31. Fei Z, Zhang X, Jiang XF, Liu WP, Wang XL, Xie L: Removal of large benign cephalonasal tumours by transbasal surgery combined with endonasal endoscopic sinus surgery and neuronavigation. **J Craniomaxillofac Surg 35:**30-34, 2007
32. Fratzoglou M, Grunert P, Leite dos Santos A, Hwang P, Fries G: Symptomatic cysts of the cavum septi pellucidi and cavum vergae: the role of endoscopic

neurosurgery in the treatment of four consecutive cases. **Minim Invasive Neurosurg 46:**243-249, 2003
33. French LA, Wild JJ, Neal D: The experimental application of ultrasonics to the localization of brain tumors; preliminary report. **J Neurosurg 8:**198-203, 1951
34. Galloway RL, Jr., Maciunas RJ, Edwards CA, 2nd: Interactive image-guided neurosurgery. **IEEE Trans Biomed Eng 39:**1226-1231, 1992
35. Giorgi C: Intraoperative fusion of field images with CT/MRI data by means of a stereotactic mechanical arm. **Minim Invasive Neurosurg 37:**53-55, 1994
36. Glasauer FE, Schlagehauff RE: Intraoperaoperative echoencephalography. **J Clin Ultrasound 1:**134-141, 1973
37. Glossop N, Hu R: Assessment of vertebral body motion during spine surgery. **Spine 22:**903-909, 1997
38. Gohr H, Wedekind T: Der Ultraschall in der Medizin. **Journal of Molecular Medicine 19:**25-29, 1940
39. Golfinos JG, Fitzpatrick BC, Smith LR, Spetzler RF: Clinical use of a frameless stereotactic arm: results of 325 cases. **J Neurosurg 83:**197-205, 1995
40. Gooding GA, Edwards MS, Rabkin AE, Powers SK: Intraoperative real-time ultrasound in the localization of intracranial neoplasms. **Radiology 146:**459-462, 1983
41. Gronningsaeter A, Kleven A, Ommedal S, Aarseth TE, Lie T, Lindseth F, et al: SonoWand, an ultrasound-based neuronavigation system. **Neurosurgery 47:**1373-1379; discussion 1379-1380, 2000
42. Gronningsaeter A, Unsgard G, Ommedal S, Angelsen BA: Ultrasound-guided neurosurgery: a feasibility study in the 3-30 MHz frequency range. **Br J Neurosurg 10:**161-168, 1996
43. Gronningsaeter A, Unsgard G, Ommedal S, Angelsen BAJ: Ultrasound-guided neurosurgery: A feasibility study in the 3-30 MHz frequency range. **British Journal of Neurosurgery 10:**161-168, 1996
44. Grunert P, Darabi K, Espinosa J, Filippi R: Computer-aided navigation in neurosurgery. **Neurosurg Rev 26:**73-99; discussion 100-101, 2003
45. Grunert P, Müller-Forsell W, Darabi K, Reisch R, Busert C, Hopf N, et al: Basic Principles and Clinical Applications of Neuronavigation and Intraoperative Computed Tomography. **Computer Aided Surgery 3:**166-173, 1998
46. Grønningsæter Å, Kleven A, Ommedal S, Årseth TE, Lie T, Lindseth F, et al: SonoWand, an Ultrasound-based Neuronavigation System. **Neurosurgery 47:**1373-1380, 2000
47. Gumprecht H, Trost HA, Lumenta CB: Neuroendoscopy combined with frameless neuronavigation. **Br J Neurosurg 14:**129-131, 2000
48. Gumprecht HK, Widenka DC, Lumenta CB: BrainLab VectorVision Neuronavigation System: technology and clinical experiences in 131 cases. **Neurosurgery 44:**97-104; discussion 104-105, 1999
49. Hammoud MA, Ligon BL, elSouki R, Shi WM, Schomer DF, Sawaya R: Use of intraoperative ultrasound for localizing tumors and determining the extent of resection: a comparative study with magnetic resonance imaging. **J Neurosurg 84:**737-741, 1996

50. Hartkens T, Hill DL, Castellano-Smith AD, Hawkes DJ, Maurer CR, Jr., Martin AJ, et al: Measurement and analysis of brain deformation during neurosurgery. **IEEE Trans Med Imaging 22:**82-92, 2003
51. Hastreiter P, Rezk-Salama C, Soza G, Bauer M, Greiner G, Fahlbusch R, et al: Strategies for brain shift evaluation. **Med Image Anal 8:**447-464, 2004
52. Hata N, Dohi T, Iseki H, Takakura K: Development of a frameless and armless stereotactic neuronavigation system with ultrasonographic registration. **Neurosurgery 41:**608-613; discussion 613-604, 1997
53. Hernes TA, Ommedal S, Lie T, Lindseth F, Lango T, Unsgaard G: Stereoscopic navigation-controlled display of preoperative MRI and intraoperative 3D ultrasound in planning and guidance of neurosurgery: new technology for minimally invasive image-guided surgery approaches. **Minim Invasive Neurosurg 46:**129-137, 2003
54. Hernes TAN, Lindseth F, Selbekk T, Wollf A, Solberg OV, Harg E, et al: Computer-assisted 3D ultrasound-guided neurosurgery: technological contributions, including multimodal registration and advanced display, demonstrating future perspectives. **The International Journal of Medical Robotics and Computer Assisted Surgery 2:**45-59, 2006
55. Hill DL, Maurer CR, Jr., Maciunas RJ, Barwise JA, Fitzpatrick JM, Wang MY: Measurement of intraoperative brain surface deformation under a craniotomy. **Neurosurgery 43:**514-526; discussion 527-518, 1998
56. Hirschberg H, Unsgaard G: Incorporation of ultrasonic imaging in an optically coupled frameless stereotactic system. **Acta Neurochir Suppl 68:**75-80, 1997
57. Hlatky R, Jackson EF, Weinberg JS, McCutcheon IE: intraoperative neuronavigation using diffusion tensor MR tractography for the resection of a deep tumor adjacent to the corticospinal tract. **Stereotact Funct Neurosurg 83:**228-232, 2005
58. Hopf NJ, Grunert P, Darabi K, Busert C, Bettag M: Frameless neuronavigation applied to endoscopic neurosurgery. **Minim Invasive Neurosurg 42:**187-193, 1999
59. Hounsfield GN: Computerised tomographic axial scanning (tomography). 1 Description of the system. **Brit J Radiol 46:**1016-1023, 1973
60. Jodicke A, Deinsberger W, Erbe H, Kriete A, Boker DK: Intraoperative three-dimensional ultrasonography: an approach to register brain shift using multidimensional image processing. **Minim Invasive Neurosurg 41:**13-19, 1998
61. Jodicke A, Springer T, Boker DK: Real-time integration of ultrasound into neuronavigation: technical accuracy using a light-emitting-diode-based navigation system. **Acta Neurochir (Wien) 146:**1211-1220, 2004
62. Kamada K, Todo T, Morita A, Masutani Y, Aoki S, Ino K, et al: Functional monitoring for visual pathway using real-time visual evoked potentials and optic-radiation tractography. **Neurosurgery 57:**121-127; discussion 121-127, 2005
63. Kanno H, Ozawa Y, Sakata K, Sato H, Tanabe Y, Shimizu N, et al: Intraoperative power Doppler ultrasonography with a contrast-enhancing agent for intracranial tumors. **J Neurosurg 102:**295-301, 2005
64. Katisko JP, Koivukangas JP: Optically neuronavigated ultrasonography in an intraoperative magnetic resonance imaging environment. **Neurosurgery 60:**373-380; discussion 380-371, 2007

65. Kato A, Yoshimine T, Hayakawa T, Tomita Y, Ikeda T, Mitomo M, et al: A frameless, armless navigational system for computer-assisted neurosurgery. Technical note. **J Neurosurg 74:**845-849, 1991
66. Keles GE, Lamborn KR, Berger MS: Coregistration accuracy and detection of brain shift using intraoperative sononavigation during resection of hemispheric tumors. **Neurosurgery 53:**556-562; discussion 562-554, 2003
67. Kelly PJ: Technology in the resection of gliomas and the definition of madness. **J Neurosurg 101:**287-294, 2004
68. Kirschner M: Die Punktionstechnik und die Elektrokoagulation des Ganglion Gasseri. **Arch. Klin. Chir 176:**581, 1933
69. Knake JE, Chandler WF, Gabrielsen TO, Latack JT, Gebarski SS: Intraoperative sonography in the nonstereotaxic biopsy and aspiration of subcortical brain lesions. **AJNR Am J Neuroradiol 4:**672-674, 1983
70. Knake JE, Chandler WF, McGillicuddy JE, Gabrielsen TO, Latack JT, Gebarski SS, et al: Intraoperative sonography of intraspinal tumors: initial experience. **AJNR Am J Neuroradiol 4:**1199-1201, 1983
71. Knake JE, Chandler WF, McGillicuddy JE, Silver TM, Gabrielsen TO: Intraoperative sonography for brain tumor localization and ventricular shunt placement. **AJR Am J Roentgenol 139:**733-738, 1982
72. Knake JE, Gabrielsen TO, Chandler WF, Latack JT, Gebarski SS, Yang PJ: Real-time sonography during spinal surgery. **Radiology 151:**461-465, 1984
73. Koivukangas J, Louhisalmi Y, Alakuijala J, Oikarinen J: Ultrasound-controlled neuronavigator-guided brain surgery. **J Neurosurg 79:**36-42, 1993
74. Koivukangas J, Ylitalo J, Alasaarela E, Tauriainen A: Three-dimensional ultrasound imaging of brain for neurosurgery. **Ann Clin Res 18 Suppl 47:**65-72, 1986
75. Kosugi Y, Watanabe E, Goto J, Watanabe T, Yoshimoto S, Takakura K, et al: An articulated neurosurgical navigation system using MRI and CT images. **IEEE Trans Biomed Eng 35:**147-152, 1988
76. Krishnan R, Raabe A, Hattingen E, Szelenyi A, Yahya H, Hermann E, et al: Functional magnetic resonance imaging integrated neuronavigation: Correlation between lesion-to-motor cortex distance and outcome. **Neurosurgery 55:**904-914, 2004
77. Krybus W, Knepper A, Adams L, Rüger R, Meyer–Ebrecht D: Navigation Support for Surgery by Means of Optical Position Detection. **Proceedings of CAR 91:**362-366
78. Kunz U, Goldmann A, Bader C, Oldenkott P: Stereotactic and ultrasound guided minimal invasive surgery of subcortical cavernomas. **Minim Invasive Neurosurg 37:**17-20, 1994
79. Kurze T, Dyck P, Barrows HS: Neurosurgical evaluation of ultrasonic encephalograph. **J Neurosurg 22:**437-440, 1965
80. Lange SC, Howe JF, Shuman WP, Rogers JV: Intraoperative ultrasound detection of metastatic tumors in the central cortex. **Neurosurgery 11:**219-222, 1982
81. Langø T: Ultrasound Guided Surgery: Image Processing and Navigation.
82. Le Roux PD, Berger MS, Wang K, Mack LA, Ojemann GA: Low grade gliomas: comparison of intraoperative ultrasound characteristics with preoperative imaging studies. **Journal of Neuro-Oncology 13:**189-198, 1992

83. Leggett WB, Greenberg MM, Gannon WE, Dekel D, Gabe CJ: The Viewing Wand: a new system for three-dimensional computed tomography-correlated intraoperative localization. **Curr Surg 48:**674-678, 1991
84. Leksell L: Echo-encephalography. I. Detection of intracranial complications following head injury. **Acta Chir Scand 110:**301-315, 1956
85. Leksell L: Echoencephalography. II. Midline echo from the pineal body as an index of pineal displacement. **Acta Chir Scand 115:**255-259, 1958
86. LeRoux PD, Berger MS, Ojemann GA, Wang K, Mack LA: Correlation of intraoperative ultrasound tumor volumes and margins with preoperative computerized tomography scans. An intraoperative method to enhance tumor resection. **J Neurosurg 71:**691-698, 1989
87. LeRoux PD, Winter TC, Berger MS, Mack LA, Wang K, Elliott JP: A comparison between preoperative magnetic resonance and intraoperative ultrasound tumor volumes and margins. **J Clin Ultrasound 22:**29-36, 1994
88. Letteboer MM, Willems PW, Viergever MA, Niessen WJ: Brain shift estimation in image-guided neurosurgery using 3-D ultrasound. **IEEE Trans Biomed Eng 52:**268-276, 2005
89. Lindner D, Trantakis C, Renner C, Arnold S, Schmitgen A, Schneider J, et al: Application of intraoperative 3D ultrasound during navigated tumor resection. **Minim Invasive Neurosurg 49:**197-202, 2006
90. Lindseth F, Kaspersen JH, Ommedal S, Lango T, Bang J, Hokland J, et al: Multimodal image fusion in ultrasound-based neuronavigation: improving overview and interpretation by integrating preoperative MRI with intraoperative 3D ultrasound. **Comput Aided Surg 8:**49-69, 2003
91. Lindseth F, Lango T, Bang J, Nagelhus Hernes TA: Accuracy evaluation of a 3D ultrasound-based neuronavigation system. **Comput Aided Surg 7:**197-222, 2002
92. Longatti P, Fiorindi A, Feletti A, Baratto V: Endoscopic opening of the foramen of magendie using transaqueductal navigation for membrane obstruction of the fourth ventricle outlets. Technical note. **J Neurosurg 105:**924-927, 2006
93. Lovstakken L, Bjaerum S, Martens D, Torp H: Blood flow imaging--A new real-time, 2-D flow imaging technique. **IEEE Trans Ultrason Ferroelectr Freq Control 53:**289-299, 2006
94. Lunsford LD, Parrish R, Albright L: Intraoperative imaging with a therapeutic computed tomographic scanner. **Neurosurgery 15:**559-561, 1984
95. Masuzawa H, Kamitani H, Sato J, Inoya H, Hachiya J, Sakai F: [Intraoperative application of sector scanning electronic ultrasound in neurosurgery (author's transl)]. **Neurol Med Chir (Tokyo) 21:**277-285, 1981
96. Masuzawa H, Kanazawa I, Kamitani H, Sato J: Intraoperative ultrasonography through a burr-hole. **Acta Neurochir (Wien) 77:**41-45, 1985
97. Mathiesen T, Peredo I, Edner G, Kihlstrom L, Svensson M, Ulfarsson E, et al: Neuronavigation for arteriovenous malformation surgery by intraoperative three-dimensional ultrasound angiography. **Neurosurgery 60:**345-350; discussion 350-341, 2007
98. Mathiesen T, Peredo I, Edner G, Kihlström L, Svensson M, Ulfarsson E, et al: NEURONAVIGATION FOR ARTERIOVENOUS MALFORMATION SURGERY BY INTRAOPERATIVE THREE-DIMENSIONAL ULTRASOUND ANGIOGRAPHY. **Neurosurgery 60:**345, 2007

99. Maurer Jr CR, Fitzpatrick JM, Wang MY, Galloway Jr RL, Maciunas RJ, Allen GS: Registration of head volume images using implantable fiducialmarkers. **Medical Imaging, IEEE Transactions on 16:**447-462, 1997
100. McDermott MW, Gutin PH: Image-guided surgery for skull base neoplasms using the ISG viewing wand. Anatomic and technical considerations. **Neurosurg Clin N Am 7:**285-295, 1996
101. McKnight TR, von dem Bussche MH, Vigneron DB, Lu Y, Berger MS, McDermott MW, et al: Histopathological validation of a three-dimensional magnetic resonance spectroscopy index as a predictor of tumor presence. **J Neurosurg 97:**794-802, 2002
102. Mercier L, LangØ T, Lindseth F, Collins DL: A review of calibration techniques for freehand 3-D ultrasound systems. **Ultrasound in medicine & biology 31:**449-471, 2005
103. Mikulis DJ, Wood ML, Zerdoner OA, Poncelet BP: Oscillatory motion of the normal cervical spinal cord. **Radiology 192:**117-121, 1994
104. Mikuni N, Okada T, Enatsu R, Miki Y, Urayama S, Takahashi JA, et al: Clinical significance of preoperative fibre-tracking to preserve the affected pyramidal tracts during resection of brain tumours in patients with preoperative motor weakness. **J Neurol Neurosurg Psychiatry 78:**716-721, 2007
105. Montalvo BM, Quencer RM: Intraoperative sonography in spinal surgery: current state of the art. **Neuroradiology 28:**551-590, 1986
106. Muacevic A, Muller A: Image-guided endoscopic ventriculostomy with a new frameless armless neuronavigation system. **Comput Aided Surg 4:**87-92, 1999
107. Nabavi A, Black PM, Gering DT, Westin CF, Mehta V, Pergolizzi RS, Jr., et al: Serial intraoperative magnetic resonance imaging of brain shift. **Neurosurgery 48:**787-797; discussion 797-788, 2001
108. Nauta HJ: Error assessment during "image guided" and "imaging interactive" stereotactic surgery. **Comput Med Imaging Graph 18:**279-287, 1994
109. Nimsky C, Ganslandt O, Cerny P, Hastreiter P, Greiner G, Fahlbush R: Quantification of, Visulaization of, and Compnsating for Brain Shift Using Intraoperative Magnetic Resonance Imaging. **Neurosurgery 47:**1070-1080, 2000
110. Nimsky C, Ganslandt O, Fahlbusch R: Implementation of fiber tract navigation. **Neurosurgery 58:**ONS-292-303; discussion ONS-303-294, 2006
111. Nimsky C, Ganslandt O, Hastreiter P, Wang RP, Benner T, Sorensen AG, et al: Intraoperative diffusion-tensor MR imaging: Shifting of white matter tracts during neurosurgical procedures - Initial experience. **Radiology 234:**218-225, 2005
112. Olivier A, Alonso-Vanegas M, Comeau R, Peters TM: Image-guided surgery of epilepsy. **Neurosurg Clin N Am 7:**229-243, 1996
113. Olivier A, Germano IM, Cukiert A, Peters T: Frameless stereotaxy for surgery of the epilepsies: preliminary experience. Technical note. **J Neurosurg 81:**629-633, 1994
114. Pelizzari CA, Chen GTY, Spelbring DR, Weichselbaum RR, Chen CT: Accurate Three-Dimensional Registration of CT, PET, and/or MR Images of the Brain. **Journal of Computer Assisted Tomography 13:**20, 1989
115. Peters TM: Image-guided surgery: From X-rays to Virtual Reality. **Computer Methods in Biomechanics and Biomedical Engineering 4:**27-57, 2000

116. Platt JF, Rubin JM, Chandler WF, Bowerman RA, DiPietro MA: Intraoperative spinal sonography in the evaluation of intramedullary tumors. **J Ultrasound Med 7:**317-325, 1988
117. Pollack IF, Albright AL, Adelson PD, Fitz CR: The role of frameless stereotactic techniques in the treatment of pediatric CNS lesions. **Pediatr Neurol 13:**209-216, 1995
118. Quencer RM: The injured spinal cord. Evaluation with magnetic resonance and intraoperative sonography. **Radiol Clin North Am 26:**1025-1045, 1988
119. Ram Z, Shawker TH, Bradford MH, Doppman JL, Oldfield EH: Intraoperative ultrasound-directed resection of pituitary tumors. **J Neurosurg 83:**225-230, 1995
120. Rasmussen IA, Jr., Lindseth F, Rygh OM, Berntsen EM, Selbekk T, Xu J, et al: Functional neuronavigation combined with intra-operative 3D ultrasound: initial experiences during surgical resections close to eloquent brain areas and future directions in automatic brain shift compensation of preoperative data. **Acta Neurochir (Wien) 149:**365-378, 2007
121. Regelsberger J: Intraoperative sonography of intra-and extramedullary tumors. **Ultrasound in Med & Biol. 31:**593-598, 2005
122. Regelsberger J, Lohmann F, Helmke K, Westphal M: Ultrasound-guided surgery of deep seated brain lesions. **Eur J Ultrasound 12:**115-121, 2000
123. Reid MH: Ultrasonic visualization of a cervical cord cystic astrocytoma. **AJR Am J Roentgenol 131:**907-908, 1978
124. Reinertsen I, Lindseth F, Unsgaard G, Collins DL: Clinical validation of vessel-based registration for correction of brain-shift. **Med Image Anal**, 2007
125. Reinges MHT, Nguyen HH, Krings T, Hutter BO, Rohde V, Gilsbach JM: Course of brain shift during microsurgical resection of supratentorial cerebral lesions: limits of conventional neuronavigation. **Acta Neurochirurgica 146:**369-377, 2004
126. Resch KD: Endo-neuro-sonography: first clinical series (52 cases). **Childs Nerv Syst 19:**137-144, 2003
127. Resch KD, Perneczky A, Schwarz M, Voth D: Endo-neuro-sonography: principles of 3-D technique. **Childs Nerv Syst 13:**616-621, 1997
128. Rhoten RL, Luciano MG, Barnett GH: Computer-assisted endoscopy for neurosurgical procedures: technical note. **Neurosurgery 40:**632-637; discussion 638, 1997
129. Roberts DW, Hartov A, Kennedy FE, Miga MI, Paulsen KD: Intraoperative brain shift and deformation: a quantitative analysis of cortical displacement in 28 cases. **Neurosurgery 43:**749-758; discussion 758-760, 1998
130. Roberts DW, Nakajima T, Brodwater B, Pavlidis J, Friets E, Fagan E, et al: Further development and clinical application of the stereotactic operating microscope. **Stereotact Funct Neurosurg 58:**114-117, 1992
131. Roberts DW, Strohbehn JW, Hatch JF, Murray W, Kettenberger H: A frameless stereotaxic integration of computerized tomographic imaging and the operating microscope. **J Neurosurg 65:**545-549, 1986
132. Robinson JR, Jr., Golfinos JG, Spetzler RF: Skull base tumors. A critical appraisal and clinical series employing image guidance. **Neurosurg Clin N Am 7:**297-311, 1996
133. Rogers JV, 3rd, Shuman WP, Hirsch JH, Lange SC, Howe JF, Burchiel K: Intraoperative neurosonography: application and technique. **AJNR Am J Neuroradiol 5:**755-760, 1984

134. Roth J, Biyani N, Beni-Adani L, Constantini S: Real-time neuronavigation with high-quality 3D ultrasound SonoWand in pediatric neurosurgery. **Pediatr Neurosurg 43:**185-191, 2007
135. Rubin JM: Power doppler. **Eur Radiol 9 Suppl 3:**S318-322, 1999
136. Rubin JM, Dohrmann GJ: Efficacy of intraoperative US for evaluating intracranial masses. **Radiology 157:**509-511, 1985
137. Rubin JM, Dohrmann GJ: Intraoperative neurosurgical ultrasound in the localization and characterization of intracranial masses. **Radiology 148:**519-524, 1983
138. Rubin JM, Dohrmann GJ: The spine and spinal cord during neurosurgical operations: real-time ultrasonography. **Radiology 155:**197-200, 1985
139. Rubin JM, Dohrmann GJ, Greenberg M, Duda EE, Beezhold C: Intraoperative sonography of meningiomas. **AJNR Am J Neuroradiol 3:**305-308, 1982
140. Rubin JM, Hatfield MK, Chandler WF, Black KL, DiPietro MA: Intracerebral arteriovenous malformations: intraoperative color Doppler flow imaging. **Radiology 170:**219-222, 1989
141. Rubin JM, Mirfakhraee M, Duda EE, Dohrmann GJ, Brown F: Intraoperative ultrasound examination of the brain. **Radiology 137:**831-832, 1980
142. Ryan MJ, Erickson RK, Levin DN, Pelizzari CA, Macdonald RL, Dohrmann GJ: Frameless stereotaxy with real-time tracking of patient head movement and retrospective patient-image registration. **J Neurosurg 85:**287-292, 1996
143. Sandeman DR, Gill SS: The impact of interactive image guided surgery: the Bristol experience with the ISG/Elekta viewing Wand. **Acta Neurochir Suppl 64:**54-58, 1995
144. Schiffbauer H: Neuronavigation in brain tumor surgery. **Department of Neurosurgery, Oulu**, 1999
145. Schlondorff G, Mosges R, Meyer-Ebrecht D, Krybus W, Adams L: [CAS (computer assisted surgery). A new procedure in head and neck surgery]. **Hno 37:**187-190, 1989
146. Schroeder HW, Wagner W, Tschiltschke W, Gaab MR: Frameless neuronavigation in intracranial endoscopic neurosurgery. **J Neurosurg 94:**72-79, 2001
147. Selbekk T, Bang J, Unsgaard G: Strain processing of intraoperative ultrasound images of brain tumours: initial results. **Ultrasound Med Biol 31:**45-51, 2005
148. Sergeeva O, Uhlemann F, Schackert G, Hergeth C, Morgenstern U, Steinmeier R: Integration of intraoperative 3D-ultrasound in a commercial navigation system. **Zentralbl Neurochir 67:**197-203, 2006
149. Sipos EP, Tebo SA, Zinreich SJ, Long DM, Brem H: In Vivo Accuracy Testing and Clinical Experience with the ISG Viewing Wand. **Neurosurgery 39:**194, 1996
150. Smith KR, Frank KJ, Bucholz RD: The NeuroStation--a highly accurate, minimally invasive solution to frameless stereotactic neurosurgery. **Comput Med Imaging Graph 18:**247-256, 1994
151. Smith SJ, Vogelzang RL, Marzano MI, Cerullo LJ, Gore RM, Neiman HL: Brain edema: ultrasound examination. **Radiology 155:**379-382, 1985
152. Solberg OV, Lindseth F, Torp H, Blake RE, Nagelhus Hernes TA: Freehand 3D Ultrasound Reconstruction Algorithms—A Review. **Ultrasound in Medicine & Biology 33:**991-1009, 2007
153. Spetzger U, Laborde G, Gilsbach JM: Frameless neuronavigation in modern neurosurgery. **Minim Invasive Neurosurg 38:**163-166, 1995

154. Spiegel EA, Wycis HJ, Marks M, Lee A: Stereotactic apparatus for operations. **Science 106:**439-450, 1947
155. Stadlbauer A, Moser E, Gruber S, Nimsky C, Fahlbusch R, Ganslandt O: Integration of biochemical images of a tumor into frameless stereotaxy achieved using a magnetic resonance imaging/magnetic resonance spectroscopy hybrid data set. **J Neurosurg 101:**287-294, 2004
156. Sure U, Benes L, Bozinov O, Woydt M, Tirakotai W, Bertalanffy H: Intraoperative landmarking of vascular anatomy by integration of duplex and Doppler ultrasonography in image-guided surgery. Technical note. **Surgical Neurology 63:**133-141, 2005
157. Sutcliffe JC, Battersby RD: Intraoperative ultrasound-guided biopsy of intracranial lesions: comparison with freehand biopsy. **Br J Neurosurg 5:**163-168, 1991
158. Takizawa T: Isocentric stereotactic three-dimensional digitizer for neurosurgery. **Stereotact Funct Neurosurg 60:**175-193, 1993
159. Tan KK, Grzeszczuk R, Levin DN, Pelizzari CA, Chen GT, Erickson RK, et al: A frameless stereotactic approach to neurosurgical planning based on retrospective patient-image registration. Technical note. **J Neurosurg 79:**296-303, 1993
160. Tanaka K, Ito K, Wagai T: The localization of brain tumors by ultrasonic techniques. A clinical review of 111 cases. **J Neurosurg 23:**135-147, 1965
161. Tirakotai W, Miller D, Heinze S, Benes L, Bertalanffy H, Sure U: A novel platform for image-guided ultrasound. **Neurosurgery 58:**710-718; discussion 710-718, 2006
162. Trantakis C, Tittgemeyer M, Schneider JP, Lindner D, Winkler D, Strauss G, et al: Investigation of time-dependency of intracranial brain shift and its relation to the extent of tumor removal using intra-operative MRI. **Neurological Research 25:**9-12, 2003
163. Trobaugh JW, Richard WD, Smith KR, Bucholz RD: Frameless stereotactic ultrasonography: method and applications. **Comput Med Imaging Graph 18:**235-246, 1994
164. Trobaugh JW, Trobaugh DJ, Richard WD: Three-dimensional imaging with stereotactic ultrasonography. **Comput Med Imaging Graph 18:**315-323, 1994
165. Tronnier VM, Wirtz CR, Knauth M, Lenz G, Pastyr O, Bonsanto MM, et al: Intraoperative diagnostic and interventional magnetic resonance imaging in neurosurgery. **Neurosurgery 40:**891-900; discussion 900-892, 1997
166. Unsgaard G, Ommedal S, Muller T, Gronningsaeter A, Nagelhus Hernes TA: Neuronavigation by intraoperative three-dimensional ultrasound: initial experience during brain tumor resection. **Neurosurgery 50:**804-812; discussion 812, 2002
167. Unsgaard G, Ommedal S, Rygh O, Lindseth F: Operation of Arteriovenous Malformations Assisted by Stereoscopic Navigation-controlled Display of Preoperative Magnetic Resonance Angiography and Intraoperative Ultrasound Angiography. **Neurosurgery 56:**281-290, 2005
168. Unsgaard G, Rygh OM, Selbekk T, Muller TB, Kolstad F, Lindseth F, et al: Intra-operative 3D ultrasound in neurosurgery. **Acta Neurochir (Wien) 148:**235-253, 2006
169. Unsgaard G, Selbekk T, Brostrup Muller T, Ommedal S, Torp SH, Myhr G, et al: Ability of navigated 3D ultrasound to delineate gliomas and metastases--

comparison of image interpretations with histopathology. **Acta Neurochir (Wien) 147:**1259-1269; discussion 1269, 2005
170. van Velthoven V, Auer LM: Practical application of intraoperative ultrasound imaging. **Acta Neurochir (Wien) 105:**5-13, 1990
171. Voorhies RM, Patterson Jr RH: Preliminary experience with intra-operative ultrasonographic localization of brain tumors. **Ultra-sound in medicine. Radiology Nuclear Med October:**8-10, 1980
172. Watanabe E, Mayanagi Y, Kosugi Y, Manaka S, Takakura K: Open surgery assisted by the neuronavigator, a stereotactic, articulated, sensitive arm. **Neurosurgery 28:**792-799; discussion 799-800, 1991
173. Watanabe E, Watanabe T, Manaka S, Mayanagi Y, Takakura K: Three-dimensional digitizer (neuronavigator): new equipment for computed tomography-guided stereotaxic surgery. **Surg Neurol 27:**543-547, 1987
174. Wilberger JE, Jr., Maroon JC, Prostko ER, Baghai P, Beckman I, Deeb Z: Magnetic resonance imaging and intraoperative neurosonography in syringomyelia. **Neurosurgery 20:**599-605, 1987
175. Wild JJ, Reid JM: Further pilot echographic studies on the histologic structure of tumors of the living intact human breast. **Am J Pathol 28:**839-861, 1952
176. Wirtz CR, Albert FK, Schwaderer M, Heuer C, Staubert A, Tronnier VM, et al: The benefit of neuronavigation for neurosurgery analyzed by its impact on glioblastoma surgery. **Neurological Research 22:**354-360, 2000
177. Wirtz CR, Knauth M, Staubert A, Bonsanto MM, Sartor K, Kunze S, et al: Clinical evaluation and follow-up results for intraoperative magnetic resonance imaging in neurosurgery. **Neurosurgery 46:**1112-1120; discussion 1120-1112, 2000
178. Woydt M, Greiner K, Perez J, Krone A, Roosen K: Intraoperative color duplex sonography of basal arteries during aneurysm surgery. **J Neuroimaging 7:**203-207, 1997
179. Woydt M, Krone A, Becker G, Schmidt K, Roggendorf W, Roosen K: Correlation of intra-operative ultrasound with histopathologic findings after tumour resection in supratentorial gliomas. A method to improve gross total tumour resection. **Acta Neurochir (Wien) 138:**1391-1398, 1996
180. Woydt M, Krone A, Soerensen N, Roosen K: Ultrasound-guided neuronavigation of deep-seated cavernous haemangiomas: clinical results and navigation techniques. **British Journal of Neurosurgery 15:**485-495, 2001
181. Woydt M, Perez J, Meixensberger J, Krone A, Soerensen N, Roosen K: Intra-operative colour-duplex-sonography in the surgical management of cerebral AV-malformations. **Acta Neurochir (Wien) 140:**689-698, 1998
182. Zamorano LJ, Nolte L, Kadi AM, Jiang Z: Interactive intraoperative localization using an infrared-based system. **Stereotact Funct Neurosurg 63:**84-88, 1994
183. Zweifel HJ, Reinhardt HF, Horstmann GA, Amrein E: [CT/MRI correlated stereometry with ultrasound in brain surgery]. **Ultraschall Med 11:**72-75, 1990

PAPER 1

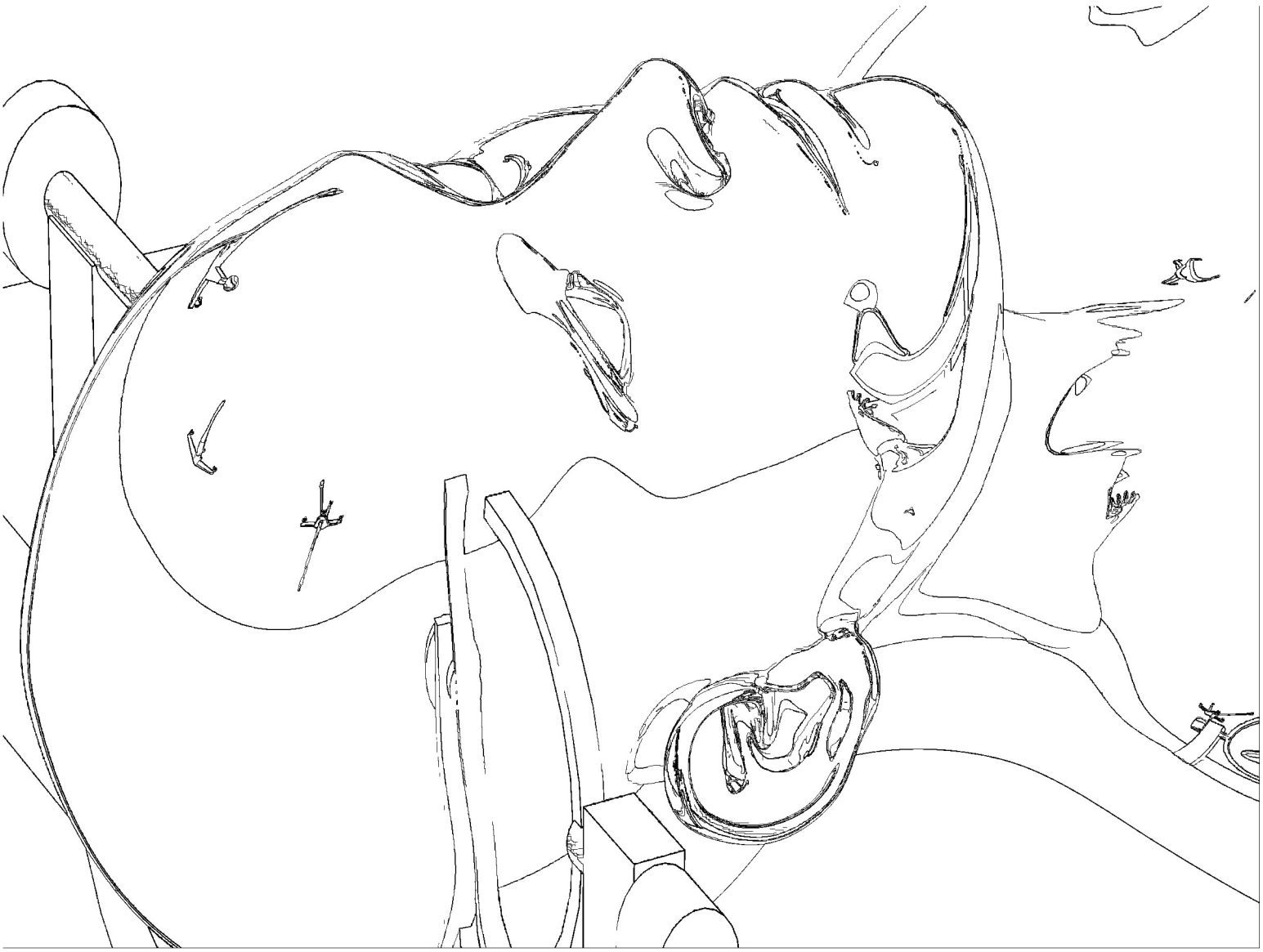

Acta Neurochir (Wien)
DOI 10.1007/s00701-008-0017-3

CLINICAL ARTICLE

Comparison of navigated 3D ultrasound findings with histopathology in subsequent phases of glioblastoma resection

Ola Morten Rygh · Tormod Selbekk · Sverre Helge Torp · Stian Lydersen · Toril Anita Nagelhus Hernes · Geirmund Unsgaard

Received: 11 November 2007 / Accepted: 22 June 2008

Abstract
Objective The purpose of the study was to compare the ability of navigated 3D ultrasound to distinguish tumour and normal brain tissue at the tumour border zone in subsequent phases of resection.
Materials and methods Biopsies were sampled in the tumour border zone as seen in the US images before and during surgery. After resection, biopsies were sampled in the resection cavity wall. Histopathology was compared with the surgeon's image findings.
Results Before resection, the tumour border was delineated by ultrasound with high specificity and sensitivity (both 95%). During resection, ultrasound had acceptable sensitivity (87%), but poor specificity (42%), due to biopsies falsely classified as tumour by the surgeon. After resection, sensitivity was poor (26%), due to tumour or infiltrated tissue in several biopsies deemed normal by ultrasound, but the specificity was acceptable (88%).
Conclusions Our study shows that although glioblastomas are well delineated prior to resection, there seem to be overestimation of tumour tissue during resection. After resection tumour remnants and infiltrated brain tissue in the resection cavity wall may be undetected. We believe that the benefits of intraoperative ultrasound outweigh the shortcomings, but users of intraoperative ultrasound should keep the limitations shown in our study in mind.

O. M. Rygh
Department of Radiology, St.Olav University Hospital, Trondheim, Norway

O. M. Rygh · S. H. Torp · G. Unsgaard
Department of Neuroscience, Norwegian University of Science and Technology, Trondheim, Norway

T. Selbekk · T. A. N. Hernes
SINTEF Health Research, Trondheim, Norway

O. M. Rygh · T. Selbekk · T. A. N. Hernes · G. Unsgaard
National Centre for 3D Ultrasound in Surgery, St.Olav University Hospital, Trondheim, Norway

S. H. Torp
Department of Pathology and Medical Genetics, St Olav University Hospital, Trondheim, Norway

S. Lydersen
Unit for Applied Clinical Research, Department of Cancer Research and Molecular Medicine, Norwegian University of Science and Technology, Trondheim, Norway

G. Unsgaard
Department of Neurosurgery, St.Olav University Hospital, Trondheim, Norway

T. A. N. Hernes
Department of Circulation and Medical Imaging, Norwegian University of Science and Technology, Trondheim, Norway

S. H. Torp
Section of Morphology, Department of Laboratory Medicine, Children's and Women's Health, Faculty of Medicine, Norwegian University of Science and Technology (NTNU), Trondheim, Norway

O. M. Rygh (✉)
Vegmesterstien 17c, 7022 Trondheim, Norway
e-mail: ola.rygh@ntnu.no

Keywords Brain tumour surgery · Biopsies · Histopathology · Intraoperative imaging · Neuronavigation · Three-dimensional ultrasound imaging

Abbreviations

US	ultrasound
3D	three dimensional
MHz	megahertz
PPV	positive predictive value
NPV	negative predictive value
ROC	receiver operating characteristics
AUC	area under curve

Background

In the surgical treatment of glioblastomas the goal is to perform the most complete resection possible without damaging normal tissue [2, 17]. Neuronavigation systems have become part of the routine tools assisting the surgeon in achieving this goal. Intraoperative imaging appears to be necessary to maintain accuracy of neuronavigation during subsequent stages of tumour resection [19, 25, 29]. To be of value, intraoperative imaging modalities must reliably discriminate between tumour and normal tissue in the subsequent stages of surgery. At present, the alternatives for intraoperative imaging in brain tumour surgery are MRI and ultrasound [10, 11, 20, 24, 31]. Although recognized to be useful for detecting residual tumour during resection [9, 30, 35, 36], it is not known how intraoperative factors affect the ability of ultrasound to delineate tumour. The aim of the present study was to assess the ability of intraoperative 3D ultrasound in neuronavigation to distinguish tumour and normal brain tissue in the tumour border zone, before, during and after resection.

Materials and methods

Patients and biopsies

Nineteen patients (four females and 15 males, average age 59, age range 45–83 years) with the final diagnosis of glioblastoma were included in the present study. The patients were included in the period 2003–2006. A total of 301 biopsies were acquired, 186 biopsies were included in this study. The study was approved by the Regional Research Ethics Committee in medicine in Mid-Norway and the patients signed an informed consent form before the operation.

Neuronavigation equipment and intraoperative 3D ultrasound imaging

A 3D ultrasound based image guidance system was used; SonoWand®, equipped with a 5 MHz probe with tracking. The biopsy forceps used in the study was equipped with a tracking frame, which enabled image guided biopsies (Fig. 1). This system is described in further detail in other papers [8, 21, 37]. Preoperative MRI (T1 with contrast enhancement, T2 and FLAIR) was imported in the neuronavigation system and used for planning and anatomical orientation, but not during biopsy sampling. 3D ultrasound data was acquired immediately before biopsy sampling in each phase (Fig. 2). When a resection cavity had been created, the cavity was filled with saline before 3D ultrasound acquisition. The saline was removed afterwards.

Image-guided biopsy sampling and analysis

The biopsies were sampled in three different phases of resection; (1) After opening the dura, immediately before starting the resection. (2) After most resection had been performed, but with some residual tumour left. (3) After completed resection, having removed all detected/known residual tumour (either detected visually or by use of intraoperative ultrasound) except in eloquent areas. The biopsy forceps was calibrated to the navigation system by positioning the tip of the biopsy forceps at a reference point on the patient reference frame (Fig. 1.) The position and trajectory of the biopsy forceps was displayed on two perpendicular image slices on the neuronavigation unit, marking the biopsy site. The surgeon's assumption on whether the biopsy was sampled in tumour or normal tissue based on the ultrasound image findings was noted at the time of biopsy sampling. The surgeon classified the biopsies as "tumour", "tumour, uncertain", "normal uncertain" and "normal". Images (snapshots) from the neuronavigation system taken at the time of biopsy sampling were stored for further processing and analysis.

The biopsies were collected from the border-zone of the tumour, not further from the assumed tumour border in the US images (as judged by the surgeon) than 7 mm and not closer than 2 mm. After completed resection however, biopsies were only collected from the resection cavity wall. Before and during resection, two to four biopsies were collected in assumed solid tumour tissue, while one to three biopsies were sampled from assumed normal brain tissue. All biopsies included in the study were postoperatively controlled to ensure that they were sampled in the 2–7 mm distance from the tumour border as defined from the navigation images. Biopsies outside the 2–7 mm area of interest were excluded, and this was the most frequent reason for exclusion of biopsies. In cases of doubt, the

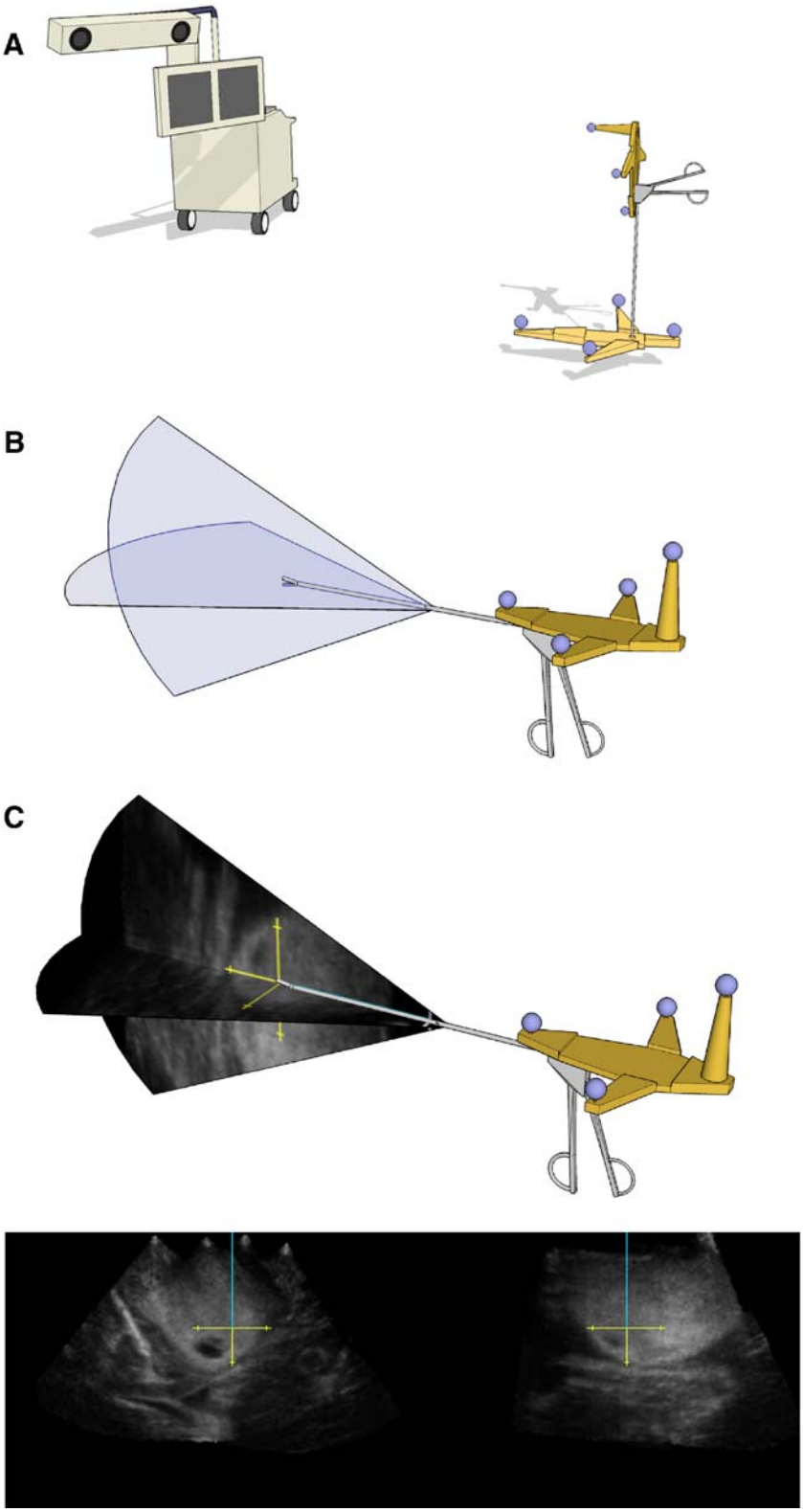

Fig. 1 Biopsy sampling method. **a** The biopsy forceps is calibrated to the navigation system by positioning the tip of the forceps in a known reference point on the patient reference frame, in the shape of a small cone with a hole in the middle. **b** Two perpendicular planes are determined by the position and trajectory of the biopsy forceps. **c** The 3D ultrasound data volume is sliced in the two perpendicular planes, displayed on screen (*bottom*). The tip of the biopsy forceps is thus indicated in the two image planes, marking the site for biopsy sampling

screenshots were analyzed with an edge-detection algorithm (described elsewhere [38]). The shortest distance between the tip of the biopsy forceps and the detected border was then found. Biopsies where the pathologist could not categorize the biopsy, for example, because of too small or traumatized biopsies, were also excluded.

The majority of biopsies (176 of 186 included biopsies) was fixed in buffered formalin and embedded in paraffin.

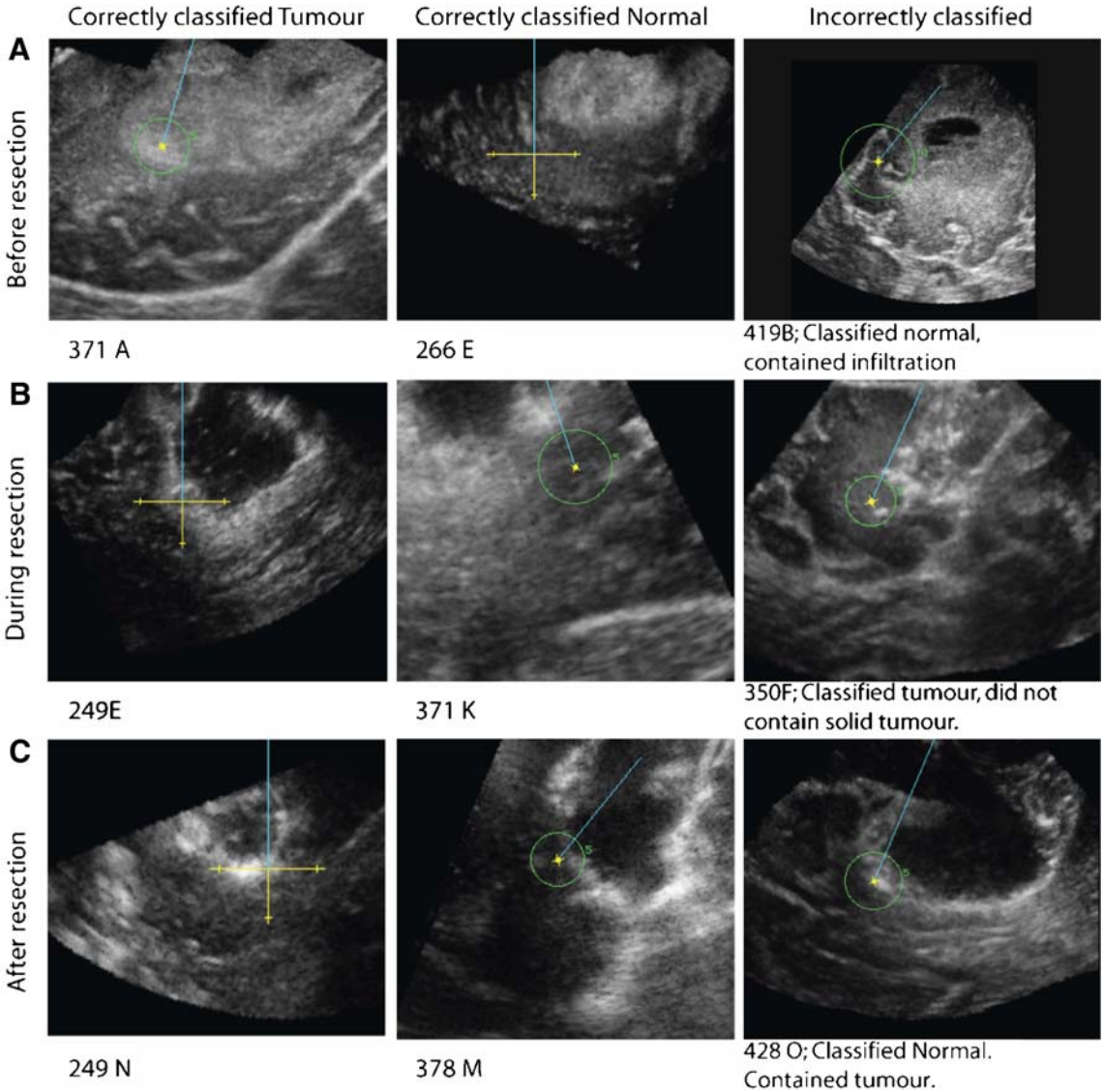

Fig. 2 Biopsy examples. **a** Screenshots from biopsy sampling before resection. *Left*: Biopsy sampled from area interpreted as tumour, confirmed by histopathology. *Middle*: Biopsy sampled from site interpreted as normal, confirmed by histopathology. *Right*: Biopsy sampled from site interpreted as normal, histopathology showed infiltration. **b** Screenshots from biopsy sampling during resection. *Left*: Biopsy sampled from site interpreted as tumour, confirmed by histopathology. *Middle*: Biopsy sampled from site interpreted as normal, confirmed by histopathology. *Right*: Biopsy sampled from site interpreted as tumour, but the pathologist saw no certain tumour tissue. **c** Screenshots from biopsy sampling after resection. *Left*: biopsy sampled from site interpreted as "tumour, uncertain", tumour confirmed by histopathology. *Middle*: Biopsy sampled from site interpreted as normal, confirmed by histopathology. *Right*: Biopsy sampled from site interpreted as normal, but histopathology showed tumour

Ten biopsies were prepared as frozen sections. The sections were stained with hematoxylin and eosin. A senior neuropathologist (SHT) examined the biopsies according to the WHO classification [1]. All histopathological analyses were performed without prior knowledge of the image information. The biopsies were classified as "tumour"/"infiltration zone"/"not tumour". All but three of the patients had a postoperative MRI within 48 h.

Statistical methods

To calculate specificity, sensitivity, PPV and NPV, the cells in the original 3×4 result table from each phase (Table 2) were combined to create a 2×2 table for each phase of the operation: Biopsies deemed "normal" and "normal, uncertain" by the surgeon were combined, and likewise biopsies deemed "tumour" and "tumour, uncertain" were combined.

Furthermore, biopsies that the pathologist classified as "infiltration zone" were combined with those classified as "tumour". The ROC curves were constructed by calculating sensitivity and specificity for the three different possible cut-off points for surgeon's judgment, one ROC curve for each phase of resection (Fig. 3).

Results

Of 301 total biopsies acquired, 186 were included in our analyses. Table 1 shows the number of biopsies included/excluded in each phase of surgery. The histopathological diagnoses of the biopsies and the corresponding ultrasound findings for each of the stages of resection are shown in Table 2. The calculated values for specificity, sensitivity, NPV and PPV are listed in Table 3. Before resection, both sensitivity and specificity were 95%, while PPV and NPV were 98% and 90%, respectively. During resection, sensitivity was 88% but specificity had dropped to 42%. PPV and NPV was 73% and 67% respectively. After resection, sensitivity was 26% and specificity was 88%, while PPV and NPV both were 62%. The ROC curve for ultrasound in each stage of surgery is displayed in Fig. 3, and the area under the curve (AUC) is stated in the figure legend.

Although comparison of ultrasound and MRI was not a part of the study protocol, 16 of the 19 patients had early postoperative MRI (within 72 h). In 13 of these 16 patients the neurosurgeon also assessed the resection grade at the end of resection using 3D ultrasound. Among these, ten patients were considered either 90–95% or >95% resected. Two of the10 patients had residual tumour on early postoperative MRI; one patient considered 90–95% resected and another considered >95% resected. The other eight patients had no residual tumour found on early postoperative MRI. In the remaining three patients (of the 13 with both early postoperative MRI and resection grade assessment), residual tumour was intentionally left behind because of unacceptable risk of neurological damage. Two of them had residual tumour on postoperative MRI, while one was considered to possibly have residual tumour.

Sixteen of the 19 patients had a good outcome with no new neurological deficits.

Two of the patients had a fair outcome with mild new neurological deficits, and one patient had a poor outcome,

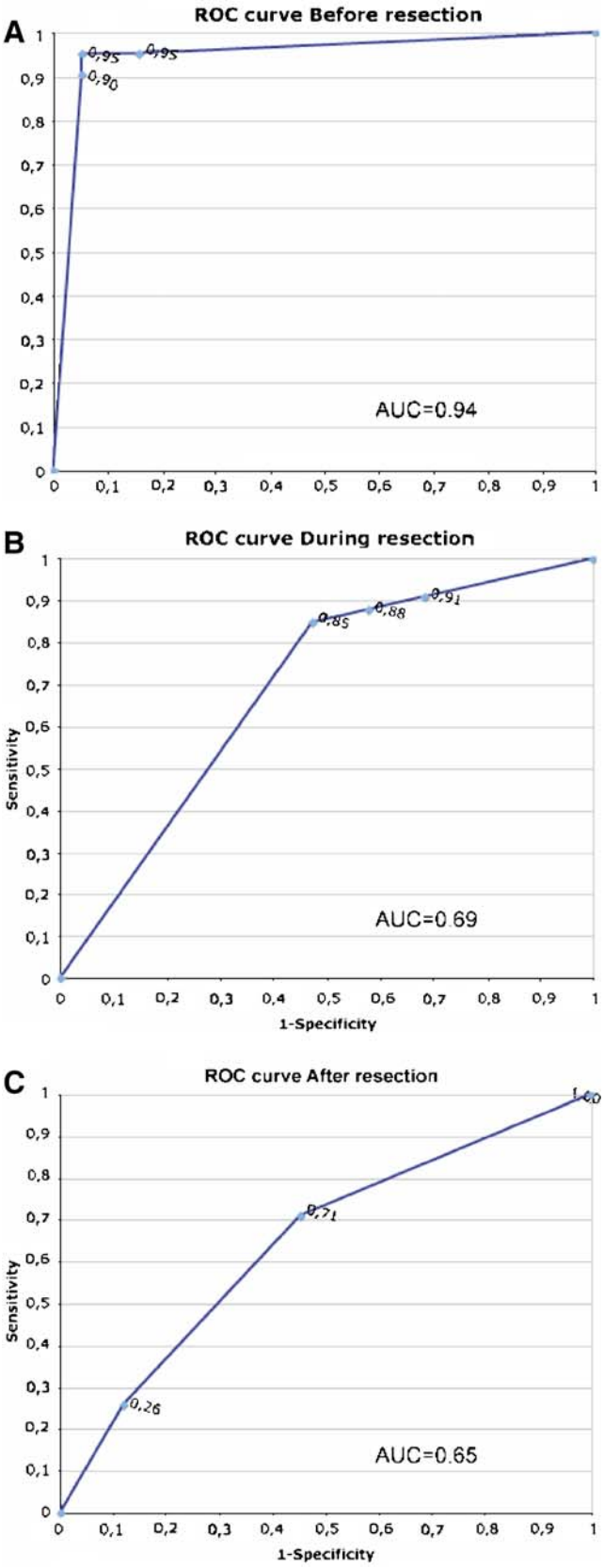

Fig. 3 ROC curves. ROC curves for the ability of ultrasound to distinguish tumour from normal tissue. **a** ROC curve before resection, showing high accuracy (AUC=0.94). **b** ROC curve during resection. Compared to the ROC curve before resection the accuracy of ultrasound is decreased. (AUC=0.69). **c** ROC curve after resection. Compared to the ROC curve before and during resection, the accuracy is further decreased (AUC=0.65)

Table 1 Biopsies

The table shows the number of biopsies sampled in each phase of the resection, and the number of biopsies excluded and included. In the lower part of the table the average number of biopsies in each patient is shown.

Parameter		Included	Excluded	Total
Total number of biopsies for patients included in study	Before resection	61	56	117
	During resection	52	47	99
	After resection	73	12	85
Average number of biopsies per patient	Before	3.2	2.9	NA
	During	2.7	2.5	NA
	After	3.8	0.6	NA
Total number of biopsies (overall)				301

with hemiparesis and aphasia. None of the patients had complications related to the procedure.

Discussion

General considerations

Delineation of gliomas poses a challenge to any imaging modality, as tumour cells infiltrate the normal brain tissue beyond the solid tumour border. In this sense, definition of a specific tumour border is impossible. For practical purposes, however, to delineate a glioblastoma usually means to outline the solid part of a tumour, of which removal is the goal of surgical resection.

Several authors have evaluated different diagnostic imaging modalities for delineation of gliomas, comparing image findings with histopathology [3, 5–7, 13, 16, 22, 23, 28, 32]. Also infiltrated brain tissue may be detected by new imaging techniques [28, 32]. In neuronavigation, intraoperative imaging is now increasingly recognized as important to amend for inaccuracy due to brain shift, and facilitate detection of residual tumour. Ultrasound and MRI are the commonly used modalities in this regard [12, 15, 26, 27, 36, 39]. However, it is not entirely known to what degree intraoperative factors affect intraoperative imaging, and the studies comparing image findings with histopathology in the intraoperative setting are scarce. Reporting on intraoperative MRI, Sutherland [34], found that intraoperatively, the contrast-enhancing margin advanced beyond the preoperatively defined contrast limits, and that biopsy samples from this zone contained tumour tissue. Knauth [14] argue that surgically induced contrast enhancement may be misinterpreted as residual tumour in intraoperative MRI, but only in one case was this confirmed with a biopsy, obtained in a contrast-enhancing area which proved to contain normal tissue. Surgically induced contrast enhancement in intraoperative MRI at the resection border, mimicking residual tumour, is also mentioned by other authors [26, 33, 39]. In ultrasound, reverberations, refraction of the ultrasound beam, artefacts due to slice thickness among others, may all cause imaging artefacts which may be misleading. During tumour resection, air bubbles, debris, blood, and the rough surface of the tumour cavity wall probably increase the occurrence of imaging artefacts in ultrasound. In addition other, unknown factors may affect the ultrasound images during the course of a tumour resection. Comparing ultrasound findings after (completed) resection, Chacko [4] found that biopsies taken from the tumour margins agreed with ultrasound image findings in the majority of samples, however, there were instances (16%) when the ultrasound reported tumour while the biopsies were negative. LeRoux et al. [18] used intraoperative ultrasound to facilitate gross total resection of brain tumours and obtained biopsies from the resection

Table 2 Image finding/histopathology of biopsies according to resection phase

The table shows the interpretation of the ultrasound image in columns and the histopathological diagnosis in rows, for each of the three subsequent phases of resection.

Resection phase	Histopathological diagnosis	Interpretation of ultrasound image			
		"Normal"	"Normal, uncertain"	"Tumour, uncertain"	"Tumour"
Before resection	Tumour	0	0	0	32
	Infiltration	2	0	2	6
	Normal	16	2	0	1
During resection	Tumour	1	0	0	22
	Infiltration	2	1	1	6
	Normal	6	2	2	9
After resection	Tumour	4	4	7	0
	Infiltration	5	10	1	0
	Normal	23	14	5	0

Table 3 Sensitivity, specificity, PPV and NPV of ultrasound for distinguishing tumour from normal tissue according to resection phase

Stage of surgery	Values	
Before resection	Sensitivity	0.95
	Specificity	0.95
	PPV	0.98
	NPV	0.90
During resection	Sensitivity	0.88
	Specificity	0.42
	PPV	0.73
	NPV	0.67
After resection	Sensitivity	0.26
	Specificity	0.88
	PPV	0.62
	NPV	0.62

The sensitivity, specificity, PPV and NPV of ultrasound in each of the subsequent resection phases is shown.

cavity wall after completed resection. They found that among 15 tumours not invading eloquent cortex and thus feasible for total resection, 11 cases (73%) had margins without solid tumour involvement although scattered tumour cells were found. Woydt et al. [40] published a study in 1996, to evaluate ultrasound findings after completed microsurgical resection of gliomas. Biopsies were obtained in (1) hyperechoic areas adjacent to the resection cavity and (2) the hyperechoic rim of the resection cavity. In group 1 (hyperechoic areas adjacent to resection cavity), high-grade glioma cases showed that 90% of biopsies contained tumour tissue, and the rest contained infiltrated tissue. For low-grade glioma cases 85% of biopsies in this group contained tumour tissue, the rest contained infiltrated tissue. Biopsies obtained at the hyperechoic rim (group 2) were heterogeneous, 26% revealed solid tumour tissue, 35% infiltration zone and 39% brain tissue (high-grade and low-grade gliomas combined). Our research group published a study in 2005 [38], comparing ultrasound findings with histopathology by obtaining tissue samples obtained in the tumour border zone before starting the resection. The ultrasound findings were in agreement with the histopathology in 77% of biopsies from glioblastoma cases and 83% and 74% for anaplastic astrocytomas and low-grade astrocytomas, respectively.

In the present paper we report on our results evaluating the ability of intraoperative ultrasound for delineation of gliobastomas before, during and after resection by comparing image findings from image guided biopsies with histopathology.

Discussion of findings

The conditions for ultrasound imaging *before resection* are probably close to optimal, and imaging artefacts should be at a minimum level. Before resection, sensitivity was 95% and specificity also was 95%. The PPV and NPV were 98% and 90%, respectively. This result shows that the ultrasound was highly accurate in delineating glioblastomas prior to resection. The sensitivity and specificity is slightly improved compared to our own study from 2005 [38]. This may be because of increased experience with ultrasound. The result also demonstrates that the sensitivity and specificity of ultrasound for predicting tumour/normal tissue, although operator dependent, is in the range of other, state of the art imaging techniques [16, 23, 28]. Thus, the sensitivity and specificity of ultrasound diagnosis in this phase serve as a baseline for comparison with subsequent phases.

During resection, a partial resection had been performed, with a resection cavity and some residual tumour left. The resection cavity wall, having a rough surface, as well as debris, small air bubbles, and blood all contribute to ultrasound imaging artefacts. The values of sensitivity and PPV were 87% and 73%; the specificity and NPV were 42% and 67%. The striking finding is a considerable decrease in specificity. This may be explained by a considerable amount of false positive biopsies; in nine biopsies, which contained normal tissue (as diagnosed by the pathologist), the diagnosis on ultrasound was “tumour”, and two were classified as “tumour, uncertain”. Several factors may explain the high false positive rate, both imaging artefacts and inherent error sources in the method of the study (discussed below). These numbers show that there may be some overestimation of tumour in this phase of surgery, but on the other hand, chances of overlooking areas with residual tumour tissue seem to be low (still high sensitivity).

After resection, leaving a cavity with the solid part of the tumour removed, biopsies were sampled in the resection cavity wall only. The same sources of imaging artefacts as discussed above also apply to this phase. The calculated values of sensitivity and PPV were 26% and 62%, while the values of specificity and NPV were 88% and 62%, respectively. The specificity was acceptable; reflecting that normal tissue in the majority of cases was correctly classified on ultrasound, important for patient safety. A sensitivity of 26% is discouraging, but calls for further considerations. First, the number of biopsies deemed “tumour” and “tumour, uncertain” were low in this stage of resection for obvious reasons. Also noteworthy is the high number of biopsies deemed “normal” and “normal, uncertain”, which contained either tumour tissue (four deemed “normal” and another four considered “normal, uncertain”) or tumour-infiltrated tissue (five deemed “normal” and ten deemed “normal, uncertain”). We are not surprised to find infiltrated brain tissue and small tumour remnants in the resection cavity wall, due to the infiltrating nature of glioblastomas. In their paper from 1996, Woydt et al. [40] reported that biopsies obtained from the “hyperechoic rim” of a resection cavity contained solid tumour (26%), infiltration zone (35%) and brain tissue (39%). For

comparison, biopsies taken from the resection cavity (regardless of image finding) wall after resection in this study have a similar, although slightly more favourable distribution; solid tumour 21%; infiltration zone 22% and normal tissue 58%. Comparison of 3D ultrasound findings at the end of resection and early postoperative MRI was not a part of the study. Still, the fact that two of ten patients considered either >95% or 90–95% resected had residual tumour on early postoperative MRI may likewise reflect difficulties in interpreting 3D ultrasound after resection, or limitations of the 3D ultrasound itself.

In summary, the diagnostic accuracy of ultrasound for delineating glioblastomas was lower in the subsequent phases of surgery than before resection. During surgery there seemed to be some overestimation of tumour, but residual tumour was rarely missed. After resection, small tumour remnants and infiltrated tissue appeared as normal tissue on ultrasound, lowering the sensitivity. Still in most cases biopsies containing normal tissue were correctly classified with ultrasound.

Limitations of the study

Important limitations of the study method must be recognized due to the fact that the 3D ultrasound technique used in this study still is not real time; the biopsy sampling in itself, although performed as gently as possible, may cause some motion of tissue. Furthermore, in some cases that the walls of the resection cavity seemed to collapse a little inwardly when removing the saline after 3D ultrasound image acquisition to what degree these effects have affected the results in this study is not known.

Small and traumatized biopsy specimens in some cases prevented optimal histological examination. The surgeon did not have the opportunity to classify tissue as infiltrated brain tissue, while the pathologist did: Whether this introduces a bias is unknown.

The diagnostic accuracy of ultrasound is user dependent. The majority of biopsies were assessed by a surgeon with long experience using 3D ultrasound (GU), and the rest of the biopsies were assessed by a surgeon with shorter, but significant experience using ultrasound. Interobserver variability analysis on the interpretation of 3D ultrasound images was not done, and this is an important limitation of the current study. In our view, interpreting 3D ultrasound is dependent on interactive navigation, and using 2D snapshots postoperatively may not be sufficient for analysis of interobserver variability. We were not able to record biopsy positions in the 3D ultrasound dataset for postoperative review and analysis.

Systematic comparison of 3D ultrasound at the end of the resection and postoperative MRI was not done as it was not part of the study protocol.

Ethical aspects

The ethical aspects of intentional sampling of biopsies in the outer border of the tumour, as seen in the US images, were given consideration. Biopsies from outside of the US indicated border were never sampled in eloquent areas.

We did not see any complications that could be related to the biopsy sampling procedure.

Conclusions

Our study shows that while ultrasound is highly accurate in delineating glioblastomas before resection it appears less accurate during and after resection. During resection there seem to be some overestimation of tumour, while small tumour remnants and infiltrated tissue in the cavity wall is underestimated after resection. Due to inherent error sources in the study design, the results must be interpreted with caution. Intraoperative 3D ultrasound still seems a reasonably reliable modality for guidance of the resection of glioblastomas as the sensitivity during resection and the specificity after completed resection are acceptable.

References

1. Albert FK, Forsting M, Sartor K, Adams HP, Kunze S (1994) Early postoperative magnetic resonance imaging after resection of malignant glioma: objective evaluation of residual tumour and its influence on regrowth and prognosis. Neurosurgery 34:45–60 discussion 60–41
2. Burger PC, Heinz ER, Shibata T, Kleihues P (1988) Topographic anatomy and CT correlations in the untreated glioblastoma multiforme. J Neurosurg 68:698–704
3. Chacko AG, Kumar NKS, Chacko G, Athyal R, Rajshekhar V (2003) Intraoperative ultrasound in determining the extent of resection of parenchymal brain tumours—a comparative study with computed tomography and histopathology. Acta Neurochirurgica 145:743–748
4. Croteau D, Scarpace L, Hearshen D, Gutierrez J, Fisher JL, Rock JP, Mikkelsen T (2001) Correlation between magnetic resonance spectroscopy imaging and image-guided biopsies: semiquantitative and qualitative histopathological analyses of patients with untreated glioma. Neurosurgery 49:823–829
5. Daumas-Duport C, Monsaigneon V, Blond S, Munari C, Musolino A, Chodkiewicz JP, Missir O (1987) Serial stereotactic biopsies and CT scan in gliomas: correlative study in 100 astrocytomas, oligo-astrocytomas and oligodendrocytomas. J Neurooncol 4: 317–328
6. Ganslandt O, Stadlbauer A, Fahlbusch R, Kamada K, Buslei R, Blumcke I, Moser E, Nimsky C (2005) Proton magnetic resonance spectroscopic imaging integrated into image-guided surgery: correlation to standard magnetic resonance imaging and tumor cell density. Neurosurgery 56:291–298 discussion 291–298
7. Grønningsæter Å, Kleven A, Ommedal S, Årseth TE, Lie T, Lindseth F, Langø T, Unsgård G (2000) SonoWand, an ultra-

sound-based neuronavigation system. Neurosurgery 47:1373–1380
8. Hammoud MA, Ligon BL, elSouki R, Shi WM, Schomer DF, Sawaya R (1996) Use of intraoperative ultrasound for localizing tumors and determining the extent of resection: a comparative study with magnetic resonance imaging. J Neurosurg 84:737–741
9. Hirschberg H, Samset E, Hol PK, Tillung T, Lote K (2005) Impact of intraoperative MRI on the surgical results for high-grade gliomas. Minim Invasive Neurosurg 48:77–84
10. Iseki H, Muragaki Y, Nakamura R, Ozawa N, Taniguchi H, Hori T, Takakura K (2005) Intelligent operating theater using intraoperative open-MRI. Magn Reson Med Sci 4:129–136
11. Katisko JP, Koivukangas JP (2007) Optically neuronavigated ultrasonography in an intraoperative magnetic resonance imaging environment. Neurosurgery 60:373–380 discussion 380–371
12. Kelly PJ, Daumas-Duport C, Scheithauer BW, Kall BA, Kispert DB (1987) Stereotactic histologic correlations of computed tomography- and magnetic resonance imaging-defined abnormalities in patients with glial neoplasms. Mayo Clin Proc 62:450–459
13. Kleihues P, Cavenee WK (eds) (2000) Pathology and genetics of tumours of the nervous system: world health organization classification of tumours. IARC, Lyon
14. Knauth M, Aras N, Wirtz CR, Dorfler A, Engelhorn T, Sartor K (1999) Surgically induced intracranial contrast enhancement: potential source of diagnostic error in intraoperative MR imaging. AJNR Am J Neuroradiol 20:1547–1553
15. Koivukangas J, Louhisalmi Y, Alakuijala J, Oikarinen J (1993) Ultrasound-controlled neuronavigator-guided brain surgery. J Neurosurg 79:36–42
16. Kracht LW, Miletic H, Busch S, Jacobs AH, Voges J, Hoevels M, Klein JC, Herholz K, Heiss WD (2004) Delineation of brain tumor extent with [11C]L-methionine positron emission tomography: local comparison with stereotactic histopathology. Clin Cancer Res 10:7163–7170
17. Lacroix M, Abi-Said D, Fourney DR, Gokaslan ZL, Shi W, DeMonte F, Lang FF, McCutcheon IE, Hassenbusch SJ, Holland E, Hess K, Michael C, Miller D, Sawaya R (2001) A multivariate analysis of 416 patients with glioblastoma multiforme: prognosis, extent of resection, and survival. J Neurosurg 95:190–198
18. LeRoux PD, Winter TC, Berger MS, Mack LA, Wang K, Elliott JP (1994) A comparison between preoperative magnetic resonance and intraoperative ultrasound tumor volumes and margins. J Clin Ultrasound 22:29–36
19. Letteboer MM, Willems PW, Viergever MA, Niessen WJ (2005) Brain shift estimation in image-guided neurosurgery using 3-D ultrasound. IEEE Trans Biomed Eng 52:268–276
20. Lindner D, Trantakis C, Renner C, Arnold S, Schmitgen A, Schneider J, Meixensberger J (2006) Application of intraoperative 3D ultrasound during navigated tumor resection. Minim Invasive Neurosurg 49:197–202
21. Lindseth F, Lango T, Bang J, Nagelhus Hernes TA (2002) Accuracy evaluation of a 3D ultrasound-based neuronavigation system. Comput Aided Surg 7:197–222
22. Lunsford LD, Martinez AJ, Latchaw RE (1986) Magnetic resonance imaging does not define tumor boundaries. Acta Radiol Suppl 369:154–156
23. McKnight TR, von dem Bussche MH, Vigneron DB, Lu Y, Berger MS, McDermott MW, Dillon WP, Graves EE, Pirzkall A, Nelson SJ (2002) Histopathological validation of a three-dimensional magnetic resonance spectroscopy index as a predictor of tumor presence. J Neurosurg 97:794–802
24. Nimsky C, Ganslandt O, Buchfelder M, Fahlbusch R (2006) Intraoperative visualization for resection of gliomas: the role of functional neuronavigation and intraoperative 1.5 T MRI. Neurol Res 28:482–487
25. Nimsky C, Ganslandt O, Cerny P, Hastreiter P, Greiner G, Fahlbush R (2000) Quantification of, visulaization of, and compensating for brain shift using intraoperative magnetic resonance imaging. Neurosurgery 47:1070–1080
26. Nimsky C, Ganslandt O, Hastreiter P, Fahlbusch R (2001) Intraoperative compensation for brain shift. Surg Neurol 56:357–364 discussion 364–355
27. Nimsky C, Ganslandt O, von Keller B, Romstock J, Fahlbusch R (2004) Intraoperative high-field-strength MR imaging: implementation and experience in 200 patients. Radiology 233:67–78
28. Price SJ, Jena R, Burnet NG, Hutchinson PJ, Dean AF, Pena A, Pickard JD, Carpenter TA, Gillard JH (2006) Improved delineation of glioma margins and regions of infiltration with the use of diffusion tensor imaging: an image-guided biopsy study. AJNR Am J Neuroradiol 27:1969–1974
29. Reinges MHT, Nguyen HH, Krings T, Hutter BO, Rohde V, Gilsbach JM (2004) Course of brain shift during microsurgical resection of supratentorial cerebral lesions: limits of conventional neuronavigation. Acta Neurochirurgica 146:369–377
30. Rubin JM, Dohrmann GJ (1985) Efficacy of intraoperative US for evaluating intracranial masses. Radiology 157:509–511
31. Sergeeva O, Uhlemann F, Schackert G, Hergeth C, Morgenstern U, Steinmeier R (2006) Integration of intraoperative 3D-ultrasound in a commercial navigation system. Zentralbl Neurochir 67:197–203
32. Stadlbauer A, Ganslandt O, Buslei R, Hammen T, Gruber S, Moser E, Buchfelder M, Salomonowitz E, Nimsky C (2006) Gliomas: histopathologic evaluation of changes in directionality and magnitude of water diffusion at diffusion-tensor MR imaging. Radiology 240:803–810
33. Steinmeier R, Fahlbusch R, Ganslandt O, Nimsky C, Buchfelder M, Kaus M, Heigl T, Lenz G, Kuth R, Huk W (1998) Intraoperative magnetic resonance imaging with the magnetom open scanner: concepts, neurosurgical indications, and procedures: a preliminary report. Neurosurgery 43:739–747 discussion 747–738
34. Sutherland GR, Kaibara T, Louw D, Hoult DI, Tomanek B, Saunders J (1999) A mobile high-field magnetic resonance system for neurosurgery. J Neurosurg 91:804–813
35. Unsgaard G, Gronningsaeter A, Ommedal S, Nagelhus Hernes TA (2002) Brain operations guided by real-time two-dimensional ultrasound: new possibilities as a result of improved image quality. Neurosurgery 51:402–411 discussion 411–402
36. Unsgaard G, Ommedal S, Muller T, Gronningsaeter A, Nagelhus Hernes TA (2002) Neuronavigation by intraoperative three-dimensional ultrasound: initial experience during brain tumor resection. Neurosurgery 50:804–812 discussion 812
37. Unsgaard G, Rygh OM, Selbekk T, Muller TB, Kolstad F, Lindseth F, Hernes TA (2006) Intra-operative 3D ultrasound in neurosurgery. Acta Neurochir (Wien) 148:235–253
38. Unsgaard G, Selbekk T, Brostrup Muller T, Ommedal S, Torp SH, Myhr G, Bang J, Nagelhus Hernes TA (2005) Ability of navigated 3D ultrasound to delineate gliomas and metastases–comparison of image interpretations with histopathology. Acta Neurochir (Wien) 147:1259–1269 discussion 1269
39. Wirtz CR, Knauth M, Staubert A, Bonsanto MM, Sartor K, Kunze S, Tronnier VM (2000) Clinical evaluation and follow-up results for intraoperative magnetic resonance imaging in neurosurgery. Neurosurgery 46:1112–1120 discussion 1120–1112
40. Woydt M, Krone A, Becker G, Schmidt K, Roggendorf W, Roosen K (1996) Correlation of intra-operative ultrasound with histopathologic findings after tumour resection in supratentorial gliomas. A method to improve gross total tumour resection. Acta Neurochir (Wien) 138:1391–1398

PAPER 2

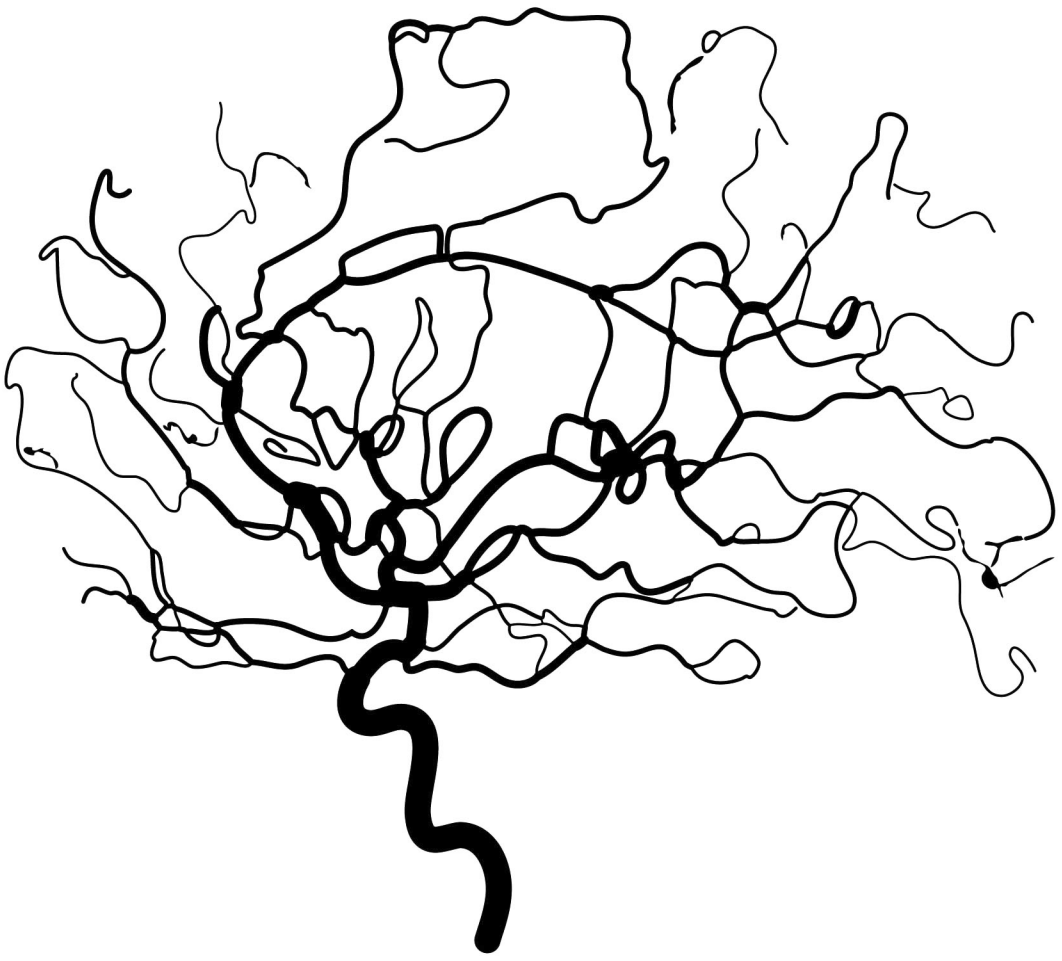

Available online at www.sciencedirect.com
ScienceDirect
Surgical Neurology 66 (2006) 581–592
SURGICAL NEUROLOGY
www.surgicalneurology-online.com

Technique-Imaging

Intraoperative navigated 3-dimensional ultrasound angiography in tumor surgery

Ola M. Rygh, MD[a,b,d,*], Toril A. Nagelhus Hernes, PhD[b,c,d], Frank Lindseth, PhD[c,d], Tormod Selbekk, MSc[c,d], Tomm Brostrup Müller, PhD, MD[a,d], Geirmund Unsgaard, PhD, MD[a,b,d]

[a]*Department of Neurosurgery, St. Olav University Hospital, 7006 Trondheim, Norway*
[b]*The Norwegian University of Science and Technology, 7006 Trondheim, Norway*
[c]*SINTEF Health Research, 7491 Trondheim, Norway*
[d]*National Centre for 3D ultrasound in Surgery, St. Olav University Hospital, 7006 Trondheim, Norway*

Received 20 January 2006; accepted 23 May 2006

Abstract

Background: Avoiding damage to blood vessels is often the concern of the neurosurgeon during tumor surgery. Using angiographic image data in neuronavigation may be useful in cases where vascular anatomy is of special interest. Since 2003, we have routinely used 3D ultrasound angiography in tumor surgery, and between January 2003 and May 2005, 62 patients with different tumors have been operated using intraoperative 3D ultrasound angiography in neuronavigation.

Methods: An ultrasound-based neuronavigation system was used. In addition to 3D ultrasound tissue image data, 3D ultrasound angiography (power Doppler) image data were acquired at different stages of the operation. The value and role of navigated 3D ultrasound angiography as judged by the surgeon were recorded.

Results: We found that intraoperative ultrasound angiography was easy to acquire and interpret, and that image quality was sufficient for neuronavigation. In 26 of 62 cases, ultrasound angiography was found to be helpful by visualizing hidden vessels adjacent to and inside the tumor, facilitating tailored approaches and safe biopsy sampling.

Conclusions: Intraoperative 3D ultrasound angiography is straightforward to use, image quality is sufficient for image guidance, and it adds valuable information about hidden vessels, increasing safety and facilitating tailored approaches. Furthermore, with updated 3D ultrasound angiography imaging, accuracy of neuronavigation may be maintained in cases of brain shift.

Keywords: Neuronavigation; Image-guided surgery; Ultrasound; Doppler ultrasonography

1. Introduction

During tumor surgery, avoiding damage to blood vessels is one of many concerns for the neurosurgeon. Neuronavigation may help the neurosurgeon to locate the position of important structures such as vessels; thus, tumor resection may be performed more safely and more radically. However, brain shift as well as registration errors may limit the overall accuracy of a neuronavigation system [3,7,9,16]. To compensate for brain shift, intraoperative imaging has been introduced in neuronavigation [1,4], thus maintaining accuracy [26,29]. In addition, residual tumor may be detected.

In our clinic, we have used neuronavigation with integrated intraoperative ultrasound imaging for guidance of tumor resection for several years [4-6,25-28]. The equipment also has capability of Doppler imaging with power Doppler for visualization of vessels. Thus, 3D ultrasound angiography image data can be acquired intraoperatively for neuronavigation. The aim of the present

Abbreviations: 3D, 3-dimensional; AVM, arteriovenous malformation; BFI, blood flow imaging; CT, computed tomography; DSA, digital subtraction angiography; FMRI, functional magnetic resonance imaging; MRI, magnetic resonance imaging; PICA, posterior inferior cerebellar artery.

* Corresponding author. St Olav University Hospital, Trondheim N-7005 Trondheim Norway. Tel.: +47 73867596; fax: +47 73867977.
E-mail address: ola.rygh@ntnu.no (O.M. Rygh).

0090-3019/$ – see front matter © 2006 Elsevier Inc. All rights reserved.
doi:10.1016/j.surneu.2006.05.060

study was to evaluate neuronavigation with intraoperative 3D ultrasound angiography (power Doppler) for image-guided resection of intracranial tumors by visualizing the vascular anatomy adjacent to and inside the tumor.

2. Patients and methods

Between January 2003 and May 2005, we have used intraoperative ultrasound angiography in 62 tumor cases. Cases selected for use of neuronavigation with 3D ultrasound angiography were those wherein neuronavigation (with 3D ultrasound) was already requested and wherein the surgeon assumed that ultrasound angiography might be of value.

We used an intraoperative ultrasound-based neuronavigation system, SonoWand (MISON AS, Trondheim, Norway), with a 4- to 8-MHz flat phased array probe with optimal focusing properties at 3 to 6 cm and with the capability of acquiring power Doppler (ultrasound angiography) images. On the ultrasound angiography images, vessels were displayed as an overlay in shades of red over the tissue image according to the power of the Doppler signal. For neuronavigation with 3D ultrasound, only power Doppler image data were applied in the present study. The ultrasound platform (a GE Vingmed Vivid FiVe unit) in SonoWand also has triplex imaging, but this cannot be imported and used for neuronavigation with 3D ultrasound.

For tracking of the ultrasound probe, a tracking frame was attached. Neuronavigation was performed with a tracked pointer device or the CUSA (Valleylab, Boulder, Colo, USA) with an attached tracking frame. Tracking of the CUSA enabled continuous monitoring of the position of the tip and the trajectory of this instrument, “online resection.” A biopsy forceps with tracking was also available for image guidance of biopsies. For acquisition of 3D ultrasound image data for navigation, the ultrasound probe was placed on the dura and tilted or translated over the area of interest by a freehand movement. The 2D ultrasound images acquired were reconstructed to a 3D ultrasound data set ready for navigation. Image acquisition and reconstruction typically took about 1 minute. The ultrasound probe was not in the operating field after the acquisition of a 3D ultrasound volume, unless additional 3D ultrasound data sets were acquired or real-time 2D imaging was needed.

The ultrasound angiography images were displayed on the screen of the navigation system, usually in addition to the preoperative MRI, which was displayed simultaneously on the same screen. With a simple pointer device, the safest surgical route to the tumor was determined with the smallest risk of vascular damage.

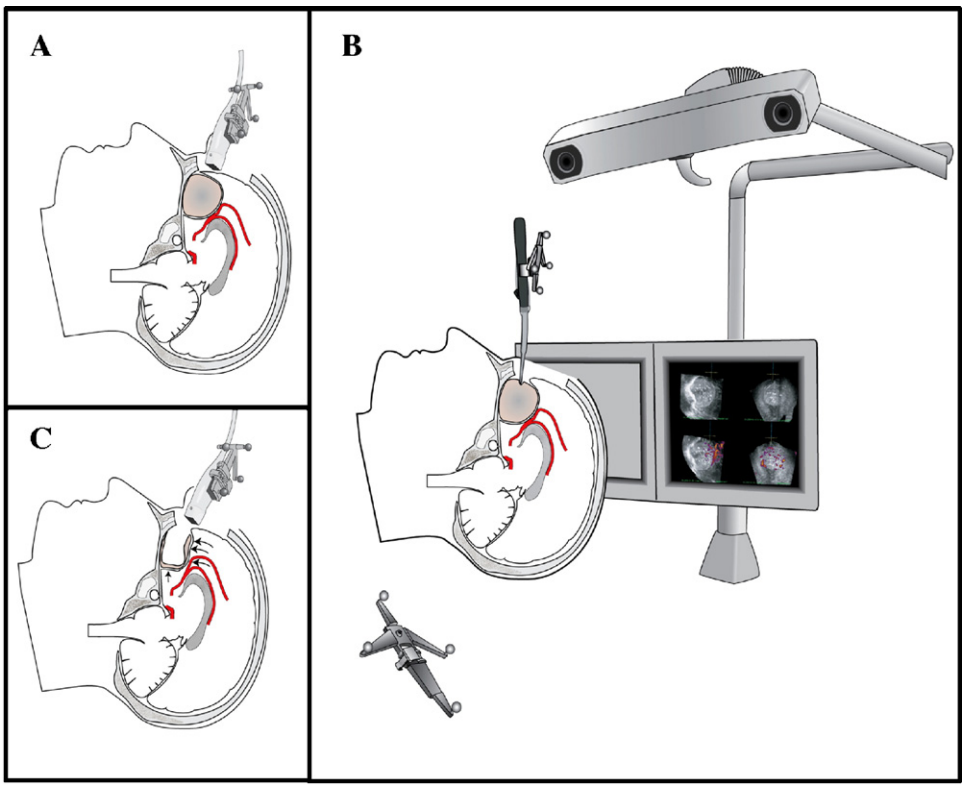

Fig. 1. Workflow in 3D ultrasound angiography. A: 3D ultrasound angiography image data are acquired by tilting or translating the probe over the area of interest. B: Then, the calibrated CUSA is used for online resection of the tumor. The navigation system displays the position of the CUSA in relation to the tumor margin and the vessels. C: After some resection, updated 3D ultrasound angiography data may be necessary because of brain shift (arrows) and is again acquired by tilting or translating the probe over the area of interest.

Table 1
List of cases

Case	Diagnosis	Location of tumor	Helpfulness of ultrasound angiography
1	Chondrosarcoma	Cavernous sinus region (left side)	Yes
2	Anaplastic astrocytoma	Left frontal lobe	No
3	Glioblastoma	Left frontal lobe	Yes
4	Low-grade astrocytoma	Right parietotemporal region	Possibly
5	Anaplastic astrocytoma	Left parietooccipital region	No
6	Chordoma	Clivus	No
7	Meningioma	Pineal region	Yes
8	Metastasis (malignant melanoma)	Right frontal lobe	Yes
9	Metastasis (lung cancer)	Left occipital lobe	No
10	Glioblastoma	Right temporal lobe	No
11	Chordoma	Cavernous sinus region (left side)	Yes
12	Metastasis (malignant melanoma)	Cavernous sinus region (right side)	Yes
13	Low-grade astrocytoma	Left medial temporal lobe (hippocampal region)	Yes
14	Metastasis (malignant melanoma)	Occipital lobe	No
15	Trigeminal schwannoma	Cavernous sinus region (right side)	Yes
16	Glioblastoma	Left parietal lobe	No
17	Low-grade astrocytoma	Right parietal lobe, close to central sulcus	Yes
18	Meningioma (sphenoid wing)	Sphenoid wing, skull base	Possibly
19	Meningioma (olfactory)	Anterior cranial fossa, midline	Yes
20	Meningioma (left convexity)	Anterior cranial fossa (left side)	No
21	Vestibular schwannoma	Cerebellopontine angle (right)	No
22	Biopsy (result: normal tissue)	Left temporal lobe, hippocampal region	No
23	Pineoblastoma	Vermis of cerebellum	No
24	Meningioma (sphenoid wing)	Sphenoid wing (right side)	Possibly
25	Meningioma (olfactory)	Anterior cranial fossa, midline	Yes
26	Anaplastic astrocytoma	Right medial temporal lobe	Yes
27	Glioblastoma	Left temporal lobe	No
28	Chordoma	Posterior fossa	No
29	Ependymoma	Posterior fossa, fourth ventricle	Yes
30	Meningioma (sphenoid wing)	Sphenoid wing (left side)	Yes
31	Low-grade astrocytoma	Temporal lobe (left)	Yes
32	Meningioma (foramen magnum)	Foramen magnum	Yes
33	Glioblastoma (biopsy only)	Parietal lobe (right)	Yes
34	Unknown lesion	Left temporal lobe	Yes
35	Meningioma (posterior fossa)	Posterior fossa	No
36	Anaplastic astrocytoma	Parietal lobe, midline	No
37	Meningioma (falx)	Falx, parietal region	Possibly
38	Glioblastoma	Right temporal lobe	No
39	Meningioma (olfactory)	Anterior cranial fossa, skull base	Possibly
40	Pilocytic astrocytoma	Posterior cranial fossa	Yes
41	Optic glioma	Extending from chiasma	Possibly
42	Meningioma (sphenoid wing)	Sphenoid wing (right side)	Yes
43	Meningioma (parasagittal)	Occipital convexity (left side, parasagittal)	No
44	Low-grade glioma	Right temporal lobe	No
45	Low-grade glioma	Right frontal lobe	Yes
46	Glioblastoma	Right occipital lobe	Possibly
47	Vestibular schwannoma	Cerebellopontine angle (right side)	No
48	Low-grade astrocytoma	Left medial temporal lobe	Yes
49	Ganglioglioma	Right temporal lobe	Possibly
50	Glioblastoma	Arising from left thalamus, intraventricular	Possibly
51	Meningioma	Sella region	No
52	Ganglioglioma	Intraventricular (left side ventricle)	No
53	Meningioma (falx)	Occipital, arising from falx (left side)	Yes
54	Meningioma (convexity)	Occipital convexity (right)	No
55	Meningioma (convexity)	Anterior cranial fossa, right convexity	Yes
56	Glioblastoma	Occipital lobe (right side)	No
57	Metastasis (breast cancer)	Right temporal lobe, sylvian fissure	Yes
58	Meningioma (convexity)	Parietal convexity meningioma, right side	No
59	Glioblastoma	Left medial frontal lobe and corpus callosum	Yes
60	Meningioma (sphenoid wing)	Sphenoid wing, skull base	Possibly
61	Vestibular schwannoma	Cerebellopontine angle, right side	No
62	Meningioma (convexity)	Parietal region, right side	No

List of patients with type of lesion, location of lesion, and usefulness of ultrasound angiography as judged by the surgeon.

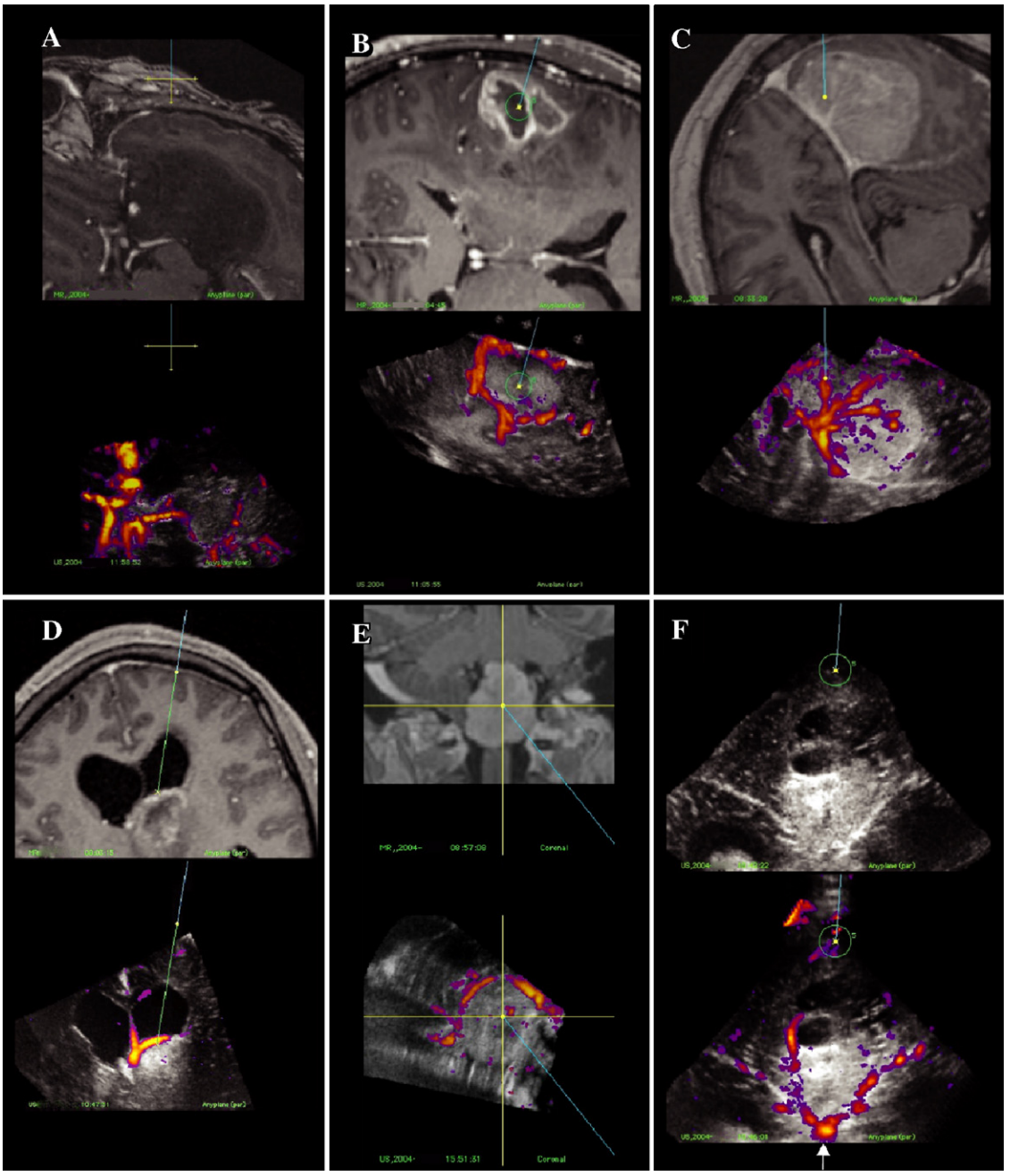

Fig. 2. Visualization of vessels. Snapshots from the neuronavigation system. A: Low-grade glioma in medial part of temporal lobe (case 26). Magnetic resonance imaging (T1 with gadolinium) (top) and ultrasound angiography (bottom). Vessels in the circle of Willis are visualized by ultrasound angiography; the tumor is partially resected. B: Glioma in right temporal lobe (case 38). Magnetic resonance imaging (T1 with gadolinium) (top) and ultrasound angiography (bottom). Vessels surrounding the tumor, probably both arterial and venous, are displayed on ultrasound angiography. The surgeon suspected that branches of the middle cerebral artery were among these vessels. From power Doppler alone, it is not possible to tell which vessels are arterial and which are venous. Being superficial, the vessels give a strong power Doppler signal. C: Meningioma originating from posterior part of falx (case 53). Magnetic resonance imaging (T1 with gadolinium) (top) and ultrasound angiography (bottom). Multiple veins inside the meningioma drain into the straight sinus. D: Thalamic glioma (case 50). Magnetic resonance imaging (T1 with gadolinium) (top) and ultrasound angiography. The thalamostriate vein is revealed by ultrasound angiography, crossing the tumor surface. E: Meningioma, foramen magnum (case 32). Magnetic resonance imaging (T1, top) and ultrasound angiography (bottom). Notice branches from vertebral arteries adjacent to the tumor. F: Pilocytic astrocytoma in posterior fossa (case 40). Ultrasound tissue (top) and ultrasound angiography (bottom). The vein of Galen is visualized (arrow) by ultrasound angiography.

Additional ultrasound and ultrasound angiography image data were acquired after some resection, if required, because of suspected brain shift or for resection control. The workflow with the equipment is summarized in Fig. 1. Additional resection was usually carried out if residual tumor was detected, except in cases where this was decided against because of unacceptable risk of neurological damage to the patient.

Table 2
Cases where navigated 3D ultrasound angiography was found helpful

Case	Diagnosis	Location of tumor	Vessel visualized	Role of navigation
1	Chondrosarcoma	Cavernous sinus region (left side)	Internal carotid artery	Visualization of hidden vessel
3	Glioblastoma	Left frontal lobe	Middle cerebral artery	Visualization of hidden vessel
7	Meningioma	Pineal region	Great cerebral vein	Visualization of hidden vessel, online CUSA resection
8	Metastasis (malignant melanoma)	Right frontal lobe	Pericallosal arteries	Visualization of hidden vessel, online CUSA resection
11	Chordoma	Cavernous sinus region (left side)	Internal carotid artery	Visualization of hidden vessel
12	Metastasis (malignant melanoma)	Cavernous sinus region (right side)	Internal carotid artery	Visualization of hidden vessel, facilitation of approach, online CUSA resection
13	Low-grade astrocytoma	Left medial temporal lobe (hippocampal region)	Middle cerebral artery	Visualization of hidden vessel
15	Trigeminal schwannoma	Cavernous sinus region (right side)	Internal carotid artery	Visualization of hidden vessel
17	Low-grade astrocytoma	Right parietal lobe, close to central sulcus	Branches from middle cerebral artery	Visualization of hidden vessel
19	Meningioma (olfactory)	Anterior cranial fossa, midline	Anterior cerebral artery	Visualization of hidden vessel, online CUSA resection
25	Meningioma (olfactory)	Anterior cranial fossa, midline	Anterior cerebral artery	Visualization of hidden vessel, online CUSA resection
26	Anaplastic astrocytoma	Right medial temporal lobe	Middle cerebral artery and internal cerebral vein	Visualization of hidden vessel, tailored approach
29	Ependymoma	Posterior fossa, fourth ventricle	Branches from PICA	Visualization of hidden vessel
30	Meningioma (sphenoid wing)	Sphenoid wing (left side)	Anterior and middle cerebral arteries	Visualization of hidden vessel, online CUSA resection
31	Low-grade astrocytoma	Left temporal lobe	Middle cerebral artery	Tailored approach, visualization of hidden vessel, online CUSA resection
32	Meningioma (foramen magnum)	Foramen magnum	Vertebral arteries	Visualization of hidden vessel, online CUSA resection
33	Glioblastoma (biopsy only)	Right parietal lobe	Smaller vessels	Safe biopsy sampling, visualization of hidden vessel
34	Unknown lesion	Left medial temporal lobe	Small cortical arteries on medial surface of temporal lobe	Tailored approach, visualization of hidden vessel
40	Pilocytic astrocytoma	Posterior cranial fossa	Vein of Galen	Visualization of hidden vessel
42	Meningioma (sphenoid wing)	Sphenoid wing (right side)	Middle cerebral artery and internal carotid	Visualization of hidden vessel, online CUSA resection
45	Low-grade glioma	Right frontal lobe	Pericallosal artery	Visualization of hidden vessel, online CUSA resection
48	Low-grade astrocytoma	Left medial temporal lobe	Middle cerebral artery	Facilitation of approach
53	Meningioma (falx)	Occipital, arising from falx (left side)	Posterior cerebral artery and straight sinus	Visualization of hidden vessel, online CUSA resection
55	Meningioma (convexity)	Right anterior cranial fossa	Pericallosal arteries	Visualization of hidden vessel, online CUSA resection
57	Metastasis (breast cancer)	Right temporal lobe in sylvian fissure	Middle cerebral artery	Visualization of hidden vessel
59	Glioblastoma	Left medial frontal lobe and corpus callosum	Pericallosal arteries	Visualization of hidden vessel, facilitation of approach, online CUSA resection

The procedures were performed by 3 surgeons, and most of the procedures (51 cases) were performed by the senior author (GU). The value and role of navigated ultrasound angiography as judged by the surgeon were recorded postoperatively in most cases. In addition, we have retrospectively reviewed all cases. The subjective judgment by the surgeon of the value of navigated ultrasound angiography was graded into 3 categories: helpful, possibly helpful, and not helpful. The degree of helpfulness was graded as helpful when navigated ultrasound angiography was used actively during the whole procedure and was considered to contribute significantly to the safe completion

of the procedure. The degree of helpfulness was considered possibly helpful when navigated ultrasound angiography was considered useful for orientation but not considered essential for safe navigation. When ultrasound angiography did not give additional valuable information for image guidance, it was deemed not helpful.

The cases are listed in Table 1.

3. Results

Between 2003 and May 2005, in 62 of 108 patients operated with image guidance, 3D ultrasound angiography was applied and evaluated. Among these patients, there were 20 meningiomas, 24 gliomas, 5 metastases, and 11 tumors of other types. There were also 2 frameless

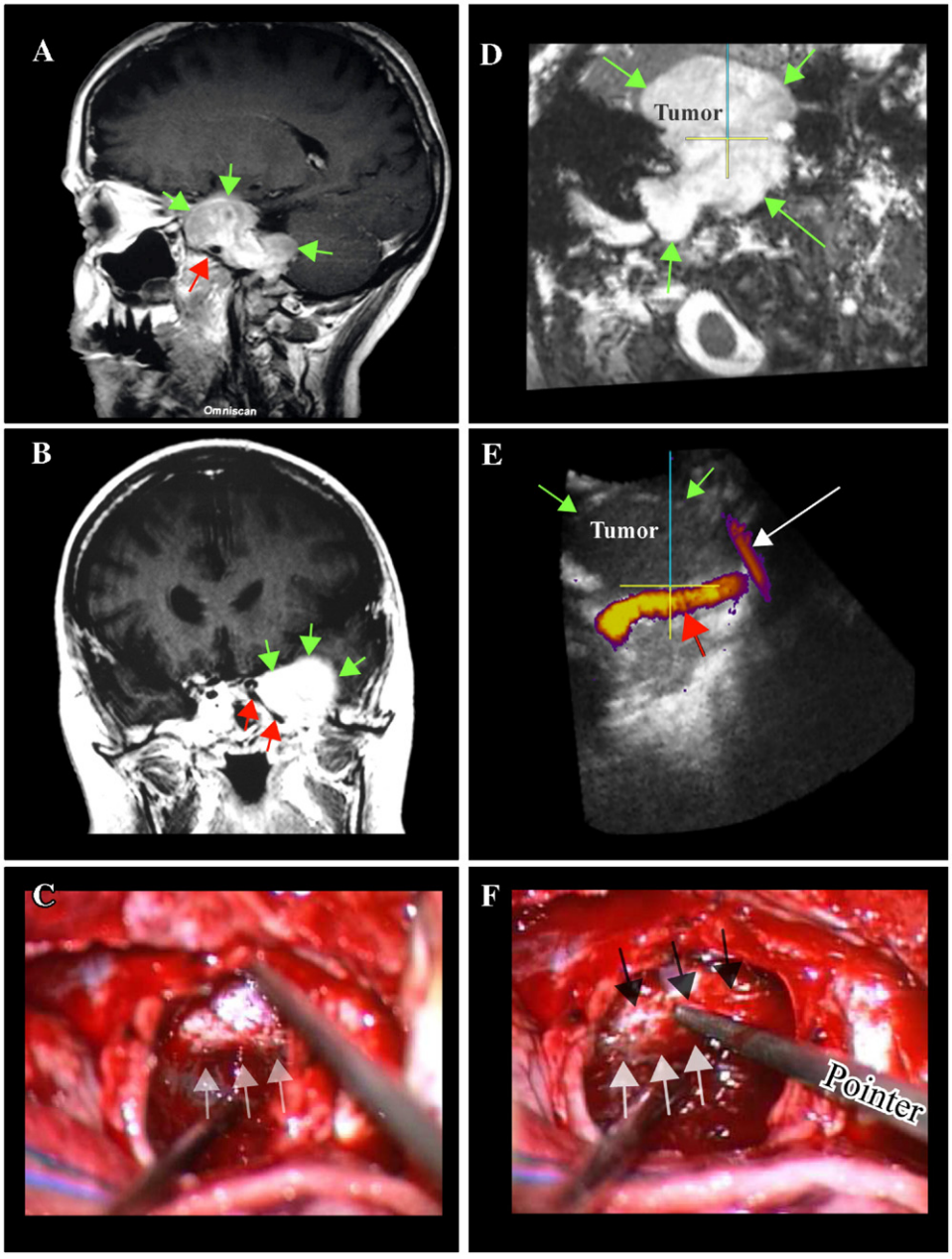

Fig. 3. Chordoma in cavernous sinus region (case 11). A: Sagittal MRI. Green arrows outline the tumor, red arrow directed at internal carotid artery. B: Coronal MRI. Green arrows outline the tumor, red arrows directed at internal carotid artery. C: Photograph from the microscope. During surgery, the internal carotid artery was revealed. White arrows directed at the internal carotid artery. D: MRI image slice from a snapshot from the navigation system during surgery. Green arrows directed at the tumor borders. E: Ultrasound angiography from the same snapshot as panel (D) visualizing the internal carotid artery (in shades of red), which in this case was adjacent to the medial parts of the tumor. The tumor in this case was hypoechogenic. Red arrow directed at artery. A flash artifact is visible upward to the right of the artery (white arrow). F: Photograph from the microscope. The pointer is directed at the internal carotid artery (indicated by white and black arrows). The snapshot from which panels (D) and (E) originate was taken about the same time this photograph was taken, demonstrating good accuracy of the ultrasound angiography navigation, as the position of the pointer directed at the artery seem to correspond with the position as indicated by the navigation system. (For interpretation of the references to color in this figure legend, the reader is referred to the web version of this article).

stereotactic biopsies performed with the use of navigated 3D ultrasound angiography.

3D ultrasound angiography image data were successfully acquired and visualized in all cases.

Both arteries and veins (Fig. 2) were visualized via ultrasound angiography. Vessels in range of the probe gave a strong Doppler signal (Fig. 2). In some cases, the simultaneous display of preoperative MRI helped to decide the identity of vessels, by giving anatomical overview, as the 3D ultrasound angiography only displayed the part of the anatomy that was covered in the 3D ultrasound image acquisition.

Image guidance with 3D ultrasound angiography was performed with a pointer device or tracked surgical instruments, such as the tracked CUSA or a tracked biopsy forceps. With tracking of the CUSA, the surgeon was able to see the position of the tip of the CUSA in relation to the tumor capsule or margin, as well as the vessels of interest (Fig. 1). We found this to be a useful safety measure during resection when there were vessels adjacent to or inside the tumor.

In some of the cases (cases 26, 31, 34, 39, 44, 49, and 50), the role of navigation with 3D ultrasound angiographic imaging was to tailor an approach with minimal invasiveness. With angiographic image guidance, a safe route to the tumor could be chosen, with less need for dissecting and visually inspecting vessels.

With tracking of the biopsy forceps, frameless stereotactic biopsies were acquired with image guidance. Angiographic imaging with ultrasound was found to be helpful in deciding sites for biopsy sampling with minimal risk of bleeding. We found that ultrasound angiography sufficiently displayed small vessels (about ≥ 0.5 mm) in the brain tissue for safe image-guided biopsy sampling. One patient in our series (case 57) had an infarction of the middle cerebral artery, which passed close to a metastasis. Except this case, we have not recorded any vascular complications in our series.

The cases where navigated ultrasound angiography was found to be helpful and the role of navigated ultrasound angiography in those cases are presented in Table 2.

In 26 (42%) of the cases, ultrasound angiography was found to be helpful, in 10 (16%) possibly helpful, and in 26 (42%) not helpful.

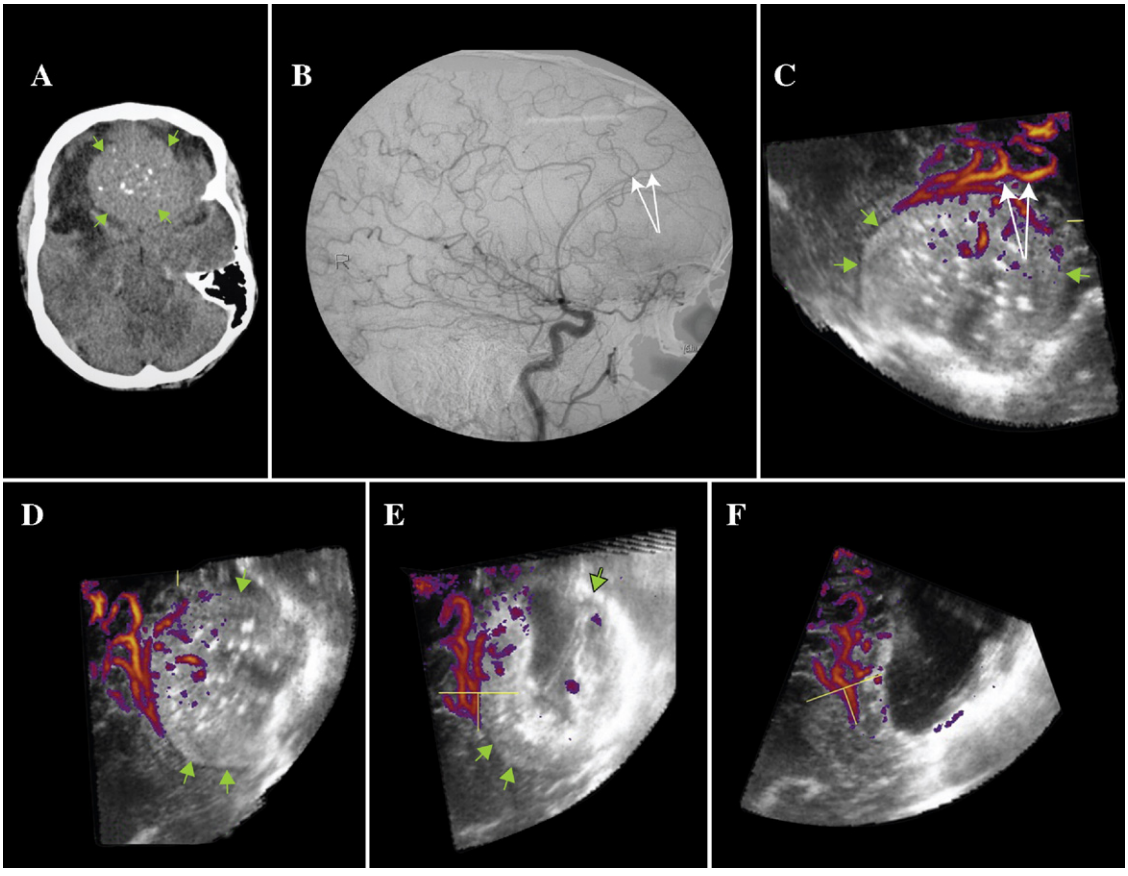

Fig. 4. Large olfactory meningioma (case 25). Green arrows outline tumor. A: CT image showing the tumor. B: DSA showing branches from the anterior cerebral artery being displaced by the tumor (white arrows). C: Ultrasound angiography showing the same branches as indicated in panel (B) from the anterior cerebral artery (white arrows) adjacent to the tumor. D: Ultrasound angiography before the resection. E: Ultrasound angiography during resection. F: Ultrasound angiography after tumor removal. The branches from the anterior cerebral artery are clearly visualized during these phases of the operation. Updated 3D ultrasound angiography image data ensure that accuracy is good even if brain shift has occurred. (For interpretation of the references to color in this figure legend, the reader is referred to the web version of this article).

4. Case descriptions

4.1. Case 11

A 58-year-old woman complained of hoarseness and swallowing difficulties. A left recurrent laryngeal nerve paresis was found on clinical examination, and MRI investigation showed a tumor in the left middle cranial fossa and jugular fossa with close anatomical relation to the internal carotid artery (Fig. 3A and B). She was operated using a pterional approach. The tumor was found to be a chordoma by frozen sections, confirmed later by histopathological analysis. Before reaching the tumor, 3D ultrasound and 3D ultrasound angiography image data were acquired. During surgery, navigating with the pointer and the calibrated CUSA showed the position of the internal carotid artery in relation to the tip of the instrument. This was found valuable for safe resection because the artery was not visible in this phase of the operation. Further dissection revealed the carotid artery (Fig. 3C), and we could verify that the navigation system showed the correct position of the artery when directing the pointer at the artery (Fig. 3E and F). Using neuronavigation with ultrasound angiography images, surgery was performed without any complications, and the patient had an uneventful recovery without any new neurological deficits.

4.2. Case 25

A 52-year-old man presented with progressive dementia. A CT scan revealed a large interhemispheric tumor in the anterior cranial fossa (Fig. 4A). Preoperative DSA showed branches of the anterior cerebral artery passing close to the tumor (Fig. 4B). An image-guided extirpation of the tumor via the bifrontal approach was performed. During surgery, intraoperative 3D ultrasound angiography showed branches from the anterior cerebral arteries and their close relation to the tumor (Fig. 4C). Debulking and resection of the tumor were performed with tracked CUSA, which enabled monitoring of the CUSA tip in relation to the vessels, clearly revealed by 3D ultrasound angiography. Several 3D ultrasound angiography image acquisitions were performed during different stages of the operation (Fig. 4D-F), ensuring that inaccuracy due to brain shift was minimal. Neuronavigation with intraoperative ultrasound angiography thus served to increase the safety of the procedure. The postoperative recovery was uneventful. At follow-up, the patient had a significant improvement in cognitive function.

5. Discussion

In image-guided surgery, angiographic imaging may be valuable in addition to tissue imaging. In image guidance of aneurysm and AVM surgery, preoperative angiographic image data, MR Angiography and CT Angiography, have successfully been imported and used in neuronavigation [2,13,20,21,27] and have been found to be valuable for localization of aneurysms and AVM feeders. In addition, in tumor surgery, preoperative angiographic image data (CT angiography and MR angiography) may be used in neuronavigation. Advanced neuronavigation with CT angiography has been found to be valuable for tailoring surgical approaches and identification of hidden vessels (ie, vessels not exposed in the surgical field) during resection [17]. However, in cases with brain shift, preoperative images may become inaccurate during surgery [3,7,16]. Intraoperative imaging, tissue and angiographic, may therefore be necessary to maintain the accuracy in neuronavigation. Both intraoperative MRI and ultrasound are modalities for acquiring intraoperative angiographic image data for use in neuronavigation. Intraoperative ultrasound integrated with neuronavigation is now a convenient alternative, as modern ultrasound Doppler technology is capable of depicting intracranial vasculature with sufficient image quality [5,6,19,24,30,31].

Sure et al [23] has reported land-marking of vessels in a conventional neuronavigation system with the help of a tracked 2D ultrasound probe using color flow Doppler and found that marking the position of vessels adjacent to a tumor facilitated image-guided tumor resection. The solution we have used enables navigation directly in the 3D ultrasound angiography images without need for land-marking on a preoperative MRI data set. In addition, updated 3D ultrasound angiographic image data may quickly be acquired and used in neuronavigation.

Not surprisingly, we found navigated 3D ultrasound angiography to be of value during surgery on tumor cases with large and important vessels adjacent to or embedded in the tumor (Table 2). Five of these cases (patients 19, 25, 30, 32, and 40) were patients with large meningiomas arising from the skull base, displacing important arteries. With online resection using the CUSA, monitoring the position of the tip of the CUSA relative to the position of vessels helped the surgeon to do a more complete resection of the meningiomas before starting the dissection of the capsule, probably reducing the traumatization of the cerebral cortex during this phase. Updated 3D ultrasound angiography image data gave angiographic images of sufficient quality for navigation during the different stages of the resection. In addition, in 9 cases (patients 10, 13, 22, 26, 31, 34, 44, 48, and 49) with tumors in the medial part of the temporal lobe, we found that visualization of vessels in the basal cistern (eg, the great cerebral vein and the middle cerebral artery) was helpful for safer resection and biopsy sampling.

In other cases, ultrasound angiography was not found helpful, such as in superficial gliomas not close to larger vessels. Nevertheless, even in such cases, unexpected vessels may give the surgeon unpleasant surprises, and confirmation that important vessels were not present close to the tumor was found reassuring by the surgeon.

In skull base surgery, the vessels are usually attached to the skull base and are therefore not subject to brain shift [3,22]. Nevertheless, in MRI-based neuronavigation, inaccuracy in image registration may still lead to inaccurate

targeting of skull base vessels. As no image registration is needed in neuronavigation based on 3D ultrasound angiography [28], this technique is still valuable because image registration errors are avoided.

One limitation of the 3D ultrasound–based neuronavigation is that covering the whole area of interest during 3D ultrasound image data acquisition can be difficult, for example, in cases with large tumors. Furthermore, in skull base surgery, the skull base itself may hinder ultrasound imaging of the entire tumor, for example, in cases where a large skull base tumor is invading both the middle and the posterior cranial fossa. Still, it is our experience that careful planning of the surgical approach and keeping in mind optimal positioning of the ultrasound probe may reduce such problems to a minimum. Moreover, simultaneous display of MRI and 3D ultrasound in neuronavigation may be helpful, giving overview and anatomical orientation in cases with large tumors that are difficult to cover entirely with ultrasound.

6. Technical considerations

For angiographic imaging with the Doppler technique, both color flow and power Doppler technique may be used. Power Doppler displays the vessels because of the power of the Doppler signal in shades of red as an overlay on the ultrasound tissue image. In contrast to color flow Doppler imaging, power Doppler does not have flow velocity or direction information but is less angle-dependent, there is no aliasing and the modality is more flow sensitive [15,18]. Because of less angle dependence, vessel continuity is also better with power Doppler than with color flow Doppler, and vessels will be visualized even if the ultrasound beam hits the vessel at angles close to 90°. In an application with free-hand 3D ultrasound image acquisition, the ultrasound beam will almost always hit a vessel with several different angles; therefore, there is minimal risk of missing a vessel when acquiring 3D ultrasound angiography image data.

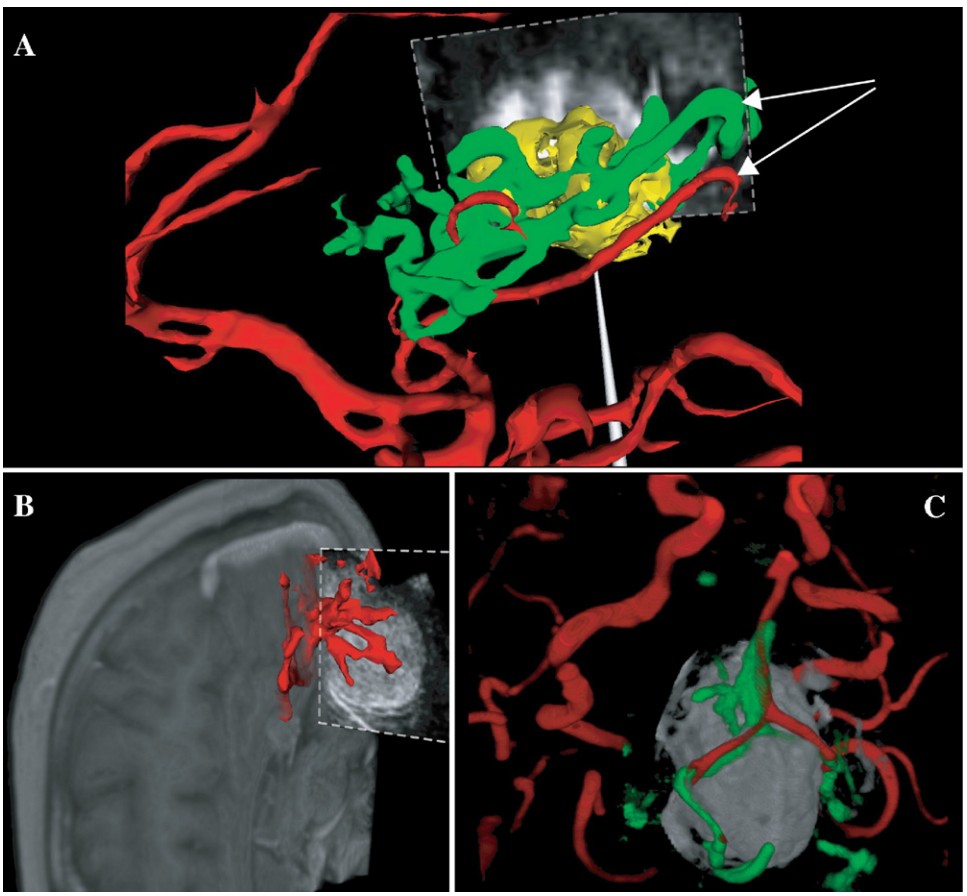

Fig. 5. Multimodal visualization. A: Glioma (same patient as in Fig 2B, case 38). Ultrasound image slice placed in a 3D scene with a segmented representation of the MR-imaged tumor (yellow). Ultrasound angiography (green) and MR angiography (red) show the vessels in relation to the tumor. The ultrasound angiography and MR angiography do not completely overlap, and this may be due to brain shift or registration error. The ultrasound angiography displays more vessels than the MR angiography, and the vessels appear thicker. Still, the vascular anatomy is recognized on both ultrasound angiography and MR angiography. The ultrasound angiography only shows parts of the anatomy. B: Meningioma (same patient as in Fig 2C, case 53). Ultrasound angiography (segmented) here shown in red. Image slices from T1 MRI and ultrasound give orientation and show the tumor. C: Foramen magnum meningioma (same patient as in Fig 2E, case 32). A volume rendered representation of the tumor is shown in grayscale, whereas MR angiography is shown in red and ultrasound angiography in green. The visualization in a 3D scene demonstrates the spatial relationships between the tumor and vessels. (For interpretation of the references to color in this figure legend, the reader is referred to the web version of this article).

In contrast to MR angiography, ultrasound angiography shows both arteries and veins at the same time. We consider this an advantage, as one usually is interested in preserving both arteries and veins during surgery. It is however not possible to discriminate between arteries and veins using the power Doppler imaging technique alone. Still, adjusting the "low velocity reject" setting on the ultrasound scanner may be helpful for showing only vessels with high flow velocities, in which case, most veins will be "filtered out." Using triplex display may also be of help to discriminate between arteries and veins by evaluating the Doppler spectrum. Using the ultrasound probe as a pointer will enable targeting of a vessel with neuronavigation while using triplex display, and in this way, it is possible to evaluate the targeted vessel with triplex. We did however use triplex in the present study. With larger vessels, it was often possible to decide whether the targeted vessel was an artery or a vein by using anatomical knowledge and comparing with arterial MR angiography in cases where this was available.

In ultrasound angiography imaging, the ultrasound data are used for simultaneous imaging of both tissue and angiographic imaging. We have not experienced wherein the quality of the ultrasound tissue part of the image is significantly decreased on ultrasound angiography images.

There are, however, some drawbacks of 3D ultrasound angiography with power Doppler. The high sensitivity of power Doppler may lead to the visualization of too many vessels, as small and surgically less important vessels are depicted. Sometimes, this may result in confusing images that are difficult to interpret. In our experience, reducing the gain setting on the ultrasound scanner may reduce this problem by filtering out the smaller vessels. For better orientation, simultaneous display of preoperative MRI and MR angiography is also useful in such cases.

Blooming may also be a problem with power Doppler, as the power Doppler signal tends to expand beyond the vessel walls; consequently, the vessels may seem larger and thicker than they really are. In addition, the 2D ultrasound image plane itself has a certain thickness that varies with the depth; thus, the resolution in the elevation direction (normal to the scan plane) of the ultrasound beam affects the image quality in 3D ultrasound. Therefore, the vessels in reconstructed (ultrasound angiography) images tend to appear bulkier when viewed on slices orthogonal to the scan plane.

Finally, power Doppler is relatively sensitive to flash artifacts, which occur as red fields or stripes (Fig. 2). Flash artifacts may, for example, occur when the probe is in a cavity filled with saline, when motion in the saline is detected by the power Doppler (Fig. 3C). This is another consequence of the high motion sensitivity of power Doppler, which can occur relatively often during free-hand 3D ultrasound angiography acquisition. Flash artifacts can be reduced with gentle movement of the probe during image acquisition and by adjustments on the ultrasound scanner, such as adjusting the lower limit for detectable flow.

The overall clinical accuracy of the SonoWand system may be as low as 2 mm in a clinical setting when using intraoperative imaging to compensate for brain shift [11]. We did not systematically measure accuracy in this study. Nonetheless, in each case a vessel was exposed in the surgical field, we directed the pointer at the artery for accuracy testing, as in Fig. 3F. In each case, we observed that the position of the pointer corresponded with the position indicated by the navigation system, as shown in Fig. 3E. Although not a precise measurement of accuracy, we found these accuracy tests to indicate that the clinical accuracy of the navigation system was satisfactory.

7. Limitations of this study

This technical evaluation study of navigated 3D ultrasound angiography demonstrates the straightforward application of neuronavigation with this imaging modality in 62 cases. To prove any benefit for the patient, a study with a different design is needed. The cases selected for evaluation of ultrasound angiography were cases wherein ultrasound-based neuronavigation was chosen in advance. Small, extra-axial tumors that were easy to localize were not included in this material because they were not operated with image guidance. In other tumor cases, which were operated with image guidance, ultrasound angiography was not used because the surgeon felt that it would not be of value. Most of the operations, and thus also the evaluation of the helpfulness of ultrasound angiography, were performed by one surgeon. Still, the 3 surgeons who participated seemed to judge the usefulness of 3D ultrasound angiography similarly. Nevertheless, different surgeons may judge the helpfulness of navigated ultrasound angiography differently, for example, some surgeons would not trust the navigation system enough to leave out dissection of important vessels. All this has to be kept in mind when interpreting the results of this study.

8. Future prospects

Ultrasound angiography still has potential for significant improvements, and developments along several venues are to be expected:

New signal processing methods such as BFI [12] may better visualize flow inside vessels and hopefully reduce the problem of blooming. Ultrasound contrast-enhancing agents have been reported to be helpful in tumor neurosurgery for assessing the vasculature close to and inside the tumor [8,14] and may improve the quality of ultrasound angiographic imaging.

New multirow probes will have a more optimal beam shape with better resolution in the elevation direction (eg, normal to the scan plane). This will further improve the image quality of ultrasound angiography because elevation resolution is a limiting factor for image quality with the present technology. Real-time 3D probes will be able to

acquire 3D ultrasound data sets directly without free hand movement, and this will minimize flash artifacts.

New multimodal visualization techniques where preoperative MR and intraoperative ultrasound are integrated in the same 3D scene are already available [10]. This may probably further enhance the surgeon's perception of anatomic and spatial relationships between tumor and adjacent vessels (Fig. 5). Diffusion tensor imaging of tracts and FMRI of eloquent cortex may also be visualized.

Furthermore, robust volume-to-volume registration techniques for registration of preoperative MR angiography data to intraoperative ultrasound angiography data may make it possible to adjust preoperative MR image data in cases of brain shift.

9. Conclusions

On the basis of our experience with navigated intraoperative ultrasound angiography, we believe that this imaging modality is sufficient for intraoperative imaging of arteries and veins. Image guidance with 3D ultrasound angiography may increase the safety in surgery of tumor cases where an important vessel is adjacent to or inside a tumor. It may facilitate tailored approaches, and frameless stereotactic biopsies may be performed with increased safety. Furthermore, with updated 3D ultrasound angiography imaging, accuracy of angio-based neuronavigation may be maintained in cases of brain shift.

Acknowledgments

This work was supported by the Norwegian Research Council.

References

[1] Albayrak B, Samdani AF, Black PM. Intra-operative magnetic resonance imaging in neurosurgery. Acta Neurochir (Wien) 2004;146:543-56 [discussion 57].

[2] Coenen VA, Dammert S, Reinges MH, et al. Image-guided microneurosurgical management of small cerebral arteriovenous malformations: the value of navigated computed tomographic angiography. Neuroradiology 2005;47:66-72.

[3] Dorward NL, Alberti O, Velani B, et al. Postimaging brain distortion: magnitude, correlates, and impact on neuronavigation. J Neurosurg 1998;88:656-62.

[4] Gronningsaeter A, Kleven A, Ommedal S, et al. SonoWand, an ultrasound-based neuronavigation system. Neurosurgery 2000; 47:1373-9 [discussion 79-80].

[5] Gronningsaeter A, Unsgard G, Ommedal S, et al. Ultrasound-guided neurosurgery: a feasibility study in the 3-30 MHz frequency range. Br J Neurosurg 1996;10:161-8.

[6] Hernes TA, Ommedal S, Lie T, et al. Stereoscopic navigation-controlled display of preoperative MRI and intraoperative 3D ultrasound in planning and guidance of neurosurgery: new technology for minimally invasive image-guided surgery approaches. Minim Invasive Neurosurg 2003;46:129-37.

[7] Hill DL, Maurer Jr CR, Maciunas RJ, et al. Measurement of intraoperative brain surface deformation under a craniotomy. Neurosurgery 1998;43:514-26 [discussion 27-28].

[8] Kanno H, Ozawa Y, Sakata K, et al. Intraoperative power Doppler ultrasonography with a contrast-enhancing agent for intracranial tumors. J Neurosurg 2005;102:295-301.

[9] Letteboer MM, Willems PW, Viergever MA, et al. Brain shift estimation in image-guided neurosurgery using 3-D ultrasound. IEEE Trans Biomed Eng 2005;52:268-76.

[10] Lindseth F, Kaspersen JH, Ommedal S, et al. Multimodal image fusion in ultrasound-based neuronavigation: improving overview and interpretation by integrating preoperative MRI with intraoperative 3D ultrasound. Comput Aided Surg 2003;8:49-69.

[11] Lindseth F, Lango T, Bang J, et al. Accuracy evaluation of a 3D ultrasound-based neuronavigation system. Comput Aided Surg 2002;7:197-222.

[12] Loevstakken L, Bjaerum S,Martens D, et al. Real-time blood motion imaging a 2D blood flow visualization technique. IEEE International Ultrasonics symposium, Montreal, Canada, Aug. 24-27, 2004. 1: 602.

[13] Muacevic A, Steiger HJ. Computer-assisted resection of cerebral arteriovenous malformations. Neurosurgery 1999;45:1164-70 [discussion 70-1].

[14] Otsuki H, Nakatani S, Yamasaki M, et al. Intraoperative ultrasound arteriography with the "Coded Harmonic Angio" technique. Report of three cases. J Neurosurg 2001;94:992-5.

[15] Riccabona M, Resch B, Eder HG, et al. Clinical value of amplitude-coded colour Doppler sonography in paediatric neurosonography. Childs Nerv Syst 2002;18:663-9.

[16] Roberts DW, Hartov A, Kennedy FE, et al. Intraoperative brain shift and deformation: a quantitative analysis of cortical displacement in 28 cases. Neurosurgery 1998;43:749-58 [discussion 58-60].

[17] Rohde V, Spangenberg P, Mayfrank L, et al. Advanced neuronavigation in skull base tumors and vascular lesions. Minim Invasive Neurosurg 2005;48:13-8.

[18] Rubin JM. Power Doppler. Eur Radiol 1999;9(Suppl 3):S318-22.

[19] Rubin JM, Hatfield MK, Chandler WF, et al. Intracerebral arteriovenous malformations: intraoperative color Doppler flow imaging. Radiology 1989;170:219-22.

[20] Russell SM, Woo HH, Joseffer SS, et al. Role of frameless stereotaxy in the surgical treatment of cerebral arteriovenous malformations: technique and outcomes in a controlled study of 44 consecutive patients. Neurosurgery 2002;51:1108-16 [discussion 16-18].

[21] Schmid-Elsaesser R, Muacevic A, Holtmannspotter M, et al. Neuronavigation based on CT angiography for surgery of intracranial aneurysms: primary experience with unruptured aneurysms. Minim Invasive Neurosurg 2003;46:269-77.

[22] Sure U, Alberti O, Petermeyer M, et al. Advanced image-guided skull base surgery. Surg Neurol 2000;53:563-72 [discussion 72].

[23] Sure U, Benes L, Bozinov O, et al. Intraoperative landmarking of vascular anatomy by integration of duplex and Doppler ultrasonography in image-guided surgery. Technical note. Surg Neurol 2005; 63:133-41.

[24] Tekula F, Pritz MB, Kopecky K, et al. Usefulness of color Doppler ultrasound in the management of a spinal arteriovenous fistula. Surg Neurol 2001;56:304-7.

[25] Unsgaard G, Gronningsaeter A, Ommedal S, et al. Brain operations guided by real-time two-dimensional ultrasound: new possibilities as a result of improved image quality. Neurosurgery 2002;51:402-11 [discussion 11-12].

[26] Unsgaard G, Ommedal S, Muller T, et al. Neuronavigation by intraoperative three-dimensional ultrasound: initial experience during brain tumor resection. Neurosurgery 2002;50:804-12 [discussion 12].

[27] Unsgaard G, Ommedal S, Rygh O, et al. Operation of arteriovenous malformations assisted by stereoscopic navigation-controlled display of preoperative magnetic resonance angiography and intraoperative ultrasound angiography. Neurosurgery 2005;56:281-90.

[28] Unsgaard G, Rygh OM, Selbekk T, et al. Intra-operative 3D ultrasound in neurosurgery. Acta Neurochir (Wien) 2006;148: 235-53.

[29] Wirtz CR, Knauth M, Staubert A, et al. Clinical evaluation and follow-up results for intraoperative magnetic resonance imaging in neurosurgery. Neurosurgery 2000;46:1112-20 [discussion 20-2].
[30] Woydt M, Greiner K, Perez J, et al. Intraoperative color duplex sonography of basal arteries during aneurysm surgery. J Neuroimaging 1997;7:203-7.
[31] Woydt M, Perez J, Meixensberger J, et al. Intra-operative colour-duplex-sonography in the surgical management of cerebral AV-malformations. Acta Neurochir (Wien) 1998;140:689-98.

Commentary

In the past several years, intraoperative imaging has gained increasing importance. With the newest medico-technical achievements such as high-field (1.5–3 T) MRI and multislice CT, a certain renaissance of intraoperative imaging has started. However, the setting up of such diagnostic tool requires a major financial background. Consequently, Unsgaard et al started to promote the intraoperative navigated ultrasound technology by introducing a 3D ultrasound navigation system. In previous publications, this group described a very nice system that is capable of producing a 3D imaging ultrasound data set that is used for navigation and can be supported by the display of preoperatively acquired corresponding MRI images. In their article, the authors demonstrate the integration of power Doppler (Duplex or color mode) signals in their 3D navigation data set. The figures, as shown by the authors, are of very high quality; let us hope that the drawbacks of the intraoperative ultrasound imaging of vessels, such as the exaggeration of the caliper (blooming), can be reduced in future.

Frequently, for us neurosurgeons, the vascular anatomy is the most interesting part to recognize in a navigational data set. Therefore, we believe that particularly the 3D visualization of the vascular anatomy, as presented here, is of major benefit during surgery of a broad variety of intracranial pathologies. In our experience, such technology is of particular benefit when vessels are encased or distorted by tumors or when evaluation of hemodynamics within a complex AVM is intended [1]. The usefulness of a similar technique for treatment of vascular lesions has also been previously illustrated by the same group [2]. One of the most interesting questions to answer in the future will be whether the ultrasound technology will allow to evaluate the neck of a clipped aneurysm to exclude a remnant.

However, alongside the economic aspect, acquisition time and quality of intraoperative visualization of the vascular anatomy are further advantages of the ultrasound technology when compared with the MRI and/or CT intraoperative imaging solutions.

Dorothea Miller, MD
Oliver Bozinov, MD
Ulrich Sure, MD
Clinic for Neurosurgery, University Hospital
Philipps-University Marburg
Marburg, 35033 Germany

References

[1] Tirakotai W, Miller D, Heinze S, Benes L, Bertalanffy H, Sure U. A novel platform for image-guided ultrasound. Neurosurgery 2006;58:710-8.
[2] Unsgaard G, Ommedal S, Rygh OM, Lindseth F. Operation of arteriovenous malformations assisted by stereoscopic navigation-controlled display of preoperative magnetic resonance angiography and intraoperative ultrasound angiography. Neurosurgery 2005;56(2 Suppl):281-90.

PAPER 3

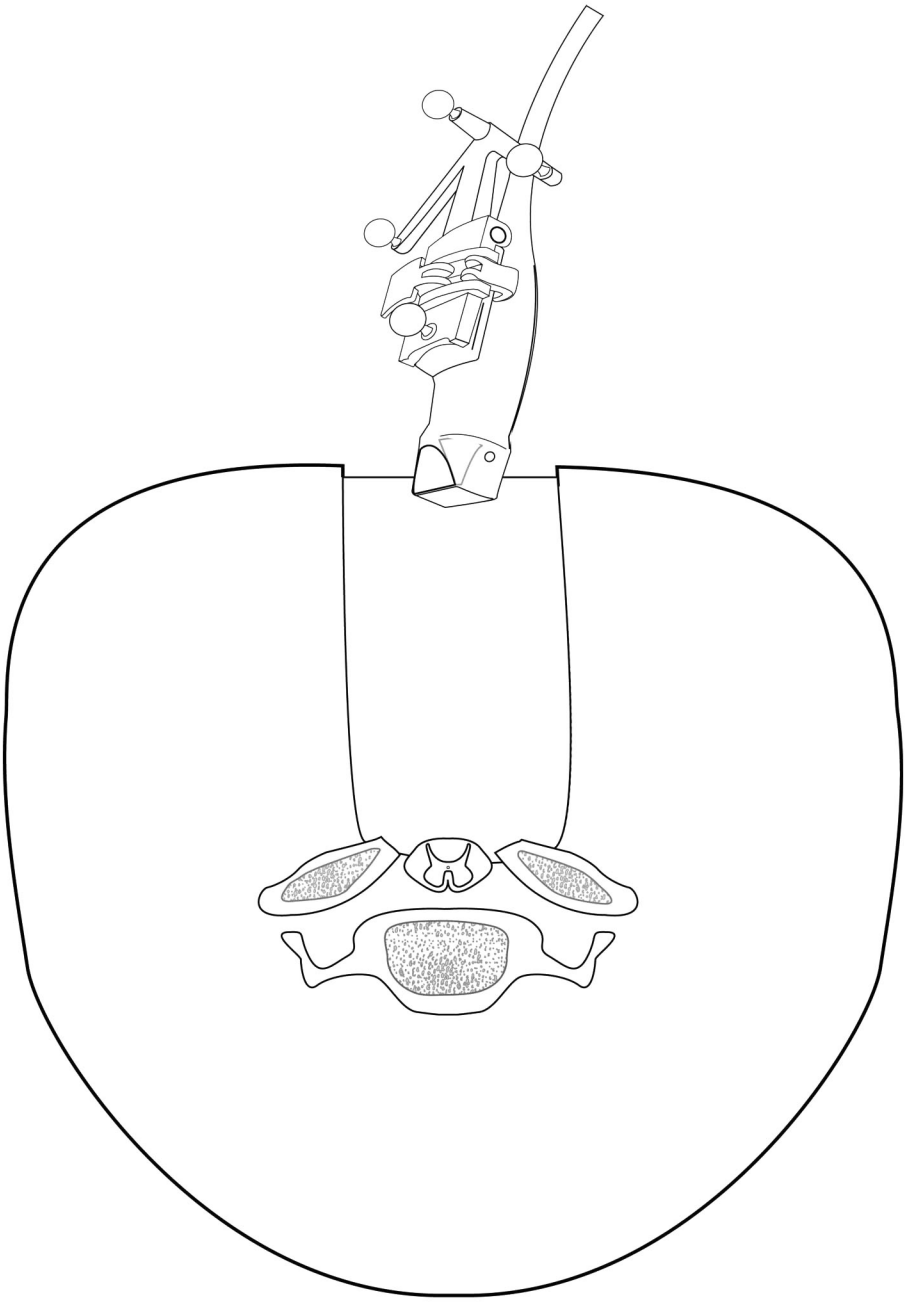

J Neurosurg Spine 5:264–270, 2006

Three-dimensional ultrasonography navigation in spinal cord tumor surgery

Technical note

Frode Kolstad, M.D., Ola M. Rygh, M.D., Tormod Selbekk, M.Sc., Geirmund Unsgaard, M.D., Ph.D., and Øystein P. Nygaard, M.D., Ph.D.

National Center of Spinal Disorders, National Center for 3D Ultrasound in Surgery, and Department of Neurosurgery, St. Olav University Hospital; The Norwegian University of Science and Technology; and SINTEF Health Research, Trondheim, Norway

✓The authors describe the technical application of three-dimensional (3D) ultrasonography navigation in spinal cord tumor surgery.

The spinal cord is a complex neurological structure in which there is the potential for causing neurological morbidity during tumor resection. Standard neuronavigation systems based on computed tomography or C-arm images are not adapted to tumor surgery in the spinal cord.

Since 2004 the authors have been using a 3D ultrasonography-based neuronavigation system. During surgery, two-dimensional ultrasound images were acquired and reconstructed into 3D image data to assist in tumor resection. The navigation cameras read the position of a patient reference frame attached to a spinous process, the ultrasonography probe, and surgical instruments. Five- and 10-MHz phased-array ultrasonography probes equipped with optical tracking frames were used for image data acquisition.

Spinal cord tumors were visualized using ultrasonography, and 3D ultrasonography–guided tumor biopsy sampling and resection were performed.

The practice of attaching the reference frame to a spinous process adjacent to the spinal cord tumor, as well as performing image acquisition just before starting the resection, reduced the possible sources of inaccuracy.

The technical application of a navigation system based on intraoperative 3D ultrasound image reconstruction seems feasible and may have the potential of improving functional outcome in association with spinal cord tumor surgery.

Key Words • three-dimensional ultrasonography • neuronavigation • spine tumor • spinal cord neoplasm

Tumors of the spinal cord account for 2 to 4% of all central nervous system tumors.[16] They are found in approximately 20% of spinal tumors in adults and 35% in children.[2] The most common histological types are glial tumors (80%).[7,9] The surgical treatment of spinal cord tumors began almost a century ago. In 1905 Cushing[3] performed decompression of a spinal cord tumor. Today most tumors are treated using microsurgical techniques after the patient undergoes detailed preoperative investigation and planning. The spinal cord, however, is a very complex neurological structure and the potential of serious operative neurological morbidity is present.[11]

Conventional neuronavigation systems have become frequently used for planning and performing spinal surgery. The systems are based on preoperative computed tomography images or C-arm perioperative images. The main indication for these guidance systems is quality control during fusion surgery involving pedicle screws. They are not applicable in spinal cord tumor surgery.

Ultrasonography has been used in guiding intraspinal surgery for many years.[10,12–14,18] Limited image quality and certain practical aspects, however, have limited its use. Technological advances in ultrasonography have been considerable in recent years. Renewed interest in ultrasonography as a practical intraoperative modality in neurosurgery has arisen due to the advent of phased-array probes with small footprints and optimal focusing at a range of depths that allow for treatment in a minimally invasive fashion. Other alternative intraoperative guidance systems focusing on soft-tissue structures in the spinal canal have not been available. One problem with 2D ultrasonography in spinal surgery is positioning of the operating instruments. When the lesion is seen on the 2D image, the

Abbreviations used in this paper: CUSA = Cavitron Ultrasonic Surgical Aspirator; MR = magnetic resonance; ROI = region of interest; 2D = two-dimensional; 3D = three-dimensional.

orientation of the probe needs to be taken into account to estimate the lesion's location in the physical space. The surgeon has to remember the position of the probe when applying practical use of the images. When acquiring the 2D images, this might be difficult when the surgical cavity has to be filled with saline and the probe subsequently removed before the instruments are inserted.

The practical limitations inherent in the use of 2D ultrasonography in spinal surgery are overcome by using a 3D ultrasonography–based navigation system. A 3D ultrasonography image volume is acquired by tilting/translating the probe over the ROI. The 3D image volume is then automatically transferred to the navigation system, and navigation based on intraoperative images can be performed directly without any registration procedure. Thus, the localization of the lesion can be accomplished by simply using a conventional navigation pointer or any other instrument equipped with a tracking frame.

The aim of this paper is to describe a new concept in which 3D ultrasonography–guided navigation is used in the resection of spinal cord tumors. The technical use is illustrated in three clinical cases.

Clinical Material and Methods

Since 2004 we have used a 3D ultrasonography–based navigation system in patients with intraspinal pathological entities. In the present report we describe the technical application of this technique in the treatment of spinal cord tumors.

The Ultrasonography-Based Neuronavigation System

The ultrasonography-based intraoperative imaging and neuronavigation system (SonoWand; Mison, Trondheim, Norway) used in the present study has three functions: as an ultrasound imager, a conventional neuronavigation system, and an integrated, ultrasound-based neuronavigation system that uses the features of both technologies.[17] The system is based on optical tracking technology and comes with precalibrated ultrasound probes optimized for neurosurgery.[5] Two different probes were used: a 5-MHz (4–8-MHz) flat phased-array probe (optimal resolution at depths 2.5–6 cm) and a 10-MHz flat phased-array probe (optimal resolution at depths 0.5–4 cm) (Fig. 1). Because the 10-MHz probe has just recently been made available for 3D navigation, most of the ultrasound images illustrating the technical use were obtained with the 5-MHz probe.

FIG. 1. Probes used in 3D ultrasound image–based navigation: the 5-MHz probe *(left)* and the 10-MHz probe *(right)*.

Navigation and Data Acquisition

To attach the reference frame to the patient, we had a spine clamp developed. This clamp was attached to a spinous process adjacent to the tumor area (Fig. 2). In one patient (see Case 1), however, the reference frame was attached to the head holder because the lesion was located in the cranial part of the cervical cord. To acquire the 3D data, the surgeon tilts or translates the probe over the ROI using his/her free hand. The 2D ultrasound images are reconstructed to a 3D data set ready for navigation. The procedure takes approximately 1 minute. The ultrasound probe is not present in the operating field after the acquisition of a 3D volume, unless additional 3D ultrasound data sets are acquired or real-time 2D imaging is wanted. The workflow of this procedure and setup of equipment is summarized in Fig. 3.

Navigation based on 3D ultrasonography can be performed directly without registration of anatomical landmarks because the images are acquired in the same coordinate system as the navigation is performed. Therefore, no patient or image registration error will affect the overall accuracy of the system when navigation based on 3D ultrasound images is utilized.[6]

FIG. 2. The spine clamp and patient reference frame. *Left:* Disassembled. *Right:* Assembled and attached to a spinous process adjacent to the laminectomy.

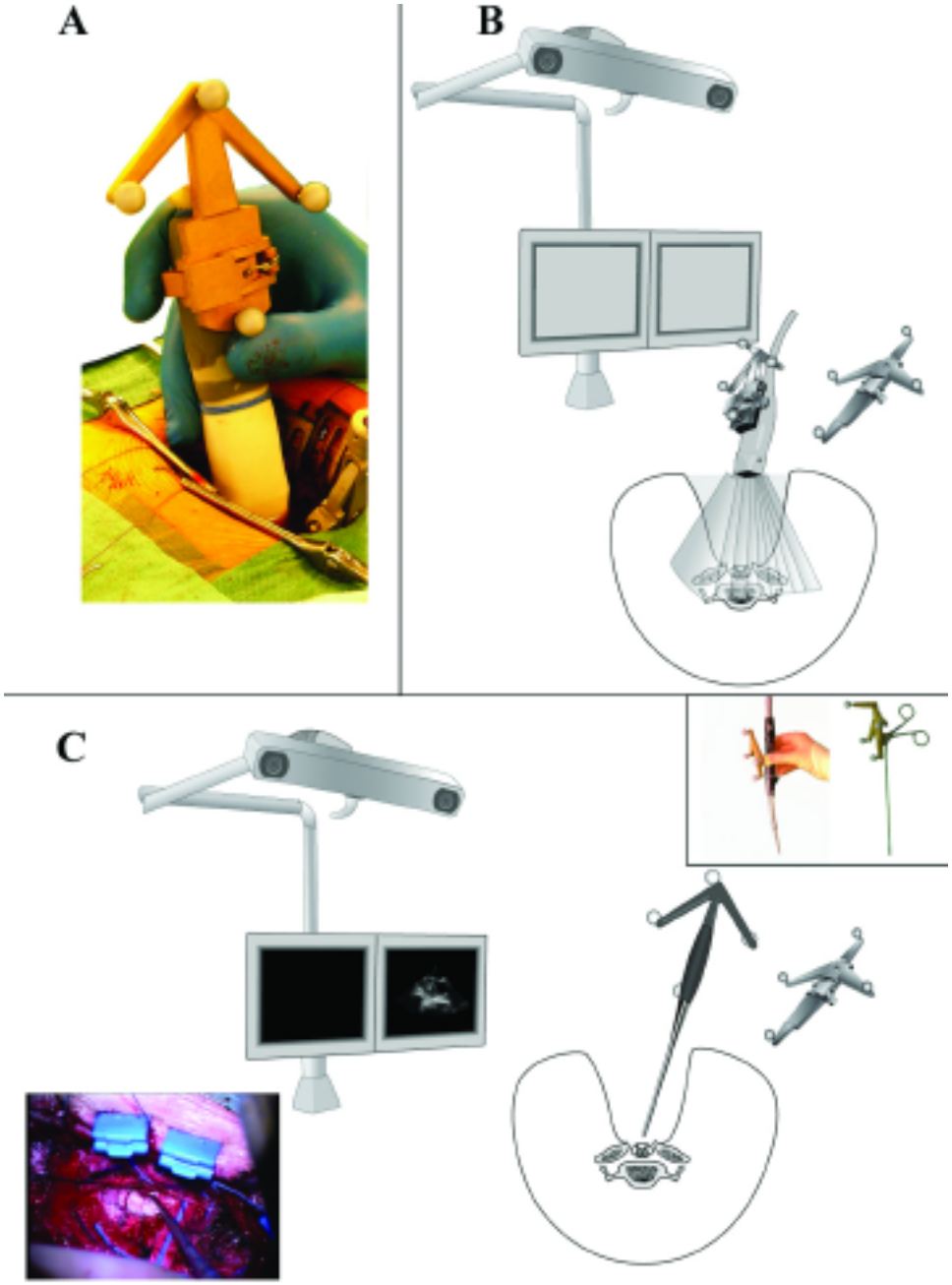

FIG. 3. Workflow in 3D ultrasonography–based spinal tumor surgery. A: The ultrasound probe with the tracking frame attached is put into the saline-filled cavity. The 2D ultrasound images can be viewed. B: By tilting and translating the probe, the 2D ultrasound images with position information are stored and reconstructed into a 3D image volume. C: With 3D ultrasound, neuronavigation can be performed using a pointer device or any tracked surgical instrument, such as the CUSA or biopsy forceps (see *inset*; photograph obtained using the operative microscope).

Neuronavigation can be performed using a tracked pointer device or with any calibrated surgical instrument—for example, a biopsy forceps, CUSA (Valleylab, Boulder, CO), or an endoscope. The trajectory and position of the pointer or surgical tool tip are displayed as a line with crosshairs or a dot (depending on the version of the navigation software) in the corresponding images. The pointer and surgical tool can be elongated virtually using an offset feature.

The display modalities commonly used are as follows: 1) orthogonal slicing (three 2D slices oriented as axial, sagittal and coronal slices) and 2) any-plane slicing (one slice defined by the axis and rotation of the pointer or custom-calibrated tool [for example, the biopsy forceps]).

The accuracy of 3D ultrasound–based navigation in which the SonoWand system is used in a laboratory setting may be as low as 1.4 mm. The accuracy in the present clinical situation can easily be tested by pointing at a de-

fined structure, such as the surface of the spinal cord, in the operative field.

Description of the Surgical Procedure

A standard laminectomy was performed, and the spine clamp with the patient-reference frame was attached to the adjacent spinous process. The operation cavity was gently filled with saline before a 3D ultrasound image data set was acquired by tilting the probe in the operation cavity, covering the ROI.

With neuronavigation based on the recently acquired 3D ultrasound image data, the pointer was used to determine the optimal site for dural opening. For frameless stereotactic biopsy sampling, a calibrated biopsy forceps was used. This tool was calibrated by pointing it at a hole in the center of the patient-reference frame. The biopsy samples were then collected using image guidance. Resection of the tumors was either done using conventional microsurgical technique or, in some of the cases, with the CUSA equipped with a tracking frame for online image-guided resection.

Updated 3D image data were obtained when required because of suspected anatomical shift or to assess the presence of residual tumor. At the end of the procedure the spine clamp was removed and the operation wound was closed.

Illustrative Cases

Case 1

This 42-year-old man presented with right-sided facial pain. Magnetic resonance imaging revealed a lesion in the spinal cord at the C-1 level. The findings were consistent with the diagnosis of a cavernous hemangioma. The patient's head was fixed with a Mayfield headholder and the patient reference frame was attached to the headholder because the lesion was located in the cranial part of the cervical medulla. During the procedure we had preoperative MR imaging data with fiducials available, and these images were registered and used for planning of the incision. A lateral suboccipital approach was performed. When the dura mater was exposed, 3D ultrasound images were acquired and used for image guidance. Both the 5- and 10-MHz probes were used; however, at this time we did not have a tracking frame available for the 10-MHz probe, and thus image guidance could be performed using the 3D ultrasound data obtained with the 5-MHz probe only. We found that both the 5- and the 10-MHz probe provided images of sufficient quality, but that of the 10-MHz probe was superior. We noticed a distinct discrepancy between the preoperative MR imaging and the intraoperative ultrasound data during navigation (Fig. 4A and B), presumably a consequence of both anatomical shift and inaccuracy in image registration of the MR imaging data.

The cavernous hemangioma was not easily visualized on the surface of the spinal cord, but by applying 3D ultrasonography navigation, an accurate site for incision in the spinal cord was defined. The lesion was extirpated using conventional microsurgical technique. Sequential intraoperative ultrasonography provided information on the extent of resection (Fig. 4C).

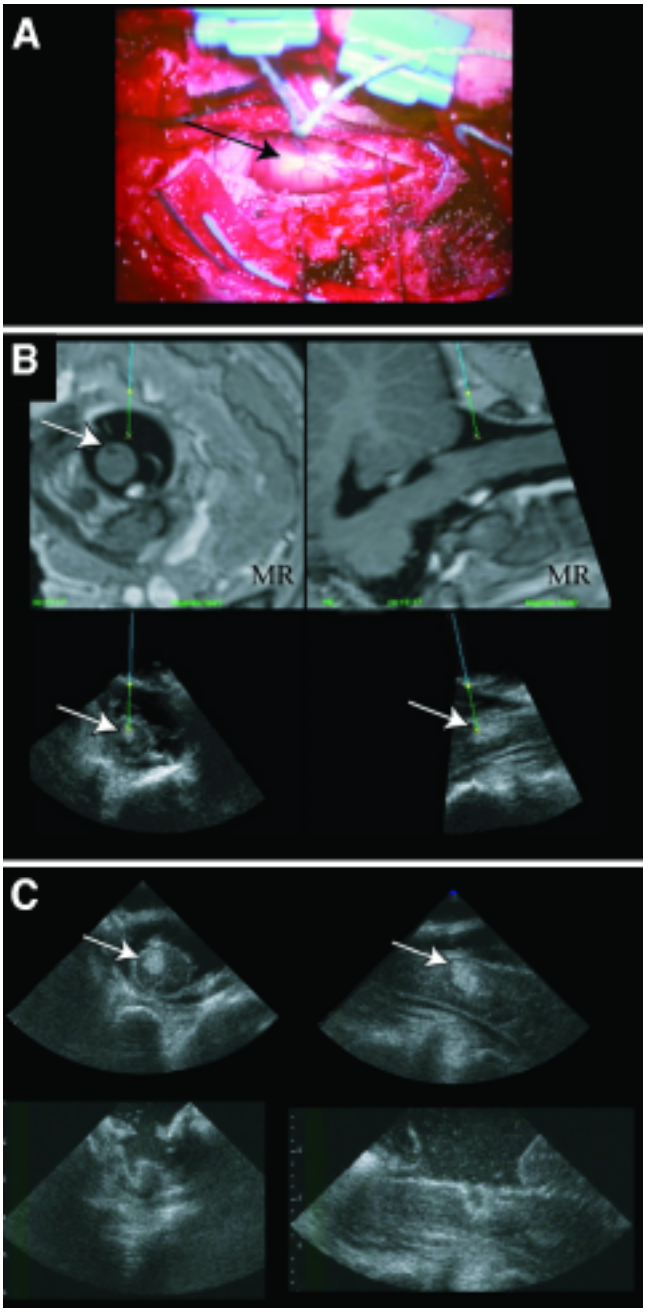

FIG. 4. Case 1. A: Intraoperative image showing a cavernous hemangioma *(black arrow)* in the upper cervical spinal cord. The position of the cavernous hemangioma was not obvious to us when inspecting the surface of the spinal cord. B: Snapshot from the neuronavigation system. In this case preoperative MR images were available, and the reference frame was attached to the headholder (in the other cases the reference frame was attached to the spine clamp). Note the shift between the MR *(upper)* and the ultrasound images *(lower)*. The *blue line* shows the position of the biopsy forceps, and the *yellow dot* indicates the tip of the instrument. The *elongated line* with the *cross* at the end demonstrates the offset feature. The *arrows* point to the cavernous hemangioma. C: Sequentially obtained ultrasound images using the 10-MHz probe. Upper row: Ultrasound images acquired prior to resection. *Arrows* point to the cavernoma. Lower row: Ultrasound images after resection of the cavernoma, in this case demonstrating the removal of the lesion.

Case 2

This 82-year-old man presented with progressive myelopathy and urinary incontinence. Imaging showed a lesion in the spinal cord at the conus level (Fig. 5A). A T11–12 laminectomy was conducted and the dura mater was exposed. The spine clamp was attached to the adjacent spinous process, and 3D ultrasound images were acquired using the 5-MHz probe.

Ultrasonography provided good visualization of the lesion (Fig. 5B). The biopsy forceps was calibrated to the navigation system, and, based on the 3D ultrasound images, a site for biopsy sampling was chosen (Fig. 5C and D). The lesion was diagnosed as an anaplastic astrocytoma.

Case 3

This 48-year-old woman with a history of breast cancer was referred to our unit. There was imaging documentation of a cystic lesion in the conus medullaris and an associated syrinx. She presented with mild gait unsteadiness. A resection of the lesion was planned. A T11–12 laminectomy was undertaken and the dura was exposed. The spine clamp was attached to the T-10 spinous process, and 3D ultrasound images were obtained using the 5-MHz probe. We did not yet have the tracking frame for the 10-MHz probe.

We found that the cysts and the solid parts of the lesion were well visualized by 3D ultrasonography (Fig. 6). Even the septa between the cysts were clearly visualized. Two-dimensional images with the 10-MHz probe were also acquired. With neuronavigation based on the 3D ultrasound images, biopsy samples were taken, the cysts fenestrated, and a limited tumor resection performed. The histological diagnosis was intramedullary ependymoma. Due to the coexisting advanced breast carcinoma and the patient's strong desire to maintain function, complete resection was not performed.

Discussion

General Considerations

Intramedullary spinal cord tumors are rare lesions, but when they occur surgery is commonly the treatment of choice. One of the most important predictors of treatment outcome is complete excision.[11]

Two-dimensional real-time ultrasonography has been used for many years to guide the anatomical identification and resection of spinal tumors, but poor image quality and certain practical aspects have limited its use. Recent refinements in image quality, however, have led to a renaissance in applying ultrasonography. New imaging modalities, such as ultrasound strain imaging, may further increase the clinical usefulness of ultrasonography in neurosurgery.[15]

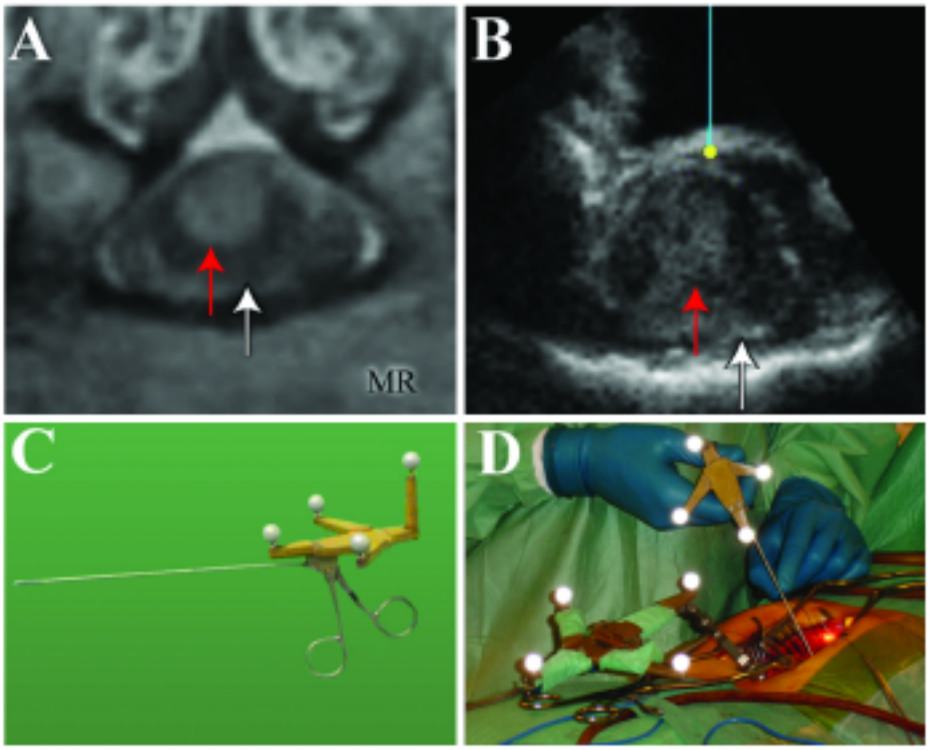

FIG. 5. Case 2. This patient harbored an anaplastic astrocytoma in the thoracic spinal cord. Using the calibrated biopsy forceps, the biopsy site was determined. The *white arrows* point to the dura mater (in A and B). A: Axial T1-weighted Gd-enhanced MR image demonstrating the enhancing tumor *(red arrow)*. B: Ultrasound image. The *blue line* with the *yellow dot* indicates the position of the biopsy forceps. The tumor *(red arrow)* is hyperdense. C: Photograph of the biopsy forceps with the tracking frame. D: Photograph of the biopsy sampling procedure.

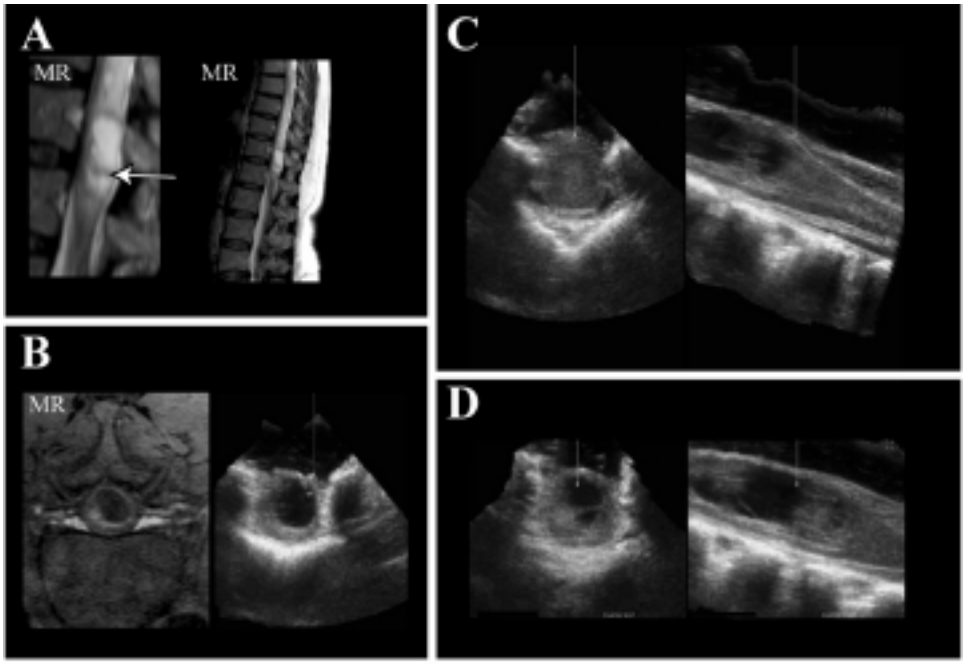

FIG. 6. Case 3. This patient harbored a cystic ependymoma. A: Sagittal MR images: the cyst, with a septum within *(arrow [left])* and an overview of the sagittal spine *(right)*. B: Axial MR image showing the cystic tumor *(left)* and the equivalent ultrasound image obtained using the navigation system *(right)*. The 3D ultrasonography provides images of high quality. C: By pointing at the medullary surface or the wall of the cystic cavity *(white line)*, the accuracy of the modality in this clinical setting can be appreciated. The *dot* at the end of the white line touches the dura. D: Ultrasound images obtained using the neuronavigation system. Note how the septum within the cyst is shown.

Ultrasonography Navigation

Three-dimensional ultrasound image guidance is an important, evolving modality. With our system, the 3D ultrasound volume is built up of 100 to 200 2D images by tilting or translating a precalibrated ultrasonography probe covering the ROI. It takes approximately 1 minute to acquire and reconstruct a 3D ultrasound volume. Three-dimensional ultrasonography–based navigation may thus be close to providing "real-time" data, but of course this depends on how often images are updated. Image-to-patient registration is not necessary because the ultrasound acquisition is performed in the same coordinate system as navigation. Definition of spatial relationships and anatomical structures is generally easier with 3D than 2D ultrasound images because the interactive reslicing and display of the image volume from any angle is possible. What makes this modality a practical tool is the preoperative registration, intraoperative sequentially obtained ultrasound images that update the situation, and the intuitive understanding of spatial relationships. Combining high-quality 3D ultrasonography with navigation is the only neuronavigation-based solution available for use in intramedullary spinal cord tumor surgery. Computed tomography– or MR imaging–based systems for this purpose are, to the best of our knowledge, not available. With the use of 3D ultrasound image guidance in spinal cord tumor surgery, resection can be guided by updated 3D ultrasound images, thus reducing the potential risk of traumatizing normal medulla.

Probes/Image Quality

High image quality and resolution are vital for successful image-guided surgery. The quality of the 3D volumes is dependent on the quality of the 2D images. Higher frequency in ultrasonography means improved resolution but also reduced tissue penetration. Contemporary probes are electronically tuned, and optimal resolution can be obtained simultaneously at a broad range of depths. In our three cases, we used a 5-MHz probe for 3D image acquisition, but now a 10-MHz probe is available for the navigation system. Because the 10-MHz probe has an optimal image quality at a closer range (0.5–4 cm), it is preferable for spinal cord tumor surgery. Anatomically the spinal canal is well suited for 10-MHz probes because the ROI is close to the probe. A phased-array probe spreads out like a fan covering a large sector, whereas the image acquired using a linear-array probe is limited to the width of the probe. This makes phased-array probes preferable. Whether better image quality and resolution will assist in differentiating between histological tumor types has yet to be proven. The same goes for new image modalities such as ultrasound strain imaging in which differences in elastic properties of the spinal cord may be visualized. The authors of a recent publication have shown that ultrasound strain imaging can discriminate the elastic properties of normal brain and low-grade astrocytoma;[15] this imaging modality may prove to be a useful adjunct to conventional ultrasonography.

Accuracy, Reference Frame, and Anatomical Shift

Several sources of inaccuracy in image-guided spinal cord surgery are present. In addition to accuracy limitations of the hardware, anatomical shifts (termed "brain shift" in cranial neurosurgery) might represent a problem. The accuracy of the SonoWand system has been tested in the laboratory setting by Lindseth and colleagues[6] and was measured to be approximately 1.4 mm.

Changing the patient from supine to prone position may cause at least the conus medullaris to change position.[19] Laminectomy and dural opening can also theoretically change the position of the spinal cord. When 3D ultrasound image acquisition is conducted immediately before the tumor resection, these sources of inaccuracy are kept to a minimum.

Furthermore, the practice of attaching the reference frame to a spinous process adjacent to the spinal cord tumor reduces inaccuracy due to small changes in patient positioning intraoperatively and thus has an advantage over attaching the reference frame to the operating table, a solution chosen by Bonsanto, et al.,[1] in syrinx surgery. Furthermore, inaccuracy due to respiratory intraoperative spinal motion[4] may be kept to a minimum when attaching the frame to the spinous process because the vertebrae and the spinal cord probably move in a similar fashion during respiration.

Other sources of inaccuracy are virtually impossible to avoid without real-time imaging. The spinal cord moves in a pulsatile fashion with each cardiac cycle. Mikulis et al.,[8] reported a pulsatile craniocaudal displacement of the cervical cord of 0.4 to 0.5 mm, whereas no definite motion was seen in the midthoracic cord or conus medullaris. This source of shift, however small, must always be kept in mind by the surgeon when using equipment such as this.

The overall clinical accuracy of this system in association with spinal cord tumor surgery has not been systematically tested because the aim of the present study was to establish and evaluate the feasibility of a method for 3D ultrasound image–guided spinal cord tumor surgery. We did, however, conduct a qualitative accuracy test in each of the operations by directing the pointer at the surface of the dura mater after 3D ultrasound image acquisition (Figs. 5 and 6), and in each case we observed that the position of the pointer suggested by the navigation system and the position of the pointer in the operation field were in near-total agreement. This shows that at least the clinical accuracy in the anteroposterior axis was satisfactory.

Conclusions

Spinal cord tumors were visualized using ultrasonography, and tumor biopsy and resection were performed guided by 3D ultrasonography navigation.

The practices of attaching the reference frame to a spinous process adjacent to the spinal cord tumor and performing image acquisition just before starting the resection reduced several sources of inaccuracy. The technical application of a navigation system based on intraoperative 3D ultrasound reconstruction seems feasible and may have the potential of improving functional outcome in spinal cord tumor surgery.

References

1. Bonsanto MM, Metzner R, Aschoff A, Tronnier V, Kunze S, Wirtz CR: 3D ultrasound navigation in syrinx surgery—a feasibility study. **Acta Neurochir (Wien) 147:**533–541, 2005
2. Constantini S, Epstein F: Primary spinal cord tumors, in Levin AV (ed): **Cancer in Central Nervous System.** New York: Churchill Livingstone, 1994, pp 127–138
3. Cushing H: The special field of neurological surgery. **John Hopkins Hosp Bull 16:** 77–87, 1905 (also published in **Cleveland Med J 4:**1–25, 1905)
4. Glossop N, Hu R: Assessment of vertebral body motion during spine surgery. **Spine 22:**903–909, 1997
5. Grønningsæter Å, Kleven A, Ommedal S, Årseth TE, Lie T, Lindseth F, et al: SonoWand, an ultrasound-based neuronavigation system. **Neurosurgery 47:**1373–1380, 2000
6. Lindseth F, Langø T, Bang J, Nagelhus Hernes TA: Accuracy evaluation of a 3D ultrasound-based neuronavigation system. **Comput Aided Surg 7:**197–222, 2002
7. Maira G, Amante P, Denaro L, Mangiola A, Colosimo C: Surgical treatment of cervical intramedullary spinal cord tumors. **Neurol Res 23:**835–842, 2001
8. Mikulis DJ, Wood ML, Zerdoner OA, Poncelet BP: Oscillatory motion of the normal cervical spinal cord. **Radiology 192:** 117–121, 1994
9. Miller DC: Surgical pathology of intramedullary spinal cord neoplasms. **J Neurooncol 47:**189–194, 2000
10. Quencer RM: The injured spinal cord. Evaluation with magnetic resonance and intraoperative sonography. **Radiol Clin North Am 26:**1025–1045, 1988
11. Raco A, Esposito V, Lenzi J, Piccirilli M, Delfini R, Cantore G: Long-term follow-up of intramedullary spinal cord tumors: a series of 202 cases. **Neurosurgery 56:**972–981, 2005
12. Regelsberger J, Fritzsche E, Langer N, Westphal M: Intraoperative sonography of intra- and extramedullary tumors. **Ultrasound Med Biol 31:**593–598, 2005
13. Reid MH: Ultrasonic visualization of a cervical cord cystic astrocytoma. **AJR Am J Roentgenol 131:**907–908, 1978
14. Rubin JM, Dohrmann GJ: The spine and spinal cord during neurosurgical operations: real-time ultrasonography. **Radiology 155:**197–200, 1985
15. Selbekk T, Bang J, Unsgaard G: Strain processing of intraoperative ultrasound images of brain tumors: initial results. **Ultrasound Med Biol 31:**45–51, 2005
16. Stein BM, McCormick PC: Intramedullary neoplasms and vascular malformations. **Clin Neurosurg 39:**361–387, 1992
17. Unsgaard G, Ommedal S, Muller T, Gronningsaeter A, Nagelhus Hernes TA: Neuronavigation by intraoperative three-dimensional ultrasound: initial experience during brain tumor resection. **Neurosurgery 50:**804–812, 2002
18. Wilberger JE Jr, Maroon JC, Prostko ER, Baghai P, Beckman I, Deeb Z: Magnetic resonance imaging and intraoperative neurosonography in syringomyelia. **Neurosurgery 20:**599–605, 1987
19. Witkamp TD, Vandertop WP, Beek FJA, Notermans NC, Gooskens RHJM, van Waes PFGM: Medullary cone movement in subjects with a normal spinal cord and in patients with a tethered spinal cord. **Radiology 220:**208–212, 2001

Manuscript received September 27, 2005.

Accepted in final form June 13, 2006.

This work was supported by the Norwegian Ministry of Health and Social Affairs and the Research Council of Norway.

Address reprint requests to: Frode Kolstad, M.D., St. Olav University Hospital, Trondheim, Olav Kyrres Gate 17, N-7005 Trondheim, Norway. email: Frode.Kolstad@ntnu.no.

PAPER 4

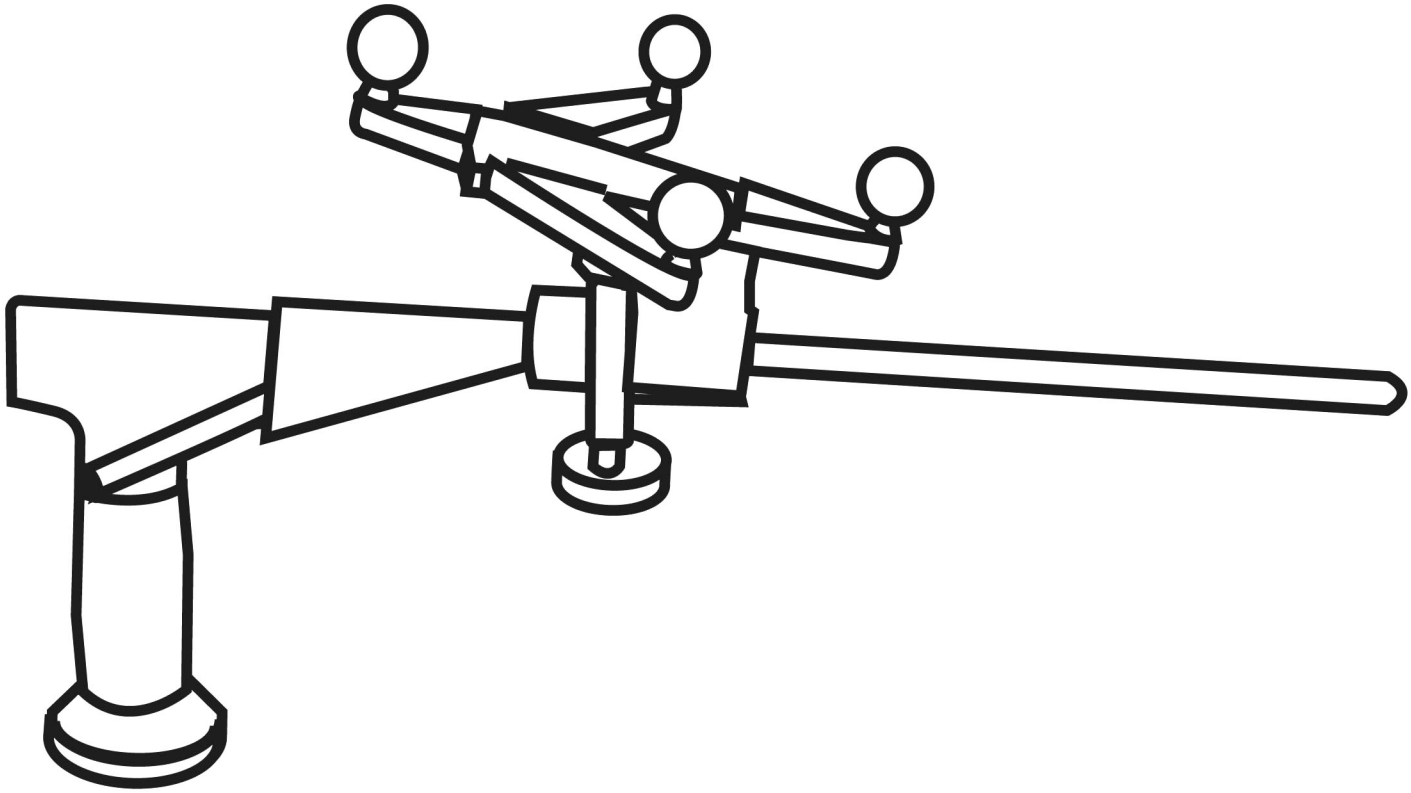

O. M. Rygh[1,2,4]
J. Cappelen[1]
T. Selbekk[3,4]
F. Lindseth[3,4]
T. A. N. Hernes[2,3,4]
G. Unsgaard[1,2,4]

Endoscopy Guided by an Intraoperative 3D Ultrasound-Based Neuronavigation System

Abstract

Objective: We have investigated the feasibility of using 3D ultrasound-based neuronavigation for guiding neuroendoscopy. **Methods:** A neuronavigation system with an integrated ultrasound scanner was used for acquiring the 3D ultrasound image data. The endoscope with a tracking frame attached was calibrated to the navigation system. The endoscope was guided based on intraoperative 3D ultrasound data in 9 operations. In 5 of the operations, ultrasound angiography data were also obtained. Updated image data (e.g., more than one 3D ultrasound dataset) were obtained in 6 of the operations. **Results:** We found that the image quality of 3D ultrasound was sufficient for image guidance of the endoscope. Planning of the entry point and trajectory as well as finding optimal sites for fenestration were successfully performed. Blood vessels were visualized by 3D ultrasound angiography. In one procedure of third ventriculostomy, the basilar artery was visualized. Updated image data were quickly obtained, and in two of the cases, a reduction of the size of cysts was demonstrated. **Conclusions:** 3D ultrasound gives accurate images of sufficiently high quality for image guidance of neuroendoscopy. Updated 3D ultrasound datasets can easily be acquired and may adjust for brain shift. Ultrasound angiography image data are also available with this technology and can visualize vessels of importance.

Key words

Ultrasound · three-dimensional ultrasound · neuronavigation · neuroendoscopy

Introduction

Advances in endoscope technology have resulted in more frequent use of neuroendoscopy. A number of different indications for using this technology exist, such as third ventriculostomy [1–3], colloid cysts [4,5], septum pellucidum cysts [6,7], intraventricular tumors [8,9], and pituitary tumors [10] among others. However, even with advances in neuroendoscopy, certain limitations still exist, such as orientation of the endoscope in abnormal anatomy, inserting the endoscope into small narrow ventricles, visualization in opaque fluids and finding small subependymal tumor masses [11].

Several methods for solving these limitations are reported. Intraoperative imaging with MRI [12,13] and ultrasound [14–19] has been used to give improved anatomical orientation in neuroendoscopic procedures. Real-time 2D ultrasound has been used to guide neuroendoscopic procedures since the 1980s and has been reported to give satisfactory images for guiding such procedures [16–19]. However, other authors find ultrasound less suitable for guiding neuroendoscopic procedures [11]. Stereotaxy has been used for finding the optimal entry point and trajectory for endoscopic procedures in the ventricular system and for third ventriculostomy [9,20,21], but still this method has its practical limitations.

Neuronavigation integrated with an endoscope seems to be a natural evolution of neuroendoscopy and is reported to give improved anatomical orientation, and to facilitate the selection of

Affiliation
[1] Department of Neurosurgery, St. Olav University Hospital, Trondheim, Norway
[2] The Norwegian University of Science and Technology, Trondheim, Norway
[3] SINTEF Health Research, Trondheim, Norway
[4] National Centre for 3D Ultrasound in Surgery, St. Olav University Hospital, Trondheim, Norway

Correspondence
Ola M. Rygh, M. D. · Department of Neurosurgery · St. Olav University Hospital Trondheim · Olav Kyrres gate 17 · 7005 Trondheim · Norway · Tel.: +47/9284/9775 · Fax: +47/7386/7977 · E-mail: ola.rygh@ntnu.no

Bibliography
Minim Invas Neurosurg 2006; 49: 1–9 © Georg Thieme Verlag KG Stuttgart · New York
DOI 10.1055/s-2005-919164
ISSN 0946-7211

Table 1 Summary of the patients treated by endoscopic procedures with neuronavigation based on 3D ultrasound

Patient	Sex/age	Diagnosis	Procedure	No. of 3D ultrasound acquisitions	US angiography used	Preoperative 3D MRI used in neuronavigation
1	F/63 years	Unilateral hydrocephalus, post-SAH	Fenestration of septum pellucidum	2	No	No
2	F/67 years	Intracerebral cysts	Fenestration of cysts	2	Yes	No
3	F/73 years	Colloid cyst, hydrocephalus	Extirpation of cyst, septostomy	1	Yes	No
4	M/19 years	Septum pellucidum cyst	Fenestration of cyst	2	Yes	No
5	M/11 years	Interhemispheric cyst	Fenestration of cyst	3	No	Yes
6	M/3 months	Multiloculated hydrocephalus	Fenestration of cysts	1	No	No
	2 years	Multiloculated hydrocephalus	Fenestration of cysts	2	Yes	No
7	M/25 years	Septum pellucidum cyst	Fenestration of cyst	1	No	No
8	M/33 years	Hydrocephalus, aqueduct stenosis	Third ventriculostomy	2	Yes	Yes

the optimal entry point and trajectory for an endoscopic procedure [7,11,20,22,23]. However, neuronavigation systems based on preoperative images in general may suffer from inaccuracy due to registration errors and brain shift [24–28].

Ultrasound image quality has improved considerably in the last decades due to technological development and application adaptation [29,30]. The combination of 2D ultrasound and tracking technology enables freehand 3D ultrasound reconstruction. This gives a 3D ultrasound dataset that can be used in a similar manner as 3D MRI datasets are used in a conventional neuronavigation system [29,30]. In addition, with 3D ultrasound, the inaccuracy caused by patient registration is avoided and updated intraoperative images can be acquired whenever needed during surgery. This technology has been reported to solve some of the challenges of navigated tumor surgery and vascular neurosurgery [29–31]. In the present study, we have investigated the feasibility of using intraoperative 3D ultrasound for image guidance in neuroendoscopy. We here report our experience with this technology in 9 procedures.

Patients and Methods

Patients

Between January 2003 and February 2005, 9 procedures in 8 patients were performed using the described system. (Two procedures were performed on patient 6 in Table **1**, at ages 3 months and 2 years). There were 3 female patients. The age of the patients ranged from 3 months to 72 years. The patients are summarized in Table **1**.

Endoscopic equipment

We used a rigid operating endoscope (Aesculap, Tuttlingen, Germany) of 6 mm outer diameter and one working channel, one irrigation channel, one overflow channel as well as the optic channel. A single chip video camera was mounted on the eyepiece for visualization and connected to a monitor.

An optical tracking frame (Mison, Trondheim, Norway), usually used with the CUSA, was used for tracking the endoscope. The tracking frame was attached to the fixation adapter for the trocar. A custom-made insert (see Fig. **3C**) for the fixation adapter was used to make the plane of the tracking frame and the endoscope parallel, necessary for correct calibration for neuronavigation. Fixation of the endoscope was accomplished with a single-arm fixation device (Aesculap, Tuttlingen, Germany).

Ultrasound and neuronavigation system

An ultrasound-based intraoperative imaging and neuronavigation system (SonoWand®, Mison, Trondheim, Norway) was used. This system may be used as an ultrasound scanner, a conventional neuronavigation system, or an integrated, ultrasound-based neuronavigation system that uses the features of both technologies [30]. The system is based on optical tracking technology, and comes with a 4–8 MHz flat phased array ultrasound probe, precalibrated for image data acquisition and optimized for neurosurgery and with optimal resolution at depths of 3–6 cm [32]. A patient reference frame is attached to the head-holder (Mayfield frame). In one case the patient reference frame was attached to the operating table, because the young age of the patient (3 months) prohibited the use of a head-holder. For tracking of the ultrasound probe, a tracking frame is attached to the probe. Neuronavigation can be performed with a tracked pointer device, or any surgical instrument with an attached tracking frame after calibration. The trajectory and position of the pointer or surgical tool tip is displayed as a line with crosshairs or a dot (depending on the version of the neuronavigation software) in the corresponding images. The pointer and surgical tool can be virtually elongated using an offset feature. The ultrasound probe is tilted or translated over the area of interest by free hand movement and the 2D ultrasound images acquired are reconstructed, making a 3D ultrasound dataset ready for navigation (Fig. **1B**). The procedure takes about one minute. The ultrasound probe is not in the operating field after the acquisition of a 3D ultrasound volume, unless additional 3D ultrasound datasets are acquired or real-time 2D imaging is needed. The workflow of this procedure and set-up of equipment are summarized in Fig. **1**.

Navigation based on 3D ultrasound can be performed directly without any patient registration with fiducials, since the images are acquired in the same coordinate system as navigation is performed. Therefore, no patient or image registration error will affect the overall accuracy of the system when navigation based on

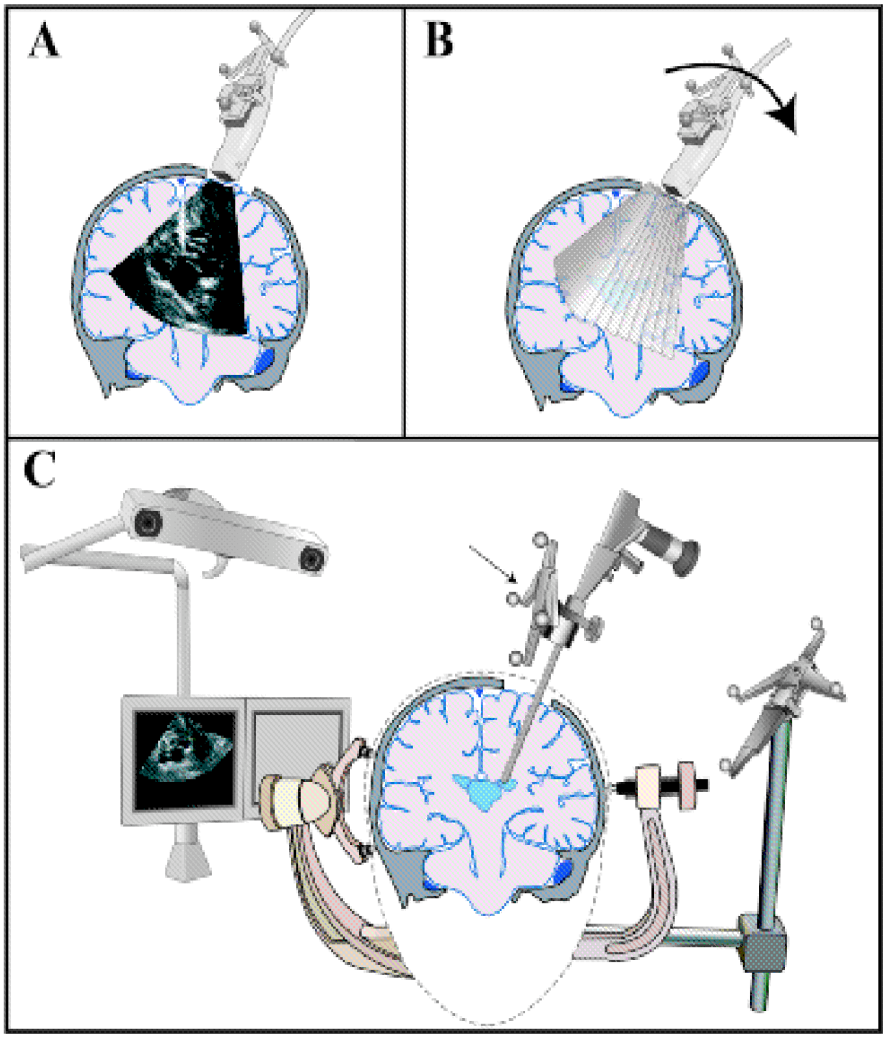

Fig. 1 Neuroendoscopy guided by 3D ultrasound. **A** The probe is placed on the dura. The anatomy and pathology are visualized by real-time 2D ultrasound. **B** During image acquisition, the probe with tracking frame is tilted or translated over the area of interest. A 3D ultrasound dataset is reconstructed from a stack of 2D images. **C** The calibrated endoscope with the tracking frame (arrow) is tracked by the navigation system and the tip position and trajectory of the endoscope are displayed on the neuronavigation screen. The patient reference frame is attached to the head-holder.

3D ultrasound is performed [24]. If neuronavigation based on preoperative MRI also is desired, patient registration of course will be necessary.

The display modalities available are: 1) Orthogonal slicing: three 2D slices are oriented as axial, sagittal and coronal slices (Fig. **2A**). 2) Anyplane slicing: One slice defined by the axis and rotation of the pointer or custom calibrated tool (for example, the endoscope) (Fig. **2B**). A plane perpendicular to the anyplane can also be added (dual anyplane) (Fig. **2C**). With a tracking frame attached, the endoscope tip and trajectory defines the slicing of the image volume (Fig. **2D**).

The overall accuracy of 3D ultrasound-based navigation using the SonoWand® system in a clinical setting may be as good as 2 mm [24].

Operative technique

All the operations were performed with neuronavigation based on 3D ultrasound. In two of the operations, preoperative MRI also was available for navigation.

The position of a small craniotomy (diameter approximately 4 cm) was chosen based on preoperative CT or MR images (but not neuronavigation) (Fig. **3A**). After cleaning the dura for blood and bone debris, sterile ultrasound gel was applied on the dura, and 3D ultrasound data were acquired (Fig. **3B**). If required, also 3D ultrasound angiography image data were acquired. The tracking frame was attached to the fixation adapter for the trocar, using the custom-made insert (Fig. **3C**). The endoscope was then calibrated to the navigation system by directing the tip of the endoscope at a small hole in the centre of the reference frame (Fig. **3D**). Based on the ultrasound images, and using the offset feature to display the trajectory of the endoscope, the best entry point and trajectory for the endoscope were decided, and a small opening in the dura was made. The endoscope was then inserted with image guidance (Fig. **3E**). The surgical procedure planned, for example, fenestration of a cyst, was then performed with the live video images from the endoscope, as well as image guidance. If updated images were required, additional 3D ultrasound datasets were obtained during the procedure. In one operation, real-time ultrasound was also used as a method for confirming the flow of CSF through the fenestration, using power Doppler.

Results

Nine procedures were performed on 8 patients during this study (Table **1**). We found the image quality of ultrasound to be satisfactory for image guidance in all cases. The ventricles as well as pathological cysts were clearly outlined and we found that the ultrasound images gave sufficient information for: 1) deciding the optimal entry point and trajectory for inserting the endoscope, especially in cases with small narrow ventricles; 2) anato-

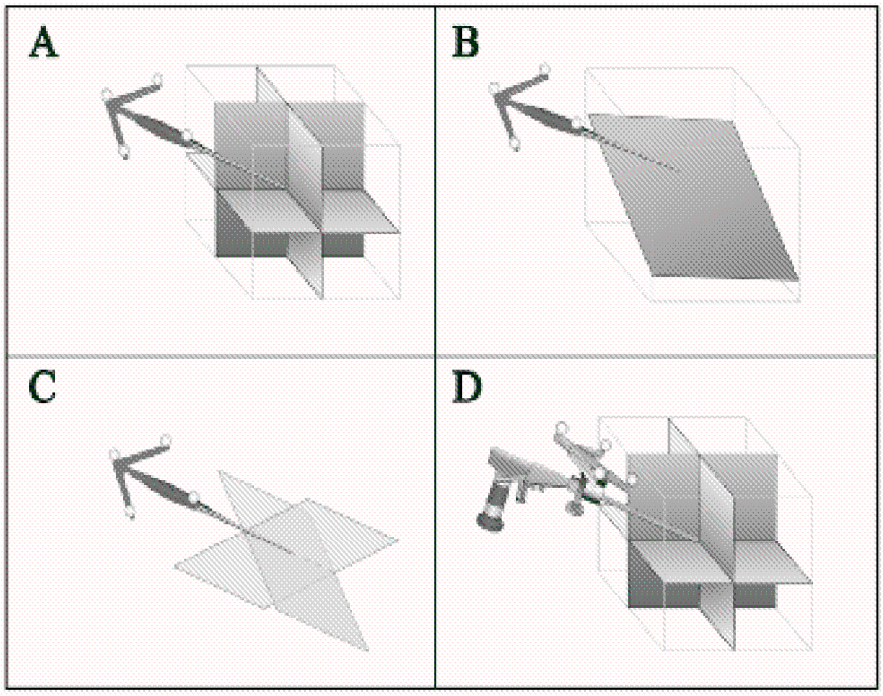

Fig. 2 Display techniques. **A** Orthogonal slices: Three orthogonal 2D slices from each 3D volume oriented as axial, sagittal and coronal slices. **B** Anyplane slices: Anyplane slices are defined by the trajectory and rotation of the pointer or surgical tool. **C** Dual anyplane slices: In dual anyplane mode an additional plane perpendicular to the first plane is added. **D** The endoscope or any surgical tool with a tracking frame, when calibrated, works as a pointer, for example, with orthogonal slices.

mical orientation during endoscopy, thus facilitating the choice of sites for fenestration of cysts; 3) quality control at the end of the procedure, excluding bleeding and in two cases verifying the reduction of size of cysts (patients 2 and 4 in Table **1**).

Even though we did not measure the clinical accuracy systematically, the general impression was that the accuracy was satisfactory. This could be confirmed by approaching a recognizable structure (for example, the foramen of Monro) with the endoscope and by comparing with the position of the endoscope tip displayed on the navigation screen.

In five of the operations ultrasound angiography also was acquired. We found that blood vessels were clearly visualized in all these cases. This was found to give particularly useful information in two cases: In patient 6, vessels in septa of multiloculated hydrocephalus were visualized (see Fig. **6B**), while in patient 8 the basilar artery could be visualized (see Fig. **6A**).

In six operations updated 3D ultrasound image data were obtained, and in two cases (cases 2 and 4), the updated ultrasound images could demonstrate the reduction of the size of a cyst. Updated ultrasound image data were acquired quickly; it typically took about a minute.

Seven of the operations were performed with only 3D ultrasound data for navigation. In two procedures we had preoperative 3D MRI with fiducials available in addition to the 3D ultrasound data (patients 5 and 8 in Table **1**).

All procedures were successful, e.g., the goal of the procedure, such as fenestration of a cyst, was reached. One patient (patient 1 in Table **1**) had postoperative meningitis, but recovered from this. We did not record any other complications at 1–2 months follow-up. The patients are summarized in the Table **1**. Two illustrative cases (patients 4 and 5 in Table **1**) are presented in detail.

Illustrative Cases

Patient 4

A man aged 19 years at the time of the operation, had episodes of loss of consciousness. A septum pellucidum cyst was found on CT and MRI investigations (Fig. **4A**). An endoscopic fenestration of the cyst to the ventricular system using navigated 3D ultrasound was planned. We did not have preoperative 3D MR images for this procedure, so only 3D ultrasound images were used for navigational guidance of the endoscope. 3D ultrasound images were acquired after making a mini-craniotomy. The ultrasound images were of sufficient quality for inserting the endoscope with navigation guidance into a narrow right ventricle (Fig. **4C**). The fenestration was done using conventional technique. The foramen of Monro was observed to be occluded by the cyst wall. Updated 3D ultrasound acquired after removing the endoscope demonstrated that the septum pellucidum cyst already was reduced somewhat in size (Fig. **4D**). It also showed the canal after removal of the endoscope, with no signs of bleeding. A postoperative CT taken the following day showed that the cyst was reduced in size (Fig. **4B**). The postoperative recovery was uneventful, and at 2 months follow-up, the patient had not had any new episodes of syncope.

Patient 5

This boy of 11 years of age at the time of the operation had been investigated because of tics in his face and arms. An interhemispheric cyst was found on investigations with CT and MRI, as well as an agenesis of the corpus callosum (Fig. **5A** and Fig. **5B**). An endoscopic fenestration of the cyst using navigated 3D ultrasound was planned. Preoperative 3D MRI with fiducials was available; consequently patient registration was done in this case. Ultrasound images were acquired through a mini-craniotomy before opening the dura and showed the interhemispheric cyst and the small ventricles clearly, in our opinion just as good as the MR images in the navigation system (Fig. **5D** and Fig. **5E**). We chose to display both the ultrasound and the MR images on

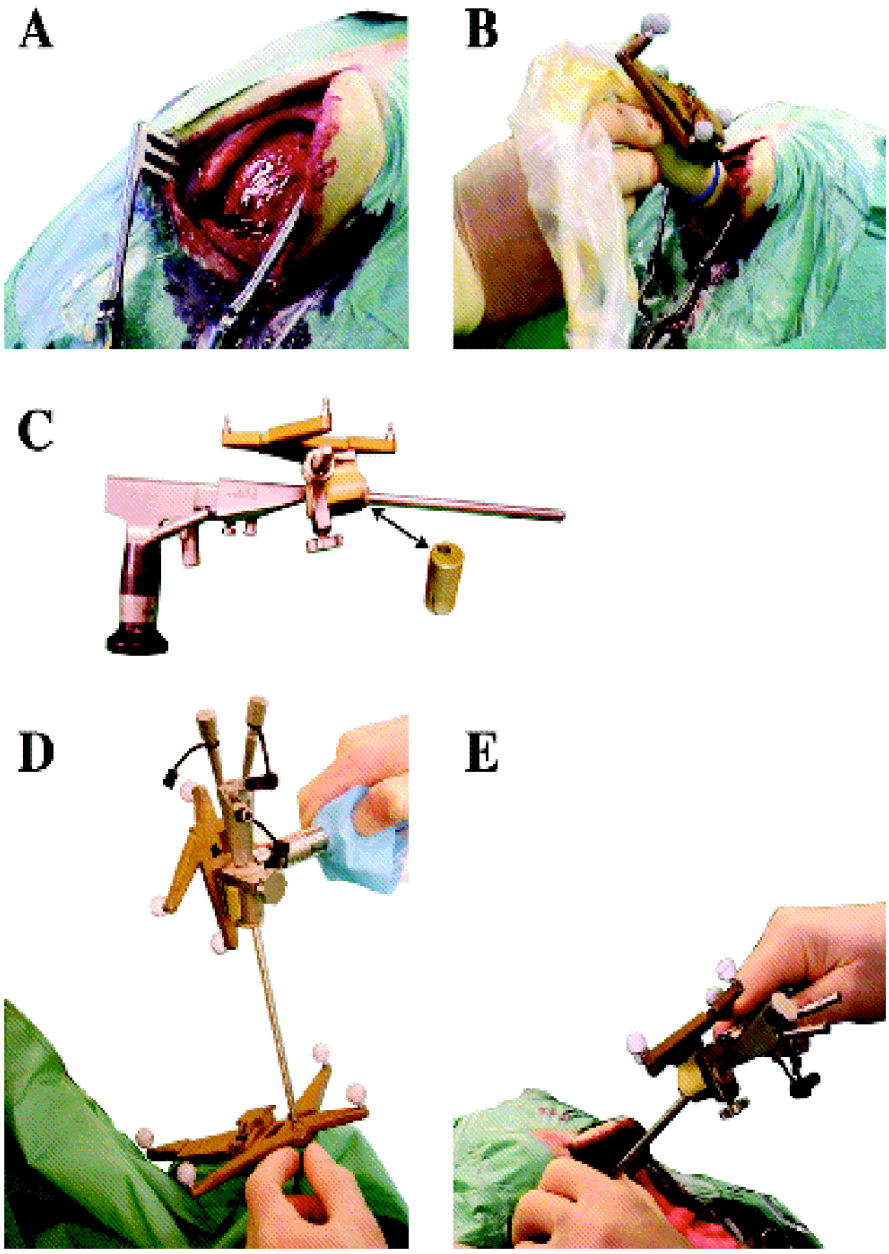

Fig. 3 Operative technique. **A** A mini-craniotomy, about 4 cm in diameter is made. **B** The ultrasound probe with a tracking frame is placed on the dura for imaging. **C** A tracking frame (in this case without marker spheres) is attached to the fixation adapter for the endoscope trocar. A custom-made insert (arrows) ensures that the plane of the tracking frame and the endoscope are parallel. **D** The neuroendoscope with the tracking frame attached is calibrated by directing the tip of the endoscope at a small hole in the centre of the reference frame. **E** With the tracking frame attached, the neuroendoscope is inserted with image guidance, based on the 3D ultrasound image data.

the navigation screen during the procedure. However, we based the operation on intraoperative 3D ultrasound knowing that these volumes were not affected by registration errors, and also that the inaccuracy due to brain shift was minimal since the 3D ultrasound was acquired just before the procedure. Neuronavigation was used to guide the endoscope into the small right lateral ventricle (Fig. **5D**). We noticed a small difference (approximately 4 mm) between the position of the endoscope tip displayed on the MRI and the ultrasound images on the navigation screen (Fig. **5E**). This difference we assumed to be caused by brain shift or registration error of the MR images. A fenestration of the cyst to the ventricle was done, as well as a fenestration from the cyst to the basal cistern. The postoperative recovery was uneventful, and a postoperative CT demonstrated that the cyst was reduced in size (Fig. **5C**). On follow-up after two months the patient's symptoms had improved considerably and he was performing better in school.

Discussion

Several ultrasound solutions have been proposed in neuroendoscopy. Real-time ultrasound has been used as an adjunct to neuroendoscopic procedures [15–18], but it has not gained popularity. This is probably due to old experiences of low image quality, as well as the fact that the probe has to be kept in the operation field for acquiring real-time images, a somewhat inconvenient concept.

More modern ultrasound solutions have also been explored. Resch et al. [16,17] developed a technique where a small sono catheter (originally developed for intravascular use) is inserted into the working canal of an endoscope, giving a 360-degree axial (to the endoscope) real-time view of the anatomy, like a "mini-CT". The solution gives good images of the anatomy in a plane axial to the endoscope, but no image ahead of the endoscope. 3D ultrasound datasets acquired on pediatric patients have been used for simulating virtual neuroendoscopies pre-

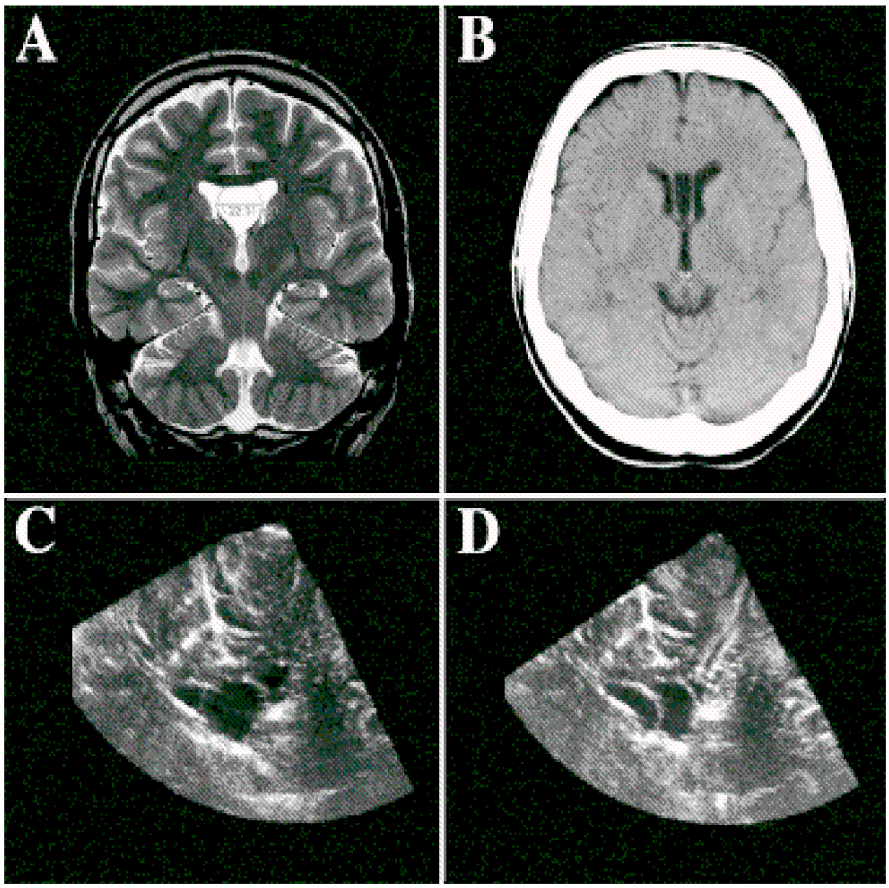

Fig. **4** Patient 4: **A** Preoperative T_2-weighted MRI, showing a septum pellucidum cyst, 22 mm in diameter, the walls of the cyst bulging into the lateral ventricles. **B** Postoperative CT, showing the septum pellucidum cyst reduced in size. **C** Ultrasound image before the procedure, clearly depicting the ventricles and the septum pellucidum cyst with its bulging walls. **D** Ultrasound image after the procedure of fenestration of the cyst. The cyst is already a little reduced in size. The channel after removal of the endoscope is also displayed, showing no signs of hematomas.

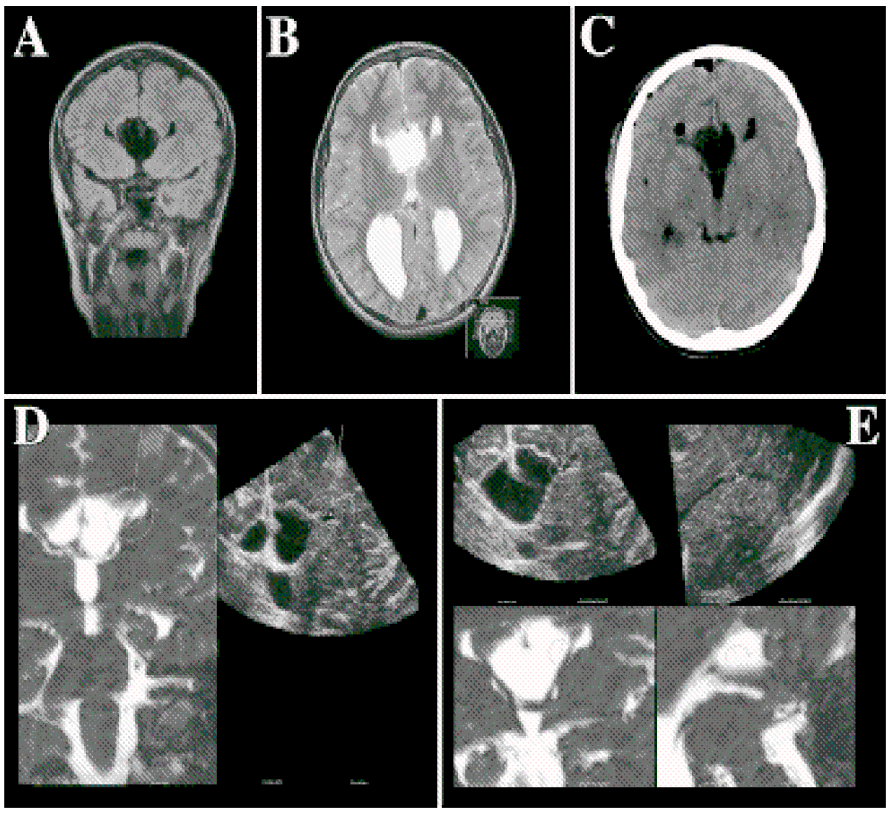

Fig. **5** Patient 5: **A** Preoperative T_1-weighted MRI showing the interhemispheric cyst and the lateral ventricles on each side. **B** Preoperative T_2-weighted MRI. **C** Postoperative CT. **D** Screenshot from the navigation system during insertion of the endoscope into the lateral ventricle. The line represents the trajectory of the endoscope, and the dot at the end of the line represents the tip of the endoscope. The two concentric rings mark the radii of 5 and 10 mm from the centre of the dot. **E** Another screenshot from the navigation system. Notice the small difference between the demonstrated position of the endoscope on the MR and the ultrasound images, about 4 mm. This difference we assumed to be caused by brain shift or registration inaccuracy.

operatively, enhancing the perception of pathoanatomy in cases of complicated anatomy [33]

Recent advances in neuronavigation technology based on preoperative CT and MRI have made neuronavigation integrated with the neuroendoscope a natural evolution in the field of neuroendoscopy. It is reported by several groups to be helpful in planning and performing endoscopic procedures [11,20,22,23,34–38].

However, ultrasound technology has also evolved and ultrasound images can be reconstructed into a 3D dataset and used

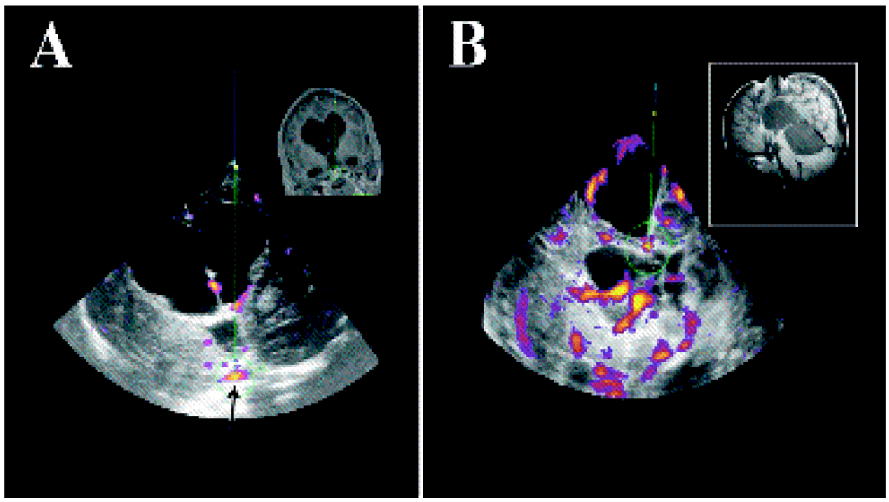

Fig. **6** Ultrasound angiography. **A** Image from patient 8 in Table **1**. Corresponding MRI is inserted in the top right corner. The vessels are highlighted in red. The yellow dot indicates the tip of the neuroendoscope, while the green line and the cross represents a virtual elongation of the neuroendoscope, "offset", useful for planning the trajectory of the endoscope. In this case the basilar artery (arrow) is depicted on ultrasound angiography. **B** Ultrasound angiography image from patient 6 in Table **1** (second operation). Preoperative MRI in the top right corner. There are numerous vessels depicted in this case of multiloculated hydrocephalus.

the same way as conventional navigation systems use preoperative image data [30]. Our experience with navigated 3D ultrasound is that it gives images of high quality and good detail, depicting the anatomy in a manner that gives good anatomical overview and orientation. We found that this was particularly useful in cases where the ventricles were small and narrow, and where the anatomy was abnormal (as in multiloculated hydrocephalus). In two cases (patients 2 and 5) this technology was considered essential for the success of the procedure, in both cases because of small narrow ventricles. The two illustrative cases presented here serve to highlight these benefits of navigated 3D ultrasound for endoscope guidance.

In our opinion, neuronavigation based on 3D ultrasound is comparable in image quality to navigation by preoperative MRI. In addition, it has a couple of advantages. When navigation of the neuroendoscope is based on 3D ultrasound images alone, the system does not require preoperative CT or MR images. This simplifies logistics, as in most cases of CT- or MRI-based neuronavigation one would require an extra set of CT or MR images for navigation purposes, both for imaging with fiducial markers and also to have as updated images as possible with good resolution and 3D protocol. When only 3D ultrasound is used for navigation, patient registration is not required, as the ultrasound images are acquired in the coordinate system of the navigation system. This means that patient registration error, otherwise one source of inaccuracy, is avoided. A small amount of time is also saved. However, as the 3D ultrasound only depicts parts of the anatomy and not the whole brain, preoperative CT or MRI can be a useful supplement for orientation, for example, in cases of large cysts where it can be a technical challenge to make an ultrasound scan which covers all of the pathology of interest.

Another benefit of this system is the possibility of doing several 3D ultrasound image acquisitions during the operation. Brain shift is a known source of inaccuracy in neuronavigation [24–28], and the inevitable loss of CSF during procedures such as those discussed here means that some brain shift is likely to occur. Some authors find that brain shift is not a problem as the live video image from the endoscope after having reached the cyst or ventricular system gives the necessary information for performing the surgery [39]. However, if the surgeon suspects that brain shift has occurred, he will of course not trust the navigation system. To have updated images increases the accuracy of the navigation and the surgeon's confidence in the technology. Often, the amount of time for acquiring updated 3D images is about one minute. To acquire new 3D ultrasound datasets, the endoscope has to be removed during image acquisition and reinserted afterwards. This may be considered a disadvantage, as removing and reinserting an endoscope might theoretically increase the risk of complications for the patient. However, this must be weighed against the risk of navigating with inaccurate image data. At the end of the procedure, a final ultrasound scan may detect bleeding, and demonstrate reduced size of fenestrated cysts as it did in two cases (patients 2 and 4 in Table **1**).

Ultrasound technology also includes Doppler technology, in our case power Doppler imaging. Thus ultrasound angiography data can be acquired and used with the navigation system. We obtained power Doppler image data during five of the operations. Power Doppler shows the blood vessels highlighted in shades of red in addition to the tissue image, according to the intensity of the Doppler (shift) signal (Fig. **6**). We found that this gave useful information as well as, for example, visualizing the position of the basilar artery in patient 8 (Fig. **6A**). In patient 6, ultrasound angiography showed blood vessels in the walls and septa of the multiple cysts (Fig. **6B**). The visualization of important vessels by ultrasound angiography may improve the safety of neuroendoscopic procedures.

In one case (patient 2 in Table **1**) we tried power Doppler for visualizing CSF flow through a fenestration using real-time 2D ultrasound, and found that this indeed was possible. Other groups have also reported that Doppler technology is able to show CSF flow [40].

Some aspects of the technique presented here might be considered disadvantages. Using ultrasound for guidance of endoscopic procedures means that one has to make a small craniotomy instead of a burr hole. We do not think that this contradicts the philosophy of minimally invasive neurosurgery, as the channel in the normal brain tissue required for the endoscope is the same as it would be with a burr hole. The larger skin incision and opening in the bone is mainly of cosmetic concern, but need not be much different than the cosmetic problems of a burr hole procedure.

A disadvantage of using only ultrasound images for neuronavigation is that surgical planning cannot be done before the craniotomy. We did not find this a restraint, as the area of the craniotomy was large enough to fine-tune the choice of position for the entry point.

We found that the tracking frame attached to the endoscope in some instances limited movement of the endoscope when it was in the deepest areas of the brain. This did not restrain the procedure in any of the operations we performed, but it is an issue that needs to be improved. In future solutions a reference frame specially designed for the endoscope must be developed.

We have not investigated 3D ultrasound navigation guidance of neuroendoscopy in pituitary surgery or other skull base approaches where the endoscope is used. Other groups have reported the use of neuronavigation integrated with endoscopy in recurrent pituitary adenomas [34]. Our own experience with modern ultrasound imaging of tumors on the skull base is that ultrasound also can depict both tumors and the normal anatomy close to the skull base in a satisfactory way. Other groups also have found ultrasound imaging to be helpful for depicting tumors near the skull base [41].

Conclusion

In summary, we found that 3D ultrasound gave satisfactory image quality for image guidance of the neuroendoscope. Neuronavigation based on 3D ultrasound improved the anatomic orientation. When using only 3D ultrasound for neuronavigation, no patient registration is necessary, thus inaccuracy due to patient registration is avoided, and logistics are simplified. Updated 3D ultrasound datasets are acquired quickly, and may adjust for brain shift. Furthermore, 3D ultrasound angiographic imaging is also available, and may improve safety as important vessels can be visualized. Based on this preliminary study, we believe that ultrasound technology will have a place in future neuroendoscopy.

Acknowledgements

The Norwegian Research Council and the Ministry of Health and Social Affairs in Norway supported this work.

References

[1] Kelly PJ. Stereotactic third ventriculostomy in patients with nontumoral adolescent/adult onset aqueductal stenosis and symptomatic hydrocephalus. J Neurosurg 1991; 75: 865–873
[2] Jones RF, Kwok BC, Stening WA, Vonau M. Neuroendoscopic third ventriculostomy. A practical alternative to extracranial shunts in noncommunicating hydrocephalus. Acta Neurochir (Suppl) 1994; 61: 79–83
[3] Kunz U, Goldmann A, Bader C, Waldbaur H, Oldenkott P. Endoscopic fenestration of the 3rd ventricular floor in aqueductal stenosis. Minim Invas Neurosurg 1994; 37: 42–47
[4] Hopf NJ, Perneczky A. Endoscopic neurosurgery and endoscope-assisted microneurosurgery for the treatment of intracranial cysts. Neurosurgery 1998; 43: 1330–1336; discussion: 1336–1337
[5] Schroeder HW, Gaab MR. Endoscopic resection of colloid cysts. Neurosurgery 2002; 51: 1441–1444; discussion: 1444–1445
[6] Lancon JA, Haines DE, Lewis AI, Parent AD. Endoscopic treatment of symptomatic septum pellucidum cysts: with some preliminary observations on the ultrastructure of the cyst wall: two technical case reports. Neurosurgery 1999; 45: 1251–1257
[7] Fratzoglou M, Grunert P, Leite dos Santos A, Hwang P, Fries G. Symptomatic cysts of the cavum septi pellucidi and cavum vergae: the role of endoscopic neurosurgery in the treatment of four consecutive cases. Minim Invas Neurosurg 2003; 46: 243–249
[8] Gaab MR, Schroeder HW. Neuroendoscopic approach to intraventricular lesions. J Neurosurg 1998; 88: 496–505
[9] Grunert P, Perneczky A, Resch K. Endoscopic procedures through the foramen interventriculare of Monro under stereotactical conditions. Minim Invas Neurosurg 1994; 37: 2–8
[10] Cappabianca P, Cavallo LM, Esposito F, de Divitiis E. Endoscopic endonasal transsphenoidal surgery: procedure, endoscopic equipment and instrumentation. Childs Nerv Syst 2004; 20: 796–801
[11] Dorward NL, Alberti O, Zhao J, Dijkstra A, Buurman J, Palmer JD, Hawkes D, Thomas DG. Interactive image-guided neuroendoscopy: development and early clinical experience. Minim Invas Neurosurg 1998; 41: 31–34
[12] Balmer B, Bernays RL, Kollias SS, Yonekawa Y. Interventional MR-guided neuroendoscopy: A new therapeutic option for children. J Pediatr Surg 2002; 37: 668–672
[13] Scholz M, Deli M, Wildforster U, Wentz K, Recknagel A, Preuschoft H, Harders A. MRI-guided endoscopy in the brain: a feasibility study. Minim Invas Neurosurg 1996; 39: 33–37
[14] Auer LM. Ultrasound stereotaxic endoscopy in neurosurgery. Acta Neurochir Suppl (Wien) 1992; 54: 34–41
[15] Auer LM. Intraoperative ultrasound as guide for neurosurgical endoscopic procedures. Acta Radiol (Supp) 1986; 369: 164–166
[16] Resch KD, Perneczky A, Schwarz M, Voth D. Endo-neuro-sonography: principles of 3-D technique. Childs Nerv Syst 1997; 13: 616–621
[17] Resch KD. Endo-neuro-sonography: first clinical series (52 cases). Childs Nerv Syst 2003; 19: 137–144
[18] Yamakawa K, Kondo T, Yoshioka M, Takakura K. Ultrasound guided endoscopic neurosurgery - new surgical instrument and technique. Acta Neurochir (Suppl) 1994; 61: 46–48
[19] Rieger A, Rainov NG, Sanchin L, Schopp G, Burkert W. Ultrasound-guided endoscopic fenestration of the third ventricular floor for non-communicating hydrocephalus. Minim Invas Neurosurg 1996; 39: 17–20
[20] Grunert P, Hopf N, Perneczky A. Frame-based and frameless endoscopic procedures in the third ventricle. Stereotact Funct Neurosurg 1997; 68: 80–89
[21] Kelly PJ, Goerss S, Kall BA, Kispert DB. Computed tomography-based stereotactic third ventriculostomy: technical note. Neurosurgery 1986; 18: 791–794
[22] Muacevic A, Muller A. Image-guided endoscopic ventriculostomy with a new frameless armless neuronavigation system. Comput Aided Surg 1999; 4: 87–92
[23] Broggi G, Dones I, Ferroli P, Franzini A, Servello D, Duca S. Image guided neuroendoscopy for third ventriculostomy. Acta Neurochir (Wien) 2000; 142: 893–898; discussion: 898–899
[24] Lindseth F, Lango T, Bang J, Nagelhus Hernes TA. Accuracy evaluation of a 3D ultrasound-based neuronavigation system. Comput Aided Surg 2002; 7: 197–222
[25] Trantakis C, Tittgemeyer M, Schneider JP, Lindner D, Winkler D, Strauss G, Meixensberger J. Investigation of time-dependency of intracranial brain shift and its relation to the extent of tumor removal using intra-operative MRI. Neurolog Res 2003; 25: 9–12
[26] Nabavi A, Black PM, Gering DT, Westin CF, Mehta V, Pergolizzi Jr RS, Ferrant M, Warfield SK, Hata N, Schwartz RB, Wells 3rd WM, Kikinis R, Jolesz FA. Serial intraoperative magnetic resonance imaging of brain shift. Neurosurgery 2001; 48: 787–797; discussion: 788–797
[27] Dorward NL, Alberti O, Velani B, Gerritsen FA, Harkness WF, Kitchen ND, Thomas DG. Postimaging brain distortion: magnitude, correlates, and impact on neuronavigation. J Neurosurg 1998; 88: 656–662
[28] Hill DL, Maurer Jr CR, Maciunas RJ, Barwise JA, Fitzpatrick JM, Wang MY. Measurement of intraoperative brain surface deformation under a craniotomy. Neurosurgery 1998; 43: 514–526; discussion: 527–518
[29] Gronningsaeter A, Kleven A, Ommedal S, Aarseth TE, Lie T, Lindseth F, Lango T, Unsgard G. SonoWand, an ultrasound-based neuronavigation system. Neurosurgery 2000; 47: 1373–1379; discussion: 1379–1380
[30] Unsgaard G, Ommedal S, Muller T, Gronningsaeter A, Nagelhus Hernes TA. Neuronavigation by intraoperative three-dimensional ultrasound:

initial experience during brain tumor resection. Neurosurgery 2002; 50: 804–812; discussion: 812
[31] Hernes TA, Ommedal S, Lie T, Lindseth F, Lango T, Unsgaard G. Stereoscopic navigation-controlled display of preoperative MRI and intraoperative 3D ultrasound in planning and guidance of neurosurgery: new technology for minimally invasive image-guided surgery approaches. Minim Invas Neurosurg 2003; 46: 129–137
[32] Grønningsæter Å, Kleven A, Ommedal S, Årseth TE, Lie T, Lindseth F, Langø T, Unsgård G. SonoWand, an Ultrasound-based Neuronavigation System. Neurosurgery 2000; 47: 1373–1380
[33] Jodicke A, Accomazzi V, Reiss I, Boker DK. Virtual endoscopy of the cerebral ventricles based on 3-D ultrasonography. Ultrasound Med Biol 2003; 29: 339–345
[34] Lasio G, Ferroli P, Felisati G, Broggi G. Image-guided endoscopic transnasal removal of recurrent pituitary adenomas. Neurosurgery 2002; 51: 132–136; discussion: 136–137
[35] Gumprecht H, Trost HA, Lumenta CB. Neuroendoscopy combined with frameless neuronavigation. Br J Neurosurg 2000; 14: 129–131
[36] Hopf NJ, Grunert P, Darabi K, Busert C, Bettag M. Frameless neuronavigation applied to endoscopic neurosurgery. Minim Invas Neurosurg 1999; 42: 187–193
[37] Rhoten RL, Luciano MG, Barnett GH. Computer-assisted endoscopy for neurosurgical procedures: technical note. Neurosurgery 1997; 40: 632–637; discussion 638
[38] Schroeder HW, Wagner W, Tschiltschke W, Gaab MR. Frameless neuronavigation in intracranial endoscopic neurosurgery. J Neurosurg 2001; 94: 72–79
[39] Burtscher J, Sweeney R, Bale R, Eisner W, Twerdy K. Neuroendoscopy based on computer assisted adjustment of the endoscope holder in the laboratory. Minim Invas Neurosurg 2003; 46: 208–214
[40] Milhorat TH, Bolognese PA. Tailored operative technique for Chiari type I malformation using intraoperative color Doppler ultrasonography. Neurosurgery 2003; 53: 899–905; discussion: 905–906
[41] Watson JC, Shawker TH, Nieman LK, DeVroom HL, Doppman JL, Oldfield EH. Localization of pituitary adenomas by using intraoperative ultrasound in patients with Cushing's disease and no demonstrable pituitary tumor on magnetic resonance imaging. J Neurosurg 1998; 89: 927–932

PAPER 5

OPERATION OF ARTERIOVENOUS MALFORMATIONS ASSISTED BY STEREOSCOPIC NAVIGATION-CONTROLLED DISPLAY OF PREOPERATIVE MAGNETIC RESONANCE ANGIOGRAPHY AND INTRAOPERATIVE ULTRASOUND ANGIOGRAPHY

Geirmund Unsgaard, Ph.D., M.D.

Department of Neurosurgery, Trondheim University Hospital, and Norwegian University of Science and Technology, Trondheim, Norway

Steinar Ommedal, B.Sc.

SINTEF Health Research, Trondheim, Norway

Ola M. Rygh, M.D.

Department of Neurosurgery, Trondheim University Hospital, and University of Science and Technology, Trondheim, Norway

Frank Lindseth, Ph.D.

SINTEF Health Research, Trondheim, Norway

Reprint requests:
Geirmund Unsgaard, Ph.D., M.D., University Hospital of Trondheim, Olav Kyrres Gate 17, N-7005 Trondheim, Norway.
Email: geirmund.unsgard@medisin.ntnu.no

Received, July 2, 2004.
Accepted, December 2, 2004.

OBJECTIVE: To study the application of navigated stereoscopic display of preoperative three-dimensional (3-D) magnetic resonance angiography and intraoperative 3-D ultrasound angiography in a clinical setting.

METHODS: Preoperative magnetic resonance angiography and intraoperative ultrasound angiography are presented as stereoscopic images on the monitor during the operation by a simple red/blue technique. Two projections are generated, one for each eye, according to a simple ray casting method. Because of integration with a navigation system, it is possible to identify vessels with a pointer. The system has been applied during operations on nine patients with arteriovenous malformations (AVMs). Seven of the patients had AVMs in an eloquent area.

RESULTS: The technology makes it easier to understand the vascular architecture during the operation, and it offers a possibility to identify and clip AVM feeders both on the surface and deep in the tissue at the beginning of the operation. All 28 feeders identified on the preoperative angiograms were identified by intraoperative navigated stereoscopy. Twenty-five were clipped at the beginning of the operation. The other three were clipped at a later phase of the operation. 3-D ultrasound angiography was useful to map the size of the nidus, to detect the degree of brain shift, and to identify residual AVM.

CONCLUSION: Stereoscopic visualization enhances the surgeon's perception of the vascular architecture, and integrated with navigation technology, this offers a reliable system for identification and clipping of AVM feeders in the initial phase of the operation.

KEY WORDS: Arteriovenous malformation, Brain shift, Intraoperative imaging, Neuronavigation, Resection control, Sonography, Stereoscopic visualization, Three-dimensional ultrasound

Neurosurgery 56[ONS Suppl 2]:ONS-281–ONS-290, 2005 DOI: 10.1227/01.NEU.0000157005.51053.41

We have available a navigation system with a module for navigated stereoscopic display of preoperative magnetic resonance angiography (MRA) and intraoperative ultrasound angiography (Doppler). The potential applications for this module are surgery on tumors close to or surrounding important vessels, aneurysm surgery, and especially arteriovenous malformation (AVM) surgery because of the challenging angioarchitecture of AVMs. We report here our initial experiences with navigated stereoscopy in AVM surgery.

Different modalities are available for treating AVMs. Radiosurgery seems to be the best way to treat small and deep-seated AVMs, especially in eloquent areas, but the risk of hemorrhage remains until the AVM is completely closed (3). AVMs may also be treated by embolization. Alone, this technique is usually not sufficient to completely close AVMs (8). Eventually, new large feeders will develop from small feeding vessels that are impossible to reach by embolization (12). Embolization is therefore used primarily in combination with microsurgery or radiosurgery. Despite the development of the embolization and radiosurgery technique, microsurgical resection remains an important treatment modality for AVMs (5).

Surgical resection can be a rather challenging procedure, especially if the AVM is large

and located in an eloquent area. The vascular architecture of the AVM vessels is usually very complex and difficult to understand at the beginning of the operation, so the common surgical technique has been to identify the draining veins and work around the nidus of the AVM, clipping the feeders as they appear in the surgical dissection groove. Preoperative embolization may be useful to reduce the flow in the AVM and thus reduce the difficulties during the dissection (12).

Another logical way to obtain an effect similar to preoperative embolization is to clip the larger feeders accessible by microsurgery as the first step in the operation. In that way, the patient could be spared an extra procedure. The feeding vessels in an AVM are usually very tortuous. Therefore, identification of the feeders at the beginning of the operation demands navigation. A conventional neuronavigation system has been used previously for this purpose (9). It can, however, be difficult to identify these tortuous vessels by looking at cross sections from three-dimensional (3-D) volumes, which is the traditional way to display image volumes. A stereoscopic display, in which the whole vessels are displayed in a true 3-D image, would probably be more helpful. We have available an ultrasound-based intraoperative imaging and navigation system with a prototype of a stereoscopic module. We report our experiences with the use of this module in AVM operations.

PATIENTS AND METHODS

Patients

Nine patients with AVMs were operated on in the period 1999 to 2002 with the assistance of the SonoWand intraoperative imaging system. The symptoms that led to the diagnosis are shown in *Table 1*. One of the patients (Patient 7) had undergone endovascular embolization of her AVM 10 years earlier. It did not cure her, but it made her epilepsy easier to control. But during the last 2 years before operation, her epilepsy was difficult to control with medication.

Seven patients had AVMs in eloquent areas. The Spetzler-Martin grade was II for four patients, III for four patients, and IV for one patient. For diagnostic work-up, all the patients underwent conventional angiography and magnetic resonance imaging (MRI). The day before the operation, they underwent 3-D MRA with fiducials. Six of the patients had intraoperative ultrasound angiography. All patients had postoperative angiography some months later.

TABLE 1. Patient demographics[a]

Patient no.	Age (yr)/sex	Symptoms	Spetzler-Martin grade	Eloquent	Localization
1	52/M	Headache, SAH	III	Yes	Parietal, right
2	19/F	Headache, syncope	II	Yes	Parietal, left
3	42/F	Headache, dizziness	IV	No	Frontal, left
4	45/F	Lower-quadrant hemianopia	III	Yes	Occipital, left
5	32/F	Strong headache	II	Yes	Occipital, left
6	47/M	Epilepsy	II	Yes	Parietal, right
7	32/F	Epilepsy	III	Yes	Parietal, right
8	52/M	ICH, visual disturbance	II	Yes	Occipital, right
9	32/M	SAH, ICH, visual disturbance	III	Yes	Occipital, right

[a] SAH, subarachnoid hemorrage; ICH, intracerebral hematoma.

Navigation Equipment

The system applied (SonoWand; MISON A/S, Trondheim, Norway) uses preoperative MRI and computed tomography, as well as intraoperative ultrasound (*Fig. 1A*) (4). MRA is registered to the patient by skin fiducials. This procedure takes approximately 10 minutes. The intraoperative 3-D ultrasound volumes are acquired within the same coordinate system as navigation is performed, so no registration is needed. The time needed from a freehand ultrasound acquisition is started until the volume is available for navigation is typically 30 seconds. Because both MRI and ultrasound are registered to/acquired in the same tracking system, no coregistration is needed. The MRA data were from a Picker (Picker International, Inc., Cleveland, OH) or a Siemens (Siemens Medical Solutions, Erlangen, Germany) 1.5-T machine with a slice thickness of 1.5 mm. The ultrasound data were obtained with a 4- to 8-MHz flat phased array probe with optimal focusing properties at 3 to 6 cm using the power Doppler modus (*Fig. 1C*). The accuracy of ultrasound-based navigation using the SonoWand system in a clinical setting has previously been reported to be less than 2 mm (7), whereas the mean phantom accuracy was measured to be 1.4 $\pm$ 0.45 mm (n = 4860).

A pointer steers the display on the monitor. The display modalities available are 1) orthogonal slices: three 2-D slices oriented in the axial, sagittal, and coronal directions (*Fig. 2A*); 2) any-plane slices: one slice defined by the position and orientation of the pointer (*Fig. 2B*); and 3) stereoscopic projections: two rendered projections (virtual reality display) from the volumes are displayed according to the orientation of the pointer (*Fig. 2C*).

Stereoscopic System

The stereoscopic display module is prototype software made available to our re-

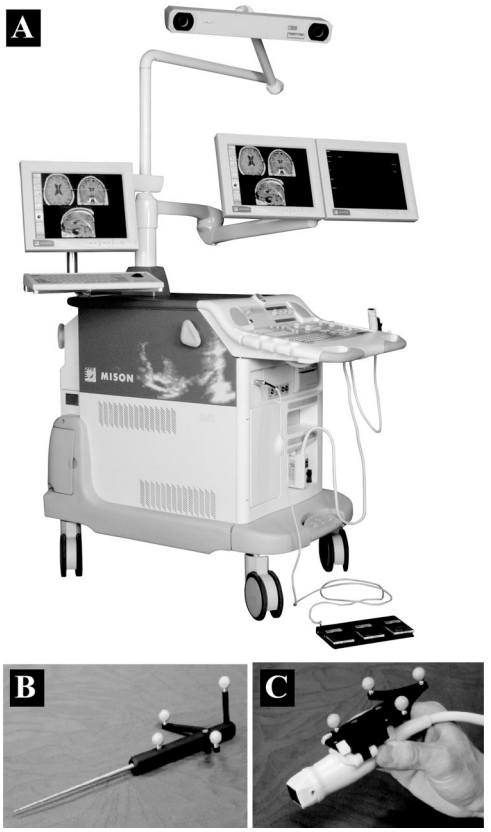

FIGURE 1. *Photographs showing equipment used.* A, *intraoperative ultrasound-based navigation system;* B, *optically tracked pointer;* C, *optically tracked ultrasound probe.*

search group for initial testing and evaluation. The module can handle both MRI and computed tomography as well as ultrasound volumes (10). To create the stereoscopic display, two perspective projections are generated, one for each eye, according to a simple ray casting technique. Each of the projections is generated by use of a semitransparent volume rendering method, in which high-intensity objects in the volume, such as blood vessels, have a low transparency and thus will hide more distant objects. The voxel values are mapped directly to color and opacity through continuous transfer function, avoiding strict classification algorithms. Each pixel in a projection is generated as a function of all the voxel values through the image volume along the beam from the observer position. The stereoscopic image is presented on the navigation monitor as simple red/blue projections.

All vessels that are visible in the angiography volume can be displayed in the stereoscopic image. MRA showed vessels down to 1.5 mm in diameter. The ultrasound angiography was just as sensitive as the MRA, but the stereoscopic display was usually more difficult to interpret (see Results). This visualization method gives the surgeon a 3-D depth view of the anatomy and vascular architecture when he or she is wearing special red/blue anaglyph glasses.

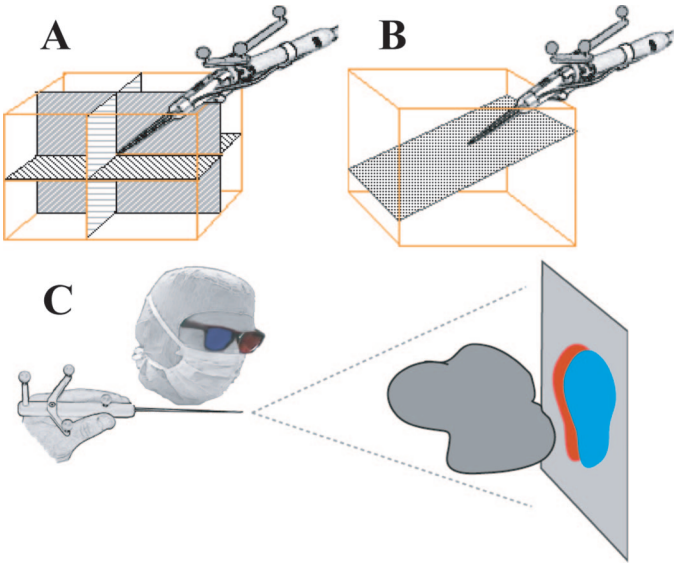

FIGURE 2. *Diagrams showing display techniques.* A, *orthogonal slicing;* B, *any-plane slicing;* C, *stereoscopic projections.*

Guidance by Stereoscopic Display

A pointer controls the stereoscopic projection interactively. Pressing a foot switch and pointing in a selected direction will change the projection view (*Fig. 3*). When the foot switch is released, the projection will be frozen, making it possible for the surgeon to interpret 3-D information from any direction during planning and surgery guidance.

The position of the pointer tip is stereoscopically displayed as a small sphere. It is also possible to set the virtual tool tip indicator ahead of its true position (i.e., using an offset). In that case, it is shown as a circle. When this virtual circle is located inside or behind a vessel in the stereoscopic display, it changes color. In that way, it is possible to determine both the direction and the distance down to a vessel from the surface of the brain (*Fig. 4*). The accuracy involved in localizing a vessel on the basis of 3-D ultrasound angiographic data using the stereoscopic module is very close to the reported navigation accuracy based on slicing a 3-D ultrasound volume (7). The only additional error source is the interpretation performed by the volume rendering module when the voxel values belonging to the object of interest are established. This error is very small, because the contrast in angiographic data (both MRI and ultrasound) is very good (see Discussion).

Procedure

At the beginning of the operations, 3-D MRA volumes were registered to the patients aided by fiducials in the usual way. During the planning phase, before the skin incision, different stereoscopic views were set for the surgeon to understand the vascular architecture and to find the projections that were most useful for dissecting the deep-seated feeders (*Fig. 3*). The strategy for the operation was decided, and a craniotomy of

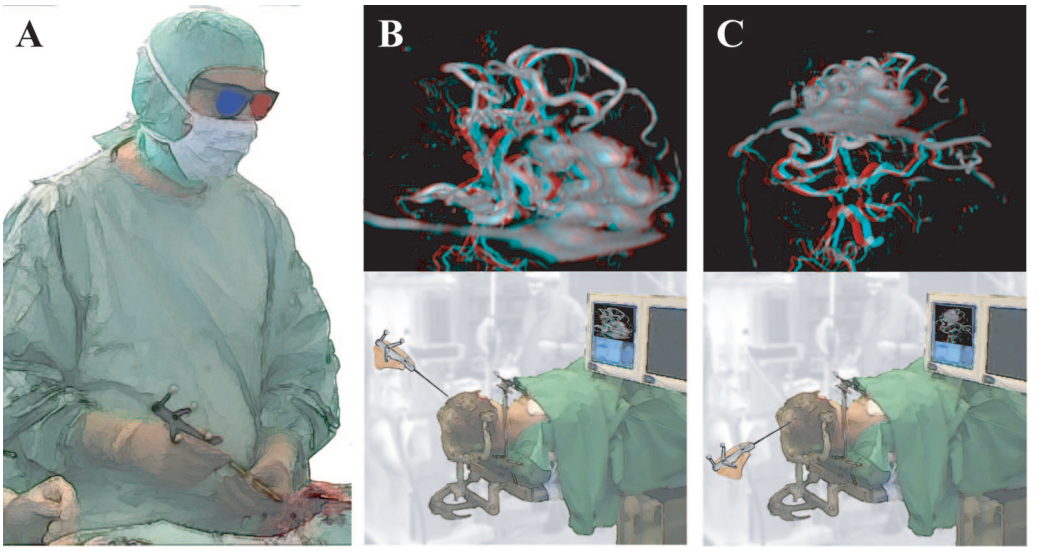

FIGURE 3. *Setting the viewpoint. The surgeon interactively changes the view using a traced pointer (*A*), and new stereoscopic projections can be seen through the red/blue glasses in real time. Two different views are seen in the figure, one from above (*B*) and one from below (*C*).*

optimal location and size could be planned. After the craniotomy and before the dura was opened, a 3-D ultrasound angiogram was acquired. This was performed by tilting and moving the probe over the area of interest. For superficial AVMs, we used gelatin standoff (1-cm-thick plate of sterile gelatin) to obtain a more optimal distance between the vessels and the probe and thus better ultrasound images. After the dura was opened, feeders that were available on the surface of the brain were identified by both the microscope and the stereoscopic visualization module before they were clipped. Then, appropriate offsets were applied to the virtual indicator to find the direction and the distance to the deep-seated feeders. After dissection, identification, and clipping of the deep-seated feeders, the nidus was dissected, the veins were clipped, and the whole AVM was removed from the operation cavity.

RESULTS

Setting of Perspective and Identification of Feeders

At the beginning of the operation, the stereoscopic perspective projection of the MRA was set in different directions. A new perspective could be set within seconds (*Fig. 3*). This was very useful. It was also useful to be able to set the viewpoint for the perspective at different distances from the AVM, changing between overview and close-up details (*Fig. 5, B* and *D*).

After the dura had been opened, the next step of the operation was to set the perspective in the same direction as the microscope or the view of the surgeon. Occasionally, it was possible to recognize feeders by simply comparing the surface view with the stereoscopic view (*Fig. 5, A* and *B*). But even superficial feeders were mostly dipping in and out of sulci, making it difficult to identify feeders on the surface without navigation. It was therefore very useful to have a pointer-driven stereoscopic view that could identify vessels on the surface (*Fig. 5, C* and *D*). In that way, the surgeon could decide which vessels on the surface were feeders, follow these feeders close to the nidus, and clip them.

In the first three operations, we did not have a stereoscopic view with offset capabilities. We therefore had to use the stereoscopic module in combination with the traditional orthogonal slicing (axial, coronal, and sagittal) of the 3-D data set to identify feeders deep in the brain tissue. When a feeder was found, it was followed a short distance to make sure it did not have the tapering of a normal vessel and to verify that it approached the nidus. This approach was possible but challenging.

When the offset feature became available in combination with the stereoscopic display technique, it was easier to find the optimal place on the surface to start the dissection as well as the direction of the dissection in the tissue to reach the deep-seated feeders (*Fig. 4*). The virtual tip (visualized as a circle) changes color when it is in or behind a vessel. In that way, it is possible to measure the distance from the surface to the feeder.

3-D Ultrasound Angiography for Correction of Brain Shift and Resection Control

Sometimes, we experienced a mismatch between the position of the pointer tip when pointing at a blood vessel and the spot in which the bright dot appeared in the stereoscopic MRA scene (*Fig. 6*). For some of the feeders, we found a disagreement of the dot and the tip of the pointer ranging from 1 to 4 mm. This disagreement could be a result of either inaccurate registration or brain shift. This disagreement can be a problem, especially when the feeder is running parallel and close to a normal vessel. 3-D ultrasound angiography acquired immediately before the identification procedure will evade the registration and brain shift problem and give an accurate location of the feeders. This discrepancy between the stereoscopic view of the MRA and the ultrasound angiography could be demonstrated on the display (*Fig. 7*), and by looking through the microscope, it was found that the ultrasound angiography

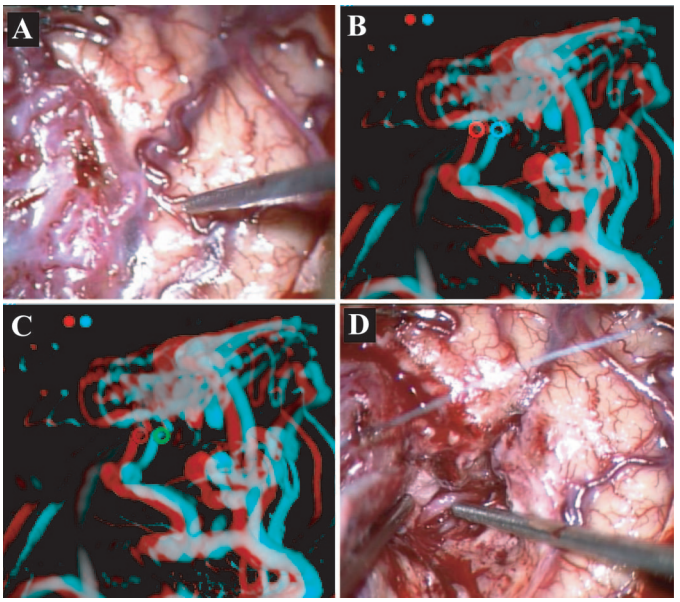

FIGURE 4. *The offset feature in the stereoscopic visualization module.* A, *intraoperative photograph showing how a pointer with appropriate offset is used to find the optimal location for starting the dissection down to one of the deep-seated feeders.* B, *in the stereoscopic view, the* dot *indicates the tip of the pointer, while the* circle *indicates the end of the offset.* C, *the same view while moving the pointer a little closer to the brain surface. Notice the change of color, indicating that the virtual circle (i.e., the offset of the pointer) is just crossing the vessel.* D, *the feeder has been dissected free and is clear for clipping.*

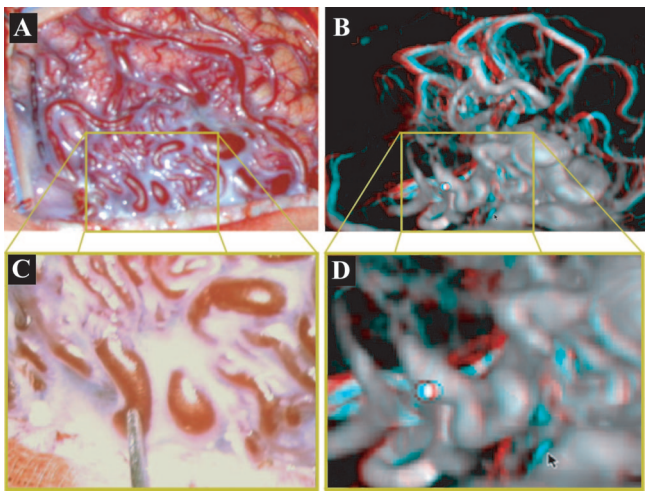

FIGURE 5. *A surface view* (A) *and a stereoscopic view* (B) *with the same perspective. A feeder is identified by pointing to a vessel* (C) *that is recognized as a feeder in the stereoscopic projection* (D).

gave the correct position. In one patient, the identification of one of the feeders was possible only because of the ultrasound angiography.

Even though ultrasound angiography can be useful to correct shift, the quality of the stereoscopic display of 3-D ultrasound angiography is not yet as good as the stereoscopic visualization of 3-D MRA. The feeders and other vessels often appear wider than they really are because of a certain smearing effect in the ultrasound angiographic scan. Ultrasound is sensitive to veins, and the simultaneous imaging of both arteries and veins sometimes makes it difficult to interpret the stereoscopic display of ultrasound angiography. Conversely, the ultrasound angiography shows the nidus better than the MRA does (*Fig. 7*). With the present quality of stereoscopic ultrasound angiography, we would prefer to have both the MRA and ultrasound angiography displayed simultaneously to better interpret the ultrasound angiography, but this is not yet available.

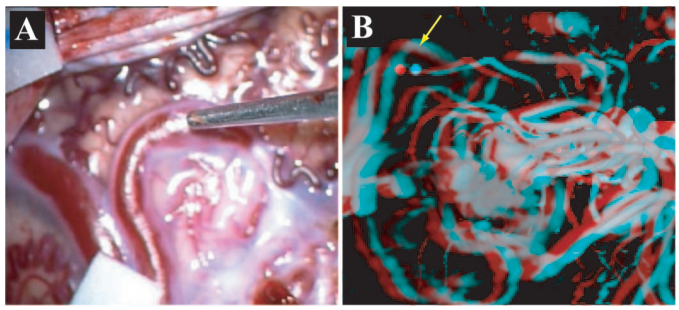

FIGURE 6. *Brain shift identification. The pointer is placed on a vessel* (A), *but the* dot *in the stereoscopic view is outside (below) the same vessel* (B). *The* arrow *indicates the expected position of the stereoscopic dot.*

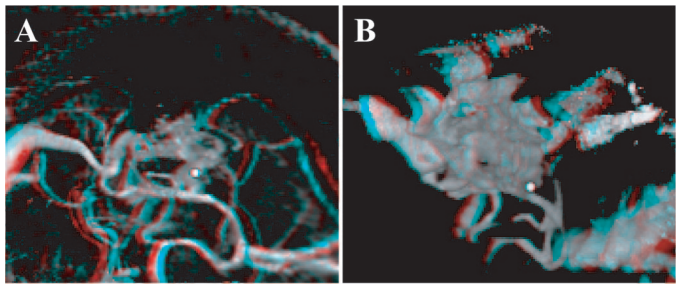

FIGURE 7. *Brain shift correction and nidus visualization. The pointer tip is placed on the vessel (as seen from the microscope), but the* dot *in the stereoscopic view of the MRA data is above the vessel* (A). *Conversely, the* dot *in the visualization of the ultrasound angiographic data is very close to the vessel* (B). *As can be seen in the figure, ultrasound angiography shows the nidus better than MRA does.*

Clipping of Feeders and Resection Control

Altogether, the nine AVM patients had 28 feeders that were described in the preoperative angiograms. Twenty-five of these feeders were clipped in the initial phase of the operation on the basis of stereoscopic information from both 3-D MRA and ultrasound angiography. The feeders were located in sulci, and it was possible to reach them by opening the sulci without traumatizing normal tissue.

The three other feeders were identified and clipped in a later phase of the operation. In one patient (Patient 7), one of

five larger feeders approached the nidus from behind the AVM, deep in the sylvian fissure. It was impossible to identify and clip this vessel early in the operation without making a dissection that could traumatize the normal tissue. This feeder was therefore left until so much of the nidus was dissected that the feeder could be reached behind the nidus.

In another patient (Patient 9), the accuracy of the registration of the MRA to the patient was insufficient. Therefore, the identification of the feeders had to be based only on the stereoscopic display of ultrasound angiography. All four feeders were identified, but for two of them, the surgeon did not trust the finding until a later phase of the operation because of the quality of the ultrasound angiographic images.

Early clipping of the feeders before dissection of the nidus greatly reduced the turgor of the nidus. In only one patient (Patient 2) did the turgor of the nidus remain high throughout the dissection, and she bled much more than expected (2000 ml). In this patient, at the end of the operation, we found a large feeder running parallel to the draining vein that was not shown on the preoperative angiogram.

We also had the impression that the trauma to the surrounding tissue was reduced, because the reduced flow in the nidus and the reduced bleeding tendency from the nidus made it easier to dissect the nidus away from the normal tissue.

Intraoperative ultrasound angiography can be used to control the extirpation (*Fig. 8*) and to detect residual AVM. In one patient (Patient 7), intraoperative 3-D ultrasound angiography revealed residual AVM that was immediately removed.

Clinical Outcome

The clinical results are shown in *Table 2*. Four of the seven patients with AVM in an eloquent area had a temporary worsening of their neurological status. One patient (Patient 7) has acquired a permanent neurological deficit. As shown in *Figure 9*, she had a Grade III AVM in the right parietal region. As expected, she sustained an immediate postoperative hemiparalysis, but after only a few days, she began to regain control, and after 3 months, her only sequela was a small paresis of her left ankle, hardly noticeable when she is walking.

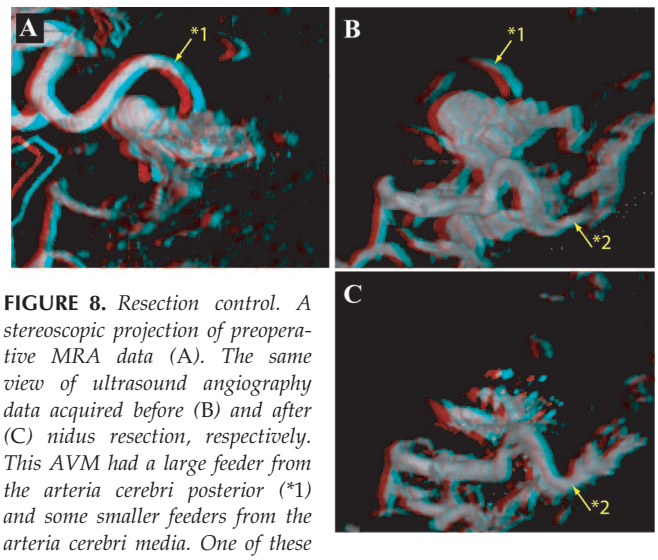

FIGURE 8. *Resection control. A stereoscopic projection of preoperative MRA data (*A*). The same view of ultrasound angiography data acquired before (*B*) and after (*C*) nidus resection, respectively. This AVM had a large feeder from the arteria cerebri posterior (*1) and some smaller feeders from the arteria cerebri media. One of these feeders, located in front of the nidus, shows considerable circulation proximal to the clipping (*2), indicating its role in supplying nutrient vessels.*

One patient (Patient 3), who had a Grade IV AVM, had to be reoperated on three times during the first postoperative night because of hemorrhage. It was initially interpreted as perfusion pressure breakthrough, but at the last operation, some residual AVM was detected and removed. After that event, we started to perform intraoperative ultrasound angiography. She also had two aneurysms, one on the anterior communicating artery, which was later coiled, and one on the internal carotid artery, which is still untreated. This patient acquired epilepsy after the operations.

The other seven patients all had excellent outcomes. One of them (Patient 6) had a postoperative hematoma, which probably was caused by high systolic blood pressure (230 mm Hg) for a short period after his awakening from the narcosis. It was removed immediately, and it did not affect his outcome. The cohort is too small to make any statement about neurological complications and outcome.

All patients underwent postoperative conventional digital subtraction angiography (DSA). No residual AVM was found.

DISCUSSION

Accuracy

In this study, navigation has been based on intraoperative ultrasound angiography as well as preoperative MRA. The navigation inaccuracies for the two modalities are independent. It is very difficult to measure the navigation inaccuracy in a clinical setting, because of 1) the lack of easily accessible well-defined structures inside the head; 2) problems with quantifying the difference between the anatomic structure/surgical tool distance as seen in the patient and the corresponding distance in the image information presented to the surgeon; and 3) the problem with distinguishing between the inaccuracy caused by the system error, the registration, and the brain shift (7). Often, we have to resolve to measure the laboratory accuracy by use of a rigid phantom and carefully list the additional error sources that apply in a clinical setting. For navigation based on preoperative MRA data, the two main error sources are the image-to-patient registration and the fact that the data are not updated to compensate for brain shift. For a rigid phantom, these errors can be made negligible. However, in a clinical setting, both errors can be considerable, especially the brain shift problem. In contrast, registration is not needed for navigation on the basis of intraoperative ultrasound, because the acquisition is made in the same coordinate system as navigation is performed, and a new acquisition can be made when needed to compensate for brain shift. The ultrasound navigation inaccuracy is therefore close to the mea-

TABLE 2. Results

Patient no.	Ultrasound angiography	Postoperative complications	Present status
1	No	Epileptic seizure, left hemiparesis	Normal
2	No	Headache	Normal
3	No	Hematoma (×3), epilepsy	Epilepsy (coiled aneurysm)
4	Yes	Small increase in hemianopia	Quadrantic hemianopia, as before operation
5	Yes	No	Normal
6	Yes	Hematoma	Normal
7	Yes	Hemiparalysis	Small paresis, left ankle
8	Yes	No	Normal
9	Yes	No	Visual disturbance, as before operation

sured laboratory inaccuracy, given that speed-of-sound issues are minimized by the system and ultrasound-based navigation is performed on a recent ultrasound volume (real-time 3-D ultrasound will eliminate the brain shift problem completely).

A thorough investigation of the ultrasound-based navigation inaccuracy using the SonoWand system was conducted by Lindseth et al. (7). The clinical inaccuracy was estimated to be less than 2 mm on the basis of slicing of tissue data, whereas the mean phantom inaccuracy was measured to be 1.4 ± 0.45 mm (n = 4860). In the present study, we used angiographic data that were visualized stereoscopically. The use of angiographic data instead of tissue data does not have any impact on accuracy. The additional error caused by stereoscopically rendering the angiographic data instead of slicing through it is also negligible, because the angiographic contrast is very good.

As opposed to navigation inaccuracy, which is a measure of the misalignment between a physical object and the image information presented (either MRI or ultrasound), fusion inaccuracy is a measure of the misalignment between the two modalities. Although fusion inaccuracy in principle tells nothing about the independent navigation inaccuracy based on MRI and ultrasound, the measure is often used as an estimate of the brain shift. However, it is important to be aware of the fact that to deduce that an observed misalignment between preoperative MRI and intraoperative ultrasound is caused by brain shift, we have to know that the system used has a very small MRA- and ultrasound-based navigation inaccuracy in the laboratory, that the preoperative MRI-to-patient registration is very accurate, and that the ultrasound display is based on a recent acquisition.

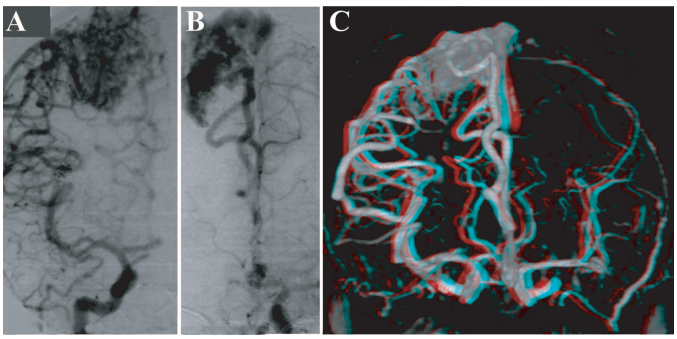

FIGURE 9. *Patient 7. A large AVM in the right parietal region is shown by the DSA images* (A *and* B) *and the stereoscopic visualization of the MRA data* (C).

In addition to direct ultrasound-based navigation, intraoperative ultrasound data can also be used to update the preoperative MRI data, which are then used for navigation. However, it is important to bear in mind that although such an indirect approach in theory could make the updated MRI-based navigation inaccuracy as small as the intraoperative ultrasound-based navigation inaccuracy, this will be very hard to achieve in practice, because automatic MRI-to-ultrasound registration is a challenging task that will introduce additional error sources.

Stereoscopic Navigation-controlled Display of MRA

To be able to approach an AVM in an optimal way, it is important to understand the 3-D vascular architecture. For better planning of the operation, Bulitt et al. (1) described the use of a program on a home personal computer to better visualize the complex 3-D vascular anatomy. This is evidently useful, but to really get help from such a 3-D visualization during dissection, it must be related to the true anatomic structures via a navigation system. Russell et al. (13) have shown the benefit of frameless stereotaxy to plan the optimal trajectory, to minimize the skin incision and the craniotomy sizes, and to confirm the AVM margins during the resection.

In the present study, we have tested a system for stereoscopic navigation-controlled display of preoperative MRA and intraoperative ultrasound angiography in planning and resection of AVMs (10). In three of the patients, we also used a program to make a preoperative stereoscopic model of the AVM. We found it useful, but it was far more useful to be able to set a stereoscopic projection over the head of the patients before the craniotomy. It helped us to decide the location of the craniotomy and to acquire an impression

of the vascular architecture relative to the structures visible on the brain surface after the craniotomy.

When we started our work with stereoscopic navigation-controlled identification and clipping of feeding arteries, we were not aware of the work by Muacevic and Steiger (9) in Munich. They used conventional navigation technology to identify and clip feeders in the initial phase of the operation. This technology is also available in our system, but we did not perform a systematic testing of the usefulness of this way of identifying feeding vessels compared with the use of stereoscopic display. In the first three operations, we did not have the stereoscopic offset, and we used the conventional orthogonal display to find deep-seated feeders. The senior author (GU) found it more difficult to trust that the vessel displayed by conventional navigation was a feeder and not an *en passant* normal vessel. The stereoscopic display made it much easier to understand the vascular architecture, because the length of the tortuous vessel was displayed, not only a cross section.

Even though stereoscopic display was superior for visualizing feeders on the basis of MRA, it also had its drawbacks. First, it was necessary to interrupt the operation to put on red/blue glasses. An operation assistant did that in a few seconds, so it was not a big problem, but it should be solved in a better way in the future by using, for example, an autostereoscopic monitor so that 3-D vision is achieved without the need for special glasses.

Another drawback, which is the same for both conventional navigation and stereoscopic display based on preoperative data, is the registration error and the brain shift. Together, these error sources can cause an error of several millimeters. By pointing at defined structures on the surface, such as the bifurcation of a vessel, it is possible to approximate the size and direction of this error. It is, however, challenging to compensate for this error in the surgeon's mind, especially when he or she is dissecting for a deep-seated feeder.

Stereoscopic 3-D Ultrasound

Intraoperative 3-D ultrasound angiography is a way to eliminate this error. In some of the AVMs, we obtained intuitive stereoscopic 3-D ultrasound angiography images that could be used to identify feeders. In one patient, a feeder was identified by ultrasound that could not be seen on preoperative 3-D MRA. Unfortunately, however, this did not work for all the AVMs, because we were not always able to generate a good stereoscopic view of the region of interest. Some possible reasons for this could be poor ultrasound data acquisitions, the presence of veins and small blood vessels that hindered sight to the relevant details, blurred representation of all blood vessels, or simply inexperience in using complex new prototype software. These issues are currently being investigated to improve the method.

Real-time two-dimensional (2-D) ultrasound has been used to localize AVMs and their feeders (2, 6, 14). We also found that 2-D ultrasound could be useful for orientation about the nidus and the feeding and draining vessels. In our hands, however, 2-D ultrasound was not sufficient for precise localization of the feeders.

Intraoperative DSA is useful for resection control in AVM surgery (11). Ultrasound may be an alternative to DSA for quality control after an assumedly complete resection (14). Even though we do not have much experience in detecting residual AVM with 3-D ultrasound angiography, we think it will have an advantage compared with 2-D ultrasound, for the following reasons: with 3-D ultrasound, it is easy to compare preoperative MRA or ultrasound angiography with the intraoperative finding. We also think that it will be proved useful to have a navigated localization of the detected residual AVM vessels.

The cohort is too small to be able to say anything about the outcome. The results we obtained by navigated stereoscopy and early clipping of feeders is probably at the level of what can be obtained by conventional methods in skilled neurovascular centers. However, it must be taken into consideration that the method has been in development and that we operate on rather few AVMs per year. A clinical evaluation of operating on AVMs with this method will necessitate a larger study.

CONCLUSION

Navigated stereoscopic display of angiography offers a technology that can be used successfully to identify and clip AVM feeders in the initial phase of the operation.

DISCLOSURE

The producer of SonoWand, MISON A/S, is a spin-off company from the National Center for 3-D Ultrasound in Surgery, Trondheim, Norway. GU holds 0.5% of the shares in this company.

REFERENCES

1. Bulitt E, Aylward S, Bernard EJ, Gerig G: Computer-assisted visualization of arteriovenous malformations on the home personal computer. **Neurosurgery** 48:576–583, 2001.
2. Cokluk C, Iygün Ö, Senel A, Celik F, Rakunt C: The guidance of intraoperative ultrasonography in the surgical treatment of arteriovenous malformation. **Minim Invasive Neurosurg** 46:169–172, 2003.
3. Gallina P, Merienne L, Meder JF, Schlienger M, Lefkopoulos D, Merland JJ: Failure in radiosurgery treatment of cerebral arteriovenous malformations. **Neurosurgery** 42:996–1004, 1998.
4. Gronningsaeter A, Kleven A, Ommedal S, Aarseth TE, Lie T, Lindseth F, Langø T, Unsgård G: SonoWand, an ultrasound-based neuronavigation system. **Neurosurgery** 46:1373–1379, 2000.
5. Heros CR, Morcos JJ: Cerebrovascular surgery: Past, present, and future. **Neurosurgery** 47:1007–1033, 2000.
6. Kitazawa K, Nitta J, Okudera H, Kobayashi S: Color Doppler ultrasound imaging in the emergency management of an intracerebral hematoma caused by cerebral arteriovenous malformations. **Neurosurgery** 42:405–407, 1998.
7. Lindseth F, Langø T, Bang J, Hernes TA: Accuracy evaluation of a 3D ultrasound-based neuronavigation system. **Comp Aided Surg** 7:197–222, 2002.

8. Mattle HP, Schroth G, Seiler RW: Dilemmas in the management of patients with arteriovenous malformations. **J Neurol** 247:917–928, 2000.
9. Muacevic A, Steiger HJ: Computer-assisted resection of cerebral arteriovenous malformations. **Neurosurgery** 45:1164–1171, 1999.
10. Nagelhus Hernes TA, Ommedal S, Lie T, Lindseth F, Langø T, Unsgaard G: Stereoscopic navigation-controlled display of preoperative MRI and intraoperative 3D ultrasound in planning and guidance of neurosurgery: New technology for minimally invasive image-guided surgery approaches. **Minim Invasive Neurosurg** 46:129–137, 2003.
11. Pietilä TA, Stendel R, Jansons J, Schilling A, Koch HC, Brock M: The value of intraoperative angiography for surgical treatment of cerebral arteriovenous malformations in eloquent brain areas. **Acta Neurochir (Wien)** 140:1161–1165, 1998.
12. Richling B, Killer M: Endovascular management of patients with cerebral arteriovenous malformations. **Neurosurg Clin N Am** 11:123–145, 2000.
13. Russell SM, Woo HH, Joseffer SS, Jafar JJ: Role of frameless stereotaxy in the surgical treatment of cerebral arteriovenous malformations: Technique and outcomes in a controlled study of 44 consecutive patients. **Neurosurgery** 51:1108–1118, 2002.
14. Woydt M, Perez J, Meixenberger J, Krone A, Soerensen N, Roosen K: Intra-operative colour-duplex-sonography in the surgical management of cerebral AV-malformations. **Acta Neurochir (Wien)** 140:689–698, 1998.

Acknowledgment

The Research Council and the Ministry of Health and Social Affairs in Norway supported this work.

COMMENTS

Despite advances in endovascular therapy, microsurgery remains essential in treatment of arteriovenous malformations (AVMs). Embolization of an AVM is performed routinely in our department, even if not all the feeders can be occluded, because it facilitates microsurgery by reducing intraoperative bleeding. Microsurgery of an AVM must be planned thoroughly. Questions that must be answered during the planning process and the procedure include: Where should the incision and the bone flap be place to enable to a sufficient exposure? Where should dissection of an AVM begin? How are the feeders located in relation to the nidus? Which vein is the draining vein, which must be left as the last to be occluded? Was the whole AVM removed?

The authors attempt to answer these questions by use of three-dimensional (3-D) magnetic resonance angiography and 3-D ultrasound. As the authors state, the number of patients is too small to draw definite conclusions regarding the effectiveness and safety of the tools used, but it is still worthwhile to attempt to find ways to perform safer and better microsurgery. With their methods, the authors were able plan the approach better and visualize the AVM to plan the dissection and occlusion of the feeders more precisely. It still is important to coagulate even the smallest feeders that probably cannot be seen with ultrasound to prevent postoperative hematomas. A very small amount of brain tissue and the feeder, which has a thin and abnormal wall, are taken within the bipolar forceps to perform coagulation in a more efficient way ("dirty" coagulation).

In this series of nine patients, two patients (22%) developed postoperative hematoma, and the other patients underwent surgery repeatedly (up to three times!) because of AVM remnants. This emphasizes the importance of postoperative or preferably intraoperative angiography, as it may be difficult to resect all parts of the AVM, even with modern techniques. However, how were the many reoperations planned and performed to localize the remnant AVM? Why was intraoperative angiography not performed during the first reoperation?

In general, to prevent postoperative hematomas during intracranial neurosurgery, it is useful to keep the patient's head elevated above level of the heart and to maintain systolic blood pressure at approximately 100 mm Hg during surgery and afterward, in the intensive care unit. After we remove large AVMs, we keep the patient sedated overnight to prevent blood pressure peaks during awakening in the immediate postoperative period. Because AVMs are quite rare and often complex, therapy for patients with AVMs should be guided by experienced neurovascular surgeons working with endovascular surgeons. As collective experience is gathered, we will learn from difficulties to enable better care for the next patient.

Mika Niemelä
Juha Hernesniemi
Helsinki, Finland

The authors report their recent experiences of AVM resection with assistance of stereoscopic navigation-controlled display of preoperative magnetic resonance angiography and intraoperative ultrasound angiography. Their application of new modalities seems to be helpful in planning skin incision, craniotomy, and imaging surgical approach just before and during operations. Visualizing 3-D vascular architecture during the brain operation may reduce vascular damage or intraoperative bleeding. As the first step in AVM surgery, dissection of main feeding arteries should be thoroughly performed, and these modalities may provide surgeons with a level of confidence. However, as the authors discuss, inaccuracy caused by registration error and brain shift should be adequately corrected by the surgeon or with more refined modalities. Furthermore, as most feeding arteries have arterial branches to the normal brain tissue and apparently normal arteries have many branches to the nidus, all vessels should be dissected to the nidus to distinguish proper feeding branches from normal branches. Feeding arteries behind the draining veins also should be explored and severed even if intraoperative ultrasound fails to detect them. The adequate control of blood supply from perforating vessels is critical. The useful contribution of the authors' modalities in these important steps during AVM surgery seems doubtful, and the necessity and accuracy of the modalities are still to be addressed and proven in an objective manner.

Kazuhiko Nozaki
Nobuo Hashimoto
Kyoto, Japan

The authors present a new technique for stereoscopic display of preoperative magnetic resonance angiography and intraoperative ultrasound angiography data. Integration and coregistration of the two techniques allow for an intraoperative navigation system that was applied to AVM surgery in this study. The

Dissertations at the Faculty of Medicine, NTNU

1977

1. Knut Joachim Berg: EFFECT OF ACETYLSALICYLIC ACID ON RENAL FUNCTION
2. Karl Erik Viken and Arne Ødegaard: STUDIES ON HUMAN MONOCYTES CULTURED *IN VITRO*

1978

3. Karel Bjørn Cyvin: CONGENITAL DISLOCATION OF THE HIP JOINT.
4. Alf O. Brubakk: METHODS FOR STUDYING FLOW DYNAMICS IN THE LEFT VENTRICLE AND THE AORTA IN MAN.

1979

5. Geirmund Unsgaard: CYTOSTATIC AND IMMUNOREGULATORY ABILITIES OF HUMAN BLOOD MONOCYTES CULTURED IN VITRO

1980

6. Størker Jørstad: URAEMIC TOXINS
7. Arne Olav Jenssen: SOME RHEOLOGICAL, CHEMICAL AND STRUCTURAL PROPERTIES OF MUCOID SPUTUM FROM PATIENTS WITH CHRONIC OBSTRUCTIVE BRONCHITIS

1981

8. Jens Hammerstrøm: CYTOSTATIC AND CYTOLYTIC ACTIVITY OF HUMAN MONOCYTES AND EFFUSION MACROPHAGES AGAINST TUMOR CELLS *IN VITRO*

1983

9. Tore Syversen: EFFECTS OF METHYLMERCURY ON RAT BRAIN PROTEIN.
10. Torbjørn Iversen: SQUAMOUS CELL CARCINOMA OF THE VULVA.

1984

11. Tor-Erik Widerøe: ASPECTS OF CONTINUOUS AMBULATORY PERITONEAL DIALYSIS.
12. Anton Hole: ALTERATIONS OF MONOCYTE AND LYMPHOCYTE FUNCTIONS IN REALTION TO SURGERY UNDER EPIDURAL OR GENERAL ANAESTHESIA.
13. Terje Terjesen: FRACTURE HEALING AN STRESS-PROTECTION AFTER METAL PLATE FIXATION AND EXTERNAL FIXATION.
14. Carsten Saunte: CLUSTER HEADACHE SYNDROME.
15. Inggard Lereim: TRAFFIC ACCIDENTS AND THEIR CONSEQUENCES.
16. Bjørn Magne Eggen: STUDIES IN CYTOTOXICITY IN HUMAN ADHERENT MONONUCLEAR BLOOD CELLS.
17. Trond Haug: FACTORS REGULATING BEHAVIORAL EFFECTS OG DRUGS.

1985

18. Sven Erik Gisvold: RESUSCITATION AFTER COMPLETE GLOBAL BRAIN ISCHEMIA.
19. Terje Espevik: THE CYTOSKELETON OF HUMAN MONOCYTES.
20. Lars Bevanger: STUDIES OF THE Ibc (c) PROTEIN ANTIGENS OF GROUP B STREPTOCOCCI.
21. Ole-Jan Iversen: RETROVIRUS-LIKE PARTICLES IN THE PATHOGENESIS OF PSORIASIS.
22. Lasse Eriksen: EVALUATION AND TREATMENT OF ALCOHOL DEPENDENT BEHAVIOUR.
23. Per I. Lundmo: ANDROGEN METABOLISM IN THE PROSTATE.

1986

24. Dagfinn Berntzen: ANALYSIS AND MANAGEMENT OF EXPERIMENTAL AND CLINICAL PAIN.
25. Odd Arnold Kildahl-Andersen: PRODUCTION AND CHARACTERIZATION OF MONOCYTE-DERIVED CYTOTOXIN AND ITS ROLE IN MONOCYTE-MEDIATED CYTOTOXICITY.
26. Ola Dale: VOLATILE ANAESTHETICS.

1987

27. Per Martin Kleveland: STUDIES ON GASTRIN.
28. Audun N. Øksendal: THE CALCIUM PARADOX AND THE HEART.
29. Vilhjalmur R. Finsen: HIP FRACTURES

1988

30. Rigmor Austgulen: TUMOR NECROSIS FACTOR: A MONOCYTE-DERIVED REGULATOR OF CELLULAR GROWTH.
31. Tom-Harald Edna: HEAD INJURIES ADMITTED TO HOSPITAL.
32. Joseph D. Borsi: NEW ASPECTS OF THE CLINICAL PHARMACOKINETICS OF METHOTREXATE.
33. Olav F. M. Sellevold: GLUCOCORTICOIDS IN MYOCARDIAL PROTECTION.
34. Terje Skjærpe: NONINVASIVE QUANTITATION OF GLOBAL PARAMETERS ON LEFT VENTRICULAR FUNCTION: THE SYSTOLIC PULMONARY ARTERY PRESSURE AND CARDIAC OUTPUT.
35. Eyvind Rødahl: STUDIES OF IMMUNE COMPLEXES AND RETROVIRUS-LIKE ANTIGENS IN PATIENTS WITH ANKYLOSING SPONDYLITIS.
36. Ketil Thorstensen: STUDIES ON THE MECHANISMS OF CELLULAR UPTAKE OF IRON FROM TRANSFERRIN.
37. Anna Midelfart: STUDIES OF THE MECHANISMS OF ION AND FLUID TRANSPORT IN THE BOVINE CORNEA.
38. Eirik Helseth: GROWTH AND PLASMINOGEN ACTIVATOR ACTIVITY OF HUMAN GLIOMAS AND BRAIN METASTASES - WITH SPECIAL REFERENCE TO TRANSFORMING GROWTH FACTOR BETA AND THE EPIDERMAL GROWTH FACTOR RECEPTOR.
39. Petter C. Borchgrevink: MAGNESIUM AND THE ISCHEMIC HEART.
40. Kjell-Arne Rein: THE EFFECT OF EXTRACORPOREAL CIRCULATION ON SUBCUTANEOUS TRANSCAPILLARY FLUID BALANCE.
41. Arne Kristian Sandvik: RAT GASTRIC HISTAMINE.
42. Carl Bredo Dahl: ANIMAL MODELS IN PSYCHIATRY.

1989

43. Torbjørn A. Fredriksen: CERVICOGENIC HEADACHE.
44. Rolf A. Walstad: CEFTAZIDIME.
45. Rolf Salvesen: THE PUPIL IN CLUSTER HEADACHE.
46. Nils Petter Jørgensen: DRUG EXPOSURE IN EARLY PREGNANCY.
47. Johan C. Ræder: PREMEDICATION AND GENERAL ANAESTHESIA IN OUTPATIENT GYNECOLOGICAL SURGERY.
48. M. R. Shalaby: IMMUNOREGULATORY PROPERTIES OF TNF-α AND THE RELATED CYTOKINES.
49. Anders Waage: THE COMPLEX PATTERN OF CYTOKINES IN SEPTIC SHOCK.
50. Bjarne Christian Eriksen: ELECTROSTIMULATION OF THE PELVIC FLOOR IN FEMALE URINARY INCONTINENCE.
51. Tore B. Halvorsen: PROGNOSTIC FACTORS IN COLORECTAL CANCER.

1990

52. Asbjørn Nordby: CELLULAR TOXICITY OF ROENTGEN CONTRAST MEDIA.
53. Kåre E. Tvedt: X-RAY MICROANALYSIS OF BIOLOGICAL MATERIAL.
54. Tore C. Stiles: COGNITIVE VULNERABILITY FACTORS IN THE DEVELOPMENT AND MAINTENANCE OF DEPRESSION.
55. Eva Hofsli: TUMOR NECROSIS FACTOR AND MULTIDRUG RESISTANCE.
56. Helge S. Haarstad: TROPHIC EFFECTS OF CHOLECYSTOKININ AND SECRETIN ON THE RAT PANCREAS.
57. Lars Engebretsen: TREATMENT OF ACUTE ANTERIOR CRUCIATE LIGAMENT INJURIES.
58. Tarjei Rygnestad: DELIBERATE SELF-POISONING IN TRONDHEIM.
59. Arne Z. Henriksen: STUDIES ON CONSERVED ANTIGENIC DOMAINS ON MAJOR OUTER MEMBRANE PROTEINS FROM ENTEROBACTERIA.
60. Steinar Westin: UNEMPLOYMENT AND HEALTH: Medical and social consequences of a factory closure in a ten-year controlled follow-up study.
61. Ylva Sahlin: INJURY REGISTRATION, a tool for accident preventive work.
62. Helge Bjørnstad Pettersen: BIOSYNTHESIS OF COMPLEMENT BY HUMAN ALVEOLAR MACROPHAGES WITH SPECIAL REFERENCE TO SARCOIDOSIS.
63. Berit Schei: TRAPPED IN PAINFUL LOVE.
64. Lars J. Vatten: PROSPECTIVE STUDIES OF THE RISK OF BREAST CANCER IN A COHORT OF NORWEGIAN WOMAN.

1991

65. Kåre Bergh: APPLICATIONS OF ANTI-C5a SPECIFIC MONOCLONAL ANTIBODIES FOR THE ASSESSMENT OF COMPLEMENT ACTIVATION.
66. Svein Svenningsen: THE CLINICAL SIGNIFICANCE OF INCREASED FEMORAL ANTEVERSION.
67. Olbjørn Klepp: NONSEMINOMATOUS GERM CELL TESTIS CANCER: THERAPEUTIC OUTCOME AND PROGNOSTIC FACTORS.
68. Trond Sand: THE EFFECTS OF CLICK POLARITY ON BRAINSTEM AUDITORY EVOKED POTENTIALS AMPLITUDE, DISPERSION, AND LATENCY VARIABLES.
69. Kjetil B. Åsbakk: STUDIES OF A PROTEIN FROM PSORIATIC SCALE, PSO P27, WITH RESPECT TO ITS POTENTIAL ROLE IN IMMUNE REACTIONS IN PSORIASIS.
70. Arnulf Hestnes: STUDIES ON DOWN´S SYNDROME.
71. Randi Nygaard: LONG-TERM SURVIVAL IN CHILDHOOD LEUKEMIA.
72. Bjørn Hagen: THIO-TEPA.
73. Svein Anda: EVALUATION OF THE HIP JOINT BY COMPUTED TOMOGRAMPHY AND ULTRASONOGRAPHY.

1992

74. Martin Svartberg: AN INVESTIGATION OF PROCESS AND OUTCOME OF SHORT-TERM PSYCHODYNAMIC PSYCHOTHERAPY.
75. Stig Arild Slørdahl: AORTIC REGURGITATION.
76. Harold C Sexton: STUDIES RELATING TO THE TREATMENT OF SYMPTOMATIC NON-PSYCHOTIC PATIENTS.
77. Maurice B. Vincent: VASOACTIVE PEPTIDES IN THE OCULAR/FOREHEAD AREA.
78. Terje Johannessen: CONTROLLED TRIALS IN SINGLE SUBJECTS.
79. Turid Nilsen: PYROPHOSPHATE IN HEPATOCYTE IRON METABOLISM.
80. Olav Haraldseth: NMR SPECTROSCOPY OF CEREBRAL ISCHEMIA AND REPERFUSION IN RAT.
81. Eiliv Brenna: REGULATION OF FUNCTION AND GROWTH OF THE OXYNTIC MUCOSA.

1993

82. Gunnar Bovim: CERVICOGENIC HEADACHE.
83. Jarl Arne Kahn: ASSISTED PROCREATION.
84. Bjørn Naume: IMMUNOREGULATORY EFFECTS OF CYTOKINES ON NK CELLS.
85. Rune Wiseth: AORTIC VALVE REPLACEMENT.
86. Jie Ming Shen: BLOOD FLOW VELOCITY AND RESPIRATORY STUDIES.
87. Piotr Kruszewski: SUNCT SYNDROME WITH SPECIAL REFERENCE TO THE AUTONOMIC NERVOUS SYSTEM.
88. Mette Haase Moen: ENDOMETRIOSIS.
89. Anne Vik: VASCULAR GAS EMBOLISM DURING AIR INFUSION AND AFTER DECOMPRESSION IN PIGS.
90. Lars Jacob Stovner: THE CHIARI TYPE I MALFORMATION.
91. Kjell Å. Salvesen: ROUTINE ULTRASONOGRAPHY IN UTERO AND DEVELOPMENT IN CHILDHOOD.

1994

92. Nina-Beate Liabakk: DEVELOPMENT OF IMMUNOASSAYS FOR TNF AND ITS SOLUBLE RECEPTORS.
93. Sverre Helge Torp: *erb*B ONCOGENES IN HUMAN GLIOMAS AND MENINGIOMAS.
94. Olav M. Linaker: MENTAL RETARDATION AND PSYCHIATRY. Past and present.
95. Per Oscar Feet: INCREASED ANTIDEPRESSANT AND ANTIPANIC EFFECT IN COMBINED TREATMENT WITH DIXYRAZINE AND TRICYCLIC ANTIDEPRESSANTS.
96. Stein Olav Samstad: CROSS SECTIONAL FLOW VELOCITY PROFILES FROM TWO-DIMENSIONAL DOPPLER ULTRASOUND: Studies on early mitral blood flow.
97. Bjørn Backe: STUDIES IN ANTENATAL CARE.
98. Gerd Inger Ringdal: QUALITY OF LIFE IN CANCER PATIENTS.
99. Torvid Kiserud: THE DUCTUS VENOSUS IN THE HUMAN FETUS.
100. Hans E. Fjøsne: HORMONAL REGULATION OF PROSTATIC METABOLISM.
101. Eylert Brodtkorb: CLINICAL ASPECTS OF EPILEPSY IN THE MENTALLY RETARDED.
102. Roar Juul: PEPTIDERGIC MECHANISMS IN HUMAN SUBARACHNOID HEMORRHAGE.
103. Unni Syversen: CHROMOGRANIN A. Phsysiological and Clinical Role.

1995

104. Odd Gunnar Brakstad: THERMOSTABLE NUCLEASE AND THE *nuc* GENE IN THE DIAGNOSIS OF *Staphylococcus aureus* INFECTIONS.
105. Terje Engan: NUCLEAR MAGNETIC RESONANCE (NMR) SPECTROSCOPY OF PLASMA IN MALIGNANT DISEASE.
106. Kirsten Rasmussen: VIOLENCE IN THE MENTALLY DISORDERED.
107. Finn Egil Skjeldestad: INDUCED ABORTION: Timetrends and Determinants.
108. Roar Stenseth: THORACIC EPIDURAL ANALGESIA IN AORTOCORONARY BYPASS SURGERY.
109. Arild Faxvaag: STUDIES OF IMMUNE CELL FUNCTION *in mice infected with* MURINE RETROVIRUS.

1996

110. Svend Aakhus: NONINVASIVE COMPUTERIZED ASSESSMENT OF LEFT VENTRICULAR FUNCTION AND SYSTEMIC ARTERIAL PROPERTIES. Methodology and some clinical applications.
111. Klaus-Dieter Bolz: INTRAVASCULAR ULTRASONOGRAPHY.
112. Petter Aadahl: CARDIOVASCULAR EFFECTS OF THORACIC AORTIC CROSS-CLAMPING.
113. Sigurd Steinshamn: CYTOKINE MEDIATORS DURING GRANULOCYTOPENIC INFECTIONS.
114. Hans Stifoss-Hanssen: SEEKING MEANING OR HAPPINESS?
115. Anne Kvikstad: LIFE CHANGE EVENTS AND MARITAL STATUS IN RELATION TO RISK AND PROGNOSIS OF CANSER.
116. Torbjørn Grøntvedt: TREATMENT OF ACUTE AND CHRONIC ANTERIOR CRUCIATE LIGAMENT INJURIES. A clinical and biomechanical study.
117. Sigrid Hørven Wigers: CLINICAL STUDIES OF FIBROMYALGIA WITH FOCUS ON ETIOLOGY, TREATMENT AND OUTCOME.
118. Jan Schjøtt: MYOCARDIAL PROTECTION: Functional and Metabolic Characteristics of Two Endogenous Protective Principles.
119. Marit Martinussen: STUDIES OF INTESTINAL BLOOD FLOW AND ITS RELATION TO TRANSITIONAL CIRCULATORY ADAPATION IN NEWBORN INFANTS.
120. Tomm B. Müller: MAGNETIC RESONANCE IMAGING IN FOCAL CEREBRAL ISCHEMIA.
121. Rune Haaverstad: OEDEMA FORMATION OF THE LOWER EXTREMITIES.
122. Magne Børset: THE ROLE OF CYTOKINES IN MULTIPLE MYELOMA, WITH SPECIAL REFERENCE TO HEPATOCYTE GROWTH FACTOR.
123. Geir Smedslund: A THEORETICAL AND EMPIRICAL INVESTIGATION OF SMOKING, STRESS AND DISEASE: RESULTS FROM A POPULATION SURVEY.

1997

124. Torstein Vik: GROWTH, MORBIDITY, AND PSYCHOMOTOR DEVELOPMENT IN INFANTS WHO WERE GROWTH RETARDED *IN UTERO*.
125. Siri Forsmo: ASPECTS AND CONSEQUENCES OF OPPORTUNISTIC SCREENING FOR CERVICAL CANCER. Results based on data from three Norwegian counties.
126. Jon S. Skranes: CEREBRAL MRI AND NEURODEVELOPMENTAL OUTCOME IN VERY LOW BIRTH WEIGHT (VLBW) CHILDREN. A follow-up study of a geographically based year cohort of VLBW children at ages one and six years.
127. Knut Bjørnstad: COMPUTERIZED ECHOCARDIOGRAPHY FOR EVALUTION OF CORONARY ARTERY DISEASE.
128. Grethe Elisabeth Borchgrevink: DIAGNOSIS AND TREATMENT OF WHIPLASH/NECK SPRAIN INJURIES CAUSED BY CAR ACCIDENTS.
129. Tor Elsås: NEUROPEPTIDES AND NITRIC OXIDE SYNTHASE IN OCULAR AUTONOMIC AND SENSORY NERVES.
130. Rolf W. Gråwe: EPIDEMIOLOGICAL AND NEUROPSYCHOLOGICAL PERSPECTIVES ON SCHIZOPHRENIA.
131. Tonje Strømholm: CEREBRAL HAEMODYNAMICS DURING THORACIC AORTIC CROSSCLAMPING. An experimental study in pigs.

1998

132. Martinus Bråten: STUDIES ON SOME PROBLEMS REALTED TO INTRAMEDULLARY NAILING OF FEMORAL FRACTURES.
133. Ståle Nordgård: PROLIFERATIVE ACTIVITY AND DNA CONTENT AS PROGNOSTIC INDICATORS IN ADENOID CYSTIC CARCINOMA OF THE HEAD AND NECK.

134. Egil Lien: SOLUBLE RECEPTORS FOR **TNF** AND **LPS**: RELEASE PATTERN AND POSSIBLE SIGNIFICANCE IN DISEASE.
135. Marit Bjørgaas: HYPOGLYCAEMIA IN CHILDREN WITH DIABETES MELLITUS
136. Frank Skorpen: GENETIC AND FUNCTIONAL ANALYSES OF DNA REPAIR IN HUMAN CELLS.
137. Juan A. Pareja: SUNCT SYNDROME. ON THE CLINICAL PICTURE. ITS DISTINCTION FROM OTHER, SIMILAR HEADACHES.
138. Anders Angelsen: NEUROENDOCRINE CELLS IN HUMAN PROSTATIC CARCINOMAS AND THE PROSTATIC COMPLEX OF RAT, GUINEA PIG, CAT AND DOG.
139. Fabio Antonaci: CHRONIC PAROXYSMAL HEMICRANIA AND HEMICRANIA CONTINUA: TWO DIFFERENT ENTITIES?
140. Sven M. Carlsen: ENDOCRINE AND METABOLIC EFFECTS OF METFORMIN WITH SPECIAL EMPHASIS ON CARDIOVASCULAR RISK FACTORES.

1999

141. Terje A. Murberg: DEPRESSIVE SYMPTOMS AND COPING AMONG PATIENTS WITH CONGESTIVE HEART FAILURE.
142. Harm-Gerd Karl Blaas: THE EMBRYONIC EXAMINATION. Ultrasound studies on the development of the human embryo.
143. Noèmi Becser Andersen:THE CEPHALIC SENSORY NERVES IN UNILATERAL HEADACHES. Anatomical background and neurophysiological evaluation.
144. Eli-Janne Fiskerstrand: LASER TREATMENT OF PORT WINE STAINS. A study of the efficacy and limitations of the pulsed dye laser. Clinical and morfological analyses aimed at improving the therapeutic outcome.
145. Bård Kulseng: A STUDY OF ALGINATE CAPSULE PROPERTIES AND CYTOKINES IN RELATION TO INSULIN DEPENDENT DIABETES MELLITUS.
146. Terje Haug: STRUCTURE AND REGULATION OF THE HUMAN UNG GENE ENCODING URACIL-DNA GLYCOSYLASE.
147. Heidi Brurok: MANGANESE AND THE HEART. A Magic Metal with Diagnostic and Therapeutic Possibilites.
148. Agnes Kathrine Lie: DIAGNOSIS AND PREVALENCE OF HUMAN PAPILLOMAVIRUS INFECTION IN CERVICAL INTRAEPITELIAL NEOPLASIA. Relationship to Cell Cycle Regulatory Proteins and HLA DQBI Genes.
149. Ronald Mårvik: PHARMACOLOGICAL, PHYSIOLOGICAL AND PATHOPHYSIOLOGICAL STUDIES ON ISOLATED STOMACS.
150. Ketil Jarl Holen: THE ROLE OF ULTRASONOGRAPHY IN THE DIAGNOSIS AND TREATMENT OF HIP DYSPLASIA IN NEWBORNS.
151. Irene Hetlevik: THE ROLE OF CLINICAL GUIDELINES IN CARDIOVASCULAR RISK INTERVENTION IN GENERAL PRACTICE.
152. Katarina Tunòn: ULTRASOUND AND PREDICTION OF GESTATIONAL AGE.
153. Johannes Soma: INTERACTION BETWEEN THE LEFT VENTRICLE AND THE SYSTEMIC ARTERIES.
154. Arild Aamodt: DEVELOPMENT AND PRE-CLINICAL EVALUATION OF A CUSTOM-MADE FEMORAL STEM.
155. Agnar Tegnander: DIAGNOSIS AND FOLLOW-UP OF CHILDREN WITH SUSPECTED OR KNOWN HIP DYSPLASIA.
156. Bent Indredavik: STROKE UNIT TREATMENT: SHORT AND LONG-TERM EFFECTS
157. Jolanta Vanagaite Vingen: PHOTOPHOBIA AND PHONOPHOBIA IN PRIMARY HEADACHES

2000

158. Ola Dalsegg Sæther: PATHOPHYSIOLOGY DURING PROXIMAL AORTIC CROSS-CLAMPING CLINICAL AND EXPERIMENTAL STUDIES
159. xxxxxxxxx (blind number)
160. Christina Vogt Isaksen: PRENATAL ULTRASOUND AND POSTMORTEM FINDINGS – A TEN YEAR CORRELATIVE STUDY OF FETUSES AND INFANTS WITH DEVELOPMENTAL ANOMALIES.
161. Holger Seidel: HIGH-DOSE METHOTREXATE THERAPY IN CHILDREN WITH ACUTE LYMPHOCYTIC LEUKEMIA: DOSE, CONCENTRATION, AND EFFECT CONSIDERATIONS.
162. Stein Hallan: IMPLEMENTATION OF MODERN MEDICAL DECISION ANALYSIS INTO CLINICAL DIAGNOSIS AND TREATMENT.

163. Malcolm Sue-Chu: INVASIVE AND NON-INVASIVE STUDIES IN CROSS-COUNTRY SKIERS WITH ASTHMA-LIKE SYMPTOMS.
164. Ole-Lars Brekke: EFFECTS OF ANTIOXIDANTS AND FATTY ACIDS ON TUMOR NECROSIS FACTOR-INDUCED CYTOTOXICITY.
165. Jan Lundbom: AORTOCORONARY BYPASS SURGERY: CLINICAL ASPECTS, COST CONSIDERATIONS AND WORKING ABILITY.
166. John-Anker Zwart: LUMBAR NERVE ROOT COMPRESSION, BIOCHEMICAL AND NEUROPHYSIOLOGICAL ASPECTS.
167. Geir Falck: HYPEROSMOLALITY AND THE HEART.
168. Eirik Skogvoll: CARDIAC ARREST Incidence, Intervention and Outcome.
169. Dalius Bansevicius: SHOULDER-NECK REGION IN CERTAIN HEADACHES AND CHRONIC PAIN SYNDROMES.
170. Bettina Kinge: REFRACTIVE ERRORS AND BIOMETRIC CHANGES AMONG UNIVERSITY STUDENTS IN NORWAY.
171. Gunnar Qvigstad: CONSEQUENCES OF HYPERGASTRINEMIA IN MAN
172. Hanne Ellekjær: EPIDEMIOLOGICAL STUDIES OF STROKE IN A NORWEGIAN POPULATION. INCIDENCE, RISK FACTORS AND PROGNOSIS
173. Hilde Grimstad: VIOLENCE AGAINST WOMEN AND PREGNANCY OUTCOME.
174. Astrid Hjelde: SURFACE TENSION AND COMPLEMENT ACTIVATION: Factors influencing bubble formation and bubble effects after decompression.
175. Kjell A. Kvistad: MR IN BREAST CANCER – A CLINICAL STUDY.
176. Ivar Rossvoll: ELECTIVE ORTHOPAEDIC SURGERY IN A DEFINED POPULATION. Studies on demand, waiting time for treatment and incapacity for work.
177. Carina Seidel: PROGNOSTIC VALUE AND BIOLOGICAL EFFECTS OF HEPATOCYTE GROWTH FACTOR AND SYNDECAN-1 IN MULTIPLE MYELOMA.

2001

178. Alexander Wahba: THE INFLUENCE OF CARDIOPULMONARY BYPASS ON PLATELET FUNCTION AND BLOOD COAGULATION – DETERMINANTS AND CLINICAL CONSEQUENSES
179. Marcus Schmitt-Egenolf: THE RELEVANCE OF THE MAJOR hISTOCOMPATIBILITY COMPLEX FOR THE GENETICS OF PSORIASIS
180. Odrun Arna Gederaas: BIOLOGICAL MECHANISMS INVOLVED IN 5-AMINOLEVULINIC ACID BASED PHOTODYNAMIC THERAPY
181. Pål Richard Romundstad: CANCER INCIDENCE AMONG NORWEGIAN ALUMINIUM WORKERS
182. Henrik Hjorth-Hansen: NOVEL CYTOKINES IN GROWTH CONTROL AND BONE DISEASE OF MULTIPLE MYELOMA
183. Gunnar Morken: SEASONAL VARIATION OF HUMAN MOOD AND BEHAVIOUR
184. Bjørn Olav Haugen: MEASUREMENT OF CARDIAC OUTPUT AND STUDIES OF VELOCITY PROFILES IN AORTIC AND MITRAL FLOW USING TWO- AND THREE-DIMENSIONAL COLOUR FLOW IMAGING
185. Geir Bråthen: THE CLASSIFICATION AND CLINICAL DIAGNOSIS OF ALCOHOL-RELATED SEIZURES
186. Knut Ivar Aasarød: RENAL INVOLVEMENT IN INFLAMMATORY RHEUMATIC DISEASE. A Study of Renal Disease in Wegener's Granulomatosis and in Primary Sjögren's Syndrome
187. Trude Helen Flo: RESEPTORS INVOLVED IN CELL ACTIVATION BY DEFINED URONIC ACID POLYMERS AND BACTERIAL COMPONENTS
188. Bodil Kavli: HUMAN URACIL-DNA GLYCOSYLASES FROM THE UNG GENE: STRUCTRUAL BASIS FOR SUBSTRATE SPECIFICITY AND REPAIR
189. Liv Thommesen: MOLECULAR MECHANISMS INVOLVED IN TNF- AND GASTRIN-MEDIATED GENE REGULATION
190. Turid Lingaas Holmen: SMOKING AND HEALTH IN ADOLESCENCE; THE NORD-TRØNDELAG HEALTH STUDY, 1995-97
191. Øyvind Hjertner: MULTIPLE MYELOMA: INTERACTIONS BETWEEN MALIGNANT PLASMA CELLS AND THE BONE MICROENVIRONMENT
192. Asbjørn Støylen: STRAIN RATE IMAGING OF THE LEFT VENTRICLE BY ULTRASOUND. FEASIBILITY, CLINICAL VALIDATION AND PHYSIOLOGICAL ASPECTS

193. Kristian Midthjell: DIABETES IN ADULTS IN NORD-TRØNDELAG. PUBLIC HEALTH ASPECTS OF DIABETES MELLITUS IN A LARGE, NON-SELECTED NORWEGIAN POPULATION.
194. Guanglin Cui: FUNCTIONAL ASPECTS OF THE ECL CELL IN RODENTS
195. Ulrik Wisløff: CARDIAC EFFECTS OF AEROBIC ENDURANCE TRAINING: HYPERTROPHY, CONTRACTILITY AND CALCUIM HANDLING IN NORMAL AND FAILING HEART
196. Øyvind Halaas: MECHANISMS OF IMMUNOMODULATION AND CELL-MEDIATED CYTOTOXICITY INDUCED BY BACTERIAL PRODUCTS
197. Tore Amundsen: PERFUSION MR IMAGING IN THE DIAGNOSIS OF PULMONARY EMBOLISM
198. Nanna Kurtze: THE SIGNIFICANCE OF ANXIETY AND DEPRESSION IN FATIQUE AND PATTERNS OF PAIN AMONG INDIVIDUALS DIAGNOSED WITH FIBROMYALGIA: RELATIONS WITH QUALITY OF LIFE, FUNCTIONAL DISABILITY, LIFESTYLE, EMPLOYMENT STATUS, CO-MORBIDITY AND GENDER
199. Tom Ivar Lund Nilsen: PROSPECTIVE STUDIES OF CANCER RISK IN NORD-TRØNDELAG: THE HUNT STUDY. Associations with anthropometric, socioeconomic, and lifestyle risk factors
200. Asta Kristine Håberg: A NEW APPROACH TO THE STUDY OF MIDDLE CEREBRAL ARTERY OCCLUSION IN THE RAT USING MAGNETIC RESONANCE TECHNIQUES

2002

201. Knut Jørgen Arntzen: PREGNANCY AND CYTOKINES
202. Henrik Døllner: INFLAMMATORY MEDIATORS IN PERINATAL INFECTIONS
203. Asta Bye: LOW FAT, LOW LACTOSE DIET USED AS PROPHYLACTIC TREATMENT OF ACUTE INTESTINAL REACTIONS DURING PELVIC RADIOTHERAPY. A PROSPECTIVE RANDOMISED STUDY.
204. Sylvester Moyo: STUDIES ON STREPTOCOCCUS AGALACTIAE (GROUP B STREPTOCOCCUS) SURFACE-ANCHORED MARKERS WITH EMPHASIS ON STRAINS AND HUMAN SERA FROM ZIMBABWE.
205. Knut Hagen: HEAD-HUNT: THE EPIDEMIOLOGY OF HEADACHE IN NORD-TRØNDELAG
206. Li Lixin: ON THE REGULATION AND ROLE OF UNCOUPLING PROTEIN-2 IN INSULIN PRODUCING ß-CELLS
207. Anne Hildur Henriksen: SYMPTOMS OF ALLERGY AND ASTHMA VERSUS MARKERS OF LOWER AIRWAY INFLAMMATION AMONG ADOLESCENTS
208. Egil Andreas Fors: NON-MALIGNANT PAIN IN RELATION TO PSYCHOLOGICAL AND ENVIRONTENTAL FACTORS. EXPERIENTAL AND CLINICAL STUDES OF PAIN WITH FOCUS ON FIBROMYALGIA
209. Pål Klepstad: MORPHINE FOR CANCER PAIN
210. Ingunn Bakke: MECHANISMS AND CONSEQUENCES OF PEROXISOME PROLIFERATOR-INDUCED HYPERFUNCTION OF THE RAT GASTRIN PRODUCING CELL
211. Ingrid Susann Gribbestad: MAGNETIC RESONANCE IMAGING AND SPECTROSCOPY OF BREAST CANCER
212. Rønnaug Astri Ødegård: PREECLAMPSIA – MATERNAL RISK FACTORS AND FETAL GROWTH
213. Johan Haux: STUDIES ON CYTOTOXICITY INDUCED BY HUMAN NATURAL KILLER CELLS AND DIGITOXIN
214. Turid Suzanne Berg-Nielsen: PARENTING PRACTICES AND MENTALLY DISORDERED ADOLESCENTS
215. Astrid Rydning: BLOOD FLOW AS A PROTECTIVE FACTOR FOR THE STOMACH MUCOSA. AN EXPERIMENTAL STUDY ON THE ROLE OF MAST CELLS AND SENSORY AFFERENT NEURONS

2003

216. Jan Pål Loennechen: HEART FAILURE AFTER MYOCARDIAL INFARCTION. Regional Differences, Myocyte Function, Gene Expression, and Response to Cariporide, Losartan, and Exercise Training.
217. Elisabeth Qvigstad: EFFECTS OF FATTY ACIDS AND OVER-STIMULATION ON INSULIN SECRETION IN MAN

218. Arne Åsberg: EPIDEMIOLOGICAL STUDIES IN HEREDITARY HEMOCHROMATOSIS: PREVALENCE, MORBIDITY AND BENEFIT OF SCREENING.
219. Johan Fredrik Skomsvoll: REPRODUCTIVE OUTCOME IN WOMEN WITH RHEUMATIC DISEASE. A population registry based study of the effects of inflammatory rheumatic disease and connective tissue disease on reproductive outcome in Norwegian women in 1967-1995.
220. Siv Mørkved: URINARY INCONTINENCE DURING PREGNANCY AND AFTER DELIVERY: EFFECT OF PELVIC FLOOR MUSCLE TRAINING IN PREVENTION AND TREATMENT
221. Marit S. Jordhøy: THE IMPACT OF COMPREHENSIVE PALLIATIVE CARE
222. Tom Christian Martinsen: HYPERGASTRINEMIA AND HYPOACIDITY IN RODENTS – CAUSES AND CONSEQUENCES
223. Solveig Tingulstad: CENTRALIZATION OF PRIMARY SURGERY FOR OVARAIN CANCER. FEASIBILITY AND IMPACT ON SURVIVAL
224. Haytham Eloqayli: METABOLIC CHANGES IN THE BRAIN CAUSED BY EPILEPTIC SEIZURES
225. Torunn Bruland: STUDIES OF EARLY RETROVIRUS-HOST INTERACTIONS – VIRAL DETERMINANTS FOR PATHOGENESIS AND THE INFLUENCE OF SEX ON THE SUSCEPTIBILITY TO FRIEND MURINE LEUKAEMIA VIRUS INFECTION
226. Torstein Hole: DOPPLER ECHOCARDIOGRAPHIC EVALUATION OF LEFT VENTRICULAR FUNCTION IN PATIENTS WITH ACUTE MYOCARDIAL INFARCTION
227. Vibeke Nossum: THE EFFECT OF VASCULAR BUBBLES ON ENDOTHELIAL FUNCTION
228. Sigurd Fasting: ROUTINE BASED RECORDING OF ADVERSE EVENTS DURING ANAESTHESIA – APPLICATION IN QUALITY IMPROVEMENT AND SAFETY
229. Solfrid Romundstad: EPIDEMIOLOGICAL STUDIES OF MICROALBUMINURIA. THE NORD-TRØNDELAG HEALTH STUDY 1995-97 (HUNT 2)
230. Geir Torheim: PROCESSING OF DYNAMIC DATA SETS IN MAGNETIC RESONANCE IMAGING
231. Catrine Ahlén: SKIN INFECTIONS IN OCCUPATIONAL SATURATION DIVERS IN THE NORTH SEA AND THE IMPACT OF THE ENVIRONMENT
232. Arnulf Langhammer: RESPIRATORY SYMPTOMS, LUNG FUNCTION AND BONE MINERAL DENSITY IN A COMPREHENSIVE POPULATION SURVEY. THE NORD-TRØNDELAG HEALTH STUDY 1995-97. THE BRONCHIAL OBSTRUCTION IN NORD-TRØNDELAG STUDY
233. Einar Kjelsås: EATING DISORDERS AND PHYSICAL ACTIVITY IN NON-CLINICAL SAMPLES
234. Arne Wibe: RECTAL CANCER TREATMENT IN NORWAY – STANDARDISATION OF SURGERY AND QUALITY ASSURANCE

2004

235. Eivind Witsø: BONE GRAFT AS AN ANTIBIOTIC CARRIER
236. Anne Mari Sund: DEVELOPMENT OF DEPRESSIVE SYMPTOMS IN EARLY ADOLESCENCE
237. Hallvard Lærum: EVALUATION OF ELECTRONIC MEDICAL RECORDS – A CLINICAL TASK PERSPECTIVE
238. Gustav Mikkelsen: ACCESSIBILITY OF INFORMATION IN ELECTRONIC PATIENT RECORDS; AN EVALUATION OF THE ROLE OF DATA QUALITY
239. Steinar Krokstad: SOCIOECONOMIC INEQUALITIES IN HEALTH AND DISABILITY. SOCIAL EPIDEMIOLOGY IN THE NORD-TRØNDELAG HEALTH STUDY (HUNT), NORWAY
240. Arne Kristian Myhre: NORMAL VARIATION IN ANOGENITAL ANATOMY AND MICROBIOLOGY IN NON-ABUSED PRESCHOOL CHILDREN
241. Ingunn Dybedal: NEGATIVE REGULATORS OF HEMATOPOIETEC STEM AND PROGENITOR CELLS
242. Beate Sitter: TISSUE CHARACTERIZATION BY HIGH RESOLUTION MAGIC ANGLE SPINNING MR SPECTROSCOPY
243. Per Arne Aas: MACROMOLECULAR MAINTENANCE IN HUMAN CELLS – REPAIR OF URACIL IN DNA AND METHYLATIONS IN DNA AND RNA
244. Anna Bofin: FINE NEEDLE ASPIRATION CYTOLOGY IN THE PRIMARY INVESTIGATION OF BREAST TUMOURS AND IN THE DETERMINATION OF TREATMENT STRATEGIES

245. Jim Aage Nøttestad: DEINSTITUTIONALIZATION AND MENTAL HEALTH CHANGES AMONG PEOPLE WITH MENTAL RETARDATION
246. Reidar Fossmark: GASTRIC CANCER IN JAPANESE COTTON RATS
247. Wibeke Nordhøy: MANGANESE AND THE HEART, INTRACELLULAR MR RELAXATION AND WATER EXCHANGE ACROSS THE CARDIAC CELL MEMBRANE

2005

248. Sturla Molden: QUANTITATIVE ANALYSES OF SINGLE UNITS RECORDED FROM THE HIPPOCAMPUS AND ENTORHINAL CORTEX OF BEHAVING RATS
249. Wenche Brenne Drøyvold: EPIDEMIOLOGICAL STUDIES ON WEIGHT CHANGE AND HEALTH IN A LARGE POPULATION. THE NORD-TRØNDELAG HEALTH STUDY (HUNT)
250. Ragnhild Støen: ENDOTHELIUM-DEPENDENT VASODILATION IN THE FEMORAL ARTERY OF DEVELOPING PIGLETS
251. Aslak Steinsbekk: HOMEOPATHY IN THE PREVENTION OF UPPER RESPIRATORY TRACT INFECTIONS IN CHILDREN
252. Hill-Aina Steffenach: MEMORY IN HIPPOCAMPAL AND CORTICO-HIPPOCAMPAL CIRCUITS
253. Eystein Stordal: ASPECTS OF THE EPIDEMIOLOGY OF DEPRESSIONS BASED ON SELF-RATING IN A LARGE GENERAL HEALTH STUDY (THE HUNT-2 STUDY)
254. Viggo Pettersen: FROM MUSCLES TO SINGING: THE ACTIVITY OF ACCESSORY BREATHING MUSCLES AND THORAX MOVEMENT IN CLASSICAL SINGING
255. Marianne Fyhn: SPATIAL MAPS IN THE HIPPOCAMPUS AND ENTORHINAL CORTEX
256. Robert Valderhaug: OBSESSIVE-COMPULSIVE DISORDER AMONG CHILDREN AND ADOLESCENTS: CHARACTERISTICS AND PSYCHOLOGICAL MANAGEMENT OF PATIENTS IN OUTPATIENT PSYCHIATRIC CLINICS
257. Erik Skaaheim Haug: INFRARENAL ABDOMINAL AORTIC ANEURYSMS – COMORBIDITY AND RESULTS FOLLOWING OPEN SURGERY
258. Daniel Kondziella: GLIAL-NEURONAL INTERACTIONS IN EXPERIMENTAL BRAIN DISORDERS
259. Vegard Heimly Brun: ROUTES TO SPATIAL MEMORY IN HIPPOCAMPAL PLACE CELLS
260. Kenneth McMillan: PHYSIOLOGICAL ASSESSMENT AND TRAINING OF ENDURANCE AND STRENGTH IN PROFESSIONAL YOUTH SOCCER PLAYERS
261. Marit Sæbø Indredavik: MENTAL HEALTH AND CEREBRAL MAGNETIC RESONANCE IMAGING IN ADOLESCENTS WITH LOW BIRTH WEIGHT
262. Ole Johan Kemi: ON THE CELLULAR BASIS OF AEROBIC FITNESS, INTENSITY-DEPENDENCE AND TIME-COURSE OF CARDIOMYOCYTE AND ENDOTHELIAL ADAPTATIONS TO EXERCISE TRAINING
263. Eszter Vanky: POLYCYSTIC OVARY SYNDROME – METFORMIN TREATMENT IN PREGNANCY
264. Hild Fjærtoft: EXTENDED STROKE UNIT SERVICE AND EARLY SUPPORTED DISCHARGE. SHORT AND LONG-TERM EFFECTS
265. Grete Dyb: POSTTRAUMATIC STRESS REACTIONS IN CHILDREN AND ADOLESCENTS
266. Vidar Fykse: SOMATOSTATIN AND THE STOMACH
267. Kirsti Berg: OXIDATIVE STRESS AND THE ISCHEMIC HEART: A STUDY IN PATIENTS UNDERGOING CORONARY REVASCULARIZATION
268. Björn Inge Gustafsson: THE SEROTONIN PRODUCING ENTEROCHROMAFFIN CELL, AND EFFECTS OF HYPERSEROTONINEMIA ON HEART AND BONE

2006

269. Torstein Baade Rø: EFFECTS OF BONE MORPHOGENETIC PROTEINS, HEPATOCYTE GROWTH FACTOR AND INTERLEUKIN-21 IN MULTIPLE MYELOMA
270. May-Britt Tessem: METABOLIC EFFECTS OF ULTRAVIOLET RADIATION ON THE ANTERIOR PART OF THE EYE
271. Anne-Sofie Helvik: COPING AND EVERYDAY LIFE IN A POPULATION OF ADULTS WITH HEARING IMPAIRMENT
272. Therese Standal: MULTIPLE MYELOMA: THE INTERPLAY BETWEEN MALIGNANT PLASMA CELLS AND THE BONE MARROW MICROENVIRONMENT

273. Ingvild Saltvedt: TREATMENT OF ACUTELY SICK, FRAIL ELDERLY PATIENTS IN A GERIATRIC EVALUATION AND MANAGEMENT UNIT – RESULTS FROM A PROSPECTIVE RANDOMISED TRIAL
274. Birger Henning Endreseth: STRATEGIES IN RECTAL CANCER TREATMENT – FOCUS ON EARLY RECTAL CANCER AND THE INFLUENCE OF AGE ON PROGNOSIS
275. Anne Mari Aukan Rokstad: ALGINATE CAPSULES AS BIOREACTORS FOR CELL THERAPY
276. Mansour Akbari: HUMAN BASE EXCISION REPAIR FOR PRESERVATION OF GENOMIC STABILITY
277. Stein Sundstrøm: IMPROVING TREATMENT IN PATIENTS WITH LUNG CANCER – RESULTS FROM TWO MULITCENTRE RANDOMISED STUDIES
278. Hilde Pleym: BLEEDING AFTER CORONARY ARTERY BYPASS SURGERY - STUDIES ON HEMOSTATIC MECHANISMS, PROPHYLACTIC DRUG TREATMENT AND EFFECTS OF AUTOTRANSFUSION
279. Line Merethe Oldervoll: PHYSICAL ACTIVITY AND EXERCISE INTERVENTIONS IN CANCER PATIENTS
280. Boye Welde: THE SIGNIFICANCE OF ENDURANCE TRAINING, RESISTANCE TRAINING AND MOTIVATIONAL STYLES IN ATHLETIC PERFORMANCE AMONG ELITE JUNIOR CROSS-COUNTRY SKIERS
281. Per Olav Vandvik: IRRITABLE BOWEL SYNDROME IN NORWAY, STUDIES OF PREVALENCE, DIAGNOSIS AND CHARACTERISTICS IN GENERAL PRACTICE AND IN THE POPULATION
282. Idar Kirkeby-Garstad: CLINICAL PHYSIOLOGY OF EARLY MOBILIZATION AFTER CARDIAC SURGERY
283. Linn Getz: SUSTAINABLE AND RESPONSIBLE PREVENTIVE MEDICINE. CONCEPTUALISING ETHICAL DILEMMAS ARISING FROM CLINICAL IMPLEMENTATION OF ADVANCING MEDICAL TECHNOLOGY
284. Eva Tegnander: DETECTION OF CONGENITAL HEART DEFECTS IN A NON-SELECTED POPULATION OF 42,381 FETUSES
285. Kristin Gabestad Nørsett: GENE EXPRESSION STUDIES IN GASTROINTESTINAL PATHOPHYSIOLOGY AND NEOPLASIA
286. Per Magnus Haram: GENETIC VS. AQUIRED FITNESS: METABOLIC, VASCULAR AND CARDIOMYOCYTE ADAPTATIONS
287. Agneta Johansson: GENERAL RISK FACTORS FOR GAMBLING PROBLEMS AND THE PREVALENCE OG PATHOLOGICAL GAMBLING IN NORWAY
288. Svein Artur Jensen: THE PREVALENCE OF SYMPTOMATIC ARTERIAL DISEASE OF THE LOWER LIMB
289. Charlotte Björk Ingul: QUANITIFICATION OF REGIONAL MYOCARDIAL FUNCTION BY STRAIN RATE AND STRAIN FOR EVALUATION OF CORONARY ARTERY DISEASE. AUTOMATED VERSUS MANUAL ANALYSIS DURING ACUTE MYOCARDIAL INFARCTION AND DOBUTAMINE STRESS ECHOCARDIOGRAPHY
290. Jakob Nakling: RESULTS AND CONSEQUENCES OF ROUTINE ULTRASOUND SCREENING IN PREGNANCY – A GEOGRAPHIC BASED POPULATION STUDY
291. Anne Engum: DEPRESSION AND ANXIETY – THEIR RELATIONS TO THYROID DYSFUNCTION AND DIABETES IN A LARGE EPIDEMIOLOGICAL STUDY
292. Ottar Bjerkeset: ANXIETY AND DEPRESSION IN THE GENERAL POPULATION: RISK FACTORS, INTERVENTION AND OUTCOME – THE NORD-TRØNDELAG HEALTH STUDY (HUNT)
293. Jon Olav Drogset: RESULTS AFTER SURGICAL TREATMENT OF ANTERIOR CRUCIATE LIGAMENT INJURIES – A CLINICAL STUDY
294. Lars Fosse: MECHANICAL BEHAVIOUR OF COMPACTED MORSELLISED BONE – AN EXPERIMENTAL IN VITRO STUDY
295. Gunilla Klensmeden Fosse: MENTAL HEALTH OF PSYCHIATRIC OUTPATIENTS BULLIED IN CHILDHOOD
296. Paul Jarle Mork: MUSCLE ACTIVITY IN WORK AND LEISURE AND ITS ASSOCIATION TO MUSCULOSKELETAL PAIN
297. Björn Stenström: LESSONS FROM RODENTS: I: MECHANISMS OF OBESITY SURGERY – ROLE OF STOMACH. II: CARCINOGENIC EFFECTS OF *HELICOBACTER PYLORI* AND SNUS IN THE STOMACH

2007

298. Haakon R. Skogseth: INVASIVE PROPERTIES OF CANCER – A TREATMENT TARGET ? IN VITRO STUDIES IN HUMAN PROSTATE CANCER CELL LINES
299. Janniche Hammer: GLUTAMATE METABOLISM AND CYCLING IN MESIAL TEMPORAL LOBE EPILEPSY
300. May Britt Drugli: YOUNG CHILDREN TREATED BECAUSE OF ODD/CD: CONDUCT PROBLEMS AND SOCIAL COMPETENCIES IN DAY-CARE AND SCHOOL SETTINGS
301. Arne Skjold: MAGNETIC RESONANCE KINETICS OF MANGANESE DIPYRIDOXYL DIPHOSPHATE (MnDPDP) IN HUMAN MYOCARDIUM. STUDIES IN HEALTHY VOLUNTEERS AND IN PATIENTS WITH RECENT MYOCARDIAL INFARCTION
302. Siri Malm: LEFT VENTRICULAR SYSTOLIC FUNCTION AND MYOCARDIAL PERFUSION ASSESSED BY CONTRAST ECHOCARDIOGRAPHY
303. Valentina Maria do Rosario Cabral Iversen: MENTAL HEALTH AND PSYCHOLOGICAL ADAPTATION OF CLINICAL AND NON-CLINICAL MIGRANT GROUPS
304. Lasse Løvstakken: SIGNAL PROCESSING IN DIAGNOSTIC ULTRASOUND: ALGORITHMS FOR REAL-TIME ESTIMATION AND VISUALIZATION OF BLOOD FLOW VELOCITY
305. Elisabeth Olstad: GLUTAMATE AND GABA: MAJOR PLAYERS IN NEURONAL METABOLISM
306. Lilian Leistad: THE ROLE OF CYTOKINES AND PHOSPHOLIPASE A_2s IN ARTICULAR CARTILAGE CHONDROCYTES IN RHEUMATOID ARTHRITIS AND OSTEOARTHRITIS
307. Arne Vaaler: EFFECTS OF PSYCHIATRIC INTENSIVE CARE UNIT IN AN ACUTE PSYCIATHRIC WARD
308. Mathias Toft: GENETIC STUDIES OF LRRK2 AND PINK1 IN PARKINSON'S DISEASE
309. Ingrid Løvold Mostad: IMPACT OF DIETARY FAT QUANTITY AND QUALITY IN TYPE 2 DIABETES WITH EMPHASIS ON MARINE N-3 FATTY ACIDS
310. Torill Eidhammer Sjøbakk: MR DETERMINED BRAIN METABOLIC PATTERN IN PATIENTS WITH BRAIN METASTASES AND ADOLESCENTS WITH LOW BIRTH WEIGHT
311. Vidar Beisvåg: PHYSIOLOGICAL GENOMICS OF HEART FAILURE: FROM TECHNOLOGY TO PHYSIOLOGY
312. Olav Magnus Søndenå Fredheim: HEALTH RELATED QUALITY OF LIFE ASSESSMENT AND ASPECTS OF THE CLINICAL PHARMACOLOGY OF METHADONE IN PATIENTS WITH CHRONIC NON-MALIGNANT PAIN
313. Anne Brantberg: FETAL AND PERINATAL IMPLICATIONS OF ANOMALIES IN THE GASTROINTESTINAL TRACT AND THE ABDOMINAL WALL
314. Erik Solligård: GUT LUMINAL MICRODIALYSIS
315. Elin Tollefsen: RESPIRATORY SYMPTOMS IN A COMPREHENSIVE POPULATION BASED STUDY AMONG ADOLESCENTS 13-19 YEARS. YOUNG-HUNT 1995-97 AND 2000-01; THE NORD-TRØNDELAG HEALTH STUDIES (HUNT)
316. Anne-Tove Brenne: GROWTH REGULATION OF MYELOMA CELLS
317. Heidi Knobel: FATIGUE IN CANCER TREATMENT – ASSESSMENT, COURSE AND ETIOLOGY
318. Torbjørn Dahl: CAROTID ARTERY STENOSIS. DIAGNOSTIC AND THERAPEUTIC ASPECTS
319. Inge-Andre Rasmussen jr.: FUNCTIONAL AND DIFFUSION TENSOR MAGNETIC RESONANCE IMAGING IN NEUROSURGICAL PATIENTS
320. Grete Helen Bratberg: PUBERTAL TIMING – ANTECEDENT TO RISK OR RESILIENCE ? EPIDEMIOLOGICAL STUDIES ON GROWTH, MATURATION AND HEALTH RISK BEHAVIOURS; THE YOUNG HUNT STUDY, NORD-TRØNDELAG, NORWAY
321. Sveinung Sørhaug: THE PULMONARY NEUROENDOCRINE SYSTEM. PHYSIOLOGICAL, PATHOLOGICAL AND TUMOURIGENIC ASPECTS
322. Olav Sande Eftedal: ULTRASONIC DETECTION OF DECOMPRESSION INDUCED VASCULAR MICROBUBBLES
323. Rune Bang Leistad: PAIN, AUTONOMIC ACTIVATION AND MUSCULAR ACTIVITY RELATED TO EXPERIMENTALLY-INDUCED COGNITIVE STRESS IN HEADACHE PATIENTS
324. Svein Brekke: TECHNIQUES FOR ENHANCEMENT OF TEMPORAL RESOLUTION IN THREE-DIMENSIONAL ECHOCARDIOGRAPHY
325. Kristian Bernhard Nilsen: AUTONOMIC ACTIVATION AND MUSCLE ACTIVITY IN RELATION TO MUSCULOSKELETAL PAIN

326. Anne Irene Hagen: HEREDITARY BREAST CANCER IN NORWAY. DETECTION AND PROGNOSIS OF BREAST CANCER IN FAMILIES WITH *BRCA1*GENE MUTATION
327. Ingebjørg S. Juel : INTESTINAL INJURY AND RECOVERY AFTER ISCHEMIA. AN EXPERIMENTAL STUDY ON RESTITUTION OF THE SURFACE EPITHELIUM, INTESTINAL PERMEABILITY, AND RELEASE OF BIOMARKERS FROM THE MUCOSA
328. Runa Heimstad: POST-TERM PREGNANCY
329. Jan Egil Afset: ROLE OF ENTEROPATHOGENIC *ESCHERICHIA COLI* IN CHILDHOOD DIARRHOEA IN NORWAY
330. Bent Håvard Hellum: *IN VITRO* INTERACTIONS BETWEEN MEDICINAL DRUGS AND HERBS ON CYTOCHROME P-450 METABOLISM AND P-GLYCOPROTEIN TRANSPORT
331. Morten André Høydal: CARDIAC DYSFUNCTION AND MAXIMAL OXYGEN UPTAKE MYOCARDIAL ADAPTATION TO ENDURANCE TRAINING

2008

332. Andreas Møllerløkken: REDUCTION OF VASCULAR BUBBLES: METHODS TO PREVENT THE ADVERSE EFFECTS OF DECOMPRESSION
333. Anne Hege Aamodt: COMORBIDITY OF HEADACHE AND MIGRAINE IN THE NORD-TRØNDELAG HEALTH STUDY 1995-97
334. Brage Høyem Amundsen: MYOCARDIAL FUNCTION QUANTIFIED BY SPECKLE TRACKING AND TISSUE DOPPLER ECHOCARDIOGRAPHY – VALIDATION AND APPLICATION IN EXERCISE TESTING AND TRAINING
335. Inger Anne Næss: INCIDENCE, MORTALITY AND RISK FACTORS OF FIRST VENOUS THROMBOSIS IN A GENERAL POPULATION. RESULTS FROM THE SECOND NORD-TRØNDELAG HEALTH STUDY (HUNT2)
336. Vegard Bugten: EFFECTS OF POSTOPERATIVE MEASURES AFTER FUNCTIONAL ENDOSCOPIC SINUS SURGERY
337. Morten Bruvold: MANGANESE AND WATER IN CARDIAC MAGNETIC RESONANCE IMAGING
338. Miroslav Fris: THE EFFECT OF SINGLE AND REPEATED ULTRAVIOLET RADIATION ON THE ANTERIOR SEGMENT OF THE RABBIT EYE
339. Svein Arne Aase: METHODS FOR IMPROVING QUALITY AND EFFICIENCY IN QUANTITATIVE ECHOCARDIOGRAPHY – ASPECTS OF USING HIGH FRAME RATE
340. Roger Almvik: ASSESSING THE RISK OF VIOLENCE: DEVELOPMENT AND VALIDATION OF THE BRØSET VIOLENCE CHECKLIST
341. Ottar Sundheim: STRUCTURE-FUNCTION ANALYSIS OF HUMAN ENZYMES INITIATING NUCLEOBASE REPAIR IN DNA AND RNA
342. Anne Mari Undheim: SHORT AND LONG-TERM OUTCOME OF EMOTIONAL AND BEHAVIOURAL PROBLEMS IN YOUNG ADOLESCENTS WITH AND WITHOUT READING DIFFICULTIES
343. Helge Garåsen: THE TRONDHEIM MODEL. IMPROVING THE PROFESSIONAL COMMUNICATION BETWEEN THE VARIOUS LEVELS OF HEALTH CARE SERVICES AND IMPLEMENTATION OF INTERMEDIATE CARE AT A COMMUNITY HOSPITAL COULD PROVIDE BETTER CARE FOR OLDER PATIENTS. SHORT AND LONG TERM EFFECTS
344. Olav A. Foss: "THE ROTATION RATIOS METHOD". A METHOD TO DESCRIBE ALTERED SPATIAL ORIENTATION IN SEQUENTIAL RADIOGRAPHS FROM ONE PELVIS
345. Bjørn Olav Åsvold: THYROID FUNCTION AND CARDIOVASCULAR HEALTH
346. Torun Margareta Melø: NEURONAL GLIAL INTERACTIONS IN EPILEPSY
347. Irina Poliakova Eide: FETAL GROWTH RESTRICTION AND PRE-ECLAMPSIA: SOME CHARACTERISTICS OF FETO-MATERNAL INTERACTIONS IN DECIDUA BASALIS
348. Torunn Askim: RECOVERY AFTER STROKE. ASSESSMENT AND TREATMENT; WITH FOCUS ON MOTOR FUNCTION
349. Ann Elisabeth Åsberg: NEUTROPHIL ACTIVATION IN A ROLLER PUMP MODEL OF CARDIOPULMONARY BYPASS. INFLUENCE ON BIOMATERIAL, PLATELETS AND COMPLEMENT
350. Lars Hagen: REGULATION OF DNA BASE EXCISION REPAIR BY PROTEIN INTERACTIONS AND POST TRANSLATIONAL MODIFICATIONS
351. Sigrun Beate Kjøtrød: POLYCYSTIC OVARY SYNDROME – METFORMIN TREATMENT IN ASSISTED REPRODUCTION

352. Steven Keita Nishiyama: PERSPECTIVES ON LIMB-VASCULAR HETEROGENEITY: IMPLICATIONS FOR HUMAN AGING, SEX, AND EXERCISE
353. Sven Peter Näsholm: ULTRASOUND BEAMS FOR ENHANCED IMAGE QUALITY
354. Jon Ståle Ritland: PRIMARY OPEN-ANGLE GLAUCOMA & EXFOLIATIVE GLAUCOMA. SURVIVAL, COMORBIDITY AND GENETICS
355. Sigrid Botne Sando: ALZHEIMER'S DISEASE IN CENTRAL NORWAY. GENETIC AND EDUCATIONAL ASPECTS
356. Parvinder Kaur: CELLULAR AND MOLECULAR MECHANISMS BEHIND METHYLMERCURY-INDUCED NEUROTOXICITY
357. Ismail Cüneyt Güzey: DOPAMINE AND SEROTONIN RECEPTOR AND TRANSPORTER GENE POLYMORPHISMS AND EXTRAPYRAMIDAL SYMPTOMS. STUDIES IN PARKINSON'S DISEASE AND IN PATIENTS TREATED WITH ANTIPSYCHOTIC OR ANTIDEPRESSANT DRUGS
358. Brit Dybdahl: EXTRA-CELLULAR INDUCIBLE HEAT-SHOCK PROTEIN 70 (Hsp70) – A ROLE IN THE INFLAMMATORY RESPONSE ?
359. Kristoffer Haugarvoll: IDENTIFYING GENETIC CAUSES OF PARKINSON'S DISEASE IN NORWAY
360. Nadra Nilsen: TOLL.LIKE RECEPTOR – EXPRESSION, REGULATION AND SIGNALING
361. Johan Håkon Bjørngaard: PATIENT SATISFACTION WITH OUTPATIENT MENTAL HEALTH SERVICES – THE INFLUENCE OF ORGANIZATIONAL FACTORS.
362. Kjetil Høydal : EFFECTS OF HIGH INTENSITY AEROBIC TRAINING IN HEALTHY SUBJECTS AND CORONARY ARTERY DISEASE PATIENTS; THE IMPORTANCE OF INTENSITY,, DURATION AND FREQUENCY OF TRAINING.
363. Trine Karlsen: TRAINING IS MEDICINE: ENDURANCE3 AND STRANGTH TRAINING IN CORONARY ARTERY DISESE AND HEALTH.
364. Marte Thuen: MANGANASE-ENHANCED AND DIFFUSION TENSOR MR IMAGING OF THE NORMAL, INJURED AND REGENERATING RAT VISUAL PATHWAY
365. Cathrine Broberg Vågbø: DIRECT REPAIR OF ALKYLATION DAMAGE IN DNA AND RNA BY 2-OXOGLUTARATE- AND IRON-DEPENDENT DIOXYGENASES
366. Arnt Erik Tjønna: AEROBIC EXERCISE AND CARDIOVASCULAR RISK FACTORS IN OVERWEIGHT AND OBESE ADOLESCENTS AND ADULTS
367. Marianne W. Furnes: FEEDING BEHAVIOR AND BODY WEIGHT DEVELOPMENT: LESSONS FROM RATS
368. Lene N. Johannessen: FUNGAL PRODUCTS AND INFLAMMATORY RESPONSES IN HUMAN MONOCYTES AND EPITHELIAL CELLS
369. Anja Bye: GENE EXPRESSION PROFILING OF *INHERITED* AND *ACQUIRED* MAXIMAL OXYGEN UPTAKE – RELATIONS TO THE METABOLIC SYNDROME.
370. Oluf Dimitri Røe: MALIGNANT MESOTHELIOMA: VIRUS, BIOMARKERS AND GENES. A TRANSLATIONAL APPROACH
371. Ane Cecilie Dale: DIABETES MELLITUS AND FATAL ISCHEMIC HEART DISEASE. ANALYSES FROM THE HUNT1 AND 2 STUDIES
372. Jacob Christian Hølen: PAIN ASSESSMENT IN PALLIATIVE CARE: VALIDATION OF METHODS FOR SELF-REPORT AND BEHAVIOURAL ASSESSMENT
373. Erming Tian: THE GENETIC IMPACTS IN THE ONCOGENESIS OF MULTIPLE MYELOMA
374. Ole Bosnes: KLINISK UTPRØVING AV NORSKE VERSJONER AV NOEN SENTRALE TESTER PÅ KOGNITIV FUNKSJON
375. Ola M. Rygh: 3D ULTRASOUND BASED NEURONAVIGATION IN NEUROSURGERY. A CLINICAL EVALUATION